CARDIOMETABOLIC BURDEN AND BIOMARKERS OF AUTONOMOUS CORTISOL SECRETION

by

ALESSANDRO PRETE

A thesis submitted to the University of Birmingham for the degree of
DOCTOR OF PHILOSOPHY

Institute of Metabolism and Systems Research
College of Medical and Dental Sciences
University of Birmingham
July 2022

UNIVERSITY OF
BIRMINGHAM

University of Birmingham Research Archive

e-theses repository

This unpublished thesis/dissertation is copyright of the author and/or third parties. The intellectual property rights of the author or third parties in respect of this work are as defined by The Copyright Designs and Patents Act 1988 or as modified by any successor legislation.

Any use made of information contained in this thesis/dissertation must be in accordance with that legislation and must be properly acknowledged. Further distribution or reproduction in any format is prohibited without the permission of the copyright holder.

ABSTRACT

The overwhelming majority of incidentally discovered adrenal tumours are benign adrenocortical tumours. These can be non-functioning (NFAT) or associated with autonomous cortisol secretion on a spectrum ranging from rare clinically overt adrenal Cushing's syndrome (CS) to much more prevalent mild autonomous cortisol secretion (MACS) without signs of CS. Here I present the characteristics of a large cohort of persons with newly diagnosed benign adrenocortical tumours.

In 1305 prospectively recruited cases, almost every second person with benign adrenocortical tumours was diagnosed with MACS. Persons with MACS had rates of cardiometabolic disease similar to CS, particularly increased prevalence and severity of hypertension and type 2 diabetes.

Urine multi-steroid profiling of these persons revealed a gradual increase in glucocorticoid excretion from NFAT over MACS to CS, whilst androgen excretion decreased. Increased glucocorticoid and 11-oxygenated androgen metabolite excretion predicted clinical outcomes including hypertension, type 2 diabetes, and the presence of bilateral adrenal tumours.

A representative group of 291 persons underwent untargeted serum metabolome profiling. Prototype-based supervised machine learning identified progressive metabolic changes in MACS and CS suggestive of lipotoxicity, dysfunctional lipid β-oxidation, and oxidative stress across the spectrum of autonomous cortisol secretion.

These results show that MACS is a prevalent cardiometabolic risk condition associated with distinct changes in the steroid and untargeted metabolome. Observed changes offer the prospect of risk stratification of affected individuals.

To Aurelio Jr.

In Ersilia, to establish the relationships that sustain the city's life, the inhabitants stretch strings from the corners of the houses, white or black or grey or black-and-white according to whether they mark a relationship of blood, of trade, authority, agency. When the strings become so numerous that you can no longer pass among them, the inhabitants leave: the houses are dismantled; only the strings and their supports remain. From a mountainside, camping with their household goods, Ersilia's refugees look at the labyrinth of taut strings and poles that rise in the plain. That is the city of Ersilia still, and they are nothing. They rebuild Ersilia elsewhere. They weave a similar pattern of strings which they would like to be more complex and at the same time more regular than the other. Then they abandon it and take themselves and their houses still farther away. Thus, when travelling in the territory of Ersilia, you come upon the ruins of abandoned cities, without the walls which do not last, without the bones of the dead which the wind rolls away: spiderwebs of intricate relationships seeking a form.

Invisible Cities – Italo Calvino

ACKNOWLEDGEMENTS

First, I wish to acknowledge Diabetes UK, the agency that has funded this work, as well as the European Society of Endocrinology and the European Union of Medical Specialists, which helped me to start my academic journey in the UK.

My gratitude goes to my supervisors, Prof Wiebke Arlt and Dr Konstantinos Manolopoulos. Thank you for your unwavering support and encouragement over the years, for your commitment to teaching, and for showing me that problems often lead to unforeseen opportunities. Your curiosity and positive attitude have been an inspiration and I feel fortunate to have you as role models for my personal and professional development.

Thank you to my collaborators within the ENSAT community, especially my friend and colleague Dr Irina Bancos: you were instrumental in the success of this work, and I will always cherish my time at the Mayo Clinic. Thank you to Prof Michael Biehl, Prof Peter Tino, and Prof Rick Dunn for teaching me a lot about machine learning and global metabolomics; thank you for your time and patience and for believing that my brain can fully grasp the amazing things you are doing! My gratitude also goes to Dr Alice Sitch, Prof Krish Nirantharakumar, Anu Subramanian, Marco Canducci, and Lida Abdi: this work wouldn't have been possible without your precious help.

To all the Arlties and the people I was privileged to meet at the IMSR over the years, especially Dr Angela Taylor, Dr Lina Schiffer, Dr Lorna Gilligan, and Dr Fozia Shaheen for your training and support. Thank you, Hannah Ivison, for just being you, and Thais Rocha, for being a good friend and a key asset to my mental health!

Thank you to my previous mentors and supervisors Prof Salvatore Corsello and Dr Carlo Rota: I became passionate about endocrinology because of you, and I will be forever grateful for what you have taught me over the years.

My gratitude goes to my friends. Daniela, you always have and always will be a pillar in my life and I am so fortunate that our paths have crossed. Manuela, I feel that our minds are beautifully intertwined, and your poise never fails to amaze me. Valentina, you stormed into my life just over a decade ago and managed to enrich it ever since. Francesca, you took a piece of my heart when we first met at university and have always kept it safe and loved. Dada, *caelum, non animum mutant qui trans mare currunt*: we may have travelled the world, but thankfully some things never change.

To my partner in crime, Jiten: thank you for being such a loving and caring person. You tolerate my erratic working patterns and always succeed in bringing me back to reality. You calmly squeezed your way into my soul, and I hope that I make you half as happy as you make me.

Finally, I want to thank my big family: a miraculous cluster of happiness and love that is as beautiful as it is rare. To my grandma Maria, your strength and determination have always been a source of inspiration. To my brother Daniele, you are a good and thoughtful person, and I am so fortunate to have you in my life. To my parents, Aurelio and Fernanda, thank you from the bottom of my heart for believing in me and for empowering me to forge my path in life. Your love and support made me the person I am today, and I will always remember that.

PUBLICATION LIST AND CONFERENCE PRESENTATIONS

During my postgraduate study within the Institute of Metabolism and Systems Research, University of Birmingham, the following articles and book chapters were accepted for publication. Invited lectures that stemmed from my research activity are also listed.

Original Research Articles

Age-dependent and sex-dependent disparity in mortality in patients with adrenal incidentalomas and autonomous cortisol secretion: an international, retrospective, cohort study.
Deutschbein T, Reimondo G, Di Dalmazi G, Bancos I, Patrova J, Vassiliadi DA, Nekić AB, Debono M, Lardo P, Ceccato F, Petramala L, **Prete A**, Chiodini I, Ivović M, Pazaitou-Panayiotou K, Alexandraki KI, Hanzu FA, Loli P, Yener S, Langton K, Spyroglou A, Kocjan T, Zacharieva S, Valdés N, Ambroziak U, Suzuki M, Detomas M, Puglisi S, Tucci L, Delivanis DA, Margaritopoulos D, Dusek T, Maggio R, Scaroni C, Concistrè A, Ronchi CL, Altieri B, Mosconi C, Diamantopoulos A, Iñiguez-Ariza NM, Vicennati V, Pia A, Kroiss M, Kaltsas G, Chrisoulidou A, Marina LV, Morelli V, Arlt W, Letizia C, Boscaro M, Stigliano A, Kastelan D, Tsagarakis S, Athimulam S, Pagotto U, Maeder U, Falhammar H, Newell-Price J, Terzolo M, Fassnacht M.
Lancet Diabetes Endocrinol. 2022 May 6:S2213-8587(22)00100-0.
doi: 10.1016/S2213-8587(22)00100-0.

Cardiometabolic Disease Burden and Steroid Excretion in Benign Adrenal Tumors: A Cross-Sectional Multicenter Study.
Prete A, Subramanian A, Bancos I, Chortis V, Tsagarakis S, Lang K, Macech M, Delivanis DA, Pupovac ID, Reimondo G, Marina LV, Deutschbein T, Balomenaki M, O'Reilly MW, Gilligan LC, Jenkinson C, Bednarczuk T, Zhang CD, Dusek T, Diamantopoulos A, Asia M, Kondracka A, Li D, Masjkur JR, Quinkler M, Ueland GÅ, Dennedy MC, Beuschlein F, Tabarin A, Fassnacht M, Ivović M, Terzolo M, Kastelan D, Young WF Jr, Manolopoulos KN, Ambroziak U, Vassiliadi DA, Taylor AE, Sitch AJ, Nirantharakumar K, Arlt W; ENSAT EURINE-ACT Investigators*.
Ann Intern Med. 2022 Mar;175(3):325-334
doi: 10.7326/M21-1737.

Modified-release Hydrocortisone in Congenital Adrenal Hyperplasia.
Merke DP, Mallappa A, Arlt W, Brac de la Perriere A, Hirschberg AL, Juul A, Newell-Price J, Perry CG, **Prete A**, Rees DA, Reisch N, Stikkelbroeck N, Tourraine P, Maltby K, Treasure FP, Porter J, Ross RJ.
J Clin Endocrinol Metab. 2021 Apr 23;106(5):e2063-e2077.
doi: 10.1210/clinem/dgab051.

Urine steroid metabolomics for the differential diagnosis of adrenal incidentalomas in the EURINE-ACT study: a prospective test validation study.
Bancos I, Taylor AE, Chortis V, Sitch AJ, Jenkinson C, Davidge-Pitts CJ, Lang K, Tsagarakis S, Macech M, Riester A, Deutschbein T, Pupovac ID, Kienitz T, **Prete A**, Papathomas TG, Gilligan LC, Bancos C, Reimondo G, Haissaguerre M, Marina L, Grytaas MA, Sajwani A, Langton K, Ivison HE, Shackleton CHL, Erickson D, Asia M, Palimeri S, Kondracka A, Spyroglou A, Ronchi CL, Simunov B, Delivanis DA, Sutcliffe RP, Tsirou I, Bednarczuk T, Reincke M, Burger-Stritt S, Feelders RA, Canu L, Haak HR, Eisenhofer G, Dennedy MC, Ueland GA, Ivovic M, Tabarin A, Terzolo M, Quinkler M, Kastelan D, Fassnacht M, Beuschlein F, Ambroziak U, Vassiliadi DA, O'Reilly MW, Young WF Jr, Biehl M, Deeks JJ, Arlt W; ENSAT EURINE-ACT Investigators.
Lancet Diabetes Endocrinol. 2020 Sep;8(9):773-781.
doi: 10.1016/S2213-8587(20)30218-7

Prevention of Adrenal Crisis: Cortisol Responses to Major Stress Compared to Stress Dose Hydrocortisone Delivery.
Prete A, Taylor AE, Bancos I, Smith DJ, Foster MA, Kohler S, Fazal-Sanderson V, Komninos J, O'Neil DM, Vassiliadi DA, Mowatt CJ, Mihai R, Fallowfield JL, Annane D, Lord JM, Keevil BG, Wass JAH, Karavitaki N, Arlt W.
J Clin Endocrinol Metab. 2020 Jul 1;105(7):2262-74.
doi: 10.1210/clinem/dgaa133.

Plasma Renin Measurements are Unrelated to Mineralocorticoid Replacement Dose in Patients With Primary Adrenal Insufficiency.
Pofi R, **Prete A**, Thornton-Jones V, Bryce J, Ali SR, Faisal Ahmed S, Balsamo A, Baronio F, Cannuccia A, Guven A, Guran T, Darendeliler F, Higham C, Bonfig W, de Vries L, Bachega TASS, Miranda MC, Mendonca BB, Iotova V, Korbonits M, Krone NP, Krone R, Lenzi A, Arlt W, Ross RJ, Isidori AM, Tomlinson JW.
J Clin Endocrinol Metab. 2020 Jan 1;105(1):dgz055.
doi: 10.1210/clinem/dgz055.

Increased Infection Risk in Addison's Disease and Congenital Adrenal Hyperplasia.
Tresoldi AS, Sumilo D, Perrins M, Toulis KA, **Prete A**, Reddy N, Wass JAH, Arlt W, Nirantharakumar K.
J Clin Endocrinol Metab. 2020 Feb 1;105(2):418-29.
doi: 10.1210/clinem/dgz006.

Natural History of Adrenal Incidentalomas With and Without Mild Autonomous Cortisol Excess: A Systematic Review and Meta-analysis.
Elhassan YS, Alahdab F, **Prete A**, Delivanis DA, Khanna A, Prokop L, Murad MH, O'Reilly MW, Arlt W, Bancos I.
Ann Intern Med. 2019 Jul 16;171(2):107-116.
doi: 10.7326/M18-3630.

The cortisol stress response induced by surgery: A systematic review and meta-analysis.
Prete A, Yan Q, Al-Tarrah K, Akturk HK, Prokop LJ, Alahdab F, Foster MA, Lord JM, Karavitaki N, Wass JA, Murad MH, Arlt W, Bancos I.
Clin Endocrinol (Oxf). 2018 Nov;89(5):554-567.
doi: 10.1111/cen.13820.

Review Articles

Clinical advances in the pharmacotherapy of congenital adrenal hyperplasia.
Prete A, Auchus RJ, Ross RJ.
Eur J Endocrinol. 2021 Nov 30;186(1):R1-R14.
doi: 10.1530/EJE-21-0794.

Approach to the Patient With Adrenal Incidentaloma.
Bancos I, **Prete A**.
J Clin Endocrinol Metab. 2021 Oct 21;106(11):3331-3353.
doi: 10.1210/clinem/dgab512.PMID: 34260734

Glucocorticoid induced adrenal insufficiency.
Prete A, Bancos I.
BMJ. **2021** Jul 12;374:n1380.
doi: 10.1136/bmj.n1380.

Steroid Metabolome Analysis in Disorders of Adrenal Steroid Biosynthesis and Metabolism.
Storbeck KH, Schiffer L, Baranowski ES, Chortis V, **Prete A**, Barnard L, Gilligan LC, Taylor AE, Idkowiak J, Arlt W, Shackleton CHL.
Endocr Rev. 2019 Dec 1;40(6):1605-1625.
doi: 10.1210/er.2018-00262.

Hypophysitis.
Prete A, Salvatori R. 2018 Aug 15. In: Feingold KR, Anawalt B, Boyce A, Chrousos G, de Herder WW, Dungan K, Grossman A, Hershman JM, Hofland J, Kaltsas G, Koch C, Kopp P, Korbonits M, McLachlan R, Morley JE, New M, Purnell J, Singer F, Stratakis CA, Trence DL, Wilson DP, editors.
Endotext [Internet]. South Dartmouth (MA): MDText.com, Inc.; 2000–2021 Oct 15.

Correspondence and Web Exclusive

Web Exclusive. Annals On Call - Are Adrenal Incidentalomas Clinically Important?
Centor RM, Bancos I, **Prete A**.
Ann Intern Med. 2022 Mar;175(3):OC1.
doi: 10.7326/A21-0007.PMID: 35286824

Comment on "A Modern Assessment of Cancer Risk in Adrenal Incidentalomas: Analysis of 2219 Patients" by Kahramangil B et al.
Chortis V, Sitch AJ, Bancos I, **Prete A**, Taylor AE, Biehl M, Deeks JJ, Arlt W.
Ann Surg. 2021 Dec 1;274(6):e887-e888.
doi: 10.1097/SLA.0000000000004804.

Response to Letter to the Editor from Chee et al: "Prevention of Adrenal Crisis: Cortisol Response to Major Stress Compared to Stress Dose Hydrocortisone Delivery".
Prete A, Taylor AE, Bancos I, Smith DJ, Foster MA, Kohler S, Fazal-Sanderson V, Komninos J, O'Neil DM, Vassiliadi DA, Mowatt CJ, Mihai R, Fallowfield JL, Annane D, Lord JM, Keevil BG, Wass JAH, Karavitaki N, Arlt W.
J Clin Endocrinol Metab. 2021 Jan 1;106(1):e407-e408.
doi: 10.1210/clinem/dgaa719.

Response to Letter to the Editor: "Prevention of Adrenal Crisis: Cortisol Response to Major Stress Compared to Stress Dose Hydrocortisone Delivery".
Prete A, Taylor AE, Bancos I, Smith DJ, Foster MA, Kohler S, Fazal-Sanderson V, Komninos J, O'Neil DM, Vassiliadi DA, Mowatt CJ, Mihai R, Fallowfield JL, Annane D, Lord JM, Keevil BG, Wass JAH, Karavitaki N, Arlt W.
J Clin Endocrinol Metab. 2021 Jan 1;106(1):e404-e406.
doi: 10.1210/clinem/dgaa712.

Urine metabolomic phenotyping for detection of adrenocortical carcinoma: still a long way to go - Authors' reply.
Bancos I, Taylor AE, Chortis V, Sitch AJ, Lang K, **Prete A**, Gilligan LC, Biehl M, Deeks JJ, Arlt W; ENSAT EURINE-ACT Investigators.
Lancet Diabetes Endocrinol. 2020 Nov;8(11):877-878.
doi: 10.1016/S2213-8587(20)30345-4.

Book chapters

Prete A, Salvatori R. Hypophysitis during Pregnancy in “Pituitary Disorders throughout the Life Cycle”, Christi M, Spring K (eds.) – Springer, 2021.

Prete A, Feliciano C, Mitchehill I, Arlt W. Congenital Adrenal Hyperplasia. Chapter 35 in “Textbook of Advanced Practice Nursing in Endocrinology”, Llahana S, Follin C, Yedinak CG, Grossman A (eds.) – Springer, 2019.

Prete A, Salvatori R, Hypophysitis (2018). In: De Groot LJ, Chrousos G, Dungan K, Feingold KR, Grossman A, Hershman JM, Koch C, Korbonits M, McLachlan R, New M, Purnell J, Rebar R, Singer F, Vinik A, editors. SourceEndotext [Internet]. South Dartmouth (MA): MDText.com, Inc.; 2000-2018 Aug 15.

Prete A, Salvatori R. Medical and Surgical Management of Hormone-Secreting Pituitary Tumours Chapter 14 in “Operative Neurosurgical Technique” 7th edition, Schmidek and Sweet (eds), Elsevier, 2018.

Prete A, Salvatori R. Management of Adults With Childhood-Onset GH Deficiency. Chapter 8 in “Pediatric Endocrinology: A Practical Clinical Guide”, 3rd edition, Radovick S and MacGillivray MH (eds.), Springer Science+Business Media New York, 2017.

Prete A, Salvatori R. Post-treatment Management of Cushing’s Disease. Chapter 9 in “Cushing’s Disease: An Often Misdiagnosed and Not So Rare Disorder”, Laws ER and Pace L (eds.), Academic Press – Elsevier, 2017.

Invited lectures

ENDO 2022 (annual conference of the Endocrine Society): Meet-the-professor session on glucocorticoid-induced adrenal insufficiency.

Society for Endocrinology Clinical Update 2022: The use of Efmody in the treatment of CAH patients.

Symposium “Steroids, mass spectrometry and endocrinology – past, present and future” (organised in 2022 by the Institute of Metabolism and Systems Research, University of Birmingham): Steroid and global metabolome changes of mild autonomous cortisol secretion.

SfE BES 2021 (annual conference of the Society for Endocrinology): Cardiometabolic disease burden and urine steroid metabolome in benign adrenocortical tumours*. I was* ***awarded the 2021 SfE Early Career Prize for clinical research by the Society for Endocrinology*** *for this presentation.*

AME 2021 (annual conference of the Italian Society for Endocrinology Associazione Medici Endocrinologi): Urine steroid metabolomics: personalised medicine for the study of adrenal disorders.

AME 2020 (annual conference of the Italian Society for Endocrinology Associazione Medici Endocrinologi): Adrenal incidentalomas – is follow-up always necessary?

AME 2019 (annual conference of the Italian Society for Endocrinology Associazione Medici Endocrinologi): Management of glucocorticoid replacement during emotional stress, fasting, and altered sleep/wake patterns.

AME 2019 (annual conference of the Italian Society for Endocrinology Associazione Medici Endocrinologi): Endocrinological causes of hypokalaemia.

Oral presentations of original research (as first or senior author)

ENDO 2022 (annual conference of the Endocrine Society): Comprehensive steroid and global metabolome analysis by mass spectrometry and machine learning to understand metabolic risk in benign adrenal tumours with mild autonomous cortisol secretion. *This presentation was* ***awarded the “outstanding abstract award” by the Endocrine Society****. (First author)*

Clinical Academics in Training Annual Conference of the Academy of Medical Sciences 2022: Comprehensive steroid and global metabolome analysis by mass spectrometry and machine learning to understand metabolic risk in benign adrenal tumours with mild autonomous cortisol secretion. *(First author)*

ENSAT 2021 (annual conference of the European Network for the Study of Adrenal Tumours): Should the 1mg-overnight dexamethasone suppression test be repeated in patients with benign adrenal incidentalomas and no overt hormone excess? *(Senior author)*

ENSAT 2020 (annual conference of the European Network for the Study of Adrenal Tumours): Urine steroid metabolomics for classification and metabolic risk stratification of benign adrenal tumours with different degrees of cortisol excess in the EURINE-ACT study. *(First author)*

SfE BES 2019 (annual conference of the Society for Endocrinology): Urine steroid metabolome analysis allows for metabolic risk stratification in 1309 prospectively recruited patients with benign adrenal tumours and different degrees of cortisol excess. *This presentation was* ***awarded the "Clinical Endocrinology Trust best clinical abstract award" by the Society for Endocrinology*** *and I was invited to deliver my talk at the Early Career Prize Plenary Session. (First author)*

ENDO 2019 (annual conference of the Endocrine Society): Mild autonomous cortisol excess in adrenal incidentalomas – metabolic risk profile and urinary steroid metabolome analysis in 1208 prospectively recruited patients. *This presentation was* ***awarded the "outstanding abstract award" by the Endocrine Society****. (First author)*

SfE BES 2018 (annual conference of the Society for Endocrinology): Timed urinary steroid profiling of patients with different degrees of cortisol excess: a proposal for a new test for the diagnosis of Cushing's syndrome. *(First author)*

Poster presentations of original research (as first or senior author)

SfE BES 2021 (annual conference of the Society for Endocrinology): Should the 1mg-overnight dexamethasone suppression test be repeated in patients with benign adrenal incidentalomas and no overt hormone excess? *(Senior author)*

SfE BES 2021 (annual conference of the Society for Endocrinology): Impact of COVID-19 on patients with primary adrenal insufficiency: a cross-sectional study. *(Senior author)*

European Congress of Endocrinology 2021 (annual conference of the European Society of Endocrinology): Modified-release hydrocortisone improves androgen excess and facilitates glucocorticoid dose reduction in patients with classic congenital adrenal hyperplasia: non-invasive monitoring in saliva and urine. *(First author)*

European Congress of Endocrinology 2021 (annual conference of the European Society of Endocrinology): Increased risk of cardiometabolic disease in patients with benign adrenal tumours with and without cortisol excess: a case-control study. *(First author)*

Diabetes UK professional conference 2020: High risk of diabetes and hypertension in patients with benign adrenal tumours associated with mild autonomous cortisol excess: Clinical characteristics and urinary steroid profiling of 1309 prospectively recruited patients. *(First author)*

ENSAT 2019 (annual conference of the European Network for the Study of Adrenal Tumours): Metabolic risk stratification by urine steroid metabolome profiling in a large prospective cohort of patients with benign adrenal tumours and different degrees of cortisol excess. *(First author)*

SfE BES 2019 (annual conference of the Society for Endocrinology): Systemic and femoral adipose tissue-specific non-targeted plasma metabolome during acute hypercortisolaemia. *(First author)*

Annual Clinical Academic Training Meeting (University of Birmingham): Mild autonomous cortisol excess in adrenal incidentalomas – metabolic risk profile and urinary steroid metabolome analysis in 1208 prospectively recruited patients. *(First author)*

ENSAT 2019 (annual conference of the European Network for the Study of Adrenal Tumours): Metabolic risk stratification by urine steroid metabolome profiling in a large prospective cohort of patients with benign adrenal tumours and different degrees of cortisol excess. *(First author)*

Adrenal Cortex Meeting 2018: Mild autonomous cortisol excess in adrenal incidentalomas – metabolic risk stratification and urinary steroid profiling in 1208 prospectively recruited patients. *(First author)*

TABLE OF CONTENTS

LIST OF FIGURES

CHAPTER 5

LIST OF TABLES

CHAPTER 5

ABBREVIATIONS

- 1mg-DST: 1mg overnight dexamethasone suppression test
- 5α-17HP: 17α-hydroxy-3α,5α-pregnanolone
- 5α-THA: 5α-tetrahydro-11-dehydrocorticosterone
- 5α-THB: 5α-tetrahydrocorticosterone
- 5α-THDOC: 5α-tetrahydro-11-deoxycorticosterone
- 5α-THF: 5α-tetrahydrocortisol
- 5PD: pregnenediol
- 5PT: pregnenetriol
- 6β-OHF: 6β-hydroxycortisol
- 11β-OHAn: 11β-hydroxyandrosterone
- 11β-OHEt: 11β-hydroxyetiocholanolone
- 11-ketoEt: 11-ketoetiocholanolone
- 16α-DHEA: 16α-hydroxy-DHEA
- 17HP: 17α-hydroxypregnanolone
- 17OHP: 17α-hydroxyprogesterone
- ACA: adrenocortical adenoma
- ACC: adrenocortical carcinoma
- ACTH: adrenocorticotropic hormone
- An: androsterone
- a-OGMLVQ: accumulative ordinal generalised matrix learning vector quantisation
- AUC-ROC: area under the receiver-operating characteristics curve
- aPR: adjusted prevalence ratio
- ARMC5: armadillo repeat containing 5 gene
- BMI: body mass index
- CAH: congenital adrenal hyperplasia
- CRH: corticotropin releasing hormone
- CS: Cushing's syndrome
- CT: computed tomography
- CYP3A4: cytochrome P450 3A4
- DHEA: dehydroepiandrosterone
- DHEAS: dehydroepiandrosterone sulfate
- DRC: direct renin concentration
- E: cortisone
- EI: electron ionisation
- ENSAT: European Network for the Study of Adrenal Tumours
- ESI: electrospray ionisation
- Et: etiocholanolone
- F: cortisol
- FDG-PET: ^{18}F-fluorodeoxyglucose positron emission tomography
- GC-MS: gas chromatography-mass spectrometry
- GMLVQ: generalised matrix learning vector quantisation
- HbA1c: glycated haemoglobin

- HILIC: hydrophilic interaction chromatography
- HPLC-MS/MS: high performance liquid chromatography-tandem mass spectrometry
- HU: Hounsfield unit
- kNN: k-nearest neighbour
- LC-MS/MS: liquid chromatography-tandem mass spectrometry
- LVQ: learning vector quantisation
- MACS: mild autonomous cortisol secretion
- MACS-1: possible MACS
- MACS-2: definitive MACS
- MRI: magnetic resonance imaging
- m/z: mass to charge ratio
- NFAT: non-functioning adrenal tumour
- NSAID: non-steroidal anti-inflammatory drug
- OCP: oral contraceptive pill
- OR: ordinal regression
- PD: pregnanediol
- p-OGMLVQ: pair ordinal generalised matrix learning vector quantisation
- PR: prevalence ratio
- PRA: plasma renin activity
- PT: pregnanetriol
- PTONE: pregnanetriolone
- SGLT2: sodium-glucose co-transporter-2
- THA: tetrahydro-11-dehydrocorticosterone
- THAldo: 3α5β-tetrahydroaldosterone
- THB: tetrahydrocorticosterone
- THDOC: tetrahydro-11-deoxycorticosterone
- THE: tetrahydrocortisone
- THF: tetrahydrocortisol
- THS: tetrahydro-11-deoxycortisol
- UFC: urinary free cortisol
- UHPLC-MS: ultra-high performance liquid chromatography-mass spectrometry

CHAPTER 1

General introduction

Content from this chapter has been published:

Approach to the Patient With Adrenal Incidentaloma.
*Bancos I, **Prete A**.*
***J Clin Endocrinol Metab. 2021** Oct 21;106(11):3331-3353.*
doi: 10.1210/clinem/dgab512.PMID: 34260734

Steroid Metabolome Analysis in Disorders of Adrenal Steroid Biosynthesis and Metabolism.
*Storbeck KH, Schiffer L, Baranowski ES, Chortis V, **Prete A**, Barnard L, Gilligan LC, Taylor AE, Idkowiak J, Arlt W, Shackleton CHL.*
***Endocr Rev. 2019** Dec 1;40(6):1605-1625.*
doi: 10.1210/er.2018-00262.

Natural History of Adrenal Incidentalomas With and Without Mild Autonomous Cortisol Excess: A Systematic Review and Meta-analysis.
*Elhassan YS, Alahdab F, **Prete A**, Delivanis DA, Khanna A, Prokop L, Murad MH, O'Reilly MW, Arlt W, Bancos I.*
***Ann Intern Med. 2019** Jul 16;171(2):107-116.*
doi: 10.7326/M18-3630.

1.1. Assessment of adrenal steroidogenesis and steroid metabolism by urine steroid metabolome analysis

1.1.1. *Overview of adrenal steroidogenesis*

The adrenal cortex, gonads and placenta are the primary sites of *de novo* steroidogenesis from cholesterol. Some of the resulting steroids can directly bind and activate steroid receptors in target cells of steroid action, whilst others require downstream activation, but may also be inactivated or diverted to other steroid pathways. This intracellular steroid pre- and post-receptor metabolism has also been termed “intracrinology” (8), explaining why circulating steroid concentrations are often not representative of observed biological hormone activity. Moreover, adrenal

steroidogenesis exhibits a diurnal rhythm and, as a result, single-timepoint serum steroid measurements only provide snapshots. This problem is circumvented by analysing 24-hour urine collections, facilitating quantitation of the net 24-hour steroid output.

The adrenal cortex is divided into three zones characterised by differential expression of steroidogenic enzymes (1) (**Figure 1.1**):

- Zona glomerulosa (outer zone): responsible for the biosynthesis of mineralocorticoids, under the co of the renin-angiotensin-aldosterone system. The active mineralocorticoid aldosterone regulates electrolyte and water absorption in the kidney, contributing to intravascular volume and blood pressure control.
- Zona fasciculata (middle zone): responsible for the biosynthesis of glucocorticoids, under the control of the hypothalamic-pituitary-adrenal axis. The active glucocorticoid cortisol regulates energy metabolism, glucose homeostasis, immune function, and stress response.
- Zona reticularis (inner zone): responsible for the biosynthesis of adrenal androgen precursors and – to a lesser extent – active androgens, under the control of the hypothalamic-pituitary-adrenal axis. Adrenal androgen precursors serve as substrates for testosterone and oestradiol biosynthesis in the gonads.

Figure 1.1: Overview of adrenal steroidogenesis, peripheral modulation of steroid bioactivity, and corresponding urine steroid metabolites. Steroids are colour-coded according to their bioactivity or commitment to a specific pathway: general precursors (yellow); mineralocorticoid precursors (light green); active mineralocorticoid (dark green); glucocorticoid precursors and inactive metabolite (light orange); active glucocorticoid (dark orange); androgen precursors (light blue); active androgens (dark blue). Corresponding urinary metabolites are shown in yellow boxes. Arrows are labelled with the catalysing enzyme and isoform. Essential co-factor proteins are also indicated: adrenodoxin (ADX): cytochrome b5 (b5); cytochrome P450 oxidoreductase (POR); PAPS synthase 2 (PAPSS2); steroidogenic acute regulatory protein (StAR). Adapted from (2).

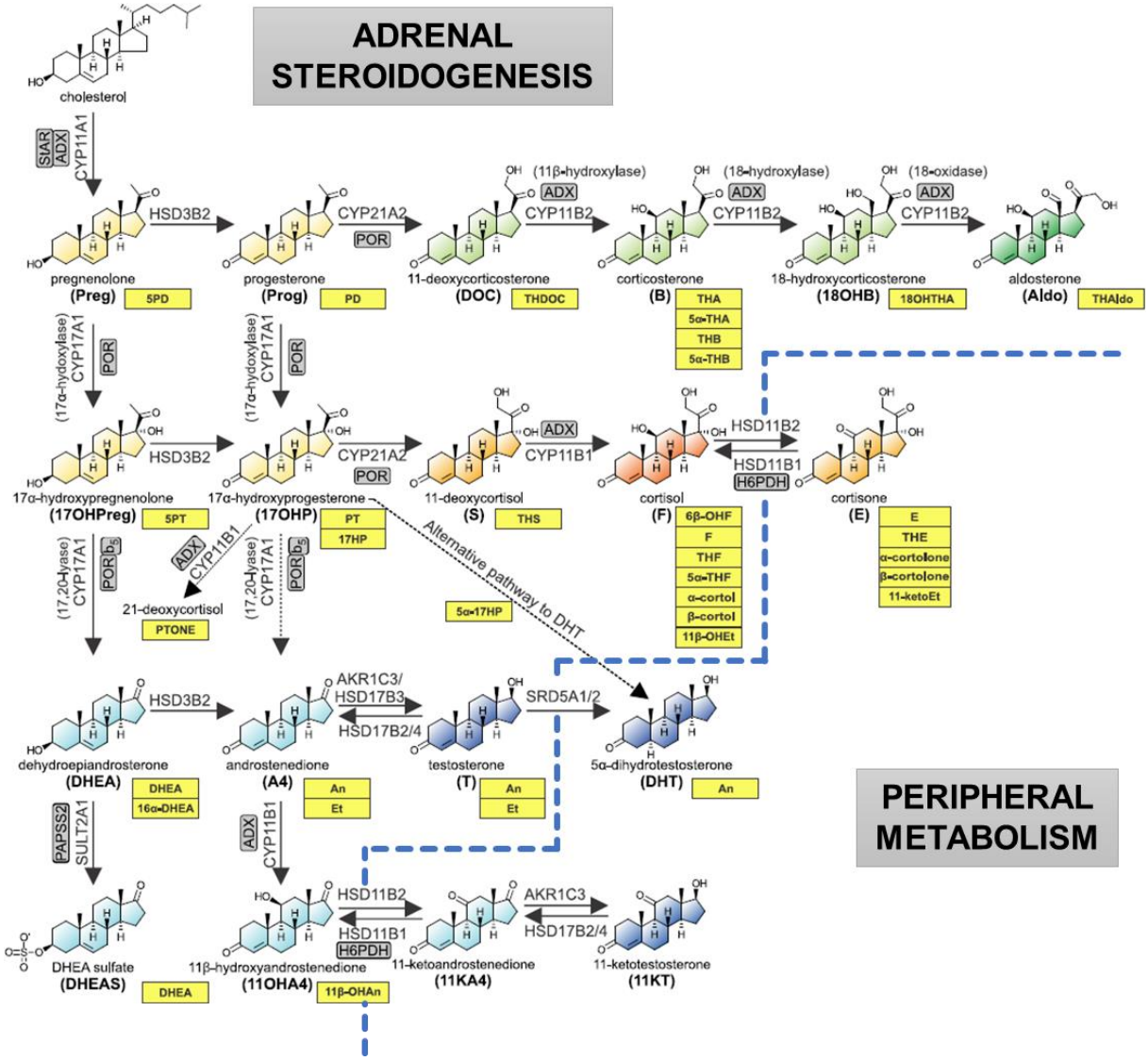

1.1.2. *Overview of steroid metabolism*

Both endogenous and exogenous steroids undergo hepatic metabolism (9), with phase 1 reactions altering the biological activity by adding or revealing functional groups that can function as targets for subsequent conjugation (phase 2) reactions. Ultimately, this results in steroid inactivation and increased water solubility, facilitating urinary excretion, which accounts for approximately 80% of steroid excretion (**Figure 1.2**) (1).

Figure 1.2: Overview of steroid metabolism. Schematic overview showing the flow of steroids from *de novo* biosynthesis in the adrenal glands and gonads to pre- and post- receptor metabolism in liver and peripheral target cells of steroid action and excretion via urine, bile, and faeces. Although the liver accounts for the majority of steroid metabolism, most peripheral tissues can express enzymes responsible for phase 1 and 2 reactions; this mechanism is responsible for tissue-specific regulation of steroid metabolism. The steroid metabolome is commonly measured in serum or 24-hour urine: the first approach provides an overview of steroid metabolism only at the time of collection, whilst the latter allows for a comprehensive analysis of steroid output and metabolism over 24 hours.

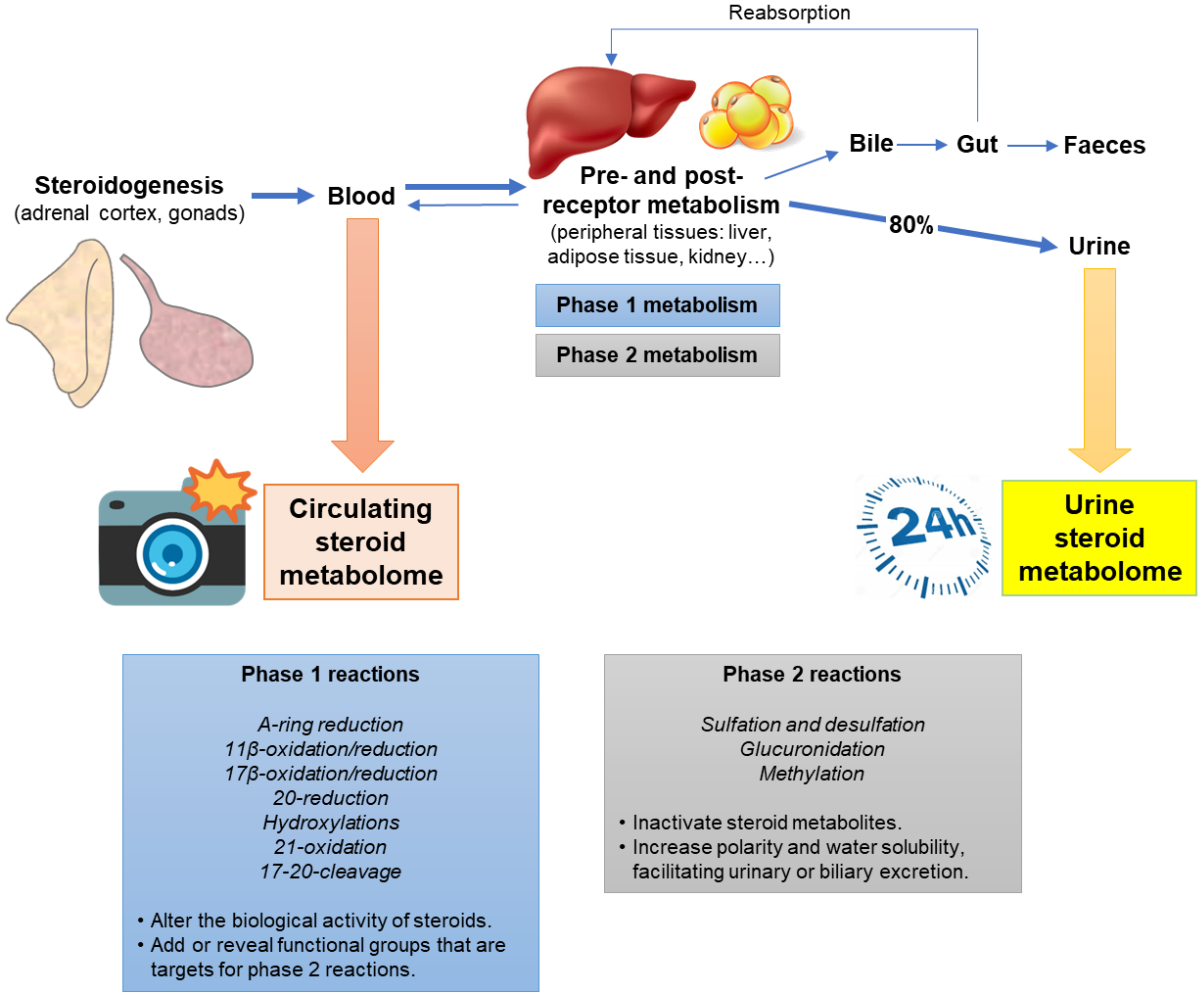

1.1.3. *Cortisol biosynthesis and metabolism*

The hypothalamic-pituitary-adrenal axis regulates the adrenal biosynthesis of glucocorticoids and androgen precursors. In short, the hypothalamus releases corticotropin-releasing hormone, which in turn stimulates the corticotrophs in the anterior pituitary to release adrenocorticotropic hormone (ACTH). ACTH then stimulates the biosynthesis of cortisol and androgen precursors. Cortisol eventually exerts a negative feedback action on the hypothalamus and pituitary preventing further stimulation of the adrenal cortex. Importantly, cortisol is secreted in a circadian fashion in healthy individuals, typically with nadir concentrations around midnight and peak concentrations in the early hours of the morning.

Pregnenolone, produced from the CYP11A1 catalysed side-chain cleavage of cholesterol, is first converted to 17α-hydroxypregnenolone by cytochrome P450 17A1 (CYP17A1) 17α-hydroxylase activity and then to 17α-hydroxyprogesterone (17OHP) by 3-β-hydroxysteroid dehydrogenase (HSD3B2). 17OHP is subsequently converted to 11-deoxycortisol by 21-hydroxylase (CYP21A2). 11-β-hydroxylase (CYP11B1) then catalyses the final step in glucocorticoid biosynthesis converting 11-deoxycortisol to cortisol (**Figure 1.3**) (1). In healthy subjects, 95% of serum cortisol is protein bound, primarily to cortisol-binding globulin (CBG) and secondarily to albumin. Five per cent of serum cortisol is free (not protein bound), and this is its bioactive form (3).

In peripheral aldosterone target tissues, cortisol is converted to inactive cortisone by the action of 11-β-hydroxysteroid dehydrogenase type 2 (HSD11B2), to prevent the activation of the mineralocorticoid receptor by cortisol (4). In the liver (and to a lesser extent adipose tissue, muscle, skin, and bone) cortisone is converted back to cortisol by 11-β-hydroxysteroid dehydrogenase type 1 (HSD11B1) (**Figure 1.3**) (4).

Figure 1.3: Overview of cortisol biosynthesis and metabolism. Schematic representation of glucocorticoids and glucocorticoid precursors, their downstream metabolism and corresponding urine metabolites. The glucocorticoid contribution to 11β-hydroxyandrosterone biosynthesis is very low in healthy individuals, with the majority (90-95%) originating from the downstream metabolism of the adrenal androgen 11β-hydroxyandrostenedione. Phase 2 reactions are not indicated in the figure.

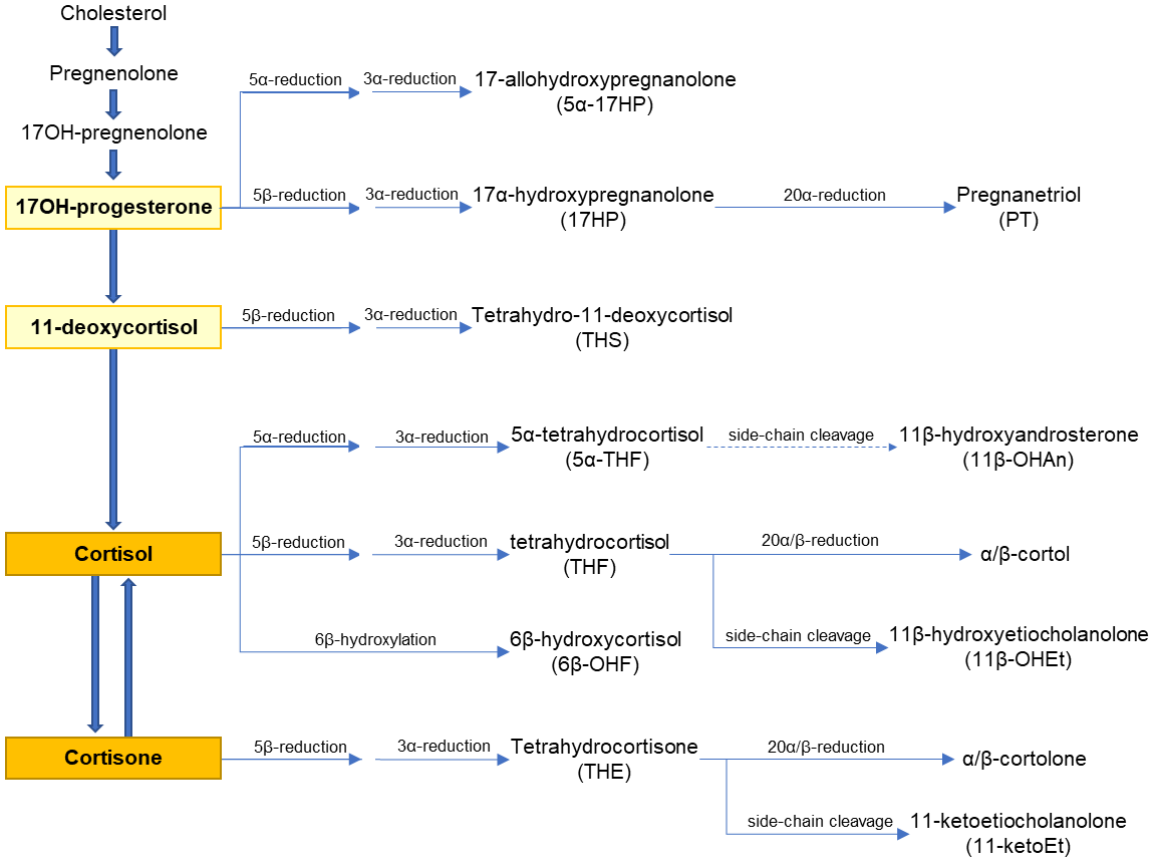

The first step in the downstream metabolism of glucocorticoids and glucocorticoid precursors, occurring primarily in the liver, is 5α/5β-reduction: 17OHP and cortisol can be either 5α- or 5β-reduced, whilst 11-deoxycortisol and cortisone are predominantly 5β-reduced (1, 5). The next step is 3α-reduction to tetrahydro or 5α-tetrahydro metabolites. Tetrahydrocortisol (THF) and tetrahydrocortisone (THE) can be further 20α/β-reduced to cortols and cortolones, respectively (1, 6, 7). THF, THE, and to a lesser extent 5α-THF, are also subject to side-chain cleavage yielding downstream metabolites. Cortisol can also be 6β-hydroxylated in the liver (1, 8).

1.1.4. *Overview of urine steroid metabolome analysis*

In the kidney, conjugated steroids are actively excreted and concentrated in the lumen of the nephron (1). Urine steroid metabolites originate from distinct circulating steroids (**Figure 1.1**; **Figure 1.3**; **Table 1.1**), and the 24-hour urine steroid metabolome serves as a magnifying glass, facilitating the detection of alterations in steroid biosynthesis or metabolism and, thus, of underlying disorders.

Mass spectrometry is uniquely suited for the analysis of the urine steroid metabolome, because of the possibility of simultaneously measuring multiple steroid metabolites. Currently, gas chromatography-mass spectrometry is the reference standard for urine steroid metabolome analysis. However, this technique is time-consuming and there have been increasing efforts in recent decades to develop ultra-high performance liquid chromatography-tandem mass spectrometry as a quicker and more cost-effective alternative (**Chapter 2**).

Table 1.1: Major urinary steroid metabolites (unconjugated form). Adapted from (2).

No.	Abbreviation	Common name	Chemical name	Metabolite of
Core steroid precursor metabolites				
1	5PD	Pregnenediol	5-Pregnene-3β,20α-diol	Pregnenolone
2	PD	Pregnanediol	5β-Pregnane-3α,20α-diol	Progesterone
3	5PT	Pregnenetriol	5-Pregnene-3β,17α,20α-triol	17α-Hydroxypregnenolone
4	PT	Pregnanetriol	5β-Pregnane-3α,17α,20α-triol	17α-Hydroxyprogesterone
5	17HP	17α-Hydroxypregnanolone	5β-Pregnane-3α,17α-diol-20-one	17α-Hydroxyprogesterone
6	5α-17HP	17α-Hydroxy-3α,5α-pregnanolone	5α-Pregnane-3α,17α-diol-20-one	17α-Hydroxyprogesterone
7	PTONE	Pregnanetriolone	5β-Pregnane-3α,17α,20α-triol-11-one	21-Deoxycortisol
8	THS	Tetrahydro-11-deoxycortisol	5β-Pregnane-3α,17α,21-triol-20-one	11-Deoxycortisol
Glucocorticoid metabolites				
9	F	Cortisol	4-Pregnene-11β,17α,21-triol-3,20-dione	Cortisol
10	6β-OHF	6β-Hydroxycortisol	4-Pregnene-6β,11β,17α,21-tetrol-3, 20-dione	Cortisol
11	THF	Tetrahydrocortisol	5β-Pregnane-3α,11β,17α,21-tetrol-20-one	Cortisol
12	5α-THF	5α-Tetrahydrocortisol	5α-Pregnane-3α,11β,17α,21-tetrol-20-one	Cortisol
13	α-cortol	α-Cortol	5β-Pregnane-3α,11β,17α,20α,21-pentol	Cortisol

14	β-cortol	β-Cortol	5β-Pregnane-3α,11β,17α,20β,21-pentol	Cortisol
15	11β-OHEt	11β-Hydroxyetiocholanolone	5β-Androstane-3α,11β-diol-17-one	Cortisol
16	E	Cortisone	4-Pregnene-17α,21-diol-3,11,20-trione	Cortisone
17	THE	Tetrahydrocortisone	5β-Pregnene-3α,17α,21-triol-11,20-dione	Cortisone
18	α-cortolone	α-Cortolone	5β-Pregnane-3α,17α,20α,21-tetrol-11-one	Cortisone
19	β-cortolone	β-Cortolone	5β-Pregnane-3α,17α,20β,21-tetrol-11-one	Cortisone
20	11-ketoEt	11-Ketoetiocholanolone	5β-Androstan-3α-ol-11.17-dione	Cortisone
Androgen and androgen precursor metabolites				
21	DHEA	Dehydroepiandrosterone	5-Androsten-3β-ol-17-one	DHEA + DHEA sulfate (DHEAS)
22	16α-DHEA	16α-Hydroxy-DHEA	5-Androstene-3β,16α-diol-17-one	DHEA + DHEAS
23	An	Androsterone	5α-Androstan-3α-ol-17-one	Androstenedione, testosterone, 5α-dihydrotestosterone
24	Et	Etiocholanolone	5β-Androstan-3α-ol-17-one	Androstenedione, testosterone
25	11β-OHAn	11β-Hydroxyandrosterone	5α-Androstane-3α,11β-diol-17-one	11β-Hydroxyandrostenedione
Mineralocorticoid and mineralocorticoid precursor metabolites				
26	THDOC	Tetrahydro-11-deoxycorticosterone	5β-Pregnane-3α,21-diol-20-one	11-Deoxycorticosterone
27	5α-THDOC	5α-Tetrahydro-11-deoxycorticosterone	5α-Pregnane-3α,21-diol-20-one	11-Deoxycorticosterone
28	THA	Tetrahydro-11-dehydrocorticosterone	5β-Pregnane-3α,21-diol-11,20-dione	11-Dehydrocorticosterone
29	5α-THA	5α-Tetrahydro-11-dehydrocorticosterone	5α-Pregnane-3α,21-diol-11,20-dione	11-Dehydrocorticosterone
30	THB	Tetrahydrocorticosterone	5β-Pregnane-3α,11β,21-triol-20-one	Corticosterone
31	5α-THB	5α-Tetrahydrocorticosterone	5α-Pregnane-3α,11β,21-triol-20-one	Corticosterone
32	THAldo	3α5β-Tetrahydroaldosterone	5β-Pregnane-3α,11β,21-triol-20-one-18-al	Aldosterone

1.2. The incidentally discovered adrenal mass and mild autonomous cortisol secretion

Adrenal tumours are commonly discovered incidentally on cross-sectional abdominal imaging performed for reasons other than adrenal mass (adrenal incidentalomas). The incidence of adrenal tumours increased 10-fold in the last two decades, with most diagnosed in older adults. In any patient with a newly discovered adrenal mass determining whether the adrenal mass is malignant and whether the adrenal mass is

hormonally active is equally important to determine the best approach. The vast majority of these tumours arise from the adrenal cortex, are benign, and do not cause specific clinical symptoms. About half of benign adrenal tumours demonstrate evidence of hormone excess. Clinically overt autonomous cortisol secretion, also known as Cushing's syndrome (CS), is rare and typically presents with distinct clinical signs such as proximal myopathy and red stretchmarks, but also with less specific metabolically adverse consequences including type 2 diabetes, hypertension, and dyslipidaemia. Mild autonomous cortisol secretion (MACS) is far more common than CS, but patients usually lack characteristic clinical signs of CS. MACS is defined by the failure to suppress serum cortisol sufficiently after overnight administration of 1mg of dexamethasone in the 1mg-dexamethasone suppression test (1mg-DST).

1.2.1. *Clinical relevance*

Adrenal tumours are commonly discovered on cross-sectional abdominal imaging in up 5-7% of adults and 10% of over 70-year-olds (9). The incidence of adrenal tumours increased 10-fold in the last two decades, in parallel to the increase in the number of abdominal computed tomography (CT) and magnetic resonance imaging (MRI) studies (10). Most of the increase in incidence was due to a more frequent discovery of smaller adrenal adenomas in older adults >65 years old, whilst the number of large and malignant tumours remained the same (10). Adrenal tumours are seen almost equally in men (45%) and women (55%), with a median age of diagnosis of 62 years. Adrenal tumours are very uncommon in children, with only 1% of all adrenal tumours diagnosed in patients <18 years old (10).

1.2.2. *Aetiology*

Adrenal tumours can be broadly divided into 5 categories: 1) adrenocortical adenomas (ACA) and nodular hyperplasia, 2) other benign lesions (myelolipomas, cysts, haematomas, other), 3) adrenocortical carcinomas (ACC), 4) other malignant tumours (metastases, sarcomas, lymphoma), and 5) phaeochromocytomas.

Population-based data demonstrated that malignant adrenal tumours are diagnosed in 8.6% of all cases, with a majority representing adrenal metastases, and only 0.3% representing ACC (10). The distribution of pathologies is different in patients referred to endocrinology, where most patients with malignant tumours are diagnosed with ACC, and only a minority with other malignant tumours (11, 12). This is likely because patients with suspected metastasis or lymphoma are evaluated by other specialities, such as medical oncology, pulmonology, and urology. In a recent study of patients with adrenal metastases, only 30% of patients with adrenal metastases were evaluated by endocrinology (13). Similarly, only 10% of patients referred for adrenal biopsy are evaluated by an endocrinologist (14).

Most benign tumours are ACAs, representing 85% of all patients with adrenal tumours (10). ACAs demonstrate biochemical evidence of adrenal hormone excess in around 50-60% of cases, most commonly MACS (9). As demonstrated by a recent population-based study, only a minority of patients with adrenal tumours undergo optimal work-up for hormone excess, missing especially patients with MACS, but also likely patients with primary aldosteronism and milder forms of CS (10). If untreated, adrenal hormone excess is associated with increased cardiometabolic risk, multiple comorbidities, and increased mortality (15-17). Thus, determining whether the adrenal mass is malignant

and whether the adrenal mass is hormonally active is equally important to determine the best management.

Adrenocortical adenoma: ACAs represent the majority of incidentally discovered adrenal tumours in both the population setting (88%) (10), as well as in the endocrine clinic (81-88%) (11, 18, 19). At the time of diagnosis, the median tumour size of ACAs is 1.5-2.5 cm, with 95-98% being <4 cm in size (10, 15, 18). Bilateral ACAs are demonstrated in around 15% of patients. On imaging, around 60% of ACAs are lipid-rich, with unenhanced Hounsfield units (HU) on unenhanced CT <10, 25% with HU between 10 and 19, and 15% with HU >20. Autonomous cortisol secretion is diagnosed in up to 35-50% of patients (**Table 1.2**) (9, 10). Notably, ACAs with overt hormone excess are often diagnosed only after incidental discovery with adrenal mass, rather than upon presentation with features of CS or primary aldosteronism (11, 19, 20).

Table 1.2: Clinical, imaging, and biochemical presentation of adrenal tumours. Abbreviations: CAH: congenital adrenal hyperplasia; CS: Cushing's syndrome; MACS: mild autonomous cortisol secretion. Adapted from (21).

	Adrenocortical adenoma	**Other benign mass**	**Adrenocortical carcinoma**	**Other malignant mass**	**Phaeochro-mocytoma**
Prevalence					
Population	84%	7%	0.3%	8%	1%
Endocrine clinic	85-90%	3-7%	1-5%	1-3%	1-8%
Mode of discovery					
Incidental	85%	90%	40%	35%	60%
Cancer staging	7%	4%	<1%	50%	<1%
Symptoms:					
- Hormone secretion	7%	<1%	40%	<1% (adr. insuff.)	30%
- Mass effect	<1%	5%	15%	5%	<1%
Other	<1%	1%	5%	10%	10% (genetic screening)
Imaging					
Tumour size					
- Median	1.5-2.5 cm	2-3 cm	10 cm	3 cm	4-5 cm
- <4 cm (%)	95%	60-70%	1%	60%	45%
Tumour laterality	15-20% bilateral	5-10% bilateral	<0.1% bilateral	24-43% bilateral	5-10% bilateral
Tumour growth	<1 cm/ 12 months	<1 cm/ 12 months	>1 cm/ 3-6 months	>1 cm/ 3-6 months	<1 cm/ 12 months
Unenhanced computed tomography (Hounsfield units, HU)	HU <10: 50-60% HU10-20:20-30% HU >20: 10-20%	HU: variable HU <0: myelolipomas HU >100: calcifications	HU <10: 0% HU 10-20: 1-2% HU >20: 98-99%	HU <10: 0% HU 10-20: 1-4% HU >20: 96-98%	HU <10: 0% HU 10-20: 1-3% HU >20: 97-99%

Magnetic resonance imaging †		Variable (depending on aetiology)			
- Chemical shift	60-80%		0%	0%	0%
- No chemical shift	20-40%		100%	100%	100%
Adrenal hormone excess					
Hormonally inactive	50-60%	100%*	20-50% show no hormone excess during routine biochemical testing (only 5% with urine steroid metabolomics). Functioning tumours most commonly cause glucocorticoid and androgen excess (alone or in combination). Isolated aldosterone excess is extremely rare.	100%	5-10%
Glucocorticoid excess	30-50% MACS; 1-3% CS	/		/	/
Aldosterone excess	5-10%	/		/	/
Androgen excess	<0.1%	/		/	/
Catecholamine excess	/	/		/	90-95%
Other	Consider CAH in the case of bilateral masses	Consider CAH in large bilateral myelolipomas		Consider primary adrenal insufficiency if bilateral adrenal involvement	/

* Rarely, adrenal hormone excess can be detected in a patient with myelolipoma (autonomous cortisol secretion, primary hyperaldosteronism). In these situations, a concomitant adenoma or hyperplasia is usually diagnosed.
† Data on the accuracy of MRI in diagnosing malignancy and phaeochromocytoma is limited; definitions of chemical shift may vary between users. Considering these limitations, a clearly lipid-rich lesion (chemical shift present) excludes malignancy and phaeochromocytoma.

Myelolipomas and other benign adrenal masses: Adrenal myelolipomas are diagnosed in 3.3-6.2% of patients with adrenal incidentalomas (**Table 1.2**). Patients usually present with a unilateral adrenal myelolipoma, at a median size of around 2-2.5 cm, however, the size may range considerably between 0.5 and >15 cm (22). Bilateral myelolipomas occur in 5% of all patients, and in 20% of patients with large tumours >6 cm (22). Benign non-cortical adrenal tumours other than myelolipomas are rare, representing altogether 1-2%, and include ganglioneuromas, cysts, haemangiomas, lymphangiomas, and schwannomas (10, 11, 18, 19, 23, 24). Imaging characteristics of these tumours vary, and diagnosis is frequently made on histology after adrenalectomy for a suspicious mass.

Phaeochromocytoma: Phaeochromocytomas represent 1.1% of patients with adrenal tumours in a population, and 4-8.5% of patients evaluated in the endocrine setting (**Table 1.2**) (10-12). Only 27% of patients are diagnosed with phaeochromocytomas

based on evaluation for symptoms of catecholamine excess, with the majority discovered incidentally (61%) or based on genetic case detection testing (12%) (25). When diagnosed incidentally or based on symptoms, phaeochromocytomas are usually large tumours with a median size of 4-5 cm, and bilateral tumours in 4-10% of cases (25). However, when diagnosed based on case detection imaging in those with known genetic predisposition, phaeochromocytomas are usually smaller, and more likely to be bilateral (25). Phaeochromocytomas usually demonstrate HU>20 on unenhanced CT scans (92%), with only 7.5% presenting HU between 10-20, and 0.5% HU of exactly 10. No phaeochromocytomas have been reported to have HU <10 (20, 25-27). Around 4% of phaeochromocytomas may be biochemically silent with normal testing for catecholamine excess (25), either due to lack of catecholamine secretion, or when detected at a smaller size with catecholamine secretion under the standard of care cut-off for measurements.

Adrenocortical carcinoma: ACCs are rare malignant adrenal tumours representing 0.3% of all adrenal tumours and 3.6% of malignant adrenal tumours in a population setting (10). However, ACC is the most common adrenal malignancy evaluated in the endocrine clinic, representing around 5% of patients seen by an endocrinologist (**Table 1.2**) (18). ACCs are discovered incidentally in 42-44% of cases (18, 20), though the subsequent work-up for hormonal excess is frequently abnormal (18). ACC presents as a unilateral mass, with most ACCs being large at the time of discovery, with a median size of 10 cm (18, 20). On imaging, ACCs are either heterogeneous tumours or demonstrate HU >20 on unenhanced CT, with a median of 35 HU (18, 20). Only 2% of ACCs are discovered at tumour size <4 cm and only 1% have HU between 10 and 20 on unenhanced CT scans (18).

Adrenal metastasis or other malignant mass: Adrenal metastasis is the most common aetiology of a malignant adrenal mass, representing 7.5% of all adrenal tumours and 86% of all malignant adrenal tumours in a population (10). However, adrenal metastases are uncommon in the endocrine clinic, with only 1 in 4 patients with adrenal metastasis undergoing endocrine work-up (10, 13, 14). Whilst the majority of adrenal metastases are discovered during imaging for cancer staging, 36% are detected incidentally (13). Patients usually present with a median mass size of 3 cm, ranging between 0.5 and 20 cm) (**Table 1.2**) (13). Bilateral adrenal metastases are common, with 24% of patients demonstrating bilateral disease at the time of initial diagnosis, and 43% of patients developing bilateral disease during follow-up (13). Preclinical or symptomatic primary adrenal insufficiency can be diagnosed in 12% of patients with bilateral adrenal metastases (13). Other very rare adrenal malignancies include lymphomas, sarcomas, and neuroblastomas (10, 18, 20).

1.2.3. *Evaluation: diagnosis of adrenal malignancy*

Diagnosis of adrenal malignancy is based on pertinent history, imaging with secondary testing including urine and serum steroid profiling, rarely, adrenal biopsy, or diagnostic adrenalectomy (**Table 1.2**).

Mode of discovery: The circumstances around the discovery of the adrenal mass could help estimate the risk of malignancy. Only 3.3% of all adrenal incidentalomas are malignant, compared with 43% of adrenal tumours discovered on cancer staging imaging in those with a history of extra-adrenal malignancy (10). Of all patients discovered with an adrenal mass, only 3% are diagnosed based on symptoms of overt

hormone excess (10). Circumstances around the discovery of the adrenal mass should be interpreted along with imaging characteristics of the adrenal mass (**Table 1.2**).

Imaging characteristics: Unenhanced CT, contrast-enhanced CT with washout characteristics, and MRI with chemical shift analysis are the most used imaging techniques in the evaluation of adrenal tumours (28-30). ^{18}F-fluorodeoxyglucose positron emission tomography (FDG-PET) scan is usually reserved for patients with a history of extra-adrenal malignancy (28-30). In addition to characterisation of tumour size, tumour borders and heterogeneity of the adrenal mass, imaging characteristics of the adrenal mass provide valuable information in the diagnosis of malignant adrenal mass and phaeochromocytoma (21, 26, 27, 30). Briefly:

- *Tumour size and laterality*: The risk of malignancy is proportional to tumour size (~5% of adrenal tumours <2 cm; ~10% of adrenal tumours between 2 and 4 cm; ~35% of adrenal tumours >4 cm) (10, 20). ACC is almost always a unilateral adrenal mass, whilst 24-43% of adrenal metastases are bilateral (13, 20). As such, patients with bilateral adrenal masses are twice as likely to be malignant when compared to unilateral adrenal tumours (10).
- *Tumour growth*: ACCs typically have explosive growth over time; other malignant tumours also increase in size, but this is frequently difficult to assess due to concomitant therapies that may affect tumour growth and often short duration of follow-up due to adrenalectomy (31). ACAs can also increase in size over time, but the rate of tumour growth is much slower than ACC; smaller ACAs are more likely to grow during follow-up (15). Phaeochromocytomas grow slowly, around 3-5 mm/year (32, 33), though the data is scarce as adrenalectomy is the standard of care for any patient with phaeochromocytoma.

- *Computed tomography and magnetic resonance imaging*: Both unenhanced CT and MRI with chemical shift analysis assess lipid content within the adrenal mass. HU measurement <10 on unenhanced CT indicates a lipid-rich lesion. HU cut-off of >10 demonstrates a sensitivity of 100% and specificity of 33-72% to detect malignancy in patients with adrenal mass (30, 34). In other words, a homogeneous adrenal mass with HU <10 can be definitely diagnosed as benign. Chemical shift analysis on MRI demonstrated a sensitivity of 86-90% and specificity of 85% in diagnosing malignant adrenal masses, with most studies being small, and with some concern of user variability (30). As both unenhanced CT and MRI assess lipid content, in general, it is not useful to obtain both studies to characterise the adrenal mass. CT washout analysis has suboptimal performance for diagnosing malignancy (30, 35, 36), and is not recommended as second-line testing of adrenal mass (28).
- *^{18}F- fluorodeoxyglucose positron emission tomography imaging*: FDG-PET has moderate-to-high accuracy in detecting adrenal malignancy (sensitivity of 82-100% and specificity of 86-96%) (30, 34, 37). False positives may occur in functioning ACAs and false negative results may occur in small metastases and when significant necrosis is present (34). Phaeochromocytomas are FDG-avid, however, FDG-PET in patients with phaeochromocytomas is not usually indicated unless metastatic or multifocal disease is suspected.

Steroid profiling: Both serum and urine steroid profiling can be valuable in the diagnostic work-up of adrenal masses. Steroid profiling has been investigated in the diagnosis of cortisol and aldosterone excess, as well as in the diagnosis of ACC (18, 38-40). Urine steroid profiling has been recently prospectively validated in a large multicentre study of 2017 patients demonstrating a high accuracy in diagnosing ACC,

especially when combined with imaging characteristics (tumour size >4 cm and HU>20 on unenhanced CT) (18). The basis of steroid profiling is that ACCs secrete steroid precursors in increased amounts, sometimes as high as 10-40 times higher than in other adrenal tumours (41). Thus, even “non-functioning” ACC on standard of care testing will be detected through urine steroid profiling, unless the tumour has lost its capacity for steroidogenesis, which is a very rare occurrence (**Table 1.2**) (18).

Adrenal biopsy: Adrenal biopsy is rarely needed in the diagnostic work-up of an adrenal mass. It may be useful in indeterminate non-functioning adrenal masses where the results of the biopsy will change management, such as patients suspected to have malignant adrenal tumours other than ACC (adrenal metastasis, sarcoma, lymphoma) or an infectious aetiology of the adrenal mass (fungal, tuberculosis) (28, 42). Adrenal biopsy has poor accuracy in diagnosing ACC and may present with a higher risk of needle track seeding and a worse prognosis, thus non-invasive diagnosis of ACC is key.

1.2.4. *Evaluation: diagnosis of adrenal hormone excess*

Clinical evaluation: The first step in the assessment of possible hormone excess in patients with adrenal incidentaloma is obtaining a detailed medical history, including family history and current medications that can affect the hormonal tests (**Figure 1.4**). The clinical course and combination of comorbidities should be investigated as well, as this may be a clue to hormone excess (**Table 1.3**).

Figure 1.4: Adrenal incidentaloma evaluation: clinical and hormonal assessment. Abbreviations: 1mg-DST, 1mg overnight dexamethasone suppression test; ACC, adrenocortical cancer; ACTH, adrenocorticotropic hormone; DHEAS, dehydroepiandrosterone sulfate. Adapted from (21).

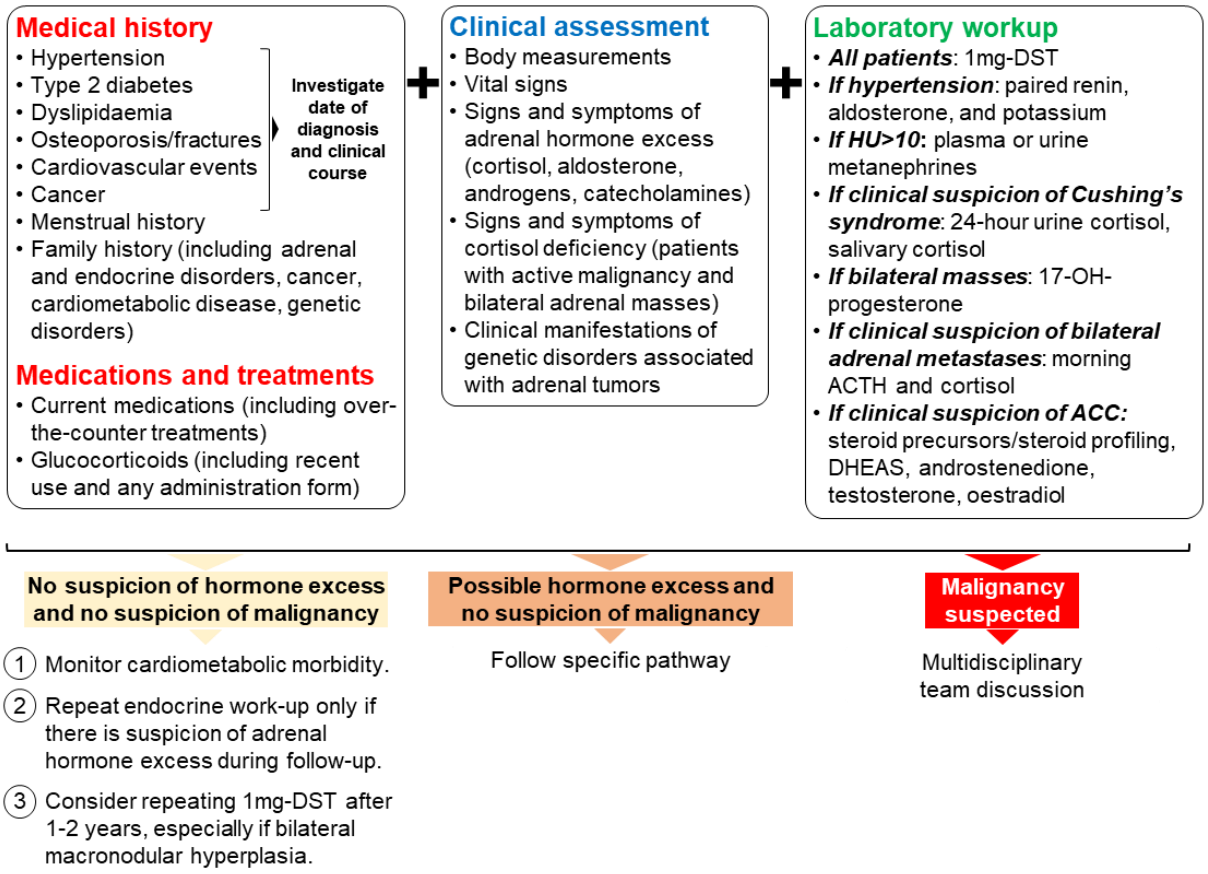

Table 1.3: Clinical manifestations of adrenal hormone excess. Abbreviations: MACS: mild autonomous cortisol secretion. Adapted from (21).

Hormone excess		General considerations	Clinical manifestations
Autonomous cortisol secretion	**MACS**	• Diagnosed in up to 50% of patients with incidentalomas. • Absence of stigmata of overt autonomous cortisol secretion (Cushing's syndrome). • Associated with frailty and increased cardiometabolic morbidity.	• Metabolic syndrome: hyperglycaemia; hypertension; dyslipidaemia; obesity. • Cardiovascular events. • Atrial fibrillation and other arrhythmias. • Osteoporosis and fragility fractures (high prevalence of asymptomatic vertebral fractures). • Anxiety/depression. • Chronic kidney disease. • Frailty
	Cushing's syndrome	• Rare (<3-5% of patients with adrenal adenomas). • Up to 50% are diagnosed during adrenal incidentaloma work-up. • Requires prompt recognition and work-up to confirm the diagnosis and offer treatment. • If untreated, it is associated with high morbidity and mortality. • Concomitant adrenal androgen excess indicates adrenocortical carcinoma.	• Stigmata of clinically overt autonomous cortisol secretion: facial plethora; dorsocervical fat pad; supraclavicular fat pads; muscle loss, proximal myopathy, and muscle weakness; easy bruising; red stretchmarks. • Increased mortality risk, mainly driven by cardiovascular and thromboembolic events. • Metabolic syndrome: hyperglycaemia; hypertension; dyslipidaemia; obesity. • Osteoporosis and fragility fractures. • Immunosuppression, susceptibility to infections. • Depression and other psychiatric disorders, insomnia, memory loss, irritability, panic attacks. • Amenorrhoea and reduced fertility. • Heart failure.
Aldosterone excess		• Incidentalomas causing primary aldosteronism are almost invariably benign. • Hypokalaemia is not required to make the diagnosis. • Associated with increased cardiometabolic risk. • Concomitant autonomous cortisol secretion (usually MACS) is common.	• Hypertension. * • Hypokalaemia (10-40% of cases). • Symptoms and complications related to hypokalaemia: polyuria and nocturia; fatigue and weakness; muscle cramps; constipation. • Cardiovascular and cerebrovascular events. • Chronic kidney disease. • Heart failure and atrial fibrillation. • Left ventricular hypertrophy. • Metabolic syndrome: hyperglycaemia; obesity. • Osteoporosis. • Depression.
Androgen excess		• Adrenal androgen excess typically indicates adrenocortical carcinoma. Androgen-producing adenomas are extremely rare. • Androgen and cortisol co-secretion (both MACS and Cushing's syndrome) is common in adrenocortical carcinoma.	Women can present with: • Hirsutism. • Oily skin and acne. • Hair loss. • Changes in libido. • Menstrual irregularities. • Metabolic syndrome (chronic androgen excess).
Catecholamine excess		• Phaeochromocytomas are increasingly diagnosed incidentally (60%). • Most patients do not have the classic "spell" symptoms. • Germline pathogenic variants are common (up to 40-50%). Syndromic associations can be a clue to the diagnosis.	• Hypertension in up to 90% of cases (paroxysmal in 50%). • Classic triad ("spell"): headaches, sweating, palpitations. • Pallor, nausea, tremor, anxiety. • Postural hypotension. • Supraventricular tachycardia. • Myocardial ischaemia/infarction. • Takotsubo cardiomyopathy and heart failure. • Hypertensive crisis triggered by stressors (e.g., surgery, colonoscopy, some medications).
* The spectrum of biochemically proven primary aldosteronism includes also subjects with normal blood pressure. Primary aldosteronism should be suspected in young normotensive subjects with unexplained hypokalaemia.			

For example, a recent diagnosis of dyslipidaemia and hypertension in a previously healthy 40-year-old individual, even if well-controlled with medical treatment, may be more relevant than a diagnosis of type 2 diabetes 10 years before the incidental finding of the adrenal mass. Questions regarding the current and recent use of glucocorticoids, which can both impact laboratory investigations and be responsible for iatrogenic CS, are a key part of the initial assessment of adrenal incidentaloma. A minority of adrenal tumours can be manifestations of numerous genetic syndromes – up to 5-10% of ACC, 25% of bilateral macronodular hyperplasia, and 40% of catecholamine-secreting tumour cases harbour germline mutations (43-45). Therefore, it is important to evaluate for possible syndromic associations that can be clues to an underlying genetic disorder during the physical examination and when collecting the medical history (43-55). Other elements that can point towards a germline pathogenic variant are young age at the time of diagnosis, familial occurrence, and bilateral adrenal masses.

Laboratory assessment: MACS is the most common hormonal abnormality observed in adrenal incidentalomas; thus, all patients should undergo a 1mg-DST (**Table 1.4**) (28, 29). The rest of the initial laboratory assessment should be personalised based on clinical and imaging characteristics: 1) if there is a history of hypertension or unexplained hypokalemia, primary aldosteronism should be ruled out by paired morning plasma renin and aldosterone measurement (56, 57); 2) if unenhanced CT HU are >10, work-up for catecholamine excess with plasma or urine metanephrines should be performed (58); 3) if ACC is suspected, elevated sex hormones and steroid precursors can noninvasively confirm this diagnosis before adrenalectomy (28) (**Table 1.4**). Additional testing may be required in patients with abnormal 1mg-DST and signs suggestive of CS (**Table 1.4**). In patients with bilateral adrenal tumours (adenomas or

myelolipomas), congenital adrenal hyperplasia should be considered. Finally, in patients with high suspicion of primary adrenal insufficiency due to bilateral infiltrative disease (bilateral adrenal metastases), morning ACTH and cortisol should be measured (**Table 1.4**) (28).

Table 1.4: Hormonal work-up in patients with adrenal tumours. Abbreviations: ACTH: adrenocorticotrophic hormone; CRH: corticotropin releasing hormone; DRC: direct renin concentration; DST: dexamethasone suppression test; CYP3A4: cytochrome P450 3A4; DHEAS: dehydroepiandrosterone sulfate; MACS: mild autonomous cortisol secretion; NSAIDs: non-steroidal anti-inflammatory drugs; OCP: oral contraceptive pill; PRA: plasma renin activity; SGLT2: sodium-glucose co-transporter-2. Adapted from (21).

Adrenal hormone abnormality	**Indication for testing**	**First-line testing**	**Second-line or confirmatory testing**	**Other considerations and remarks**
Autonomous cortisol secretion	Anyone with adrenal mass, regardless of symptoms	1mg-DST. *Abnormal result:* serum cortisol >50 nmol/L (1.8 µg/dL). *Possible causes of false-positive results:* • Oral oestrogens (e.g., OCP) • CYP3A4 inducers. • Exogenous glucocorticoids (assay interference). • Uncontrolled hyperglycaemia. • Alcoholism. • Psychiatric disorders. • Morbid obesity. • Pregnancy. • Chronic active hepatitis. • Kidney failure. • Older age. • Dementia.	• ACTH. • DHEAS. • 24h urine free cortisol (if Cushing's syndrome is suspected). • Salivary cortisol (if Cushing's syndrome is suspected). • In selected cases: repeat 1 mg-DST; perform 8 mg-DST; two-day, low-dose DST (Liddle's test); CRH test.	• ACTH-independent autonomous cortisol secretion must be confirmed before considering adrenal surgery. • Patients with adrenal hypercortisolism have abnormal DST, low ACTH, and DHEAS. • 24h urine free cortisol is usually normal in MACS. • The accuracy of salivary cortisol in MACS is low.
Aldosterone excess	Anyone with hypertension, with or without spontaneous hypokalaemia	Morning aldosterone + renin (DRC or PRA). *Abnormal result:* usually aldosterone >10 ng/dl and suppressed renin (DRC or PRA). *Possible causes of false-positive results:* * • β-blockers. • α-methyldopa • NSAIDs. • Oral oestrogens (renin measured as DRC). • Testing during the luteal phase (women of reproductive age). • Impaired renal function with hyperkalaemia. *Possible causes of false-negative results:* * • Mineralocorticoid receptor antagonists. • Diuretics. • Dihydropyridine calcium channel blockers.	Unnecessary if positive first-line test and spontaneous hypokalaemia. Otherwise: salt loading test, saline infusion test, captopril challenge or fludrocortisone test.	• Patients with confirmed primary aldosteronism will need subtype evaluation with imaging and adrenal vein sampling. • Imaging finding of adrenal mass is accurate only in 60% of cases in subtype determination. • Cortisol co-secretion is highly prevalent in primary aldosteronism (abnormal 1mg-DST is found in up to 22% of patients). †

		• ACE-inhibitors. • Angiotensin II receptor blockers. • SSRIs. • SGLT2-inhibitors.		
Catecholamine excess	Anyone with indeterminate adrenal mass (HU≥10), with or without symptoms	Plasma or 24-hour urine metanephrines. *Abnormal result:* usually >2 X upper limit of normal. *Possible causes of false-positive results:* • Collection of plasma metanephrines under not controlled conditions. • Medications: tricyclic antidepressants; psychoactive agents; prochlorperazine; L-dopa; adrenergic receptor agonists; phenoxybenzamine. • Physical stress or illness: significant illness requiring hospitalisation; congestive heart failure; panic attacks; subarachnoid bleeding; obstructive sleep apnoea. • Withdrawal from alcohol, clonidine, and other drugs. *Possible causes of false-negative results:* small phaeochromocytomas (especially with a maximum diameter <2cm). ‡	• Usually not needed unless false-positive results are suspected. § • Urinary or plasma dopamine or plasma methoxytyramine is a possible add-on test to detect tumours with dopamine hypersecretion (increased risk of malignancy).	• 24-hour urine fractionated metanephrines have excellent sensitivity and specificity. • Plasma fractionated metanephrines have excellent sensitivity but suboptimal specificity if not collected appropriately. Fasting collection after 30' in the supine position and the use of age-adjusted upper limits of normal increase specificity. • In patients with suspected phaeochromocytoma, extra-adrenal disease and associated genetic predisposition need to be considered.
Suspected steroid precursor, androgen, or oestrogen excess	Anyone suspected to have adrenocortical carcinoma, with or without symptoms	DHEAS, progesterone, 17OH-progesterone, 17OH-pregnenolone, 11-deoxycortisol, androstenedione, testosterone (women), oestradiol (men, postmenopausal women). If available, consider multi-steroid profiling (urine, blood).		• Avoid adrenal biopsy. • Open adrenalectomy is usually recommended. • Experienced adrenal surgeon is key!
	Anyone with bilateral adenomas or myelolipomas should be evaluated for congenital adrenal hyperplasia	Early-morning 17OH-progesterone (to be collected during the early follicular phase in menstruating females).	ACTH-stimulation test for cortisol and 17-OH-progesterone.	Consider genetic testing.
Adrenal insufficiency	Anyone with indeterminate bilateral masses likely to be	Morning ACTH and cortisol. If electrolyte abnormalities, test for aldosterone deficiency (paired aldosterone and renin).	Potential need for additional dynamic testing such as ACTH stimulation.	

	adrenal metastases or bilateral infiltration of other causes			

* Routine washout from potential interfering medications when assessing a patient with a newly diagnosed adrenal mass is not recommended. The main issue with interfering medications is false-negative results for mild or optimally treated primary aldosteronism cases (mostly due to non-suppressed renin). Case detection testing can be done even in patients treated with mineralocorticoid receptor antagonists, as patients with hypertension are usually treated with doses lower than those required to fully block the mineralocorticoid receptor. A suppressed renin in this scenario (especially if hypokalaemia is present) makes the diagnosis of primary aldosteronism very likely. If re-testing is required, this should be carried out in the morning, 2-4h after waking up. If it is safe to do so, interfering medications should be stopped for 2-4 weeks before testing. Alternative treatments that do not interfere with the test are verapamil, doxazosin, prazosin, terazosin, hydralazine, and moxonidine.

† Cortisol co-secretion is not only relevant from a cardiometabolic risk perspective; it may also affect the performance of adrenal vein sampling, the risk of developing adrenal insufficiency after unilateral adrenalectomy, and the rate of clinical success after surgery.

‡ Smaller catecholamine-secreting tumours may have negative metanephrine test results. This is relevant for smaller incidentalomas with HU>10 and especially for patients with known genetic disorders associated with phaeochromocytoma who undergo routine surveillance imaging for other manifestations of their disease. In such cases, it is therefore appropriate to re-test patients if the initial test was negative and the adrenal mass increases in size and/or the patient develops symptoms of catecholamine excess during follow-up.

§ Tricyclic antidepressants and other psychoactive agents should be tapered down and discontinued at least two weeks before re-testing. Selective serotonin reuptake inhibitors should not significantly affect the screening tests.

Laboratory assessment of autonomous cortisol secretion: 1mg-DST is the best initial test to diagnose MACS, which is suspected if serum cortisol is >50 nmol/L (1.8 mcg/dL) (**Table 1.4**) (28). The ESE-ENSAT guidelines on adrenal incidentalomas classify MACS possible or definitive based on the 1mg-DST serum cortisol (28):

- Possible MACS (MACS-1): 1mg-DST serum cortisol 50-138 nmol/L (1.8-5.0 µg/dL).
- Definitive MACS (MACS-2): 1mg-DST serum cortisol >138 nmol/L (5.0 mcg/dL).

The concomitant measurement of serum dexamethasone can inform about the bioavailability of the drug if false-positive results due to abnormal metabolism or absorption of the drug are suspected (59, 60) (**Table 1.4**). Additional tests, such as dehydroepiandrosterone sulfate (DHEAS) and adrenocorticotropic hormone (ACTH) can confirm the degree of autonomous cortisol secretion and ACTH independence. When CS is suspected, 24-hour urine cortisol and late-night salivary cortisol can be used to confirm the diagnosis (61). Notably, in patients with MACS, 24-hour urine cortisol and midnight salivary cortisol are frequently normal (62-67).

Laboratory assessment of aldosterone excess: Numerous antihypertensive classes and other medications can affect renin and aldosterone measurements, and this should be taken into consideration when interpreting the results (**Table 1.4**) (57, 68). However, discontinuing medications to screen for primary aldosteronism is routinely not recommended; this is more convenient for patients and results can often offer valuable information to guide future tests, if necessary (**Table 1.4**) (56, 57).

Laboratory assessment of catecholamine excess: Urinary or plasma metanephrines are the test of choice for case detection of phaeochromocytoma (69). Both tests have excellent diagnostic sensitivity (70), with plasma metanephrines having a slightly better performance if measured in controlled conditions (70, 71). Several medications,

diseases, and pre-analytical factors can lead to false-positive results and must be taken into consideration when testing patients (**Table 1.4**).

1.2.5. *Management of non-functioning benign adrenal masses*

Imaging follow-up: The European Society of Endocrinology Consensus Guidelines advise against repeated imaging in homogeneous adrenal incidentalomas <4cm with unenhanced CT tumour attenuation of HU ≤10 (28). This recommendation should also be extended to clearly benign adrenal diseases such as haemorrhage without an underlying solid component, simple cysts, and small myelolipomas. A prospective study in 2017 patients with newly diagnosed adrenal tumours (18) and two large retrospective studies in adrenal incidentalomas (72, 73) have recently confirmed that the risk of ACC in adrenal masses <4cm (regardless of HU) is extremely low. These studies also provide strong evidence that in addition to the tumour size cut-off of 4cm, the HU cut-off of 20 is a more specific cut-off to exclude ACC (18, 72, 73). A systematic review and meta-analysis investigating the natural history of adrenal incidentalomas found no cases of malignant transformation in over 2800 adrenal incidentalomas initially classified as benign adrenocortical adenomas (15).

In the case of non-functioning lipid-poor small adrenal incidentaloma, additional testing is warranted and may include 1) follow-up imaging in 3-12 months, 2) additional testing at the time of the diagnosis, such as alternative imaging or steroid profiling, or 3) adrenalectomy. Follow-up should be selected based on the pre-test probability of phaeochromocytoma, smaller ACC or other malignancy.

Another class of adrenal incidentalomas that may benefit from repeated imaging are larger myelolipomas. Despite being benign tumours, myelolipomas >3.5cm tend to

grow over time and carry a small risk of compressive symptoms and bleeding when the maximum diameter exceeds 6 cm (22).

Clinical and hormonal follow-up: Patients with benign non-functioning adrenal tumours (NFAT) carry a surprisingly high prevalence of cardiometabolic disease at the time of diagnosis (**Table 1.5**) and were also found to have an increased risk of incident pre-diabetes and type 2 diabetes during follow-up (9, 15, 74), which is possibly linked to a mild cortisol excess that is not picked up by the 1mg-DST (74, 75). Therefore, it is prudent to screen these patients for comorbid conditions and optimise their treatment as appropriate.

Table 1.5: Summary of the meta-analysis of the cardiometabolic comorbidities. This is reported as a pooled meta-analysis for all patients with non-functioning adrenal tumours (NFAT) and mild autonomous cortisol secretion (MACS). Adapted from (15).

	Pooled mean duration of follow-up (range) in months	Prevalence (%) of comorbidity at baseline	Proportion (%) of patients newly developing comorbidity	Proportion (%) of patients worsening their comorbidity
Hypertension				
NFAT	59.1 (12–277.2)	58.2 (CI 95% 55.0–61.4)	5.2 (CI 95% 3.7–6.9)	4.8 (CI 95% 2.9–7.0)
MACS	59.8 (12–204)	64.0 (CI 95% 58.2–69.6)	8.4 (CI 95% 4.6– 13.0)	13.4 (CI 95% 8.9–18.7)
Obesity/weight gain				
NFAT	52.4 (12–186)	38.8 (CI 95% 33.3–44.4)	8.7 (CI 95% 5.6–12.3)	-
MACS	53.2 (12–178)	41.0 (CI 95% 32.1–50.1)	21.0 (CI 95% 13.8–29.0)	-
Dyslipidaemia				
NFAT	66.8 (12–277.2)	33.8 (CI 95% 30.5–37.2)	6.9 (CI 95% 5.0–9.1)	4.3 (CI 95% 2.1–7.1)
MACS	59.8 (12–204)	34.1 (CI 95% 28.5–39.9)	5.7 (CI 95% 2.6–9.7)	6.8 (CI 95% 3.3–11.3)
Type 2 diabetes				
NFAT	68.1 (12–277.2)	14.4 (CI 95% 11.9–17.1)	5.3 (CI 95% 3.5–7.3)	0.0 (CI 95% 0.0–1.0)
MACS	62.8 (12–204)	28.1 (CI 95% 22.8–33.8)	4.7 (CI 95% 1.8–8.5)	9.2 (CI 95% 4.6–14.8)
Cardiovascular events				
NFAT	69.7 (18–320)	8.7 (CI 95% 6.5–11.2)	6.4 (CI 95% 4.5–8.6)	-
MACS	58.2 (12–320)	6.3 (CI 95% 3.1–10.3)	15.5 (CI 95% 10.7–20.8)	-

The risk of developing overt hormone excess in patients initially diagnosed with either NFAT or MACS during long-term follow-up is very low (<0.1%) (15); however, 4-22% of patients with adrenal incidentalomas initially classified as non-functioning can develop an abnormal 1mg-DST during follow-up (15, 62, 76-78). Therefore, a repeated 1mg-DST can be considered to detect possible MACS. It is otherwise not

recommended to routinely repeat hormonal investigations in patients with NFAT unless there is a clinical concern (e.g., onset or worsening of a comorbid condition potentially linked to cortisol excess or new unexplained hypokalaemia possibly pointing to previously unrecognised primary aldosteronism) (15, 28). Exceptions are small lipid-poor adrenal incidentalomas with a higher pre-test probability of phaeochromocytoma (e.g., known germline mutation associated with catecholamine-secreting tumours), where repeated biochemical testing is warranted in case of tumour growth, and repeated imaging should be considered if an increase in metanephrines is noted (**Table 1.4**).

1.2.6. *Primary adrenal Cushing's syndrome*

Clinically overt CS presents with characteristic signs and symptoms (facial plethora, dorsocervical fat pad, red stretchmarks, easy bruising, proximal myopathy) but also less specific ones (metabolic syndrome, centripetal obesity, acne, hirsutism, oligomenorrhea) (**Table 3**) (61, 79). Most cases of CS are due to excess adrenal stimulation by ACTH, either due to a pituitary tumour (Cushing's disease; 70-75%) or ectopic ACTH secretion (10-15%). However, in the remaining 10-15%, primary adrenal CS is the cause of disease, mostly due to a glucocorticoid-secreting ACA or, less frequently, an ACC (79). More rarely, primary adrenal CS is caused by primary bilateral macronodular adrenal hyperplasia (due to *AMRC5* mutations in 25-80% of cases) (43), or primary pigmented nodular adrenocortical disease due to inactivating *PRKAR1A* mutations (79). Mutations in the *PRKACA* gene have been identified as a frequent cause of autonomous cortisol secretion in unilateral adrenal adenomas due to somatic driver mutations, but also as a rare germline mutation underlying bilateral macronodular adrenal hyperplasia (80).

Management: Adrenalectomy is the therapy of choice in patients with an adrenal tumour causing CS (**Figure 1.5**). In any patient with an abnormal 1mg-DST, however, it is imperative to confirm that the autonomous cortisol secretion is ACTH-independent before referring the patients for adrenal surgery, as more than 30% of patients with Cushing's disease can have adrenal nodules that are either coincidental or secondary to chronic ACTH stimulation (81, 82).

Figure 1.5: Approach to adrenal adenoma with autonomous cortisol secretion. Abbreviations: 1mg-DST, 1mg overnight dexamethasone suppression test; 8mg-DST, 8mg overnight dexamethasone suppression test; ACTH, adrenocorticotropic hormone; *ARMC5*, Armadillo Repeat Containing 5 gene; DHEAS, dehydroepiandrosterone sulfate; MACS, mild autonomous cortisol secretion. Adapted from (21).

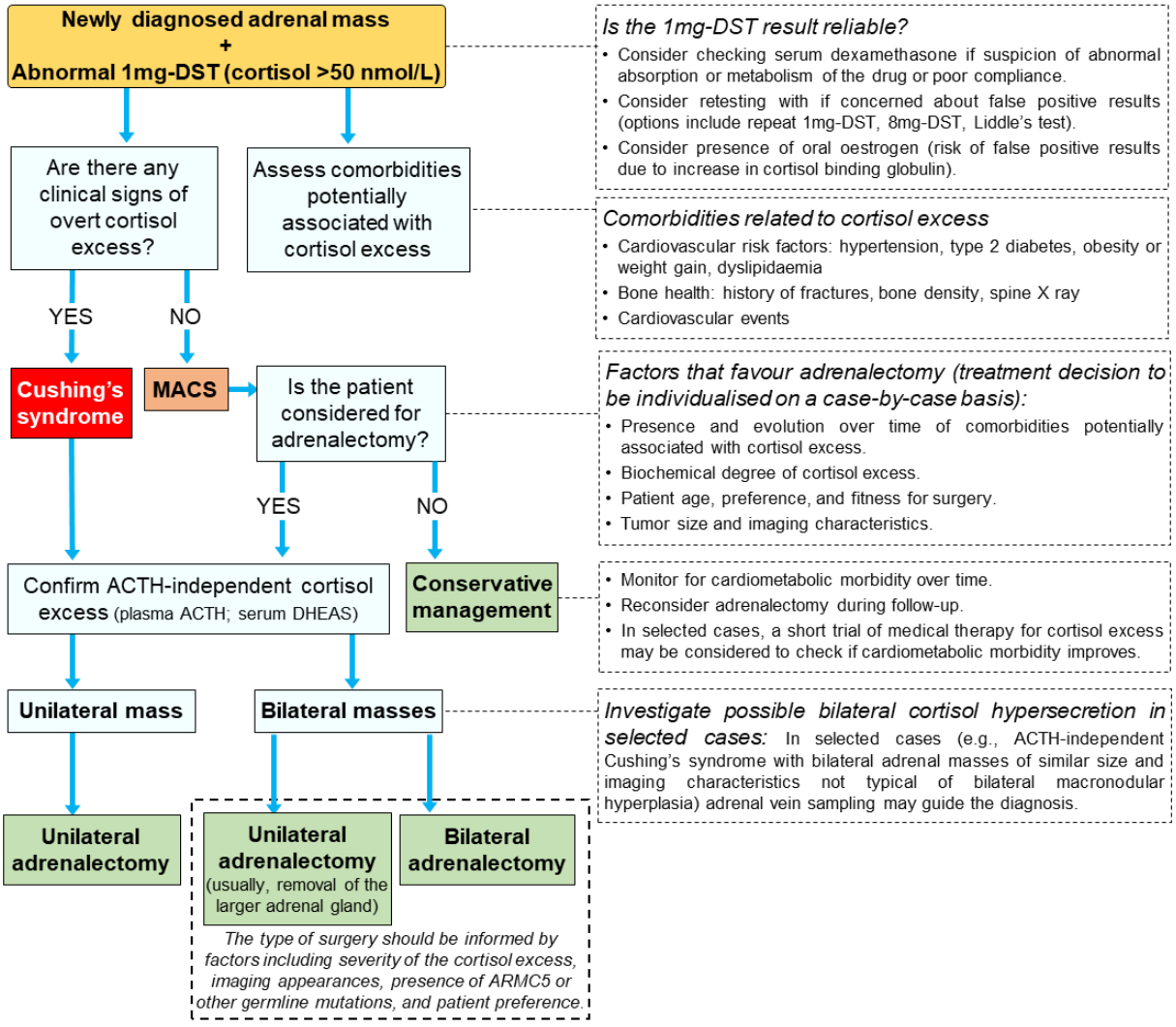

1.2.7. *Management of mild autonomous cortisol secretion*

MACS (adrenal incidentaloma + abnormal 1mg-DST + absent stigmata of CS) is the most common hormonal abnormality diagnosed in 30-50% of patients with adrenal mass (9, 28, 77). MACS is increasingly recognised as a clinically relevant cardiometabolic condition. A systematic review and meta-analysis of more than 4000 patients with benign adrenal incidentalomas found a prevalence of hypertension (64%), obesity (41%), dyslipidaemia (34%), type 2 diabetes (28%), and cardiovascular events (6%) in patients with MACS that is remarkably higher than expected for Western populations (**Table 1.5**) (15). These comorbidities were more likely to develop and worsen in patients with MACS as compared to those with NFAT. An increased risk of frailty, cardiovascular events, and mortality has also been reported in MACS (15, 17, 83-87). These patients have also been found to carry a significant risk of osteoporosis and (mostly asymptomatic) vertebral fractures (46-82%), as compared to 13-23% of patients with non-functioning adrenal incidentalomas (88-90). A population-based study in patients with adrenal incidentalomas that included a mix of patients with non-functioning adrenal adenomas and patients with MACS demonstrated an increased prevalence and incidence of fractures when compared to reference subjects from the same population (91).

Intervention vs. conservative management: The detection of MACS poses the therapeutic dilemma of whether to carefully observe and pursue medical management of metabolic comorbidities or to select adrenalectomy. A meta-analysis of small, mostly retrospective studies with heterogeneous definitions of MACS has shown that patients with MACS undergoing adrenalectomy experience an improvement in blood pressure, glycaemic control, dyslipidaemia, and a reduction of body weight (92). Another study

found that adrenalectomy reduces the risk of incident vertebral fractures in patients with MACS (93). Three small-scale studies have tested the potential use of medical treatment with mifepristone or metyrapone to reduce the cortisol excess in MACS and the authors reported beneficial effects on several metabolic parameters (94-96). These data suggest that MACS is a remediable cause of increased cardiometabolic risk; however, the evidence is mostly based on small, heterogeneous studies and randomised controlled trials comparing adrenalectomy to conservative management in this population are needed to conclusively answer this question. Until more evidence becomes available and reliable markers for metabolic risk stratification are identified, the therapeutic decision must be individualised considering clinical, biochemical, and imaging parameters, as well as the patient's preferences (**Figure 1.5**). A patient who is younger at the time of diagnosis, presenting with a higher degree of MACS, a more recent onset or exacerbation of potential cortisol-related comorbidities is more likely to benefit from adrenalectomy, both short and long-term. Plasma ACTH and serum DHEAS can help define the severity of the autonomous cortisol secretion (97-99), even though the first may not be reliable due to preanalytical challenges of sample collection and the latter is typically reduced in postmenopausal women who make up the vast majority of MACS cases (77). If it is decided to manage MACS conservatively, it is imperative to monitor the patient over time and optimise the treatment of the comorbidities potentially associated with cortisol excess, including hypertension, type 2 diabetes, dyslipidaemia, bone loss, and asymptomatic vertebral fractures. The patient's overall risk profile should be re-evaluated every 1-2 years and adrenalectomy re-discussed, if appropriate.

Management of bilateral adrenal masses: The high prevalence of autonomous cortisol secretion in patients with bilateral adrenal incidentalomas (more frequently MACS) poses diagnostic and therapeutic challenges when surgery is thought to be beneficial (**Figure 1.5**). Several authors have suggested the removal of the largest adrenal gland if the masses are unequal in size (28). This approach prevents the life-long need for glucocorticoid and mineralocorticoid replacement and is associated with an initial remission rate of up to 97%, including temporary postoperative adrenal insufficiency and improvement of comorbidities related to cortisol excess (100). Nonetheless, recurrence is observed in 20-70% of cases, and up to 33% of patients undergo contralateral adrenalectomy during follow-up to control the hypercortisolism (100, 101). Bilateral adrenalectomy as the initial treatment strategy can be considered in patients with ACTH-independent CS and bilateral adrenal enlargement of similar size (100). Adrenal venous sampling to identify the site of dominant cortisol secretion is a promising technique that has shown good performance but is not standardised (102, 103).

1.3. Project aims and objectives

The aim of this thesis was to investigate the clinical and metabolic consequences of autonomous cortisol secretion, with a particular focus on MACS, by answering the following questions:

What is the cardiometabolic burden of MACS?

To answer this question, the largest cohort to date of prospectively recruited persons with benign adrenal tumours and different degrees of autonomous cortisol secretion

was recruited, comprising 1305 subjects (EURINE-ACT study). The prevalence and severity of cardiometabolic disease (hypertension, type 2 diabetes, dyslipidaemia) in persons with MACS and CS were compared to those with NFAT.

What are the effects of MACS on steroid metabolism?

To answer this question, 24-hour urine steroid metabolite profiling by mass spectrometry was carried out on 1305 EURINE-ACT subjects with benign adrenal tumours. Linear regression and prototype-based supervised machine learning were applied to stratify persons according to the degree of autonomous cortisol secretion, comparing MACS and CS to NFAT.

What are the effects of MACS on global metabolism?

To answer this question, untargeted serum metabolome analysis by mass spectrometry was carried out in a representative sub-cohort of 291 EURINE-ACT subjects with benign adrenal tumours employing liquid chromatography-mass spectrometry. Prototype-based supervised machine learning was used to select the most relevant metabolites that change across the spectrum of autonomous cortisol secretion and inform the biological interpretation of the results.

Can a metabolic signature of increased cardiometabolic risk be identified in MACS?

To answer this question, persons with MACS were stratified based on clinical outcomes (hypertension, type 2 diabetes, presence of bilateral tumours) and linear regression and supervised machine learning applied to the 24-hour urine steroid metabolite profiling results.

CHAPTER 2

General methods

Content from this chapter has been published:

Steroid Metabolome Analysis in Disorders of Adrenal Steroid Biosynthesis and Metabolism.
*Storbeck KH, Schiffer L, Baranowski ES, Chortis V, **Prete A**, Barnard L, Gilligan LC, Taylor AE, Idkowiak J, Arlt W, Shackleton CHL.*
***Endocr Rev. 2019** Dec 1;40(6):1605-1625.*
doi: 10.1210/er.2018-00262.

Urine steroid metabolomics for the differential diagnosis of adrenal incidentalomas in the EURINE-ACT study: a prospective test validation study.
*Bancos I, Taylor AE, Chortis V, Sitch AJ, Jenkinson C, Davidge-Pitts CJ, Lang K, Tsagarakis S, Macech M, Riester A, Deutschbein T, Pupovac ID, Kienitz T, **Prete A**, Papathomas TG, Gilligan LC, Bancos C, Reimondo G, Haissaguerre M, Marina L, Grytaas MA, Sajwani A, Langton K, Ivison HE, Shackleton CHL, Erickson D, Asia M, Palimeri S, Kondracka A, Spyroglou A, Ronchi CL, Simunov B, Delivanis DA, Sutcliffe RP, Tsirou I, Bednarczuk T, Reincke M, Burger-Stritt S, Feelders RA, Canu L, Haak HR, Eisenhofer G, Dennedy MC, Ueland GA, Ivovic M, Tabarin A, Terzolo M, Quinkler M, Kastelan D, Fassnacht M, Beuschlein F, Ambroziak U, Vassiliadi DA, O'Reilly MW, Young WF Jr, Biehl M, Deeks JJ, Arlt W; ENSAT EURINE-ACT Investigators.*
Lancet Diabetes Endocrinol. 2020 Sep;8(9):773-781.
doi: 10.1016/S2213-8587(20)30218-7

2.1. Principles of urine steroid metabolite profiling by mass spectrometry

Steroid biosynthesis and metabolism are reflected by the serum steroid metabolome and, in even more detail, by the 24-hour urine steroid metabolome, which can provide valuable insights into alterations of steroid flow and output indicative of underlying conditions. Mass spectrometry-based steroid metabolome profiling has allowed for the identification of unique multi-steroid signatures associated with disorders of steroid biosynthesis and metabolism that can be used for personalised approaches to diagnosis, differential diagnosis, and prognostic prediction. In addition, steroid metabolome analysis has been used successfully as a discovery tool, for the identification of novel steroidogenic disorders and pathways as well as revealing insights into the pathophysiology of adrenal disease (104, 105).

Traditionally, gas chromatography-mass spectrometry (GC-MS) has been employed for comprehensive urine steroid metabolite profiling. Serum steroids are now increasingly analysed by high performance liquid chromatography-tandem mass spectrometry (HPLC-MS/MS), overtaking the use of immunoassays, which are recognised as compromised by cross-reactivity. In the routine clinical biochemistry context, HPLC-MS/MS is primarily used for single steroid analysis; however, recent years have seen the emergence of multi-steroid mass spectrometry analysis of serum, plasma, saliva, and urine steroid metabolites (75, 104-108).

Steroids all share a similar structure, with some sharing the same atomic composition and mass, and it is therefore important for the mass spectrometer to be able to distinguish between different steroids. This can be achieved in two ways. First, the measurement of the steroid analytes by the mass spectrometer is preceded by a chromatographic step during which the steroids are physically separated from each other, ensuring that each steroid reaches the mass spectrometer at a specific time. Secondly, the mass spectrometer can filter different steroids based on their mass to charge (m/z) ratios and in so doing distinguish between steroids of different mass.

2.1.1. *Basic principles of chromatography*

Chromatography allows for the separation of analytes by differential interaction with a mobile and a stationary phase. The mobile phase is usually either a gas or liquid in which the analyte is dissolved, whilst the stationary phase is a solid matrix held in place by a structure such as a column. During chromatography, the mobile phase passes over the stationary phase and the analytes interact with both phases; of note, different analytes have different degrees of interaction with the two phases. This results in

different retention times within the column, allowing for the separation of analytes. Analytes that interact more with the stationary phase are retained for longer, as compared to those with less interaction that are eluted earlier. This separation allows for each analyte to be delivered to the mass spectrometer at a given time.

Separation of analytes in the gas phase – gas chromatography: The instrument consists of an oven containing the chromatography column, coupled at the front end to an injection port where liquid samples are introduced and volatilised. GC for steroid analysis utilises long columns made of fused silica tubing coated internally with a permanently bonded non-polar stationary phase. An inert gas, usually helium, is used as the mobile phase at a constant flow rate. Derivatisation of steroids (commonly trimethylsilylation of hydroxyl groups and oxime formation of carbonyls) is required for GC-MS to ensure the stability and volatility of the analytes, as well as to promote reproducible fragmentation patterns (**Section 2.1.2**). The disadvantage of GC is that a mandatory deconjugation step is required before derivatisation to ensure the availability of reactive groups. This results in lengthy sample preparation times with are not conducive to high throughput analysis. Nonetheless, the resolving capacity of GC has ensured that this technique has remained the reference standard for urinary steroid profiling.

Separation of analytes in the liquid phase – high-performance liquid chromatography: HPLC makes use of one of two types of stationary phase chemistries, namely the normal phase or reverse phase. During normal phase chromatography, the stationary phase is polar and the mobile phase is non-polar, whilst the opposite is true of reverse phase chromatography. In general, reverse phase chromatography is preferred for steroid analysis due to the hydrophobic nature of steroids. The hydrophobic stationary

phase consists of a silica-based resin (in the form of small beads) to which hydrophobic alkyl chains are covalently bound. These chains typically range from 8 to 18 carbons in length, with C18 columns being a popular choice for steroid analysis. The steroids are introduced into the column in a polar aqueous mobile phase containing a low concentration of organic solvent. Being hydrophobic, the steroids favour interactions with the hydrophobic column and are therefore initially retained. Over time, the concentration of the organic solvent (often methanol or acetonitrile) in the mobile phase is increased leading to a decrease in the polarity. As the polarity decreases, the more polar steroids have increased interaction with the mobile phase and are therefore eluted first. Elution then continues in order of polarity as the amount of organic solvent is increased until the least polar steroids have sufficient interaction with the mobile phase to be eluted.

2.1.2. *Basic principles of mass spectrometry*

A mass spectrometer measures charged particles (ions) and consist of three basic components: an ion source; a mass analyser; a detector.

Ion source to ionise analytes in the gas phase: As the mass spectrometer only measures ions, the first step is to ionise the analytes and ensure the ions are in the gas phase. During GC, the analytes reaching the mass spectrometer are already in the gas phase and electron ionisation is typically used to bombard analytes with a stream of free electrons causing the analytes to fragment into smaller charged molecules. This fragmentation is reproducible and results in characteristic fragments with m/z values that serve as fingerprints of each analyte. During LC, analytes reach the mass spectrometer in a liquid mobile phase. The ion source, therefore, needs to

ionise the analytes and remove the liquid, which is commonly achieved by electrospray ionisation (ESI). During ESI, the column effluent flows through a high-voltage needle and exits as a fine spray of highly charged droplets. These droplets are directed towards an opening in the mass spectrometer by an electric field, whilst a stream of heated gas, often nitrogen, is directed at the droplets, causing the solvent to evaporate (desolvation). The reduction in droplet size causes the charge density on the droplet surface to rise until the surface tension of the solvent is exceeded by the electrostatic repulsion at which point a Coulombic explosion occurs. This causes the formation of significantly smaller more stable droplets, which deposit their charge onto the analytes as the solvent is further evaporated, a process which may include further Coulombic explosions. This leads to the formation of charged precursor ions that are free to enter the mass spectrometer. The electric field can also be switched between positive (ESI+) and negative (ESI-) modes to select for positively or negatively charged ions. Steroids, which are neutral, generate positive ions and are therefore analysed in positive mode. There are, however, exceptions to this rule such as conjugated steroids, oestrogens, and aldosterone, which ionise better in negative mode.

Mass analyser to sort and select ions based on m/z ratios: Ions each carry a single charge. As a result, steroids that differ in molecular mass will differ in their m/z ratio. The most commonly used mass analyser that sorts and shuttles selected ions to the detector is a quadrupole, consisting of four parallel cylindrical metal rods. Each rod sits at a corner of a square, creating an area in the middle of the square through which the ions can travel. An electric field is established between the rods by the superposition of both a direct current and radiofrequency voltage, with opposite rods being paired. Using this electric field, the ions that have entered the mass spectrometer are

accelerated through the quadrupole towards the detector. Different frequencies are then applied to oscillate the polarity between paired rods leading to the selection or filtering of ions of a selected m/z ratio. At the correct frequency, an ion of the selected m/z value will form a stable trajectory through the centre of the quadrupole, whilst other ions are ejected. Modern mass spectrometers can scan rapidly for different m/z ratios allowing the operator to select for specific m/z ranges or for multiple analyte-specific m/z ratios. GC-MS and LC-MS analysis of steroids more commonly utilise single quadrupole and triple quadrupole, respectively.

Detector: The ions that are selected by the mass analyser set off a cascade of electron emissions as they hit the detector. The first ion is accelerated towards a metal plate inducing the emission of multiple electrons, which are further accelerated to another plate causing the emission of additional electrons. This is repeated several times leading to an amplified stream of electrons being emitted and directed towards a metal anode which converts the input to an electric signal. The intensity of this signal is then recorded for each incident m/z value leading to the production of a mass spectrum. The readout from the mass spectrometer coupled with chromatography is a chromatogram, with individual peaks ideally representing individual steroids. The area under the peak is proportional to the concentration of the steroid thereby allowing for quantitation when compared to a calibration series.

2.1.3. *GC-MS and LC-MS/MS for steroid hormone analysis*

LC-MS/MS is widely available and increasingly used for steroid hormone analysis, whilst GC-MS remains a key discovery tool for the comprehensive analysis of the steroid metabolome (**Figure 2.1**).

Figure 2.1: Overview of GC-MS and LC-MS/MS for steroid hormone analysis.

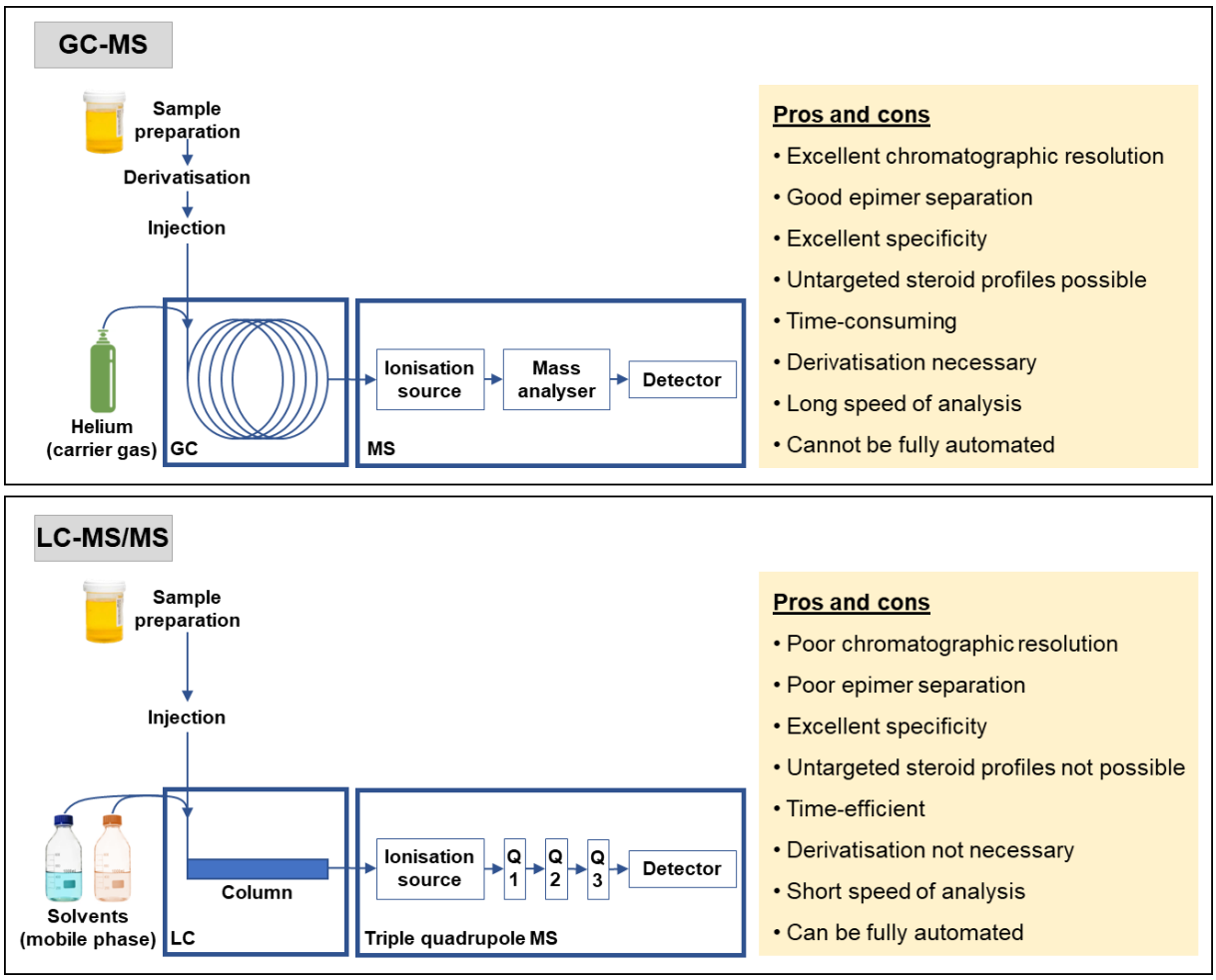

GC-MS is time-consuming and requires additional steps for sample preparation including hydrolysis of conjugates and derivatisation. Nonetheless, GC-MS can be utilised in comprehensive and targeted (selected ion) mode (109); a comprehensive (full scan) GC-MS chromatogram contains all steroids excreted and the dataset can be searched for any required analyte. This is not possible with LC-MS/MS, which has a worse chromatographic resolution because of the need for shorter run times. Thus, GC-MS remains a crucial asset for the discovery of new steroid metabolic pathways, whilst LC-MS/MS has the potential of translating steroid profiling to routine clinical use.

2.2. Principles of untargeted serum and plasma metabolome profiling by ultra-high performance liquid chromatography-mass spectrometry

Metabolic profiling (or metabolomics) is the identification and quantification of the small molecules (usually smaller than 1,500 Da) constituting the metabolome. Metabolites include amino acids, organic acids, nucleotides, lipids, amines, sugars, vitamins, hormones, etc., which play essential roles in biological systems. Therefore, metabolomics can provide invaluable insights into the pathophysiology of human diseases and biomarker discovery (110). Metabolomics can be targeted or untargeted; the first is usually deductive and allows for the accurate quantification of predefined metabolites (e.g., urine steroid metabolite profiling), whilst the second tends to be inductive and aimed at knowledge discovery by large-scale metabolic profiling (**Figure 2.2**).

Figure 2.2: Overview of omics. The branches of omics aim at the collective characterisation and quantification of molecules that translate into the phenotype of an organism, from the genome to the metabolome. The interaction between the genome and the environment (e.g., age, sex, diet, physical activity), as well as disease states, affects the phenotype and is reflected by changes in the metabolome, resulting in a "metabolic fingerprint".

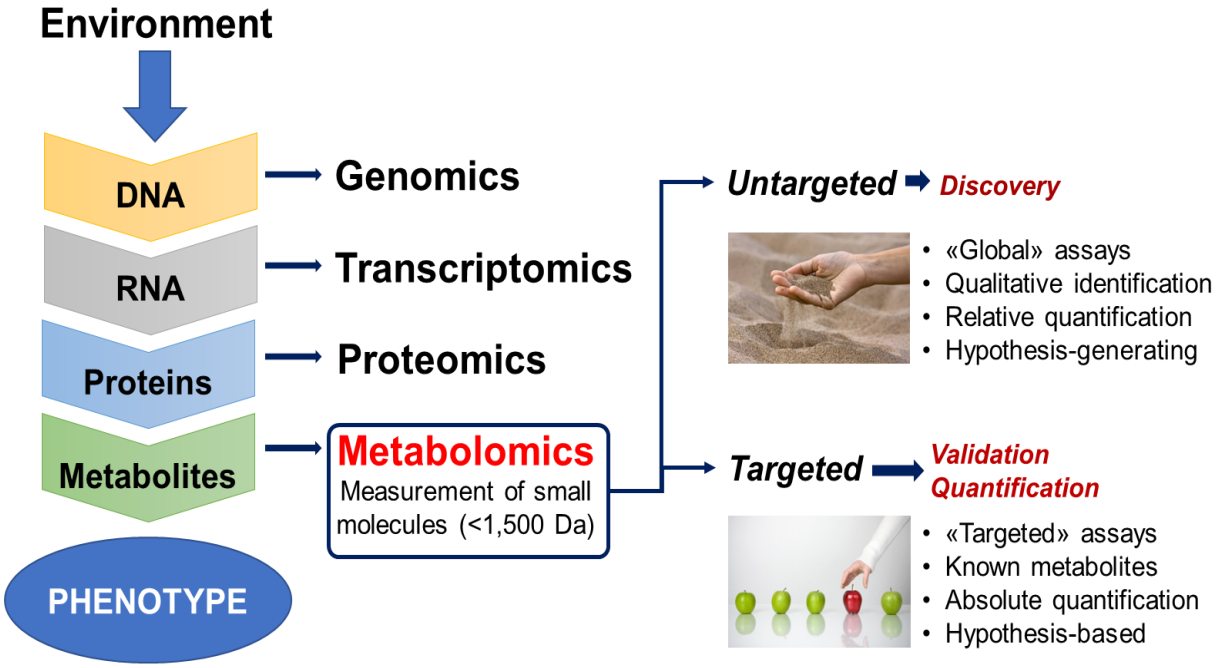

Mass spectrometry and nuclear magnetic resonance spectroscopy are the most used platforms for metabolic profiling, and for untargeted metabolomics multiple analytical platforms are typically needed to increase the number of metabolites detected, which is usually in the thousands (110). Serum and plasma are biofluids commonly used for untargeted metabolomics since their collection is minimally invasive and the circulating metabolome incorporates metabolic processes of different parts of the body.

The workflow of serum and plasma untargeted metabolome profiling by ultra-high performance liquid chromatography-mass spectrometry (UHPLC-MS) includes the following steps (110, 111):

1. Experimental design: Because of the variability of the metabolome in the context of normal physiology and environmental factors, medium-to-large numbers of samples are typically required to have more confidence that the changes observed in the metabolome are related to the outcomes of interest (e.g., a disease state, drug efficacy, or lifestyle changes) and reduce the false discovery rate.

2. Sample collection and storage: The experimental design should include protocols for standardised sample collection. Because of the intrinsic variability of the metabolome, it is crucial to minimise as much as possible other sources of variability, for example collecting different biofluids (serum, plasma), using different anticoagulants for plasma separation (lithium heparin is the preferred anticoagulant for large-scale metabolic profiling), collecting biofluids at different times of the day or not in the fasting state. Immediately after collection, samples should be frozen and stored at -80°C until analysed. Furthermore, multiple thaw/freeze cycles should be avoided to minimise the risk of sample degradation.

3. Sample preparation for UHPLC-MS: Sample preparation involves steps such as deproteinisation, lyophilisation and reconstitution in an aqueous/organic solvent mixture to remove high-molecular-weight molecules. Sample preparation on ice is recommended to decrease enzyme activity in plasma or serum and minimise the risk of sample degradation. For further details see (110, 111).

4. Data acquisition by UHPLC-MS (usually using multiple analytical platforms): In a typical application of untargeted metabolome profiling by UHPLC-MS, 2,000-7,000 features are detected, with a greater number detected in electrospray positive rather than electrospray negative ion mode. When analysing samples and interpreting untargeted metabolome profiling data, it is important to:

- Avoid systematic bias (e.g., injection order matching sample preparation order): the order of each analytical run is assigned randomly but the composition of each batch should be representative of the overall study population.
- Ensure reproducibility: quality control samples need to be analysed throughout an analytical run to assess the quality of the data and guarantee reproducibility for each metabolite measured.

5. Data pre-processing: It involves multiple stages (110, 111):

- Deconvolution, peak picking, and peak assignment: raw data (chromatograms) are pre-processed and structured in a format (relative concentrations) suitable for analysis. A range of software is available to ensure that the same metabolic feature is aligned and identified across multiple samples.
- Signal drift, batch effect correction, and quality assurance: if a metabolite does not pass quality assurance when compared to quality control samples, it is disregarded.

- Metabolite identification: it is important to make a distinction between metabolic feature and metabolite: a metabolic feature corresponds to a chromatographic peak with associated retention time and unique m/z. A metabolite can correspond to multiple metabolic features; therefore, the number of metabolic features is higher than the number of actual metabolites present in the sample. Furthermore, there are chromatographic peaks that are not identified because of the partial knowledge of the metabolome. The inability to definitively identify all metabolic features in a sample is one of the main limitations of untargeted metabolomics.

6. Data analysis and biological interpretation: A variety of methods can be used to analyse large-scale metabolome profiling results. Because of the wealth of information generated by this approach, machine learning is an attractive method to recognise intrinsic patterns in data and inform underlying metabolic processes (111). In **Chapter 5** the application of supervised machine learning to untargeted serum metabolomics data of persons with benign adrenal tumours and different degrees of autonomous cortisol secretion is presented.

2.3. Principles of machine learning

Machine learning is a series of computer programs designed to recognise intrinsic patterns in data. Machine learning is designed to perform complex tasks, including handling large amounts of data or variables, as well as processing changing data, i.e., the programs regularly adapt based on new information. Broadly, machine learning can be used for the following purposes (**Figure 2.3**):

- Clustering (unsupervised learning): it answers the question “are there intrinsic differences within the data leading to natural clusters?”.
- Classification (supervised learning): it answers the question “can the class a sample belongs to be predicted, provided that there are discrete classes in the data?”.
- Regression (supervised learning): it answers the question “can data be used to extrapolate and predict a continuous variable?”.

Figure 2.3: Overview of machine learning algorithms. Unsupervised machine learning should be considered when the aim is to explore data without a specific goal, the information contained in the data is unknown, or the aim is to reduce the dimensions of the data. Supervised machine learning takes a known set of input data (training set) and known responses to the data (output) and trains a model to generate predictions for the response to new input data. Supervised models “learn” from the data they are exposed to – the more data are used, the more robust and generalisable the model will be.

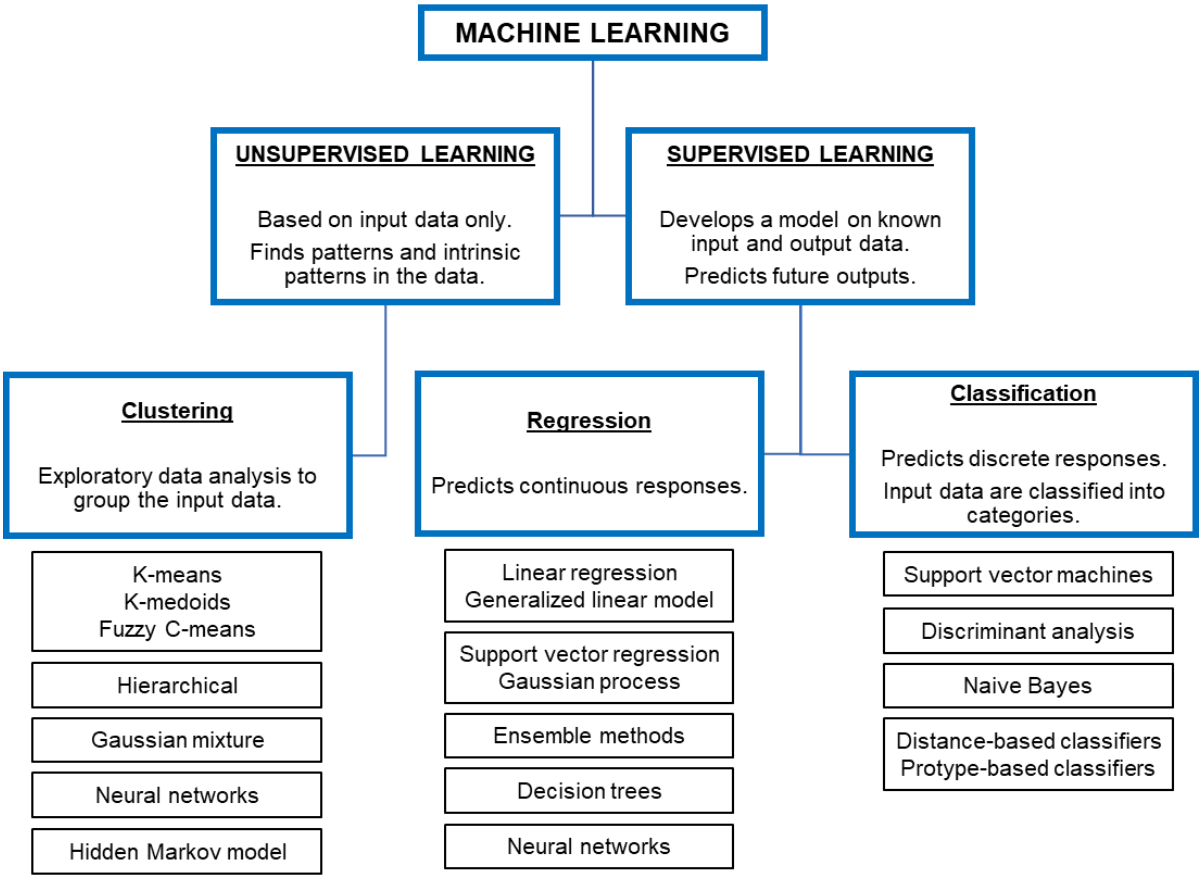

The choice of the most appropriate method depends on several considerations, including the answer to the following questions:

- What is the question machine learning is set to answer?

- What are the intrinsic properties of the population studied and of the data used?
- How many groups are to be compared?
- How many features (i.e., individual independent variables) will be used?
- What is the desired output of the model?
- What model characteristics are more desirable – speed of training, memory usage, predictive accuracy, transparency (white box vs. black box models, i.e., how easy it is to understand why a model made its predictions)?

The following section will only focus on supervised machine learning algorithms known as classifiers, which categorise data into a set of classes. More specifically, prototype-based supervised classifiers will be discussed since the algorithms used in **Chapters 4 and 5** for the analysis of the steroid and untargeted metabolome data belong to this category. For a comprehensive overview of the topic please refer to (112).

2.3.1. *Distance-based classifiers*

The basis of distance-based classifiers is the comparison of distances (or dissimilarities) of observations with a set of labelled reference data points. Distance-based models are intuitive, flexible, and transparent, meaning that the model is accountable in terms of how it makes its decisions (open box models) (112).

k-Nearest neighbour (kNN) classifier: One of the most popular and simple distance-based classifiers. kNN assumes that objects near to each other are similar and categorises objects based on the classes of their nearest neighbours. This approach can be complex for large datasets, computationally expensive, characterised by slower prediction speed, and highly affected by outliers.

Prototype-based classifiers: Build on the concept of the kNN classifier but simplify the classification task by generating representative examples (known as prototypes or exemplars) of a given class. In other words, a class prototype is a manufactured sample vector placed in a higher dimensional space so that most of the training samples belonging to that class are closest to the prototype (113). Prototype-based classifiers learn prototypes of a given class (e.g., a disease state) and compare new/unknown datasets (e.g., the metabolome data of one subject) to the class prototypes. The (dis)similarity between the dataset and the prototype is judged based on the "distance" between the two and the classification decision is made based on which prototype is nearest to the dataset. The classification decision is made in a multi-dimensional space where the number of dimensions corresponds to the number of features in the dataset. As compared to kNN, this approach is much simpler and less affected by outliers (112), and such characteristics make prototype-based classifiers attractive and widely used for handling large datasets in biomedical research.

CHAPTER 3

The cardiometabolic burden of autonomous cortisol secretion associated with benign adrenal tumours

Content from this chapter has been published:

Cardiometabolic Disease Burden and Steroid Excretion in Benign Adrenal Tumors: A Cross-Sectional Multicenter Study.
***Prete A**, Subramanian A, Bancos I, Chortis V, Tsagarakis S, Lang K, Macech M, Delivanis DA, Pupovac ID, Reimondo G, Marina LV, Deutschbein T, Balomenaki M, O'Reilly MW, Gilligan LC, Jenkinson C, Bednarczuk T, Zhang CD, Dusek T, Diamantopoulos A, Asia M, Kondracka A, Li D, Masjkur JR, Quinkler M, Ueland GÅ, Dennedy MC, Beuschlein F, Tabarin A, Fassnacht M, Ivović M, Terzolo M, Kastelan D, Young WF Jr, Manolopoulos KN, Ambroziak U, Vassiliadi DA, Taylor AE, Sitch AJ, Nirantharakumar K, Arlt W; ENSAT EURINE-ACT Investigators*.*
***Ann Intern Med. 2022** Mar;175(3):325-334*
doi: 10.7326/M21-1737.

3.1. Introduction

In the ENSAT EURINE-ACT study, the largest prospective study to date on newly diagnosed adrenal masses, benign adrenal tumours were the most common underlying entity, representing 1513 (89.7%) of 1686 incidentally discovered adrenal masses (18). Benign adrenal masses can be non-functioning adrenal tumours (NFAT) or autonomously overproduce steroids, most frequently cortisol. Autonomous cortisol secretion can be clinically overt (Cushing's syndrome, CS) or diagnosed based on abnormal 1mg-dexamethasone suppression test results (1mg-DST) in patients with incidentally discovered adrenal tumours lacking clinical signs of CS (mild autonomous cortisol secretion, MACS). Whilst CS is a well-established cause of increased cardiometabolic morbidity and mortality, the evidence regarding the impact of MACS on cardiometabolic disease risk is scarce and heterogeneous. In a recent systematic

review and meta-analysis of studies reporting on the prevalence of cardiometabolic comorbid conditions in persons with NFAT and MACS (15), hypertension was the most common occurrence (64.0% in MACS vs. 58.2% in NFAT). Persons with MACS were more likely to present with prediabetes (50.0% vs. 14.4%) and type 2 diabetes (28.1% vs. 14.4%), whilst the prevalence of dyslipidaemia was at a similar level in MACS and NFAT (approximately 34%). However, evidence regarding the cardiometabolic risk of persons with MACS is almost exclusively derived from observational studies of small sample size, thereby limiting the interpretation of the results. Here, we report the results of a cross-sectional study investigating the clinical characteristics and cardiometabolic burden in 1305 prospectively recruited persons with benign adrenal tumours and different degrees of autonomous cortisol secretion.

3.2. Methods

3.2.1. *Subject selection*

Persons with benign adrenal tumours were drawn from the ENSAT EURINE-ACT study (18), which had prospectively recruited adults (≥18 years) with newly diagnosed adrenal tumours >1cm from 2011 to 2016 through 14 secondary and tertiary care centres with expertise in the management of adrenal tumours in 11 countries, participating in the European Network for the Study of Adrenal Tumours (ENSAT; www.ensat.org). We included all EURINE-ACT participants who were diagnosed with benign adrenocortical adenomas and had undergone standardised endocrine assessment for exclusion of autonomous cortisol secretion (61, 114), with

measurement of endocrine parameters carried out in the recruitment centre. We excluded participants with confirmed primary aldosteronism diagnosed according to current guidelines (57) and participants with autonomous cortisol secretion due to bilateral macronodular adrenal hyperplasia. We included 1305 (82%) of 1588 otherwise eligible persons with benign adrenal tumours, as 283 had no available results for the 1-mg overnight dexamethasone suppression test (1mg-DST) that is required for the diagnosis of MACS (**Figure 3.1**).

Figure 3.1: Flow-chart of patient inclusion.

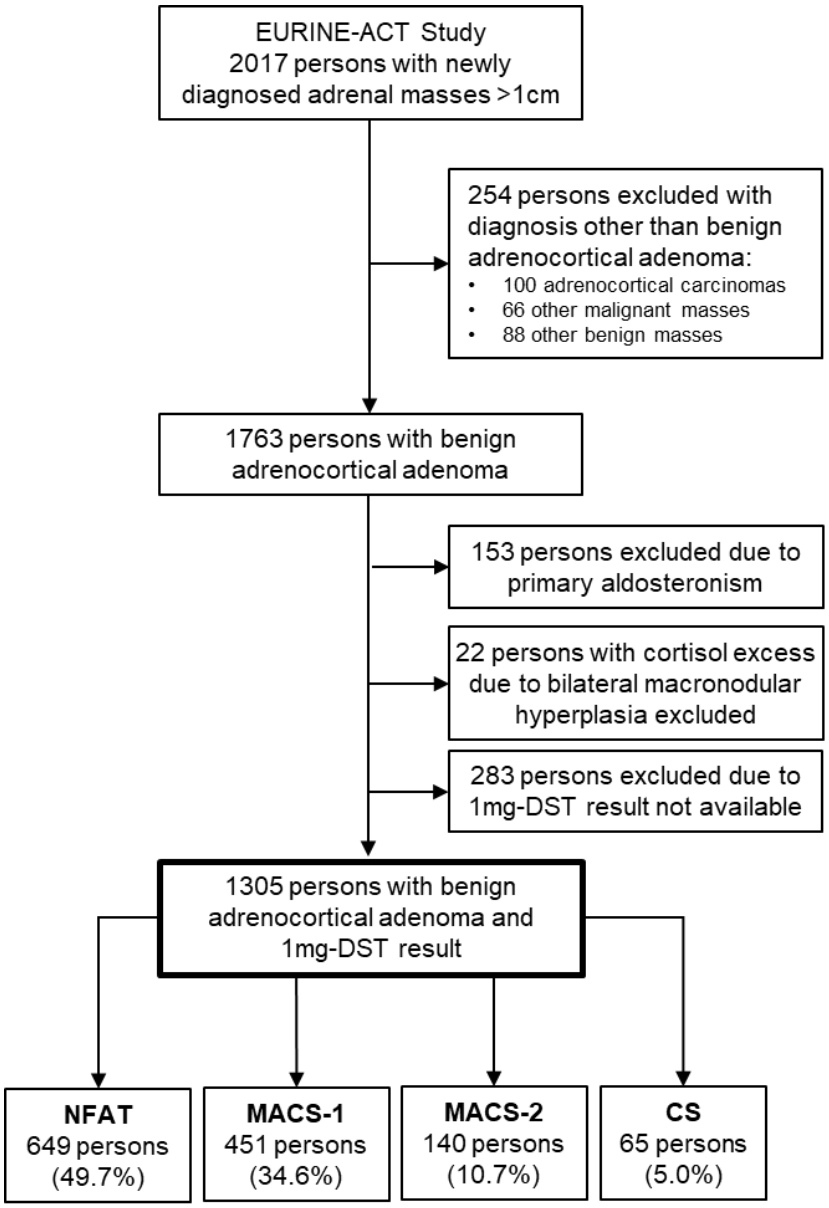

In accordance with recent guidelines (28), we defined the presence of MACS as failure to suppress morning serum cortisol concentration to <50 nmol/L during the 1mg-DST in the absence of clinical features indicative of CS (e.g., proximal myopathy, moon face, dorsocervical and supraclavicular fat pads, purple striae). Persons with MACS were further subdivided into MACS-1 (possible mild autonomous cortisol secretion; serum cortisol in the 1mg-DST 50-138 nmol/L) and MACS-2 (definitive mild autonomous cortisol secretion; serum cortisol in the 1mg-DST >138 nmol/L) (28). Persons with current or recent (<6 months) intake of drugs known to alter steroid synthesis or metabolism were excluded. All centres had ethical approval for pseudonymised phenotype recording in the online ENSAT database and all participants of the EURINE-ACT study provided written informed consent.

We used the information available at the time of adrenal tumour diagnosis (baseline assessment). Variables obtained through the online ENSAT database included demographic data (sex, age, body mass index, BMI), tumour characteristics (maximum diameter and location), information about cardiometabolic morbidity (hypertension, dysglycaemia, dyslipidaemia), and endocrine test results (adrenocorticotropic hormone, ACTH; serum dehydroepiandrosterone sulfate, DHEAS; 24-hour urinary free cortisol, UFC). We then asked each site to review the available information against their local databases to obtain any variables that were missing in the online ENSAT database (for details see **Table 3.1**).

Table 3.1: Clinical assessments, methods for data collection and analysis, and definition of clinical outcomes in the ENSAT EURINE-ACT study.

Type of clinical assessments carried out to assess cardiometabolic risk	Nurse- or doctor-led clinical assessment which included:
	• Collection of medical data including:
	  ○ Demographics.
	  ○ General health.
	  ○ Longstanding illness.
	  ○ Doctor-diagnosed hypertension.
	  ○ Doctor-diagnosed diabetes.
	  ○ Prescribed medicines.
	• Anthropometric measurements including height and weight.
	• Blood sample including glycated haemoglobin (carried out at the discretion of the medical professional).
	• Collection of radiological information concerning the newly diagnosed adrenal tumour(s) including:
	  ○ Maximum tumour diameter.
	  ○ Tumour location.
	• Laboratory work-up to exclude adrenal steroid excess including:
	  ○ 1mg-overnight dexamethasone suppression test.*
	  ○ Adrenocorticotropic hormone.
	  ○ Serum dehydroepiandrosterone sulfate.
	  ○ 24-hour urinary free cortisol.
	• Physical exam to exclude signs of adrenal steroid excess.

Clinical and laboratory data analysis and collection	• Anthropometric measurements were carried out at the recruiting centres. Height was measured to the nearest cm. Weight was measured in kg (one decimal place) using clinically validated scales. • Laboratory work-up was carried out at the recruiting centre according to standardised local protocols which were in agreement with the 2016 European Society of Endocrinology/ENSAT guidelines on adrenal incidentalomas, the Endocrine Society guidelines on Cushing's syndrome, and the Endocrine Society guidelines on primary aldosteronism (28, 57, 61). Laboratory measurements were carried out at the clinical laboratory of each recruiting centre. • Clinical information was collected through the online ENSAT database. Access to the ENSAT database occurs through a unified, security-driven portal that allows targeted upload of pseudonymised patient data. The principal investigator at each recruiting centre was responsible for data entry in the ENSAT database. All data collectors with access to the ENSAT database had to undergo training on how to use the online platform and the same person was responsible at each site for data entry throughout the study. • After recruitment was completed, we asked each site to review the available information against their local databases to obtain any variables that were missing in the online ENSAT database. Any variable that was inconsistent with the rest of the available records was queried and resolved with each site.
Definitions of clinical outcomes – hypertension	Hypertension was defined as: • Doctor-diagnosed hypertension at the time of the clinical assessment (i.e., the patient presented with a previous diagnosis of hypertension from a medical doctor), or • Treatment with anti-hypertensives at the time of the clinical assessment.
Definitions of clinical outcomes – treatment with 3 or more anti-hypertensives	The outcome was defined as the combination of: • Diagnosis of hypertension (see criteria above), and • Treatment with three or more anti-hypertensive medications at the time of the clinical assessment.

Definitions of clinical outcomes – pre-diabetes	The outcome was defined as glycated haemoglobin 5.7-6.4% (39–47 mmol/mol).	
Definitions of clinical outcomes – type 2 diabetes	Diabetes was defined as: • Doctor-diagnosed diabetes at the time of the clinical assessment (i.e., the patient presented with a previous diagnosis of diabetes from a medical doctor), or • Treatment with anti-diabetes medications at the time of the clinical assessment, or • Glycated haemoglobin ≥6.5% (48 mmol/mol) at the time of the clinical assessment. Type 1 diabetes was excluded based on clinical assessment and medical history.	
Definitions of clinical outcomes – type 2 diabetes treated with insulin	The outcome was defined as the combination of: • Diagnosis of type 2 diabetes (see criteria above), and • Treatment with any type of injectable insulin at the time of the clinical assessment.	
Definitions of clinical outcomes – dyslipidaemia	The outcome was defined as treatment with lipid-lowering agents other than for secondary cardiovascular prevention at the time of the clinical assessment. Persons on treatment following a major cardiovascular event such as ischemic heart disease and stroke (secondary prevention) were excluded. Blood samples for lipids taken at the time of the clinical assessment were not considered for the diagnosis of dyslipidaemia.	
Percentage of subjects for whom the information on clinical outcomes and anthropometric measurements was missing at the time of the clinical assessment†	Hypertension	0.1%
	Treatment with 3 or more anti-hypertensives	0
	Glucose metabolism status	25.6%
	Type 2 diabetes treated with insulin	0
	Dyslipidaemia	1.1%
	Body mass index	2.1%
Percentage of subjects for whom the information on biochemical results was missing at the time of the clinical assessment†	1mg-overnight dexamethasone suppression test	0
	Adrenocorticotropic hormone	19.2
	Serum dehydroepiandrosterone sulfate	25.4
	24-hour urinary free cortisol	31.7

* Four German centres did not perform the 1mg-DST in patients lacking clinical signs of overt cortisol excess (Cushing's syndrome) during the initial stages of recruitment (see also Table 3.2).
† This information refers to the 1305 patients included in this study.

3.2.2. *Definitions of cardiometabolic outcomes*

We calculated the prevalence of hypertension, prediabetes, type 2 diabetes, and dyslipidaemia considering the clinical information available at the time of adrenal tumour diagnosis. We also identified subjects with a more severe clinical phenotype, specifically those with hypertension treated with ≥3 anti-hypertensives and those requiring insulin to manage their type 2 diabetes (for details see **Table 3.1**).

Hypertension: Participants were considered as having hypertension if they had a doctor diagnosis or if they were prescribed medications for hypertension.

Treatment with ≥3 anti-hypertensives: Participants with hypertension were chosen for subgroup analysis to study the prescription of ≥3 antihypertensives as an outcome, in line with established American Heart Association criteria (115).

Glucose metabolism status: Participants were considered as having type 2 diabetes if they had a doctor diagnosis or if they were prescribed antidiabetic medications. Prediabetes and type 2 diabetes were also diagnosed based on glycated haemoglobin results according to American Diabetes Association criteria (116).

Type 2 diabetes requiring insulin: Participants with type 2 diabetes were chosen for subgroup analysis to study insulin therapy as an outcome.

Dyslipidaemia: The prescription of lipid-lowering agents was considered a proxy for dyslipidaemia. We only considered subjects taking lipid-lowering agents other than for secondary cardiovascular prevention, after excluding those with a history of stroke, cerebral haemorrhage, cerebral thrombosis, ischemic heart disease, or angina, in line with American College of Cardiology/American Heart Association criteria (117).

3.2.3. *Statistical analysis*

Poisson regression with robust variance (118) was fitted to obtain crude and adjusted prevalence ratios (PR) of hypertension, prediabetes, type 2 diabetes, and dyslipidaemia in persons with MACS-1, MACS-2, and CS using NFAT as the reference group. The models were adjusted for age, sex, and BMI. To provide prevalence ratios using Poisson models, the categorical glucose metabolism outcome variable was replaced with two separate binary outcomes: (a) dysglycaemia (combination of pre-diabetes and type 2 diabetes – subjects with NFAT and normal glucose metabolism were used as the reference) and (b) type 2 diabetes (the combined group of subjects with NFAT and with either pre-diabetes or normal glucose metabolism was used as the reference). In sub-groups of subjects with hypertension and type 2 diabetes, Poisson regression models were fitted to estimate the crude and adjusted PRs of treatment with ≥3 anti-hypertensives and insulin use, respectively. Missing data for the clinical outcomes were replaced using multiple imputation using chained equations through logistic models with the following covariates: age, sex, and BMI category. Resistant hypertension, type 2 diabetes and insulin treatment were imputed within a conditional sample of subjects with hypertension, dyslipidaemia, and type 2 diabetes, respectively. Outside these conditional samples, missing values for these variables were replaced with the conditional constant (0/absent).

Associations between continuous outcomes were determined by linear regression after log-transformation of all outcomes to reduce skewness in the dataset. Associations between the log-transformed outcome and the variable of interest were reported as sympercents (119); models were adjusted for age, sex, and BMI. Statistical analyses were carried out using Stata Statistical Software: Release 16 (College Station, TX: StataCorp LLC) and GraphPad Prism 9 (San Diego, CA: GraphPad Software Inc.).

3.3. Results

3.3.1. *Clinical and endocrine characteristics*

Between 2011 and 2016, 1305 persons with newly diagnosed non-aldosterone producing adenomas underwent a 1mg-DST and were prospectively assessed for clinical signs of cortisol excess (**Figure 3.1**, **Table 3.2**).

Table 3.2: Centre-specific distribution of ENSAT EURINE-ACT study participants with benign adrenocortical adenomas categorised according to autonomous cortisol secretion. Abbreviations: 1mg-DST, 1mg-overnight dexamethasone suppression test; CS, Cushing's syndrome; MACS, mild autonomous cortisol secretion; NFAT, non-functioning adrenal tumour.

Centre	EURINE-ACT participants with benign adrenocortical adenomas*, n (%)	EURINE-ACT participants with benign adrenocortical adenomas and available 1mg-DST result†, n (%)	NFAT, n (%)	MACS-1, n (%)	MACS-2, n (%)	CS, n (%)
Athens, Greece	215 (13.5)	206 (15.8)	106 (51.5)	70 (34.0)	17 (8.3)	13 (6.3)
Birmingham, UK	209 (13.2)	196 (15.0)	105 (53.6)	61 (31.1)	23 (11.7)	7 (3.6)
Warsaw, Poland	199 (12.5)	196 (15.0)	100 (51.0)	71 (36.2)	19 (9.7)	6 (3.1)
Rochester, MN, USA	203 (12.8)	175 (13.4)	94 (53.7)	52 (29.7)	20 (11.4)	9 (5.1)
Zagreb, Croatia	116 (7.3)	116 (8.9)	57 (49.1)	42 (36.2)	12 (10.3)	5 (4.3)
Turin, Italy	89 (5.6)	85 (6.5)	38 (44.7)	40 (47.1)	5 (5.9)	2 (2.4)
Belgrade, Serbia	68 (4.3)	68 (5.2)	39 (57.4)	27 (39.7)	2 (2.9)	0 (0)
Würzburg, Germany	103 (6.5)	56 (4.3)	19 (33.9)	18 (32.1)	12 (21.4)	7 (12.5)
Bordeaux, France	57 (3.6)	47 (3.6)	24 (51.1)	16 (34.0)	4 (8.5)	3 (6.4)
Munich, Germany	109 (6.9)	43 (3.3)	17 (39.5)	13 (30.2)	6 (14.0)	7 (16.3)
Galway, Ireland	45 (2.8)	42 (3.2)	27 (64.3)	11 (26.2)	3 (7.1)	1 (2.4)
Bergen, Norway	34 (2.1)	34 (2.6)	6 (17.6)	17 (50.0)	9 (26.5)	2 (5.9)
Berlin, Germany	108 (6.8)	23 (1.8)	7 (30.4)	9 (39.1)	5 (21.7)	2 (8.7)
Dresden, Germany	33 (2.1)	18 (1.4)	10 (55.6)	4 (22.2)	3 (16.7)	1 (5.6)
TOTAL	**1588**	**1305 (100.0)**	**649 (49.7)**	**451 (34.6)**	**140 (10.7)**	**65 (5.0)**

* After exclusion of participants with primary aldosteronism and participants with autonomous cortisol secretion due to primary bilateral macronodular adrenal hyperplasia.
† These are the EURINE-ACT participants included in this study.

Less than half of them achieved normal suppression of serum cortisol after the 1mg-DST (NFAT n=649, 49.7%). The vast majority of those with abnormal results lacked the distinctive clinical features of overt cortisol excess (MACS-1, n=451 [34.6%]; MACS-2, n=140 [10.7%]), whilst 65 (5.0%) were diagnosed with clinically overt CS including 37 incidentally discovered cases. Women represented 67.3% of the subjects included in the study and the female predominance was most pronounced in MACS-2 (73.6%) and CS (86.2%) (**Table 3.3**).

Table 3.3: Demographics, radiological, and biochemical parameters of EURINE-ACT participants with benign adrenocortical adenomas who underwent assessment for autonomous cortisol secretion. Values are reported as median (interquartile range), unless otherwise stated. Abbreviations: 1mg-DST, 1mg-overnight dexamethasone suppression test; ACTH, adrenocorticotropic hormone; BMI, body mass index; DHEAS, dehydroepiandrosterone sulfate; UFC, urinary free cortisol. NFAT, non-functioning adrenal tumours; MACS, mild autonomous cortisol secretion; CS, Cushing's syndrome.

	Overall cohort (n=1305)	**NFAT (n=649)**	**MACS-1 (n=451)**	**MACS-2 (n=140)**	**Adrenal CS (n=65)**
Women, n (%)	878 (67.3)	416 (64.1)	303 (67.2)	103 (73.6)	56 (86.2)
Age (years)	60 (52-67)	58 (51-65)	64 (56-71)	63 (54-69)	48 (38-60)
BMI (kg/m^2)	29.0 (25.4-33.4)	29.4 (25.8-33.9)	28.8 (25.1-33.1)	28.6 (24.0-32.9)	28.7 (25.2-31.7)
- Lean (BMI <25), n (%)	292 (22.9)	129 (20.6)	106 (23.8)	42 (30.0)	15 (23.4)
- Overweight (BMI 25-30), n (%)	429 (33.6)	202 (32.2)	160 (35.9)	41 (29.3)	26 (40.6)
- Obesity (BMI ≥30), n (%)	556 (43.5)	296 (47.2)	180 (40.4)	57 (40.7)	23 (35.9)
Maximum tumour diameter (mm)*	26 (19-36)	22 (16-30)	30 (23-38)	32 (24-44)	30 (26-38)
Tumour location:					
- Left adrenal, n (%)	616 (47.2)	323 (49.8)	196 (43.5)	63 (45.0)	34 (52.3)
- Right adrenal, n (%)	391 (30)	219 (33.7)	119 (26.4)	35 (25.0)	18 (27.7)
- Bilateral, n (%)	298 (22.8)	107 (16.5)	136 (30.2)	42 (30.0)	13 (20.0)
Serum cortisol in the 1mg-DST (nmol/L)	51 (33-92)	33 (27-41)	72 (60-93)	200 (165-283)	435 (271-574)
Plasma ACTH (pmol/L)	2.38 (1.34-3.96)	3.00 (1.89-4.89)	2.20 (1.30-3.43)	1.43 (0.55-2.60)	0.66 (0.55-1.43)
Serum DHEAS (µmol/L)	1.40 (0.70-2.70)	1.90 (1.00-3.40)	1.14 (0.65-2.19)	0.83 (0.40-1.85)	0.54 (0.23-1.58)
24-hour UFC (nmol/24h)	132 (66-226)	127 (66-207)	141 (69-229)	130 (47-207)	472 (149-1319)

* For bilateral tumours, the maximum diameter of the larger adrenal mass was considered.

The median age at the time of adrenal tumour diagnosis was 60 years (interquartile range 52-67 years). Subjects with MACS were older than those with NFAT (**Figure 3.2A**). By contrast, CS was diagnosed at a younger age (median 48 years, interquartile range 38-60 years) (**Table 3.3**). Subjects with abnormal 1mg-DST results had larger adrenal tumours, with over half of those with tumours >2 cm failing to suppress serum cortisol during the 1mg-DST (**Figure 3.2B**).

Plasma ACTH was negatively associated with 1mg-DST results (**Table 3.4**), which was reflected in a progressive decrease in ACTH from MACS-1 over MACS-2 to CS (**Table 3.3**, **Figure 3.2C**). Serum DHEAS had a similar trend, but the differences among groups were less pronounced (**Table 3.4**, **Figure 3.2D**).

Persons with MACS were almost twice as likely to present with bilateral tumours than persons with NFAT (30.1% vs. 16.5%) (**Table 3.3**). Persons with bilateral tumours had abnormal 1mg-DST results in 62.3% and presented with larger adrenal masses (the maximum diameter of the larger adrenal mass was considered), lower plasma ACTH, and higher 24-hour UFC (**Table 3.5**).

Figure 3.2: Endocrine assessment results. Distribution of serum cortisol (median, range) after the 1mg-overnight dexamethasone suppression test (1mg-DST) according to age (A) and maximum tumour diameter (B) in subjects without clinical signs of Cushing's syndrome. Plasma ACTH (C) and serum DHEAS (D) measured in these subjects are shown as boxplots, with boxes representing the median and interquartile range, and whiskers representing the 5th to 95th centile. The dotted lines in panels A and B represent the cortisol cut-offs that separate non-functioning adrenal tumours (NFAT) from possible mild autonomous cortisol secretion (MACS-1) and definitive mild autonomous cortisol secretion (MACS-2).

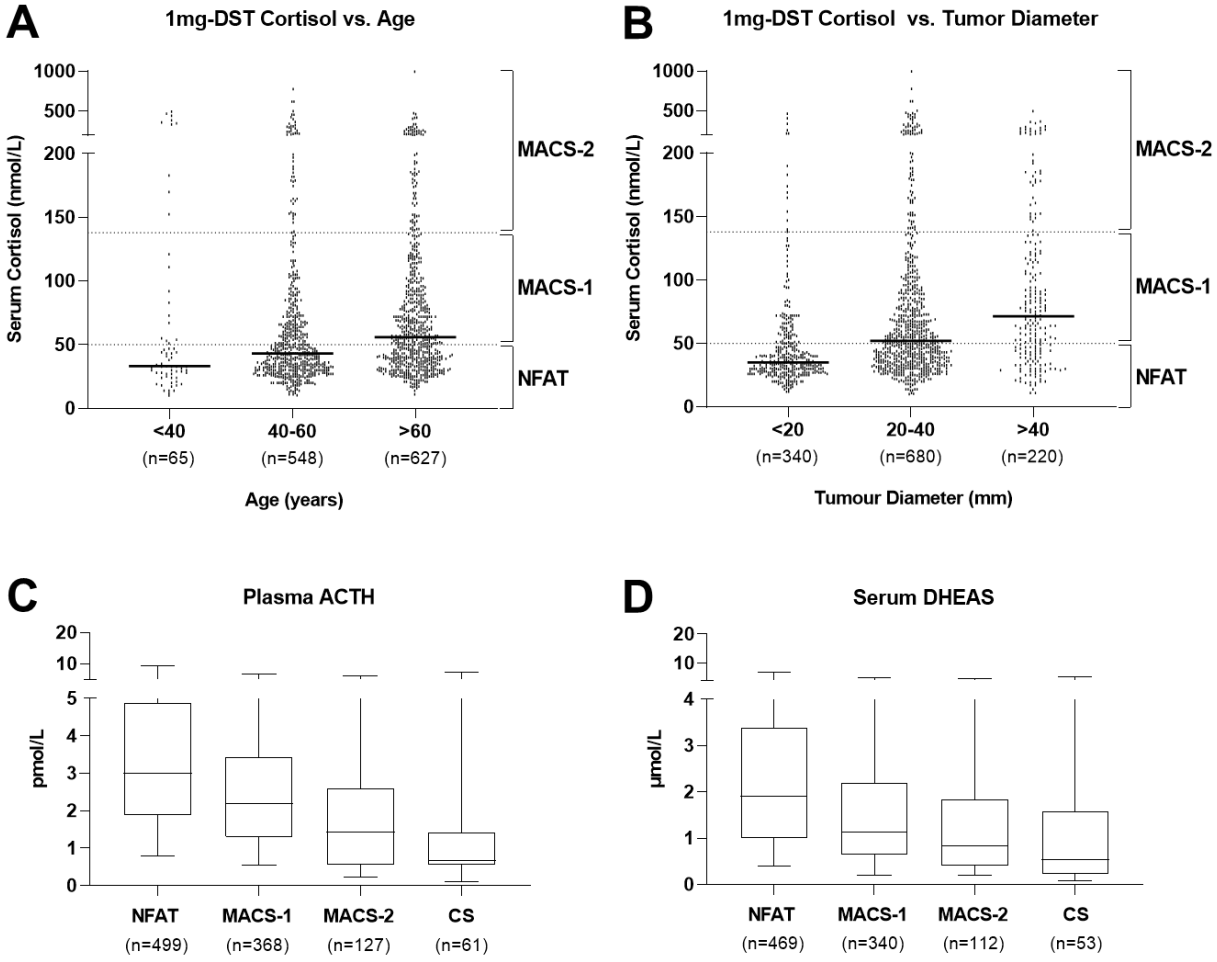

Table 3.4: Associations between clinical, radiological, and biochemical parameters of persons with benign adrenocortical tumours and different degrees of autonomous cortisol secretion. Percentage changes are reported, derived from the linear regression with log-transformed outcomes. All models were adjusted by age, sex, and BMI. Abbreviations: 1mg-DST, 1mg-overnight dexamethasone suppression test; ACTH, adrenocorticotropic hormone; CS, Cushing's syndrome; DHEAS, dehydroepiandrosterone sulfate; MACS, mild autonomous cortisol secretion; NFAT, non-functioning adrenal tumour; UFC, urinary free cortisol.

Outcome	Variables			
	1mg-DST	Maximum tumour diameter	Plasma ACTH	Serum DHEAS
	Percentage change (95% CI)	Percentage change (95% CI)	Percentage change (95% CI)	Percentage change (95% CI)
All subjects (n=1305)				
Maximum tumour diameter	0.08 (0.06, 0.11)			
Plasma ACTH	-0.28 (-0.33, -0.24)	-0.86 (-1.22, -0.49)		
Serum DHEAS	-0.24 (-0.29, -0.19)	-0.92 (-1.32, -0.53)	3.88 (2.04, 5.72)	
24-hour UFC	0.19 (0.14, 0.24)	0.82 (0.38, 1.26)	-2.01 (-4.20, 0.18)	1.93 (-1.60, 5.46)
After excluding subjects with CS (n=1240)				
Maximum tumour diameter	0.13 (0.10, 0.17)			
Plasma ACTH	-0.30 (-0.36, -0.24)	-0.76 (-1.10, -0.41)		
Serum DHEAS	-0.24 (-0.31, -0.17)	-0.93 (-1.32, -0.55)	3.32 (1.52, 5.13)	
24-hour UFC	0.07 (-0.01, 0.14)	0.71 (0.29, 1.14)	-1.25 (-3.37, 0.88)	4.17 (0.67, 7.68)

Table 3.5: Clinical characteristics of ENSAT EURINE-ACT study participants with benign adrenocortical adenomas comparing participants with unilateral vs. those with bilateral adrenocortical tumours. Persons with Cushing's syndrome were excluded from the analysis because of their low number (n=65). Values are reported as median (interquartile range), unless otherwise stated. The analysis of cardiometabolic outcomes is based on a Poisson regression model (unilateral tumours used as the reference). Results are reported as prevalence ratios and 95% confidence intervals (CI); both unadjusted and age-, sex-, and BMI-adjusted prevalence ratios are reported. Missing cardiometabolic outcome data were replaced using multiple imputation using chained equations with age, sex, and BMI as covariates. Imputations for treatment with ≥3 anti-hypertensives, type 2 diabetes and insulin treatment were conditional to persons with hypertension, dysglycaemia and type 2 diabetes, respectively. Abbreviations: 1mg-DST, 1mg-overnight dexamethasone suppression test; ACTH, adrenocorticotropic hormone; BMI, body mass index; DHEAS, dehydroepiandrosterone sulfate; MACS, mild autonomous cortisol secretion; NFAT, non-functioning adrenal tumour; UFC, urinary free cortisol.

	NFAT and MACS combined (n=1240)		**NFAT only (n=649)**		**MACS only (n=591)**	
	Unilateral tumours (n=955)	**Bilateral tumours (n=285)**	**Unilateral tumours (n=542)**	**Bilateral tumours (n=107)**	**Unilateral tumours (n=413)**	**Bilateral tumours (n=178)**
Women, n (%)	631 (66.1)	190 (66.7)	350 (64.6)	66 (61.7)	281 (68.0)	124 (69.7)
Age (years)	61 (52-67)	60 (54-68)	59 (50-65)	58 (53-65)	64 (56-71)	62 (55-70)
BMI (kg/m^2)	29.2 (25.3-33.7)	28.7 (25.4-33.0)	29.6 (25.8-34.1)	28.7 (25.9-33.4)	28.9 (24.7-33.1)	28.7 (25.4-32.4)
- Lean (BMI <25), n (%)	216 (22.6)	61 (21.4)	108 (19.9)	21 (19.6)	108 (26.2)	40 (22.5)
- Overweight (BMI 25-30), n (%)	294 (30.8)	109 (38.2)	163 (30.1)	39 (36.4)	131 (31.7)	70 (39.3)
- Obesity (BMI ≥30), n (%)	420 (44.0)	113 (39.6)	249 (45.9)	47 (43.9)	171 (41.4)	66 (37.1)
Maximum tumour diameter (mm)*	25 (18-35)	29 (20-37)	21 (15-30)	23 (18-30)	30 (23-40)	30 (24-40)
1mg-DST (nmol/L)	45 (31-75)	62 (41-100)	33 (27-40)	34 (29-43)	83 (63-135)	85 (65-134)
Plasma ACTH (pmol/L)	2.64 (1.54-4.18)	2.02 (1.29-3.51)	3.07 (2.02-4.89)	2.42 (1.56-4.73)	2.01 (1.15-3.26)	1.83 (1.20-3.00)
Serum DHEAS (µmol/L)	1.44 (0.73-2.81)	1.39 (0.79-2.61)	1.90 (0.97-3.42)	1.90 (1.11-2.84)	1.02 (0.51-2.08)	1.17 (0.68-2.05)
24-hour UFC (nmol/24h)	127 (58-204)	174 (86-254)	124 (63-196)	177 (83-257)	127 (55-213)	168 (94-246)
Hypertension, n (%)	649 (67.9)	213 (74.7)	3413(63.3)	73 (68.2)	306 (74.1)	140 (78.7)
Unadjusted prevalence ratios (95% CI)	1.10 (1.01-1.19)		1.08 (0.93-1.25)		1.06 (0.96-1.17)	
Adjusted prevalence ratios (95% CI)	1.08 (1.00-1.17)		1.06 (0.92-1.22)		1.07 (0.98-1.17)	
Use of ≥3 anti-hypertensives, n (%)†	228 (35.2)	92 (43.4)	115 (33.5)	27 (37.7)	113 (37.1)	65 (46.4)
Unadjusted prevalence ratios (95% CI)	1.23 (1.02-1.49)		1.12 (0.80-1.57)		1.25 (0.98-1.59)	
Adjusted prevalence ratios (95% CI)	1.28 (1.06-1.55)		1.21 (0.87-1.69)		1.28 (1.01-1.62)	
Dysglycaemia, n (%)	475 (49.7)	166 (58.3)	262 (48.4)	58 (54.7)	212 (51.4)	108 (60.4)
Unadjusted prevalence ratios (95% CI)	1.17 (1.03-1.34)		1.28 (0.91-1.39)		1.17 (0.99-1.39)	
Adjusted prevalence ratios (95% CI)	1.15 (1.02-1.31)		1.09 (0.89-1.34)		1.20 (1.01-1.41)	
Type 2 diabetes, n (%)	283 (29.6)	81 (28.3)	146 (26.9)	26 (24.0)	137 (33.3)	55 (30.8)
Unadjusted prevalence ratios (95% CI)	0.95 (0.76-1.19)		0.89 (0.59-1.35)		0.92 (0.70-1.22)	
Adjusted prevalence ratios (95% CI)	0.94 (0.76-1.16)		0.86 (0.58-1.28)		0.95 (0.73-1.24)	

Insulin treatment, n (%)‡	68 (23.9)	14 (17.7)	27 (18.9)	1 (5.8)	40 (29.1)	13 (23.3)
Unadjusted prevalence ratios (95% CI)	0.74 (0.42-1.30)		0.29 (0.05-1.79)		0.80 (0.45-1.44)	
Adjusted prevalence ratios (95% CI)	0.75 (0.43-1.30)		0.32 (0.05-1.91)		0.82 (0.46-1.47)	
Dyslipidaemia, n (%)	303 (31.7)	95 (33.6)	155 (28.5)	32 (30.4)	148 (35.9)	63 (35.4)
Unadjusted prevalence ratios (95% CI)	1.06 (0.87-1.28)		1.06 (0.77-1.46)		0.99 (0.78-1.25)	
Adjusted prevalence ratios (95% CI)	1.04 (0.86-1.25)		1.02 (0.75-1.39)		1.01 (0.80-1.28)	

* For bilateral tumours, the maximum diameter of the larger adrenal mass was considered.
† Considering only subjects with a diagnosis of hypertension.
‡ Considering only subjects with a diagnosis of type 2 diabetes.

3.3.2. *Cardiometabolic burden*

In comparison to NFAT, subjects with MACS-2 and CS showed higher prevalence of hypertension (age-, sex-, and BMI-adjusted prevalence ratios [aPRs] 1.15 [95%CI 1.04-1.27] and 1.37 [95%CI 1.16-1.62], respectively) (**Table 3.6**, **Figure 3.3A**) and more often required ≥3 anti-hypertensives, increasing with the degree of autonomous cortisol secretion (MACS-2 aPR 1.31 [95%CI 1.02-1.68] and CS aPR 2.22 [95%CI 1.62-3.05]) (**Table 3.6**, **Figure 3.3B**).

The prevalence of type 2 diabetes was increased in subjects with CS (aPR 1.62 [95%CI 1.08-2.42]). In a subgroup analysis of persons with type 2 diabetes, both MACS-2 and CS more often required insulin treatment (aPR 1.89 [95%CI 1.01-3.52] and 3.06 [95%CI 1.60-5.85], respectively) (**Table 3.6**, **Figure 3.3B**).

The prevalence of dyslipidaemia did not differ from NFAT in MACS and CS.

Table 3.6: Cardiometabolic disease burden in benign adrenocortical tumours with different degrees of autonomous cortisol secretion. A series of Poisson regression models with robust variance was employed to investigate the cardiometabolic burden of 1305 persons from the EURINE-ACT study. Unadjusted and adjusted prevalence ratios are reported; adjusted models included age, sex and BMI as covariates. Missing outcome data were replaced using multiple imputation using chained equations with age, sex, and BMI as covariates. Imputations for treatment with ≥3 anti-hypertensives, type 2 diabetes and insulin treatment were conditional to persons with hypertension, dysglycaemia and type 2 diabetes, respectively. Abbreviations: NFAT, non-functioning adrenal tumours; MACS, mild autonomous cortisol secretion; CS, Cushing's syndrome.

	NFAT (n=649)	MACS-1 (n=451)	MACS-2 (n=140)	Adrenal CS (n=65)
Hypertension, n (%)	416 (64.1)	339 (75.2)	107 (76.4)	47 (72.3)
Prevalence ratios (95% CI)		1.17 (1.08-1.27)	1.19 (1.07-1.33)	1.13 (0.96-1.33)
Adjusted prevalence ratios (95% CI)		1.07 (0.99-1.16)	1.15 (1.04-1.27)	1.37 (1.16-1.62)
Treatment with ≥3 anti-hypertensives, n (%)[*]	142 (34.3)	132 (39.1)	46 (43.0)	27 (57.4)
Prevalence ratios (95% CI)		1.14 (0.94-1.38)	1.25 (0.97-1.63)	1.68 (1.26-2.23)
Adjusted prevalence ratios (95% CI)		1.12 (0.92-1.37)	1.31 (1.02-1.68)	2.22 (1.62-3.05)
Dysglycaemia, n (%)[†]	321 (49.5)	243 (53.9)	77 (55.0)	32.4 (49.8)
Prevalence ratios (95% CI)		1.09 (0.97-1.23)	1.11 (0.91-1.35)	1.01 (0.75-1.34)
Adjusted prevalence ratios (95% CI)		1.00 (0.89-1.13)	1.07 (0.89-1.29)	1.23 (0.92-1.65)
Type 2 diabetes, n (%)	171 (26.4)	145 (32.2)	47 (33.7)	20 (31.5)
Prevalence ratios (95% CI)		1.22 (1.00-1.49)	1.27 (0.95-1.72)	1.19 (0.80-1.78)
Adjusted prevalence ratios (95% CI)		1.10 (0.91-1.33)	1.23 (0.92-1.64)	1.62 (1.08-2.42)
Insulin treatment, n (%)[‡]	29 (16.9)	37 (25.8)	15 (32.6)	8 (41.0)
Prevalence ratios (95% CI)		1.53 (0.92-2.56)	1.94 (1.05-3.59)	2.44 (1.25-4.76)
Adjusted prevalence ratios (95% CI)		1.45 (0.83-2.52)	1.89 (1.01-3.52)	3.06 (1.60-5.85)
Dyslipidaemia, n (%)	187 (28.8)	161 (35.7)	50 (35.9)	10 (15.7)
Prevalence ratios (95% CI)		1.24 (1.04-1.47)	1.24 (0.96-1.60)	0.54 (0.30-0.97)
Adjusted prevalence ratios (95% CI)		1.08 (0.91-1.29)	1.18 (0.91-1.52)	0.76 (0.43-1.32)

[*] Considering only subjects with a diagnosis of hypertension (n=909).
[†] Dysglycaemia includes subjects with pre-diabetes and type 2 diabetes.
[‡] Considering only subjects with a diagnosis of type 2 diabetes (n=383).

Figure 3.3: Impact of different degrees of autonomous cortisol secretion on the cardiometabolic risk. Poisson regression models with robust variance exploring the cardiometabolic risk of persons with mild autonomous cortisol secretion (MACS) and adrenal Cushing's syndrome (CS) in comparison to persons with non-functioning adrenal tumours (NFAT). Age-, sex-, and BMI-adjusted prevalence ratios and 95% confidence intervals are reported. Panel A: adjusted prevalence ratios for hypertension, dysglycaemia, type 2 diabetes, and dyslipidaemia. Panel B: adjusted prevalence ratios for treatment with ≥3 anti-hypertensives (in subjects with hypertension) and insulin (in subjects with type 2 diabetes).

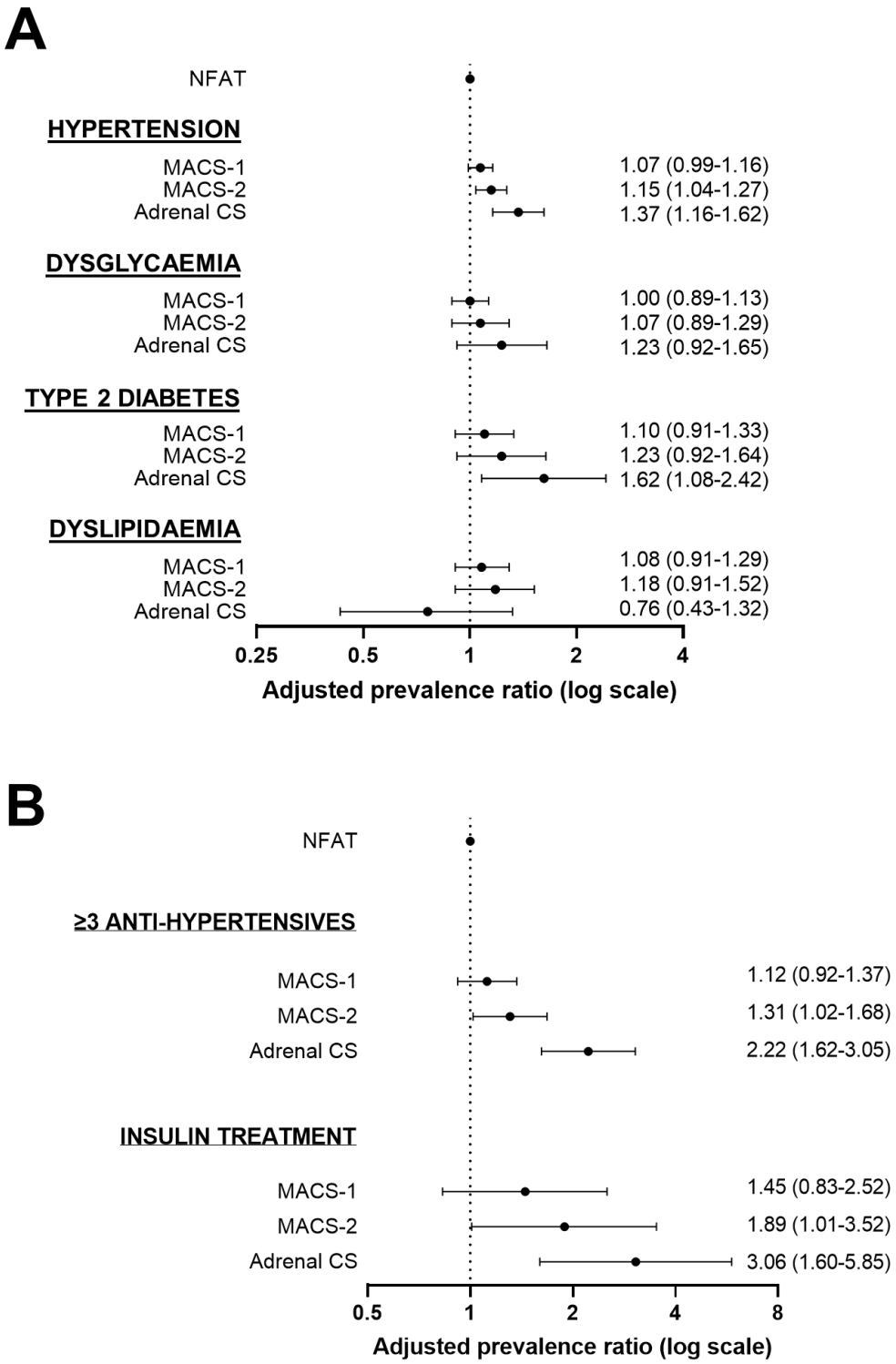

None of the available clinical or biochemical characteristics (such as tumour diameter, 1mg-DST results considered as a continuous variable, plasma ACTH, serum DHEAS, and 24-hour UFC) correlated in a clinically meaningful way with the presence of cardiometabolic disease in the EURINE-ACT study participants (**Table 3.7**).

Persons with bilateral adrenal tumours more often required ≥3 anti-hypertensives (43.4% vs. 35.2% in unilateral tumours; aPR 1.28 [95%CI 1.06-1.55]) and were more frequently diagnosed with dysglycaemia (58.3% vs. 49.7%; aPR 1.15 [95%CI 1.02-1.31]) (**Table 3.5**). When we further stratified these observations according to the 1mg-DST results, only persons with bilateral tumours and MACS had an increased cardiometabolic burden (**Table 3.5**).

Table 3.7: Poisson regression models to investigate the relationship between cardiometabolic disease and clinical, radiological, and biochemical parameters. Relationships are reported as prevalence ratios and 95% confidence intervals (CI). Unadjusted and adjusted prevalence ratios are reported; adjusted models included age, sex, and BMI as covariates. All continuous exposure variables (1mg-DST, tumour diameter, plasma ACTH, serum DHEAS, and 24-hour UFC) were scaled to clinically meaningful incremental units, as indicated in the "Variables" column. Missing outcome data were replaced using multiple imputation using chained equations with age, sex, and BMI as covariates. Imputations for treatment with ≥3 anti-hypertensives, type 2 diabetes and insulin treatment were conditional to persons with hypertension, dysglycaemia and type 2 diabetes, respectively. Abbreviations: 1mg-DST, 1mg-overnight dexamethasone suppression test; ACTH, adrenocorticotropic hormone; DHEAS, dehydroepiandrosterone sulfate; UFC: urinary free cortisol.

Variable		Hypertension	Treatment with ≥3 anti-hypertensives	Dysglycaemia	Type 2 diabetes	Insulin treatment	Dyslipidaemia
		Prevalence ratio (95% CI)	Prevalence ratio (95% CI)	Prevalence ratio (95% CI)	Prevalence ratio (95% CI)	Prevalence ratio (95% CI)	Prevalence ratio (95% CI)
All subjects (n=1305)							
1mg-DST (unit: 10 nmol/L)	Unadj.	1.00 (1.00-1.01)	1.01 (1.00-1.01)	1.00 (0.99-1.00)	1.00 (1.00-1.01)	1.01 (1.00-1.02)	1.00 (0.99-1.00)
	Adj.	1.01 (1.00-1.01)	1.01 (1.01-1.02)	1.00 (1.00-1.01)	1.01 (1.00-1.01)	1.02 (1.00-1.03)	1.00 (0.99-1.01)
Maximum tumour diameter (unit: 5mm)	Unadj.	1.00 (0.99-1.02)	1.01 (0.98-1.04)	1.00 (0.98-1.02)	1.00 (0.97-1.04)	1.02 (0.96-1.08)	0.97 (0.95-1.00)
	Adj.	1.00 (0.99-1.02)	1.01 (0.98-1.04)	0.99 (0.97-1.02)	1.00 (0.97-1.04)	1.02 (0.96-1.08)	0.97 (0.95-1.00)
Bilateral tumours	Unadj.	1.10 (1.02-1.19)	1.17 (0.97-1.41)	1.17 (1.03-1.33)	0.97 (0.78-1.20)	0.77 (0.46-1.30)	1.06 (0.88-1.28)
	Adj.	1.08 (1.01-1.17)	1.21 (1.00-1.45)	1.15 (1.02-1.30)	0.95 (0.77-1.17)	0.78 (0.47-1.29)	1.04 (0.86-1.24)
Plasma ACTH (unit: 1.1 pmol/L)	Unadj.	0.99 (0.98-1.01)	0.97 (0.93-1.01)	1.00 (0.98-1.02)	1.01 (0.99-1.04)	1.00 (0.95-1.05)	1.00 (0.98-1.03)
	Adj.	0.99 (0.97-1.01)	0.95 (0.91-1.00)	1.00 (0.98-1.02)	1.01 (0.98-1.05)	0.99 (0.94-1.05)	0.99 (0.96-1.02)
Serum DHEAS (unit: 0.5 µmol/L)	Unadj.	0.99 (0.98-1.00)	0.99 (0.97-1.01)	0.98 (0.97-1.00)	0.99 (0.96-1.01)	0.94 (0.87-1.01)	0.95 (0.92-0.98)
	Adj.	1.00 (0.99-1.01)	0.99 (0.96-1.01)	0.99 (0.98-1.01)	1.00 (0.98-1.02)	0.96 (0.89-1.03)	0.96 (0.93-0.99)
24-hour UFC (unit: 25 nmol/24h)	Unadj.	1.00 (1.00-1.00)	1.01 (1.00-1.01)	1.00 (0.99-1.01)	1.00 (0.99-1.01)	0.99 (0.96-1.02)	0.99 (0.98-1.00)
	Adj.	1.00 (1.00-1.01)	1.01 (1.00-1.02)	1.00 (1.00-1.01)	1.01 (1.00-1.02)	1.00 (0.97-1.03)	1.00 (0.99-1.01)
After excluding subjects with CS (n=1240)							
1mg-DST (unit: 10 nmol/L)	Unadj.	1.00 (1.00-1.01)	1.01 (1.00-1.02)	1.00 (0.99-1.01)	1.01 (1.00-1.02)	1.01 (1.00-1.03)	1.01 (1.00-1.02)
	Adj.	1.00 (1.00-1.01)	1.01 (1.00-1.02)	1.00 (0.99-1.01)	1.00 (1.00-1.01)	1.01 (0.99-1.03)	1.01 (1.00-1.02)
	Unadj.	1.00 (0.99-1.02)	1.00 (0.97-1.03)	0.99 (0.97-1.01)	1.00 (0.97-1.03)	1.02 (0.95-1.09)	0.98 (0.95-1.01)

Maximum tumour diameter (unit: 5mm)	Adj.	1.00 (0.99-1.01)	1.00 (0.97-1.03)	0.99 (0.97-1.01)	1.00 (0.97-1.03)	1.01 (0.95-1.08)	0.98 (0.95-1.00)
Bilateral tumours	Unadj.	1.10 (1.01-1.19)	1.23 (1.02-1.49)	1.17 (1.03-1.34)	0.95 (0.76-1.19)	0.74 (0.43-1.30)	1.06 (0.87-1.28)
	Adj.	1.08 (1.00-1.17)	1.28 (1.06-1.55)	1.15 (1.02-1.31)	0.94 (0.76-1.16)	0.75 (0.43-1.30)	1.04 (0.86-1.25)
Plasma ACTH (unit: 1.1 pmol/L)	Unadj.	0.99 (0.98-1.01)	0.98 (0.94-1.02)	1.00 (0.98-1.02)	1.01 (0.99-1.04)	1.01 (0.97-1.05)	1.00 (0.97-1.02)
	Adj.	0.99 (0.98-1.01)	0.97 (0.92-1.01)	1.00 (0.98-1.02)	1.02 (0.99-1.05)	1.01 (0.97-1.06)	0.99 (0.95-1.02)
Serum DHEAS (unit: 0.5 µmol/L)	Unadj.	0.99 (0.98-1.00)	0.99 (0.97-1.01)	0.98 (0.97-1.00)	0.99 (0.96-1.01)	0.95 (0.89-1.03)	0.94 (0.91-0.97)
	Adj.	1.00 (0.99-1.01)	0.99 (0.97-1.01)	0.99 (0.97-1.01)	1.00 (0.98-1.02)	0.97 (0.91-1.05)	0.95 (0.92-0.98)
24-hour UFC (unit: 25 nmol/24h)	Unadj.	1.00 (0.99-1.00)	1.00 (0.99-1.01)	1.00 (0.99-1.01)	1.00 (0.99-1.02)	0.96 (0.90-1.02)	1.00 (0.99-1.01)
	Adj.	1.00 (1.00-1.01)	1.01 (0.99-1.02)	1.01 (1.00-1.01)	1.01 (1.00-1.02)	0.97 (0.91-1.03)	1.01 (0.99-1.02)

3.4. Discussion

In this cross-sectional study, we showed that persons with benign adrenal tumours diagnosed with MACS-2 and adrenal CS had an increased prevalence and severity of hypertension as compared to NFAT. Persons with adrenal CS were also more likely to have a diagnosis of type 2 diabetes and persons with MACS-2 and CS who had type 2 diabetes more often required insulin therapy to achieve adequate glycaemic control. Our data demonstrate that persons with MACS-2 carry an increased cardiometabolic burden similar to that observed in CS, even if they do not display typical features of clinically overt cortisol excess.

These findings were generated utilising the largest ever prospectively recruited group of persons with benign adrenal tumours, the ENSAT EURINE-ACT study (18). We classified subjects into four subgroups, NFAT, MACS-1, MACS-2, and CS, based on 1mg-DST results and clinical presentation, according to the criteria defined in the 2016 European Society of Endocrinology/ENSAT guidelines on adrenal incidentalomas (28). Increased cardiometabolic risk is a well-established feature of clinically overt CS, whilst the evidence regarding a metabolically adverse impact of MACS has been limited by small study sizes and heterogeneous definitions of diagnosis and clinical outcomes (15). However, a picture of increased cardiometabolic disease burden and frailty in persons with MACS has emerged from previous studies (15, 21, 120-122). Two very recent studies (17, 86) have also reported increased mortality risk in persons with MACS, with younger women and those with post-dexamethasone cortisol ≥138 nmol/L, i.e., MACS-2, carrying the highest risk.

Our data demonstrate in a large prospective group that failure to suppress serum cortisol in the 1mg-DST increased the prevalence of cardiometabolic disease in

persons with MACS and CS. Though cardiometabolic disease burden was not increased in MACS-1, urinary multi-steroid profiling by mass spectrometry demonstrated decreased androgen excretion and increased excretion of cortisol (**Chapter 4**). Our data suggest that NFAT, MACS-1 and MACS-2 represent a gradually progressive continuum, which is also supported by the fact that approximately 4-22% of subjects with NFAT develop MACS over time (15, 78). To explore this further, we stratified the EURINE-ACT NFAT group at a more granular level according to their 1mg-DST result, demonstrating an increased cardiometabolic burden with each 10 nmol/L increment in serum cortisol in the 1-mg DST (**Figure 3.4**). We speculate that a subgroup of subjects with NFAT may have underlying autonomous cortisol secretion that is not detected when applying the current diagnostic criteria for autonomous cortisol secretion, namely the 1mg-DST.

Figure 3.4: Prevalence of hypertension, type 2 diabetes, and dyslipidaemia in subjects with non-functioning adrenal tumours (NFAT; post-dexamethasone serum cortisol <50 nmol/L) stratified according to serum cortisol concentrations after 1mg dexamethasone overnight in 10 nmol/L increments. The dotted lines represent the prevalence of cardiometabolic disease in the entire NFAT group.

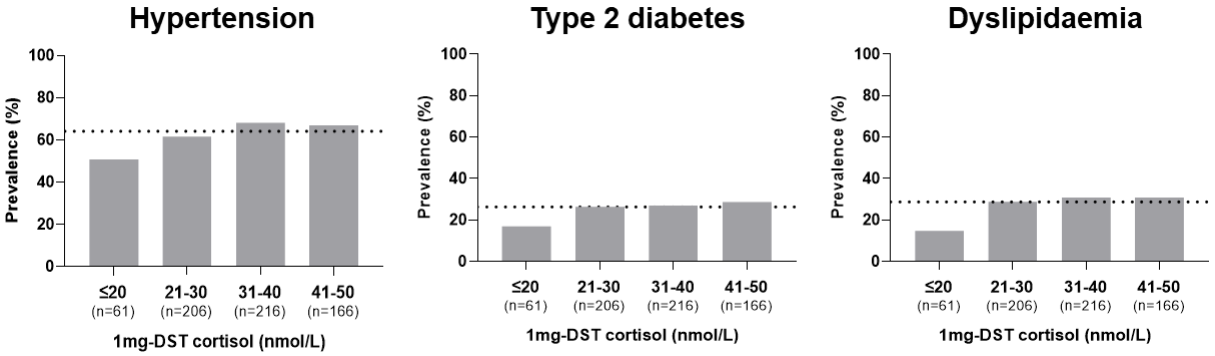

In our study of 1305 persons with benign adrenal tumours, 45.3% fulfilled the diagnostic criteria for MACS according to 1mg-DST results. The prevalence of MACS in our study is higher than previously reported, though direct comparison is hampered because of the heterogeneous approaches to the definition of MACS before the 2016

consensus (28), including different DST protocols and cut-offs and the combination of DST results with other parameters such as ACTH, 24-hour urinary free cortisol excretion, and salivary cortisol (15). However, a retrospective study in 198 persons with adrenal incidentalomas diagnosed MACS in 34.8% of cases according to the same diagnostic criteria we used in this study (77).

Persons included in the study were predominantly women and more than half of those were over the age of 60 at the time of adrenal tumour diagnosis; the demographics of our prospectively recruited study participants resemble those of large retrospective studies on adrenal incidentalomas (12, 20, 123). We also found that the proportion of women increased with the degree of autonomous cortisol secretion, corroborating previous observations that autonomous cortisol secretion predominantly affects women (77, 124).

Previous smaller studies found that subjects with bilateral and larger tumours are more likely to be diagnosed with MACS (125, 126). We found in our much larger study that individuals with MACS and bilateral tumours were more frequently diagnosed with dysglycaemia and prescribed ≥3 anti-hypertensives. We did not include subjects with autonomous cortisol secretion due to primary bilateral macronodular adrenal hyperplasia in whom this diagnosis had been ascertained by typical imaging findings, positive family history and/or documentation of gene mutations in germline DNA. Primary bilateral macronodular adrenal hyperplasia is an exceedingly rare cause of hypercortisolism that regularly presents with MACS. Thus, some further cases of undiagnosed primary bilateral macronodular adrenal hyperplasia in our study cannot be ruled out (43).

Strengths of our study include the prospective recruitment, the large sample size, and the standardised classification of different degrees of autonomous cortisol secretion. To our knowledge, this is the largest prospective study to establish the extent of the cardiometabolic disease burden in persons with benign adrenal tumours with and without autonomous cortisol secretion.

Weaknesses of our study include its cross-sectional design, precluding the collection of longitudinal data about cardiometabolic outcomes, and the absence of a comparator group of persons who also underwent imaging under similar circumstances but without being diagnosed with an adrenal tumour. Routine biochemical assessments were not standardised across participating centres and not measured in a centralised fashion. However, whilst we acknowledge that results for 24-hour UFC, plasma ACTH, and serum DHEAS should be interpreted with caution, inter-assay variability of serum cortisol measurements is unlikely to affect the cut-off of 50 nmol/L used to diagnose MACS (127). We could not include 283 (18%) of the overall 1588 eligible ENSAT EURINE-ACT participants with benign adrenal tumours in this study as they had no recorded 1mg-DST results at the time of adrenal tumour diagnosis. Therefore, a degree of selection bias is possible and should be considered when interpreting the high prevalence of MACS in our study. However, 213 of the 283 persons excluded due to missing 1-mg DST results were recruited by the four German centres that initially did not test their participants with the 1-mg DST, which makes a relevant impact of selection bias unlikely.

In conclusion, our study demonstrates that MACS-2 and CS are clinically highly relevant metabolic risk conditions, which predominantly affect women and come with an increased prevalence of hypertension and type 2 diabetes, and present with a more

severe clinical phenotype than persons with NFAT. Affected individuals should receive a comprehensive cardiovascular risk assessment at the time of adrenal tumour diagnosis, with particular attention to blood pressure and glucose metabolism.

CHAPTER 4

Urine steroid metabolomics to dissect the impact of autonomous cortisol secretion on steroid metabolism

Content from this chapter has been published:

Cardiometabolic Disease Burden and Steroid Excretion in Benign Adrenal Tumors: A Cross-Sectional Multicenter Study.
***Prete A**, Subramanian A, Bancos I, Chortis V, Tsagarakis S, Lang K, Macech M, Delivanis DA, Pupovac ID, Reimondo G, Marina LV, Deutschbein T, Balomenaki M, O'Reilly MW, Gilligan LC, Jenkinson C, Bednarczuk T, Zhang CD, Dusek T, Diamantopoulos A, Asia M, Kondracka A, Li D, Masjkur JR, Quinkler M, Ueland GÅ, Dennedy MC, Beuschlein F, Tabarin A, Fassnacht M, Ivović M, Terzolo M, Kastelan D, Young WF Jr, Manolopoulos KN, Ambroziak U, Vassiliadi DA, Taylor AE, Sitch AJ, Nirantharakumar K, Arlt W; ENSAT EURINE-ACT Investigators*.*
***Ann Intern Med. 2022** Mar;175(3):325-334*
doi: 10.7326/M21-1737.

Urine steroid metabolomics for the differential diagnosis of adrenal incidentalomas in the EURINE-ACT study: a prospective test validation study.
*Bancos I, Taylor AE, Chortis V, Sitch AJ, Jenkinson C, Davidge-Pitts CJ, Lang K, Tsagarakis S, Macech M, Riester A, Deutschbein T, Pupovac ID, Kienitz T, **Prete A**, Papathomas TG, Gilligan LC, Bancos C, Reimondo G, Haissaguerre M, Marina L, Grytaas MA, Sajwani A, Langton K, Ivison HE, Shackleton CHL, Erickson D, Asia M, Palimeri S, Kondracka A, Spyroglou A, Ronchi CL, Simunov B, Delivanis DA, Sutcliffe RP, Tsirou I, Bednarczuk T, Reincke M, Burger-Stritt S, Feelders RA, Canu L, Haak HR, Eisenhofer G, Dennedy MC, Ueland GA, Ivovic M, Tabarin A, Terzolo M, Quinkler M, Kastelan D, Fassnacht M, Beuschlein F, Ambroziak U, Vassiliadi DA, O'Reilly MW, Young WF Jr, Biehl M, Deeks JJ, Arlt W; ENSAT EURINE-ACT Investigators.*
Lancet Diabetes Endocrinol. 2020 Sep;8(9):773-781.
doi: 10.1016/S2213-8587(20)30218-7

4.1. Research strategy

We analysed the 24-hour urinary steroid metabolome of the 1305 EURINE-ACT study participants with benign adrenocortical adenomas and available 1mg-overnight dexamethasone suppression test (1mg-DST; see also **Chapter 3**). Subjects were stratified based on the degree of autonomous cortisol secretion and clinical outcomes (**Figure 4.1A**).

Figure 4.1: Overview of the analysis of the 24-hour urinary steroid metabolome in persons with adrenal tumours. Panel A: overview of the research strategy and methods used. Panel B: The 32 steroid metabolites measured by gas chromatography-mass spectrometry (GC-MS) are schematically mapped onto the steroidogenic pathways leading to glucocorticoid, androgen, and mineralocorticoid biosynthesis. The 17 steroid metabolites measured by liquid chromatography-tandem mass spectrometry (LC-MS/MS) are circled in red.

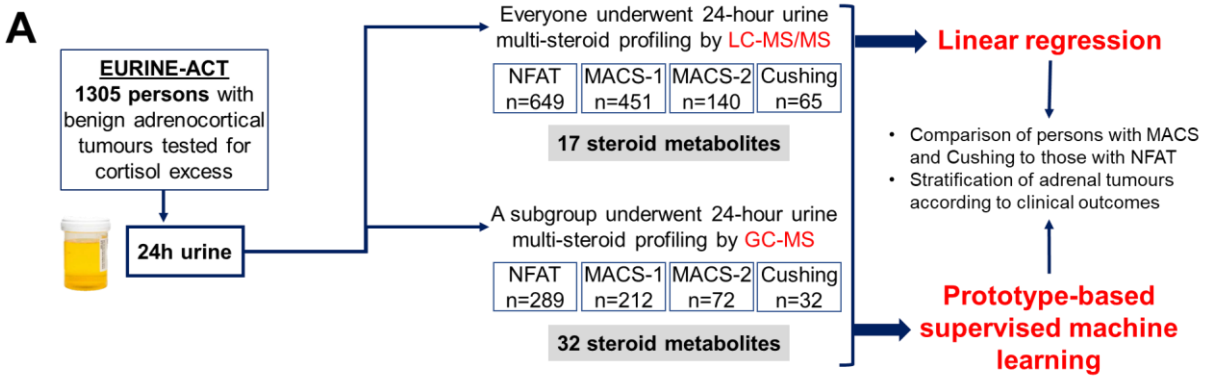

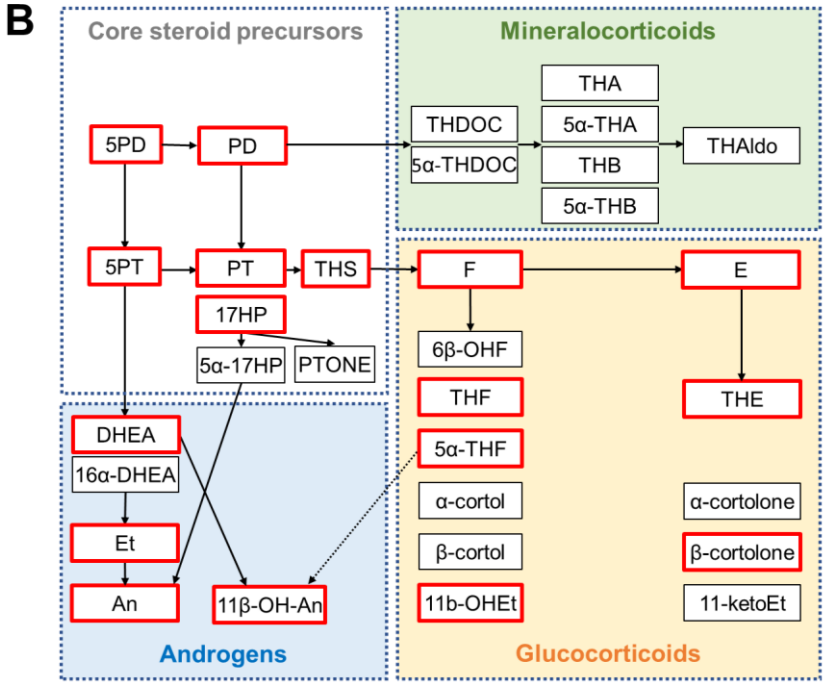

Steroid metabolite nomenclature	
5PD	Pregnenediol
PD	Pregnanediol
5PT	Pregnenetriol
PT	Pregnanetriol
17HP	17α-Hydroxypregnanolone
5α-17HP	17α-Hydroxy-3α,5α-pregnanolone
PTONE	Pregnanetriolone
THS	Tetrahydro-11-deoxycortisol
F	Cortisol
6β-OHF	6β-Hydroxycortisol
THF	Tetrahydrocortisol
5α-THF	5α-Tetrahydrocortisol
α-cortol	α-cortol
β-cortol	β-cortol
11β-OHEt	11β-Hydroxyetiocholanolone
E	Cortisone
THE	Tetrahydrocortisone
α-cortolone	α-Cortolone
β-cortolone	β-Cortolone
11-ketoEt	11-Ketoetiocholanolone
DHEA	Dehydroepiandrosterone
16α-DHEA	16α-Hydroxy-DHEA
An	Androsterone
Et	Etiocholanolone
11β-OHAn	11β-Hydroxyandrosterone
THDOC	Tetrahydro-11-deoxycorticosterone
5α-THDOC	5α-Tetrahydro-11-deoxycorticosterone
THA	Tetrahydro-11-dehydrocorticosterone
5α-THA	5α-Tetrahydro-11-dehydrocorticosterone
THB	Tetrahydrocorticosterone
5α-THB	5α-Tetrahydrocorticosterone
THAldo	3α5β-Tetrahydroaldosterone

All EURINE-ACT study participants (649 with non-functioning adrenal tumours [NFAT]; 451 with possible mild autonomous cortisol secretion [MACS-1]; 140 with definitive mild autonomous cortisol secretion [MACS-2]; 65 with adrenal Cushing's syndrome [CS]) underwent 24-hour urine analysis by liquid chromatography-tandem mass spectrometry (LC-MS/MS), with quantification of 17 distinct adrenal steroid metabolites (**Figure 4.1B**). A representative subgroup of these persons also underwent gas chromatography-mass spectrometry (GC-MS) analysis (289 NFAT, 212 MACS-1, 72

MACS-2, 32 CS). GC-MS allowed for the detection of 32 adrenal steroid metabolites, which offer a more comprehensive overview of adrenal steroidogenesis than LC-MS/MS, with quantification of steroid precursors, androgen, mineralocorticoid, and glucocorticoid metabolites (**Figure 4.1B**).

First, the 24-hour urine steroid metabolome was analysed using linear regression models adjusted for age, sex, and BMI, focusing on the following outcomes: difference in the steroid excretion of adrenal tumours based on the degree of autonomous cortisol secretion; stratification of adrenal tumours based on clinical outcomes (type 2 diabetes; hypertension; presence of bilateral tumours).

Whilst this descriptive approach is a well-established method to adjust for confounding variables, it only allows to look at one metabolite at a time and cannot be used for classification. Therefore, I looked at ways to assess the urine steroid metabolome as a whole. To this end steroid metabolomics was used, i.e., the combination of mass spectrometry-based steroid analysis with machine learning-based approaches (18, 75, 128-130). Specifically, two types of supervised machine learning methods were used (**Chapter 2**), generalised matrix learning vector quantisation (GMLVQ) and ordinal regression (OR) based on learning vector quantisation. These machine learning methods look at all the urinary steroid metabolites and create an “ideal” example (called prototype) for each class (e.g., NFAT, MACS, CS). The machine learning algorithm then compares the urinary steroid metabolome of each sample to the prototype of interest and determines how “close” the sample is to the prototype. In essence, these methods are trained to a) compare samples to the prototypes, b) determine how accurately they can separate samples belonging to different classes, and c) establish how relevant each steroid metabolite is in this separation. Both

GMLVQ and OR can be used for two-class (e.g., NFAT vs. MACS) and multiple-class problems (e.g., NFAT vs. MACS-1 vs. MACS-2 vs. CS). The main difference between the two methods is that OR assumes that there is a natural order of the classes (e.g., NFAT → MACS-1 → MACS-2 → CS), whilst GMLVQ does not. Hence, if the OR algorithm assigns a sample to the wrong class, the error is considered more serious when the two classes are far apart (e.g., mislabelling an NFAT case as CS is more serious than mislabelling an NFAT case as MACS-1). In contrast, GMLVQ assigns the same weight to mislabelling errors. For this reason, in this study OR was used for the multi-class classification of NFAT, MACS, and CS, and GMLVQ for two-class problems, since GMLVQ and OR yield the same results in this context.

4.2. Methods

4.2.1. *Subjects*

The clinical characteristics of the subjects included in the 24-hour urine multi-steroid profiling are reported in **Table 4.1**. All EURINE-ACT study participants (**Chapter 3**) provided a 24-hour urine sample at the time of the baseline assessment for their newly diagnosed adrenal masses. The volume of the 24-hour collection was recorded and the samples were aliquoted on the day of collection and stored locally at -20 °C. The samples were transported on dry ice to the University of Birmingham, United Kingdom, for centralised 24-hour urine multi-steroid profiling in the Steroid Metabolome Analysis Core of the Institute of Metabolism and Systems Research.

Table 4.1: Clinical characteristics of the persons who underwent 24-hour urine multi-steroid profiling. Values are reported as median (interquartile range), unless otherwise stated. Abbreviations: BMI, body mass index.

	NFAT (n=649)	MACS-1 (n=451)	MACS-2 (n=140)	Adrenal CS (n=65)
Women, n (%)	416 (64.1)	303 (67.2)	103 (73.6)	56 (86.2)
Age at diagnosis (years)	58 (51-65)	64 (56-71)	63 (54-69)	48 (38-60)
BMI (kg/m^2)	29.4 (25.8-33.9)	28.8 (25.1-33.1)	28.6 (24.0-32.9)	28.7 (25.2-31.7)
Hypertension, n (%)	416 (64.1)	339 (75.2)	107 (76.4)	47 (72.3)
Type 2 diabetes, n (%)	171 (26.4)	145 (32.2)	47 (33.7)	20 (31.5)
Bilateral tumours, n (%)	107 (16.5)	136 (30.2)	42 (30.0)	13 (20.0)

4.2.2. *Urine multi-steroid metabolite profiling*

Gas chromatography-mass spectrometry: From each 24-hour urine collection, 1mL of urine was used for extraction of free and conjugated steroids by solid-phase extraction. Derivatisation to form methyloxime trimethyl silyl ethers followed enzymatic hydrolysis and re-extraction. GC-MS was carried out on an Agilent 5973 instrument operating in selected-ion-monitoring to detect and quantify 32 steroid metabolites. Full details on the method can be found in (75, 109).

Liquid chromatography-tandem mass spectrometry: From each 24-hour urine collection, 400µL of urine was used for steroid metabolite extraction. After the addition of deuterated steroid standards (DHEA-d6, Cortisol-d4, Etio-d5, THE-d5, THS-d5), samples were deconjugated by hydrolysis. Thereafter, the solution underwent solid phase extraction using Sep Pak C18 cartridges prior to mass spectrometry analysis. A Waters Xevo mass spectrometer with an ACQUITY ultra-high performance chromatography system with an HSS T3, 1.8µm, 1.2x50mm column was used to analyse the steroids in positive ionisation mode. For positive identification and quantification of a steroid, the analyte had to have two matching multiple reaction monitoring mass transitions (precursor/product transitions) and an identical retention time relative to an authentic steroid standard. Steroids were quantified compared to a

calibration series using standard concentrations of each steroid standard ranging from 10 to 5000ng/mL, with the inclusion of a blank, prepared in a steroid-free synthetic urine matrix. Each steroid concentration was calculated relative to an assigned internal standard. Full details on the method can be found in (18).

4.2.3. *Linear regression analysis of GC-MS and LC-MS/MS data*

Associations between 24-hour urine steroid excretion measurements and the variable of interest (categories based on 1mg-DST results [NFAT, MACS-1, MACS-2, CS]; diagnosis of hypertension; diagnosis of type 2 diabetes; presence of bilateral tumours) were determined by linear regression after log-transformation of all outcomes to reduce skewness in the dataset. Associations between the log-transformed outcome and the variable of interest were reported as sympercents (119) and all models were adjusted for age, sex, and BMI. Linear regression models were generated using Stata Statistical Software: Release 16 (College Station, TX: StataCorp LLC) and GraphPad Prism 9 (San Diego, CA: GraphPad Software Inc.).

4.2.4. *Machine learning analysis of LC-MS/MS data*

Generalised matrix learning vector quantisation (GMLVQ): The mathematical details of GMLVQ, a prototype-based classification method and extension of Learning Vector Quantisation (LVQ) have been described elsewhere (131-134). GMLVQ has been applied to multi-steroid urine metabolome data in previous studies (18, 75). In brief, 24-hour excretion values of the steroid metabolites were log-transformed and subsequently z-score normalised with respect to the means and standard deviations observed in the data set. The resulting set of multi-dimensional vectors (one dimension

for each steroid), together with the class membership (NFAT, MACS-1, MACS-2, CS, hypertension yes/no, type 2 diabetes yes/no, bilateral tumours yes/no) served as input for the machine learning analysis. For each classifier experiment, the dataset was randomly split into a training and a validation set (90% and 10% of cases, respectively), which were used to evaluate the performance of GMLVQ of each experiment. Each experiment was repeated at least 30 times and the performance was measured as the average area under the receiver-operating characteristics curve (AUC-ROC). At each run, the data set was balanced independently with respect to the smallest class by undersampling the majority-class (113). The relevance of steroid metabolites for the classification was determined as the indices of the highest values of the relevance matrix diagonal on average over the multiple training processes. In this analysis, the GMLVQ implementation Version 3.0 from (134) was used.

Ordinal regression (OR): OR refers to a setting which predicts categories of an ordinal scale. Data samples are labelled by categories or ranks which are discrete and finite. These categories have a natural order, and the difference between consecutive ranks is not measured. OR problem refers to embedding samples such that they are ordered regarding their labels. When the ordering of a sample assigned to a different class is violated, an error occurs. OR problems can be addressed by regular classification or regression techniques; however, algorithms which consider the ordering of class labels are preferred because they account for the unknown and uneven distance between ordinal classes. Extension of LVQ to OR algorithms (135-138) and multi-class classification (139) are considered examples of OR. OR based on LVQ (accumulative ordinal generalised matrix learning vector quantisation, a-OGMLVQ) was proposed by Tang and Tiño (135) to solve the ordinal regression problems in a learning vector

quantisation or LVQ-based framework. a-OGMLVQ, which extends the previous algorithm pair OGMLVQ (p-OGMLVQ), has intuitive rules to update the parameters and its cost function is more realistic and reasonable. Unlike the previous methods, a-OGMLVQ considers a unified cost for all prototypes, and the bandwidth of the prototypes' weights is adapted automatically. As a result, the updated rules indicate the global ordinal relations between the prototype classes.

4.3. Results

4.3.1. *Urine steroid metabolome analysis across the spectrum of autonomous cortisol secretion*

The 24-hour urine steroid metabolite excretion measured by GC-MS and LC-MS/MS is reported in **Table 4.2** and **Table 4.3**, respectively.

Analysis by linear regression adjusted for age, sex, and BMI: There was good agreement between GC-MS and LC-MS/MS, with the two methods showing very comparable trends of urine steroid metabolite excretion across the spectrum of autonomous cortisol secretion (**Figure 4.2** and **Figure 4.3**). Compared with persons with NFAT, those with MACS-1, MACS-2, and CS showed a gradual decrease in the 24-hour urinary excretion of androgen metabolites (androsterone, etiocholanolone, dehydroepiandrosterone [DHEA], and 16α-hydroxy-DHEA) and of pregnenetriol and 17α-hydroxy-3α,5α-pregnanolone, the metabolites of the DHEA precursors 17-hydroxypregnenolone and 17α-hydroxyprogesterone, respectively. Conversely, there was a progressive increase – most pronounced in persons with CS – in the 24-hour

urinary excretion of cortisol and its metabolites, and of tetrahydro-11-deoxycortisol (THS), the metabolite of the immediate cortisol precursor 11-deoxycortisol. In persons with MACS-2 and CS, the excretion of cortisone was also increased. In persons with CS, an increased 24-hour urine excretion of the mineralocorticoid metabolites tetrahydro-11-deoxycorticosterone and tetrahydrocorticosterone was also observed.

Analysis by machine learning: OR was applied to LC-MS/MS results to classify persons with adrenal tumours and different degrees of autonomous cortisol secretion (**Figure 4.4**). The two-dimensional projection of the steroid metabolome on the first and second eigenvector of Λ shows a gradual progression across the spectrum of autonomous cortisol secretion from NFAT to CS (**Figure 4.4A**); however, there is considerable overlap across the classes, with the OR algorithm correctly classifying 38.7% of cases (**Figure 4.4B**). Glucocorticoid (cortisol, tetrahydrocortisone) and androgen metabolites (androsterone) were the most relevant steroids for the classification (**Figure 4.4C**). As a further step, GMLVQ was applied to LC-MS/MS results of persons with adrenal incidentalomas to classify NFAT and MACS in a two-class problem (**Figure 4.5**). The algorithm achieved moderate accuracy for the classification, with AUC-ROC of 0.75 and androsterone, cortisol, and 11β-hydroxyandrosterone representing the most relevant metabolites. The MACS prototype was characterised by lower steroid precursor and androgen metabolites, and higher glucocorticoid metabolites.

Table 4.2: 24-hour urine steroid excretion measured by gas chromatography-mass spectrometry (GC-MS). Steroid excretion is expressed in µg/24h and reported as median (interquartile range) in 24-h urine collected persons with non-functioning adrenal tumours (NFAT), mild autonomous cortisol secretion (MACS-1 and MACS-2 listed separately), and clinically overt Cushing's syndrome.

Metabolite	NFAT (n=289)	MACS-1 (n=212)	MACS-2 (n=72)	Cushing (n=32)
Core steroid precursor metabolites				
Pregnenediol (5PD)	283 (147-512)	217 (132-400)	220 (141-355)	347 (200-674)
Pregnanediol (PD)	144 (95-247)	119 (79-194)	124 (70-229)	351 (153-590)
Pregnenetriol (5PT)	112 (57-197)	69 (43-122)	65 (43-124)	95 (55-217)
Pregnanetriol (PT)	332 (209-549)	269 (166-440)	279 (151-462)	260 (184-554)
17α-Hydroxypregnanolone (17HP)	99 (44-178)	72 (39-152)	85 (41-155)	91 (58-218)
17α-Hydroxy-3α,5α-pregnanolone (5α-17HP)	9 (4-20)	6 (3-12)	5 (3-14)	4 (3-11)
Pregnanetriolone (PTONE)	17 (10-33)	20 (11-39)	17 (9-39)	31 (12-58)
Tetrahydro-11-deoxycortisol (THS)	99 (56-147)	103 (78-155)	152 (83-248)	325 (157-567)
Glucocorticoid metabolites				
Cortisol (F)	64 (41-100)	73 (48-109)	80 (56-142)	240 (138-492)
6β-Hydroxycortisol (6β-OHF)	106 (70-163)	132 (76-212)	166 (99-271)	500 (259-978)
Tetrahydrocortisol (THF)	1393 (980-1960)	1642 (1153-2215)	1813 (1316-2313)	4280 (2215-7114)
5α-Tetrahydrocortisol (5α-THF)	993 (585-1622)	1025 (510-1736)	702 (365-1552)	1076 (505-1643)
α-Cortol	286 (208-386)	350 (255-478)	396 (259-482)	724 (484-1215)
β-Cortol	386 (270-544)	440 (306-625)	480 (289-673)	978 (503-1590)
11β-Hydroxyetiocholanolone (11β-OHEt)	279 (129-443)	304 (129-534)	407 (122-654)	624 (243-1387)
Cortisone (E)	88 (62-128)	95 (69-131)	104 (73-147)	216 (158-330)
Tetrahydrocortisone (THE)	2395 (1775-3394)	2445 (1554-3364)	2401 (1570-3531)	4593 (2466-7318)
α-Cortolone	973 (680-1291)	970 (714-1361)	1044 (732-1470)	1957 (1249-2420)
β-Cortolone	487 (349-670)	485 (363-741)	503 (327-735)	963 (442-1323)
11-Ketoetiocholanolone (11-ketoEt)	319 (176-490)	316 (158-509)	347 (140-581)	388 (207-843)
Androgen and androgen precursor metabolites				
Dehydroepiandrosterone (DHEA)	68 (32-171)	34 (20-72)	30 (20-70)	26 (14-64)
16α-Hydroxy-DHEA (16α-DHEA)	138 (56-365)	75 (40-180)	81 (38-192)	52 (23-110)
Androsterone (An)	625 (289-1117)	288 (129-644)	239 (90-482)	195 (75-391)
Etiocholanolone (Et)	666 (342-1209)	417 (219-742)	418 (179-865)	394 (217-1137)
11β-Hydroxyandrosterone (11β-OHAn)	383 (259-593)	382 (239-680)	369 (216-752)	427 (255-832)
Mineralocorticoid and mineralocorticoid precursor metabolites				
Tetrahydro-11-deoxycorticosterone (THDOC)	13 (9-21)	11 (8-19)	13 (8-23)	23 (12-45)
5α-Tetrahydro-11-deoxycorticosterone (5α-THDOC)	3 (2-6)	3 (2-5)	3 (2-6)	4 (2-7)
Tetrahydro-11-dehydrocorticosterone (THA)	87 (58-128)	78 (51-124)	66 (38-115)	85 (49-155)
5α-Tetrahydro-11-dehydrocorticosterone (5α-THA)	70 (49-107)	73 (46-100)	56 (44-80)	75 (35-145)
Tetrahydrocorticosterone (THB)	99 (66-162)	102 (65-153)	100 (61-167)	175 (101-330)
5α-Tetrahydrocorticosterone (5α-THB)	210 (139-352)	195 (108-365)	152 (69-267)	169 (78-301)
3α5β-Tetrahydroaldosterone (THAldo)	27 (19-39)	30 (20-40)	32 (17-44)	41 (21-54)

Table 4.3: 24-hour urine steroid excretion measured by liquid chromatography-tandem mass spectrometry (LC-MS/MS). Steroid excretion is expressed in µg/24h and reported as median (interquartile range) in 24-h urine collected by persons with non-functioning adrenal tumours (NFAT), mild autonomous cortisol secretion (MACS-1 and MACS-2 listed separately), and clinically overt Cushing's syndrome.

Metabolite	NFAT (n=649)	MACS-1 (n=451)	MACS-2 (n=140)	Cushing (n=65)
Core steroid precursor metabolites				
Pregnenediol (5PD)	81 (55-144)	64 (55-106)	56 (55-105)	89 (55-158)
Pregnanediol (PD)	328 (190-597)	281 (157-479)	254 (149-503)	536 (206-813)
Pregnenetriol (5PT)	92 (49-177)	63 (43-126)	56 (43-101)	71 (43-115)
Pregnanetriol (PT)	333 (179-567)	257 (143-465)	210 (118-452)	222 (145-368)
17α-Hydroxypregnanolone (17HP)	69 (39-135)	63 (37-127)	51 (32-108)	74 (45-116)
Tetrahydro-11-deoxycortisol (THS)	141 (87-222)	142 (91-239)	177 (90-271)	317 (181-500)
Glucocorticoid metabolites				
Cortisol (F)	45 (28-65)	54 (32-82)	57 (33-92)	151 (76-344)
Tetrahydrocortisol (THF)	1362 (914-2011)	1460 (888-2165)	1563 (998-2293)	3163 (1466-6425)
5α-Tetrahydrocortisol (5α-THF)	568 (287-986)	543 (267-947)	506 (206-823)	642 (315-1088)
11β-Hydroxyetiocholanolone (11β-OHEt)	305 (120-541)	335 (135-613)	413 (156-769)	602 (182-1310)
Cortisone (E)	73 (47-105)	76 (47-108)	82 (49-115)	141 (95-317)
Tetrahydrocortisone (THE)	2223 (1457-3409)	2181 (1334-3329)	2323 (1296-3170)	3812 (1939-5865)
β-Cortolone	634 (401-964)	624 (389-989)	658 (341-937)	998 (622-1632)
Androgen and androgen precursor metabolites				
Dehydroepiandrosterone (DHEA)	26 (22-54)	22 (22-30)	22 (22-24)	22 (22-22)
Androsterone (An)	577 (258-1034)	290 (127-642)	191 (97-474)	167 (61-314)
Etiocholanolone (Et)	540 (264-1073)	364 (167-747)	329 (144-689)	331 (221-725)
11β-Hydroxyandrosterone (11β-OHAn)	541 (292-874)	551 (306-973)	523 (254-778)	524 (295-847)

Figure 4.2: 24-hour urinary steroid excretion measured by GC-MS in persons with possible mild autonomous cortisol secretion (MACS-1), definitive mild autonomous cortisol secretion (MACS-2), and clinically overt Cushing's syndrome compared to non-functioning adrenal tumours (NFAT). The urinary excretion of each steroid metabolite in persons with MACS-1, MACS-2, and adrenal CS was compared with values in persons with NFAT by using a linear regression model with the log-transformed steroid metabolite as the outcome (adjusted for age, sex, and body mass index). Associations between the log-transformed outcome and the variable of interest are reported as sympercents (mean percentage change and 95% confidence interval).

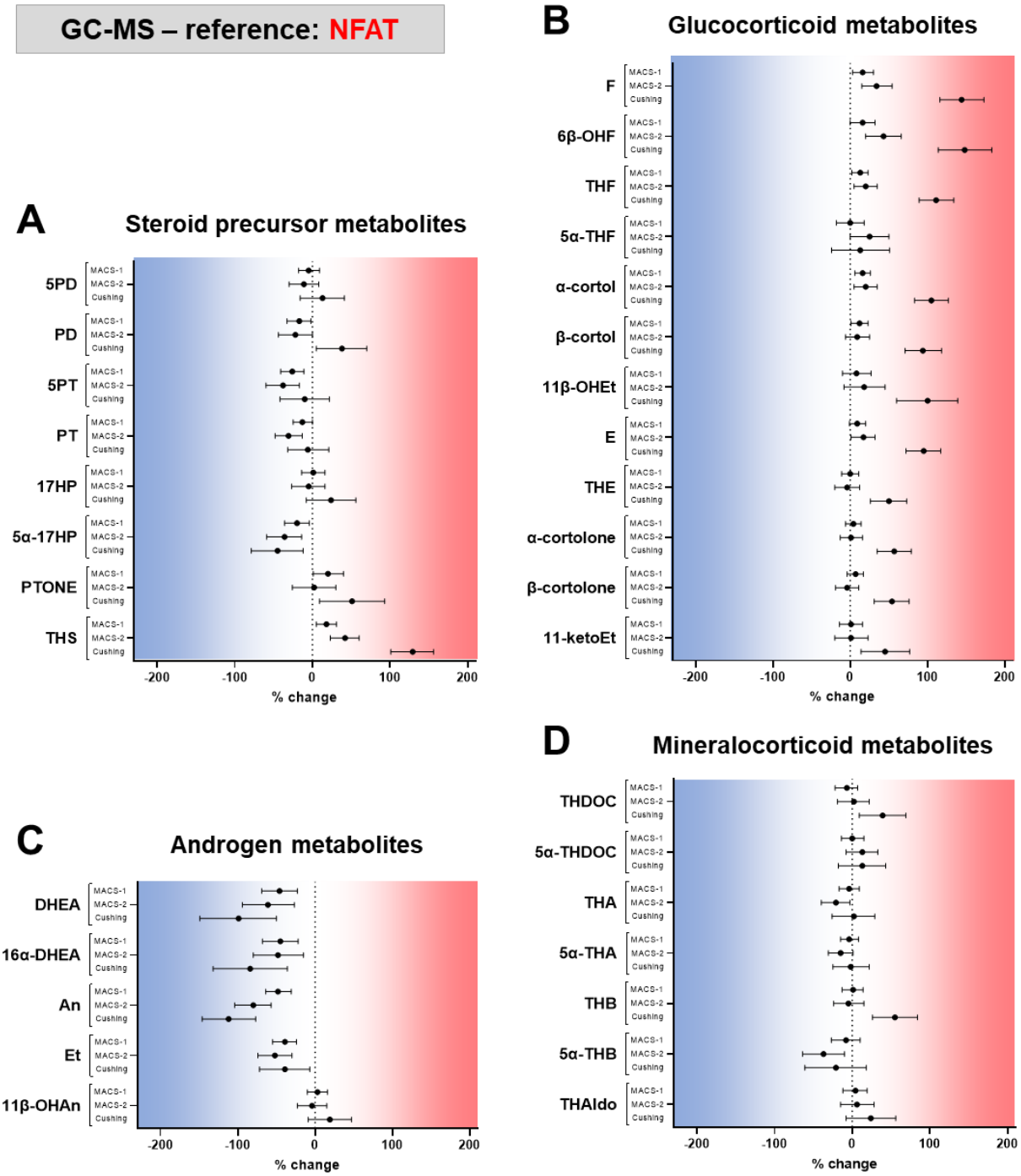

Figure 4.3: 24-hour urinary steroid excretion measured by LC-MS/MS in persons with possible mild autonomous cortisol secretion (MACS-1), definitive mild autonomous cortisol secretion (MACS-2), and clinically overt Cushing's syndrome compared to non-functioning adrenal tumours (NFAT). The urinary excretion of each steroid metabolite in persons with MACS-1, MACS-2, and adrenal CS was compared with values in persons with NFAT by using a linear regression model with the log-transformed steroid metabolite as the outcome (adjusted for age, sex, and body mass index). Associations between the log-transformed outcome and the variable of interest are reported as sympercents (mean percentage change and 95% confidence interval).

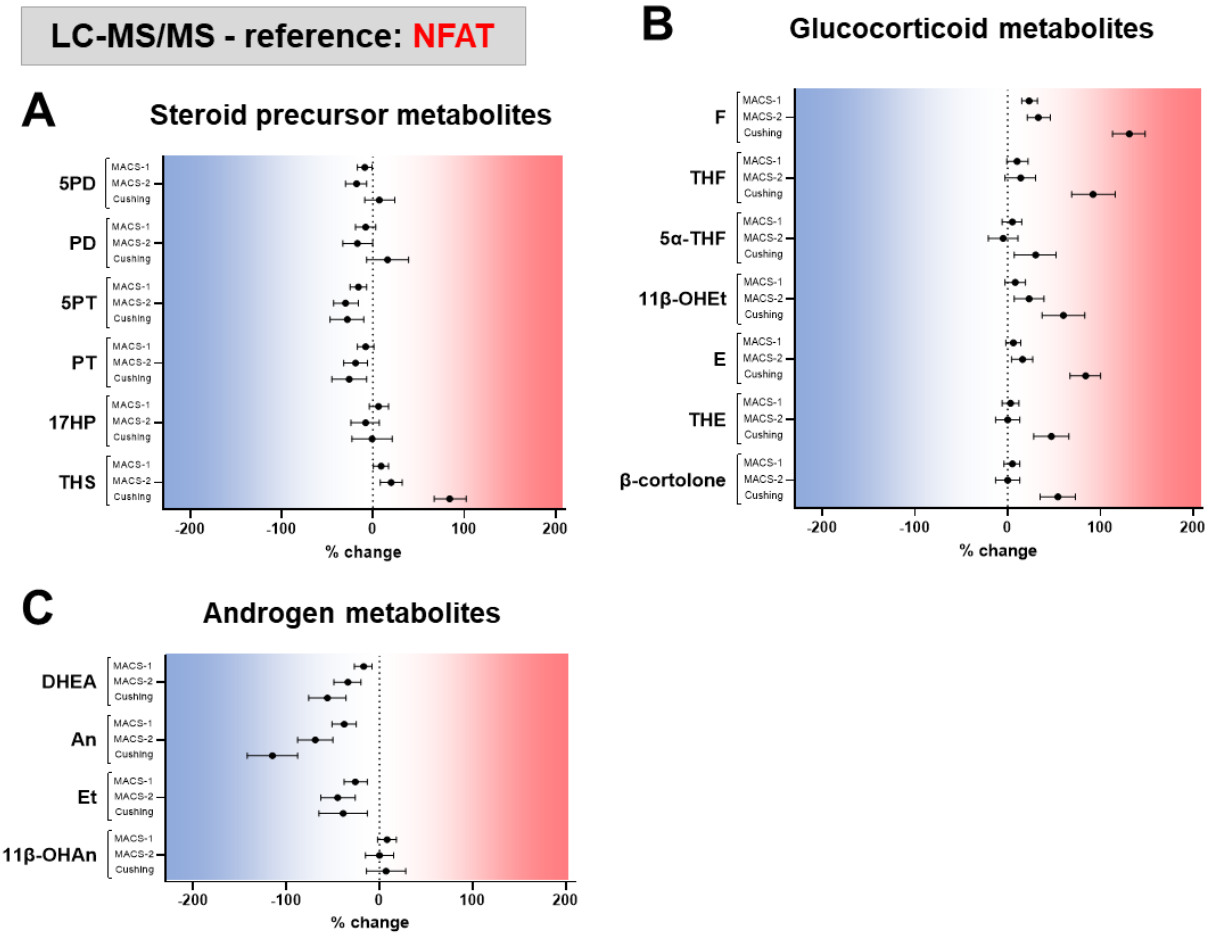

Figure 4.4: Ordinal regression to classify persons with non-functioning adrenal tumours (NFAT), possible mild autonomous cortisol secretion (MACS-1), definitive mild autonomous cortisol secretion (MACS-2), and clinically overt Cushing's syndrome based on 24-hour urinary steroid excretion. Urine steroid metabolites were measured by LC-MS/MS. The results are averaged over 30 selected independent runs. Panel A: two-dimensional embedding of the samples; each dot is the projection of the entire steroid metabolome of a person with adrenal tumours; the big circles represent the class prototypes. Panel B: confusion matrix for multi-class classification (class 1, NFAT; class 2, MACS-1; class 3, MACS-2; class 4, Cushing) of the predicted class (output class) and the true class (target class); the number of observations and the percentage of the total number of observations are shown in each cell; the column on the far right shows the positive predictive value and false discovery rate for each class; the row at the bottom shows the true positive and false negative rates; the cell in the bottom right reports the overall accuracy. Panel C: relevance (mean ± standard deviation) of each steroid metabolite for the multi-class classification; metabolites on the left-hand side of the graph are more relevant for the classification.

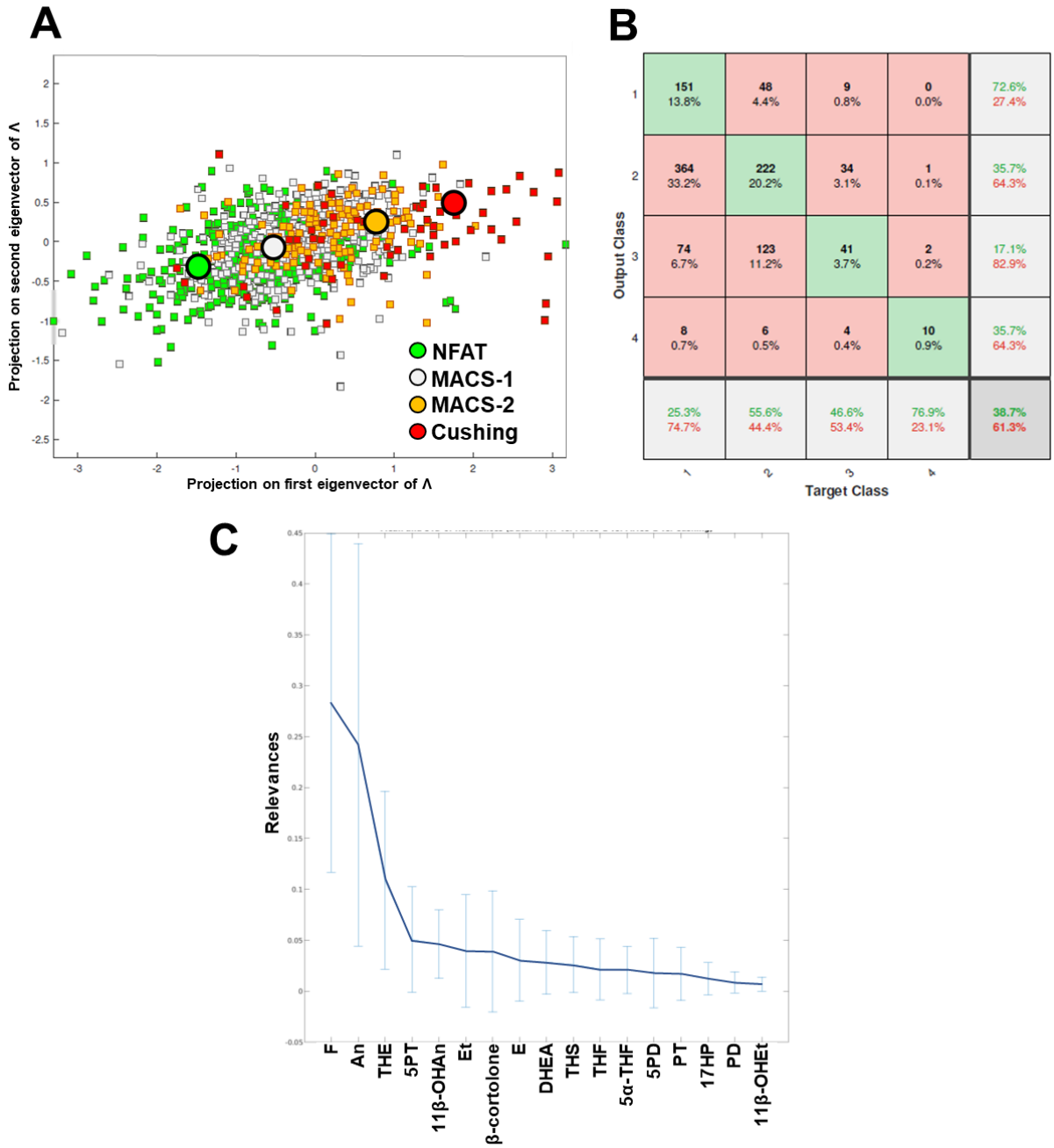

Figure 4.5: Generalised matrix learning vector quantisation to classify persons with non-functioning adrenal tumours (NFAT) and mild autonomous cortisol secretion (MACS) based on 24-hour urinary steroid excretion. Urine steroid metabolites were measured by LC-MS/MS. The results are averaged over 30 selected independent runs. Data of persons with possible MACS (MACS-1) and definitive MACS (MACS-2) have been combined. Panel A: two-dimensional embedding of the samples; each dot is the projection of the entire steroid metabolome of a person with adrenal tumours; the big circles represent the class prototypes. Panel B: training receiver operating characteristic (ROC) curve showing the performance of a classification model. Panel C: prototype vectors for the 17 steroid metabolites of the two classes (1, 5PD; 2, PD; 3, 5PT; 4, PT; 5, 17HP; 6, THS; 7, F; 8, THF; 9, 5α-THF; 10, 11β-OHEt; 11, E; 12, THE; 13, β-cortolone; 14, DHEA; 15, An; 16, Et; 17, 11β-OHAn); columns above and below the 0 represent increased or decreased steroid excretion relative to the other class, respectively, and the height of the column indicates the degree of the change. Panel D: relevance (mean ± standard deviation) of each steroid metabolite for the multi-class classification; metabolites on the left-hand side of the graph are more relevant for the classification.

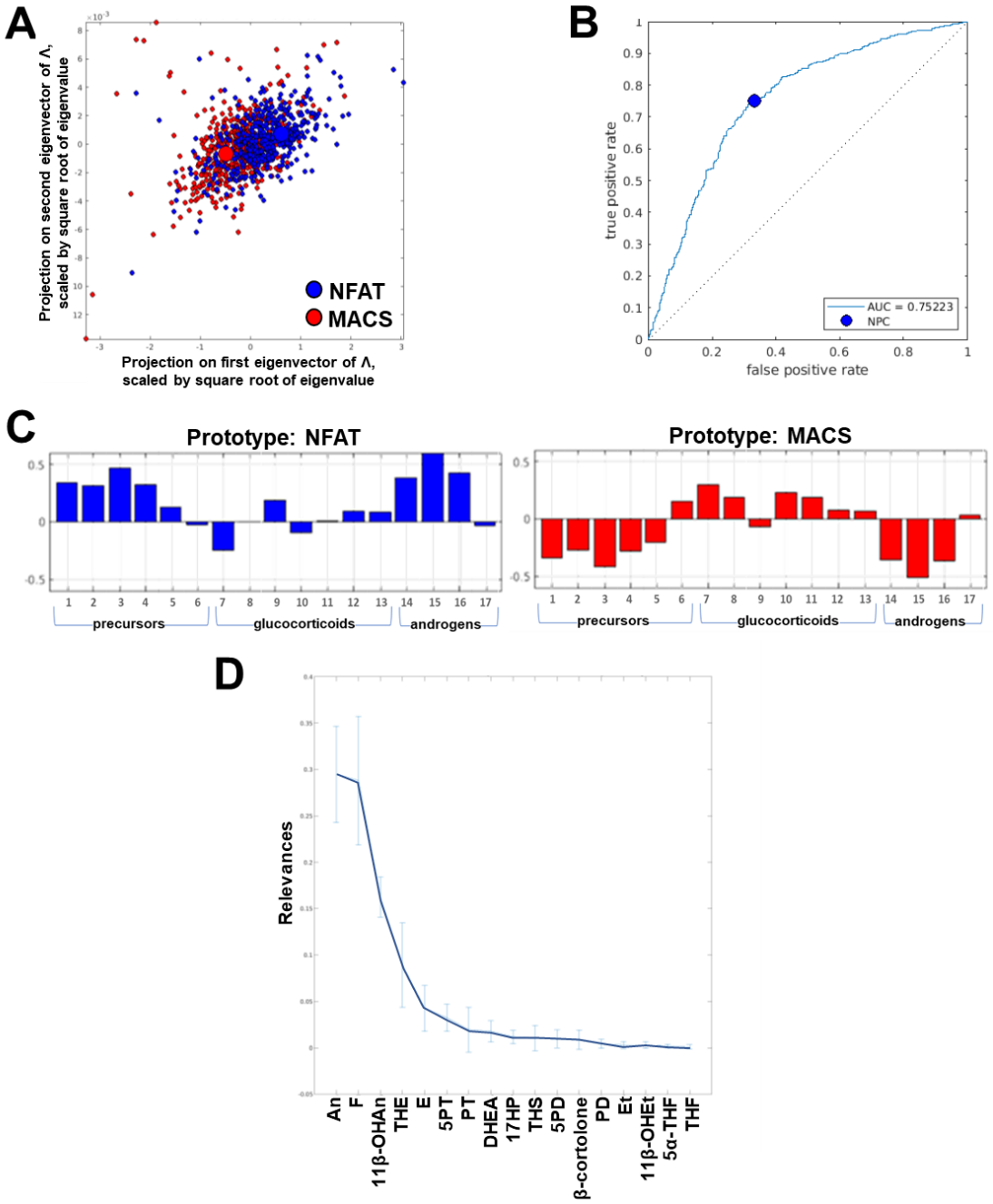

4.3.2. *Urine steroid metabolome analysis and clinical outcomes*

In **Chapter 3** I showed that persons with MACS carried an increased risk and severity of hypertension and type 2 diabetes and were more likely to present with bilateral adrenal tumours. Moreover, persons with MACS and bilateral tumours had a higher cardiometabolic burden and were more likely to present with larger tumours, lower ACTH, and higher 24-hour urinary free cortisol excretion. Therefore, I investigated whether the urine steroid metabolome can be used for metabolic stratification of persons with adrenal tumours. To this end, the urine steroid metabolome was dichotomised based on clinical outcomes (hypertension, type 2 diabetes, and bilateral adrenal tumours; **Table 4.1** and **Figures 4.6-4.14**), with a focus on persons with incidentally discovered adrenal tumours (NFAT and MACS). The analysis was restricted to LC-MS/MS urine steroid metabolome data, which were available for the entire EURINE-ACT cohort.

Hypertension: Persons with NFAT and MACS with hypertension tended to have increased urine glucocorticoid metabolite excretion, which was more pronounced in MACS (**Figure 4.6**). Interestingly, there was higher androgen metabolite excretion in persons with hypertension, especially those with abnormal 1mg-DST results, with 11β-hydroxyandrosterone being among the top markers identified by GMLVQ (**Figures 4.7** and **4.8**).

Type 2 diabetes: Glucocorticoid metabolite excretion was not significantly increased in persons with type 2 diabetes. However, 11β-hydroxyandrosterone excretion was increased (**Figure 4.9**) and – again – this was one of the top markers to classify persons with adrenal incidentalomas and type 2 diabetes by GMLVQ (**Figures 4.10** and **4.11**).

Bilateral adrenal tumours: Glucocorticoid metabolite excretion was increased in persons with bilateral adrenal tumours, particularly in MACS (**Figure 4.12**). There was also a significantly increased excretion of the glucocorticoid precursor THS. These results were mirrored by GMLVQ, with the algorithm prototypes of persons with bilateral tumours characterised by higher glucocorticoid metabolites (**Figures 4.13** and **4.14**) and TSH representing the top marker to classify persons with MACS and bilateral tumours (**Figure 4.14D**).

Figure 4.6: 24-hour urinary steroid excretion in persons with non-functioning adrenal tumours (NFAT) and mild autonomous cortisol secretion (MACS), with and without hypertension. Steroid metabolites were measured by LC-MS/MS. The urinary excretion of each metabolite in persons with hypertension was compared to persons without hypertension (reference) by using a linear regression model with the log-transformed steroid metabolite as the outcome (adjusted for age, sex, and body mass index). Associations between the log-transformed outcome and the variable of interest are reported as sympercents (mean percentage change and 95% confidence interval). Persons with MACS were analysed together with NFAT (left panels) and separately (right panels).

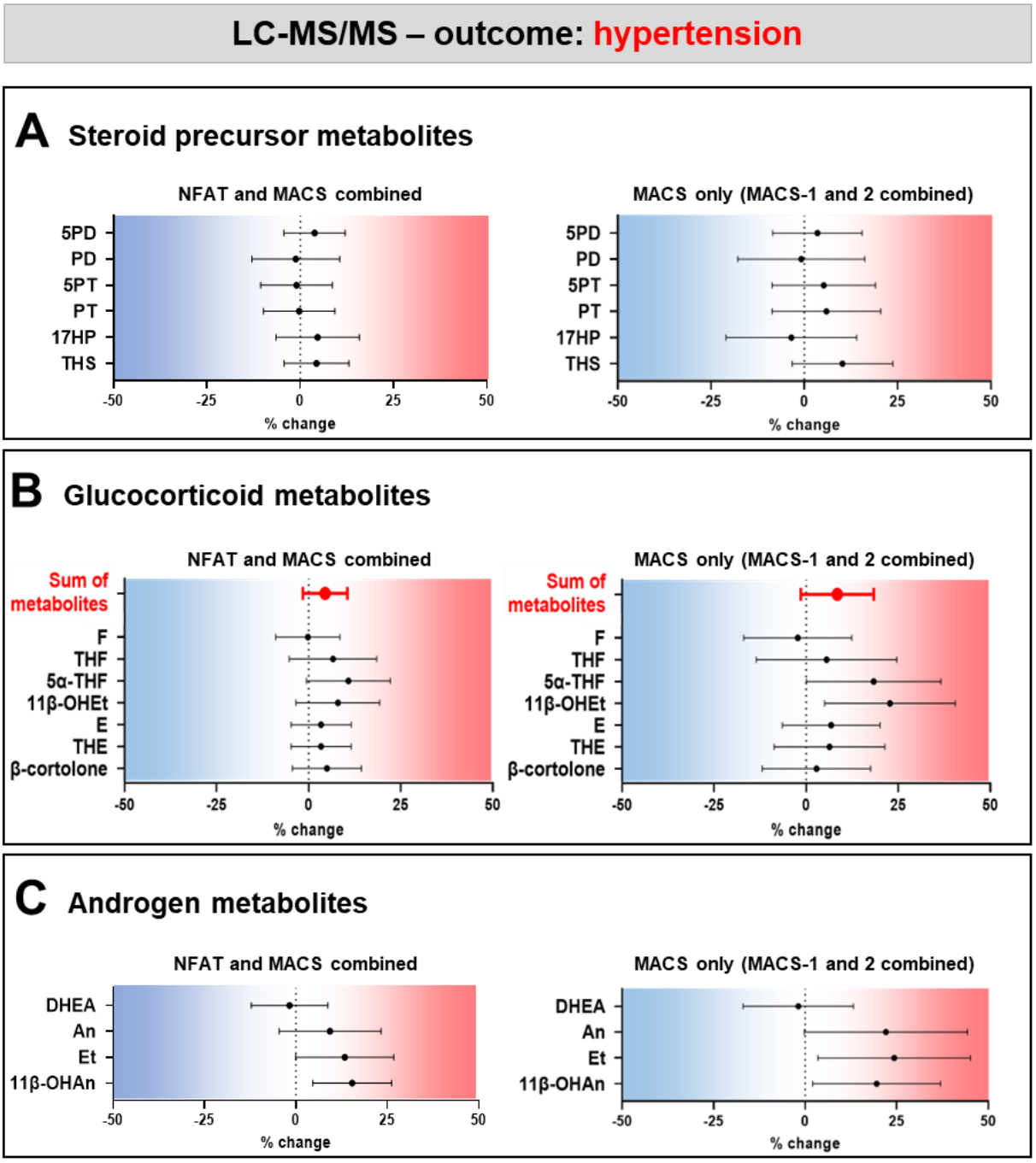

Figure 4.7: Generalised matrix learning vector quantisation to classify persons with adrenal incidentalomas, with and without hypertension, based on 24-hour urinary steroid excretion. Urine steroid metabolites were measured by LC-MS/MS. The results are averaged over 30 selected independent runs. Data of persons with non-functioning adrenal tumours (NFAT) and mild autonomous cortisol secretion (MACS) were combined. Panel A: two-dimensional embedding of the samples; each dot is the projection of the entire steroid metabolome of a person with adrenal tumours; the big circles represent the class prototypes. Panel B: training receiver operating characteristic (ROC) curve showing the performance of a classification model. Panel C: prototype vectors for the 17 steroid metabolites of the two classes (1, 5PD; 2, PD; 3, 5PT; 4, PT; 5, 17HP; 6, THS; 7, F; 8, THF; 9, 5α-THF; 10, 11β-OHEt; 11, E; 12, THE; 13, β-cortolone; 14, DHEA; 15, An; 16, Et; 17, 11β-OHAn); columns above and below the 0 represent increased or decreased steroid excretion relative to the other class, respectively, and the height of the column indicates the degree of the change. Panel D: relevance (mean ± standard deviation) of each steroid metabolite for the multi-class classification; metabolites on the left-hand side of the graph are more relevant for the classification.

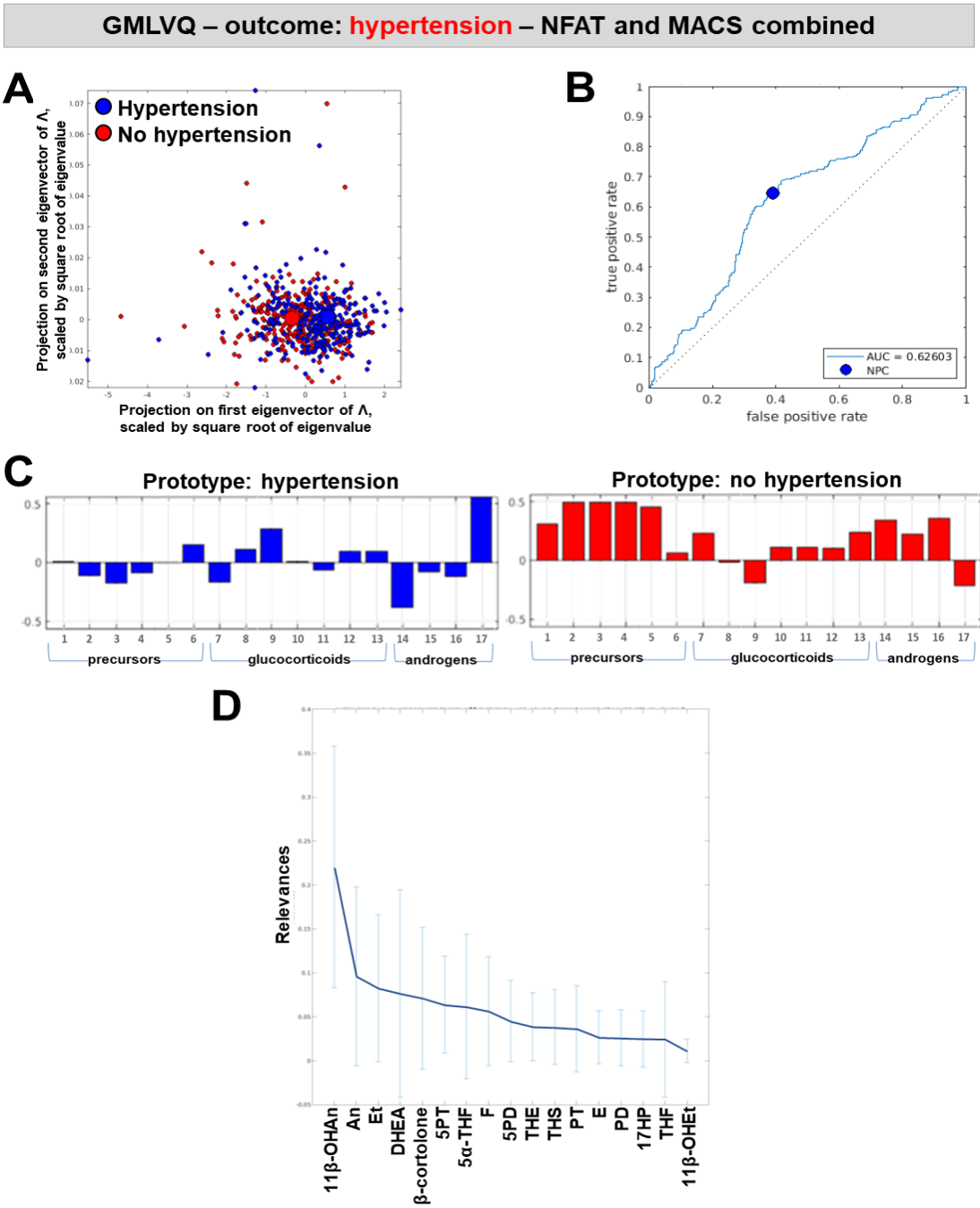

Figure 4.8: Generalised matrix learning vector quantisation to classify persons with mild autonomous cortisol secretion (MACS), with and without hypertension, based on 24-hour urinary steroid excretion. Urine steroid metabolites were measured by LC-MS/MS. The results are averaged over 30 selected independent runs. Data of persons with possible and definitive MACS were combined. Panel A: two-dimensional embedding of the samples; each dot is the projection of the entire steroid metabolome of a person with adrenal tumours; the big circles represent the class prototypes. Panel B: training receiver operating characteristic (ROC) curve showing the performance of a classification model. Panel C: prototype vectors for the 17 steroid metabolites of the two classes (1, 5PD; 2, PD; 3, 5PT; 4, PT; 5, 17HP; 6, THS; 7, F; 8, THF; 9, 5α-THF; 10, 11β-OHEt; 11, E; 12, THE; 13, β-cortolone; 14, DHEA; 15, An; 16, Et; 17, 11β-OHAn); columns above and below the 0 represent increased or decreased steroid excretion relative to the other class, respectively, and the height of the column indicates the degree of the change. Panel D: relevance (mean ± standard deviation) of each steroid metabolite for the multi-class classification; metabolites on the left-hand side of the graph are more relevant for the classification.

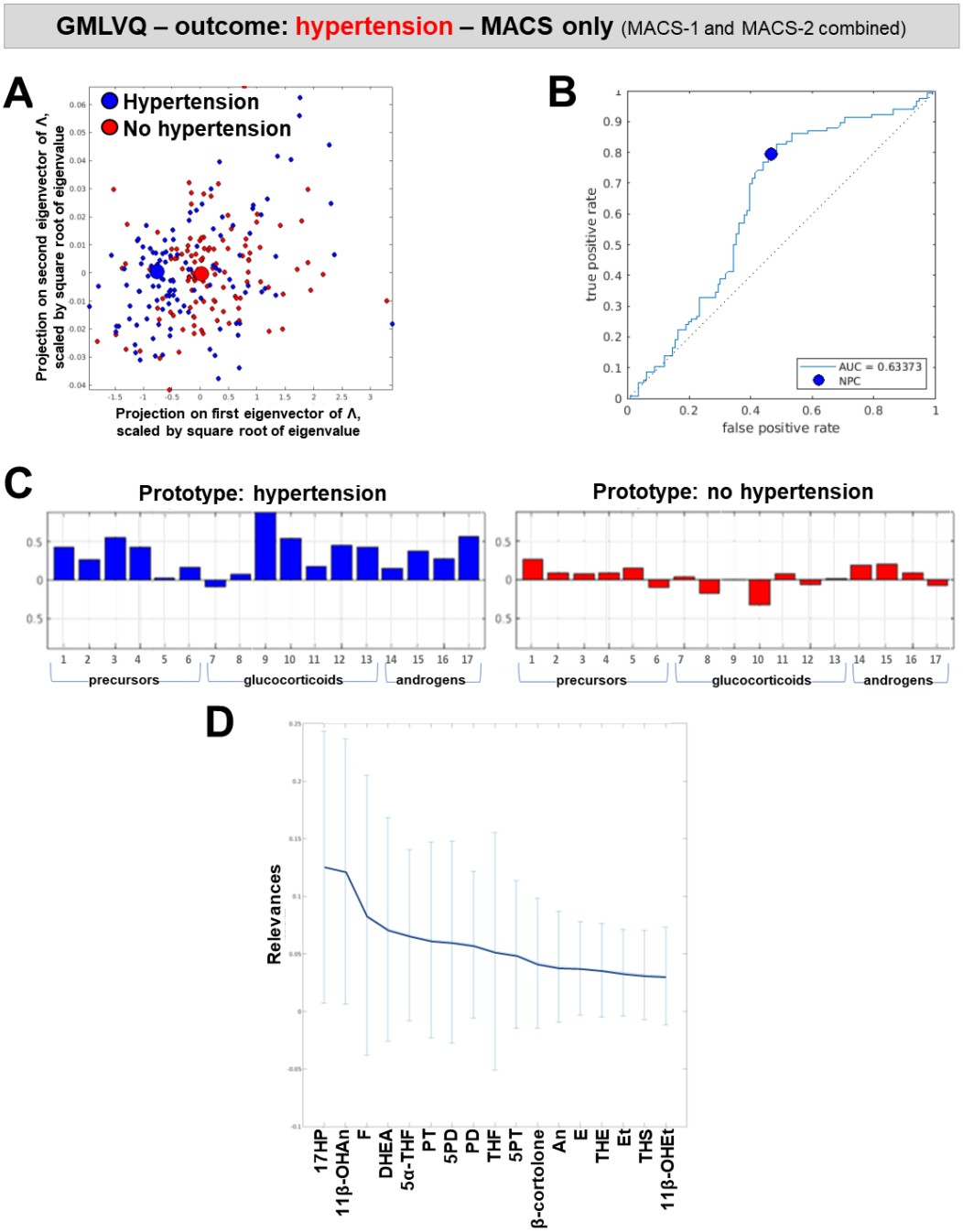

Figure 4.9: 24-hour urinary steroid excretion in persons with non-functioning adrenal tumours (NFAT) and mild autonomous cortisol secretion (MACS), with and without type 2 diabetes. Steroid metabolites were measured by LC-MS/MS. The urinary excretion of each metabolite in persons with type 2 diabetes was compared to persons without type 2 diabetes (reference) by using a linear regression model with the log-transformed steroid metabolite as the outcome (adjusted for age, sex, and body mass index). Associations between the log-transformed outcome and the variable of interest are reported as sympercents (mean percentage change and 95% confidence interval). Persons with MACS were analysed together with NFAT (left panels) and separately (right panels).

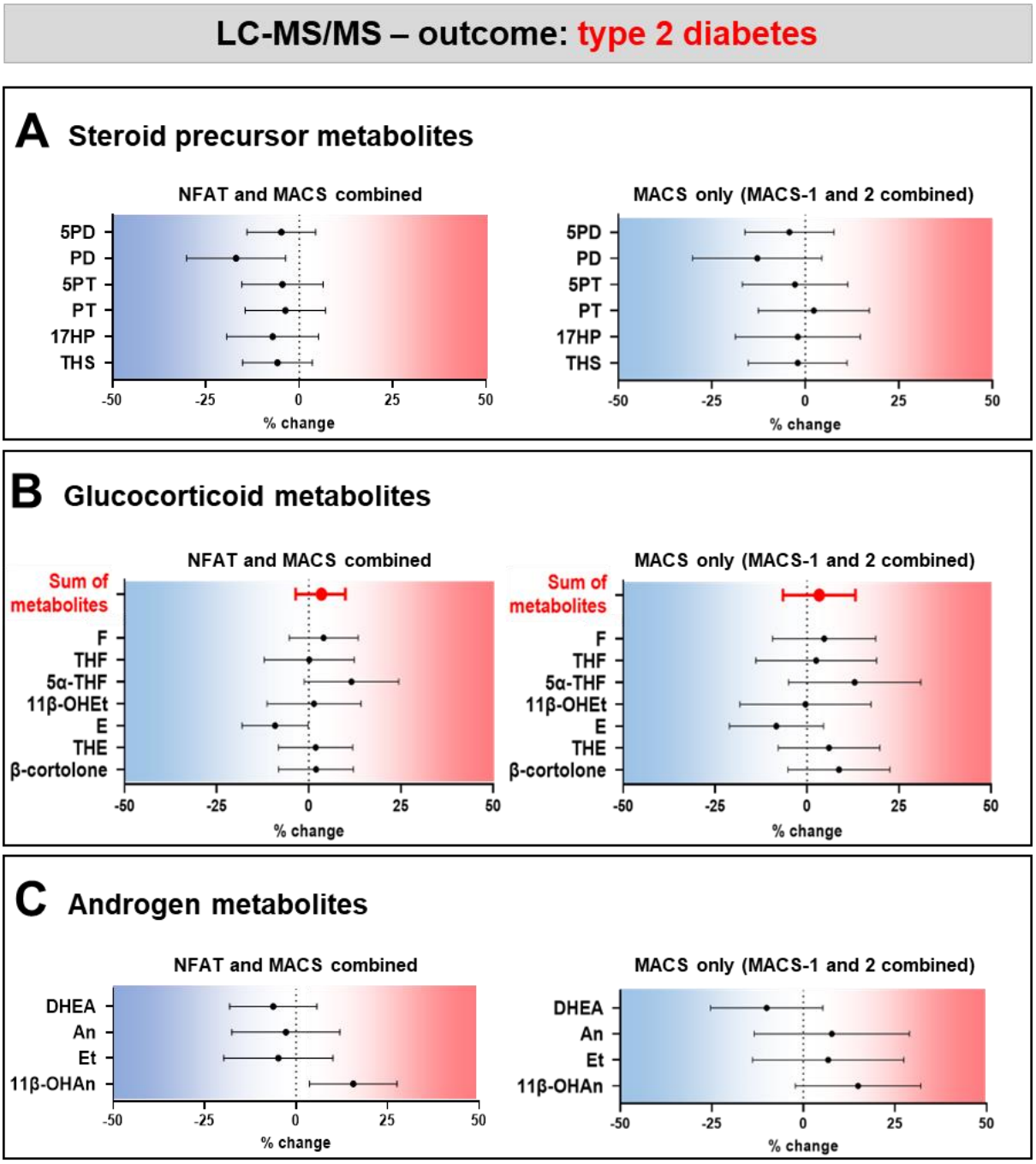

Figure 4.10: Generalised matrix learning vector quantisation to classify persons with adrenal incidentalomas, with and without type 2 diabetes, based on 24-hour urinary steroid excretion. Urine steroid metabolites were measured by LC-MS/MS. The results are averaged over 30 selected independent runs. Data of persons with non-functioning adrenal tumours (NFAT) and mild autonomous cortisol secretion (MACS) were combined. Panel A: two-dimensional embedding of the samples; each dot is the projection of the entire steroid metabolome of a person with adrenal tumours; the big circles represent the class prototypes. Panel B: training receiver operating characteristic (ROC) curve showing the performance of a classification model. Panel C: prototype vectors for the 17 steroid metabolites of the two classes (1, 5PD; 2, PD; 3, 5PT; 4, PT; 5, 17HP; 6, THS; 7, F; 8, THF; 9, 5α-THF; 10, 11β-OHEt; 11, E; 12, THE; 13, β-cortolone; 14, DHEA; 15, An; 16, Et; 17, 11β-OHAn); columns above and below the 0 represent increased or decreased steroid excretion relative to the other class, respectively, and the height of the column indicates the degree of the change. Panel D: relevance (mean ± standard deviation) of each steroid metabolite for the multi-class classification; metabolites on the left-hand side of the graph are more relevant for the classification.

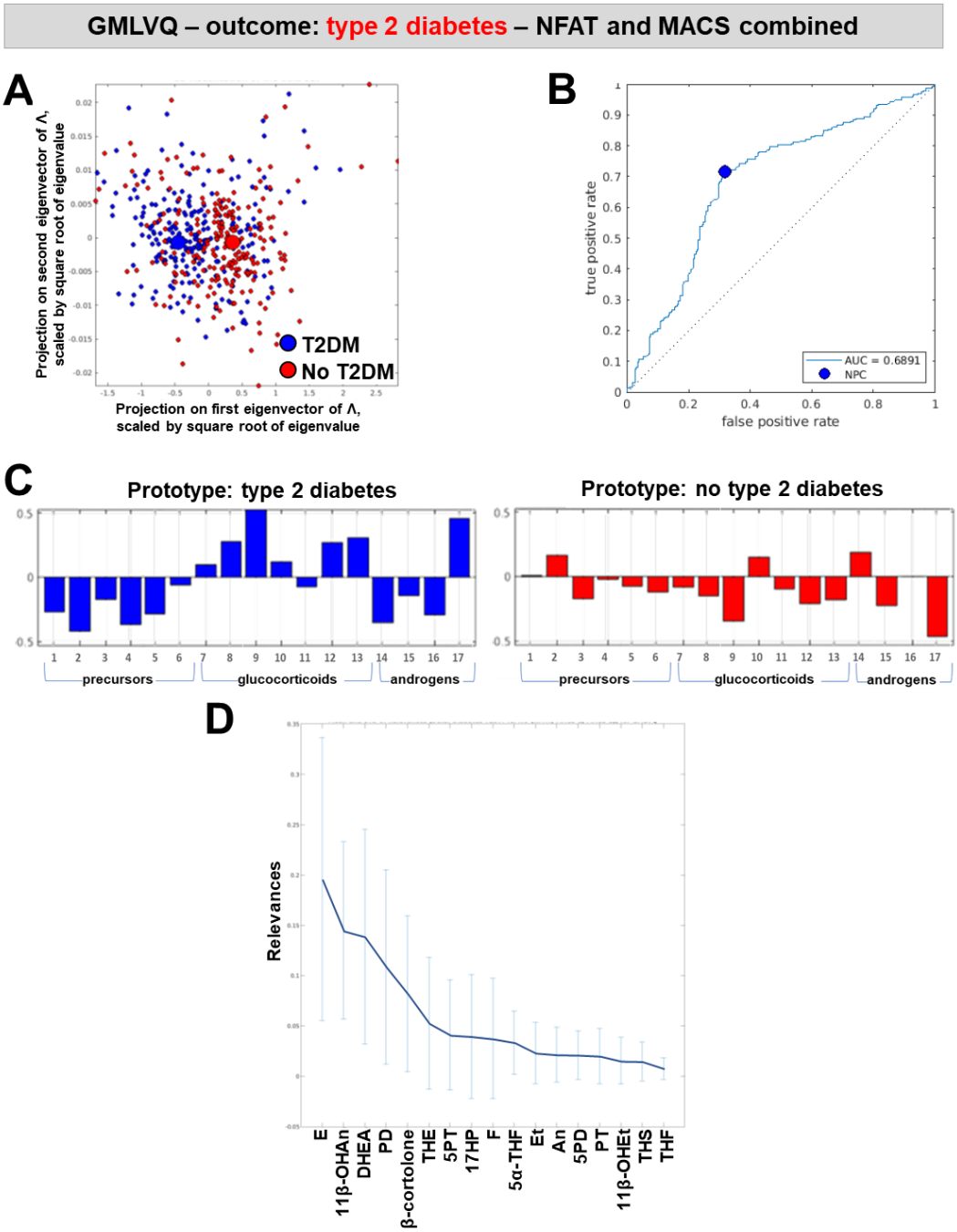

Figure 4.11: Generalised matrix learning vector quantisation to classify persons with mild autonomous cortisol secretion (MACS), with and without type 2 diabetes, based on 24-hour urinary steroid excretion. Urine steroid metabolites were measured by LC-MS/MS. The results are averaged over 30 selected independent runs. Data of persons with possible and definitive MACS were combined. Panel A: two-dimensional embedding of the samples; each dot is the projection of the entire steroid metabolome of a person with adrenal tumours; the big circles represent the class prototypes. Panel B: training receiver operating characteristic (ROC) curve showing the performance of a classification model. Panel C: prototype vectors for the 17 steroid metabolites of the two classes (1, 5PD; 2, PD; 3, 5PT; 4, PT; 5, 17HP; 6, THS; 7, F; 8, THF; 9, 5α-THF; 10, 11β-OHEt; 11, E; 12, THE; 13, β-cortolone; 14, DHEA; 15, An; 16, Et; 17, 11β-OHAn); columns above and below the 0 represent increased or decreased steroid excretion relative to the other class, respectively, and the height of the column indicates the degree of the change. Panel D: relevance (mean ± standard deviation) of each steroid metabolite for the multi-class classification; metabolites on the left-hand side of the graph are more relevant for the classification.

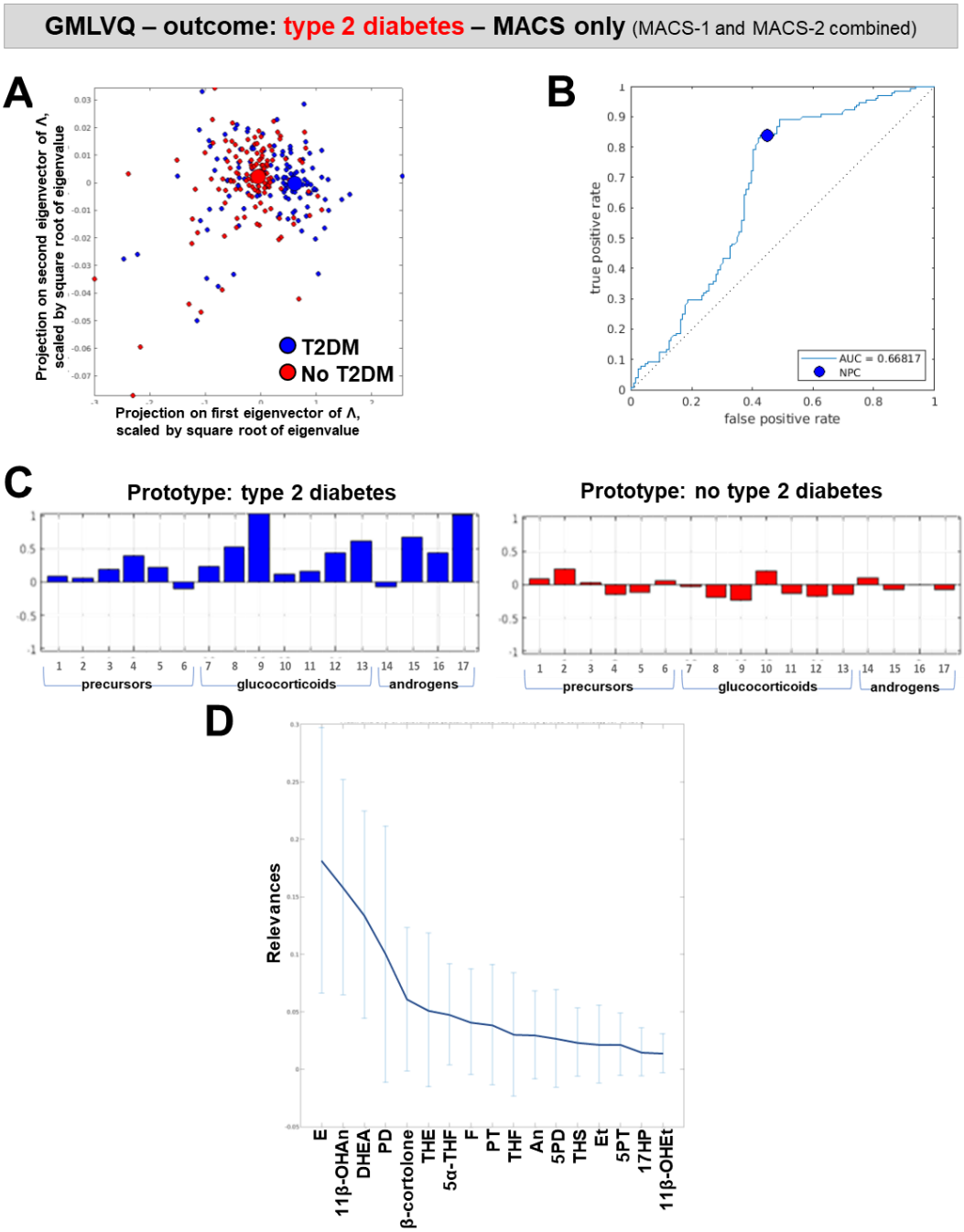

Figure 4.12: 24-hour urinary steroid excretion in persons with non-functioning adrenal tumours (NFAT) and mild autonomous cortisol secretion (MACS), with and without bilateral adrenal masses. Steroid metabolites were measured by LC-MS/MS. The urinary excretion of each metabolite in persons with bilateral adrenal masses was compared to persons with unilateral masses (reference) by using a linear regression model with the log-transformed steroid metabolite as the outcome (adjusted for age, sex, and body mass index). Associations between the log-transformed outcome and the variable of interest are reported as sympercents (mean percentage change and 95% confidence interval). Persons with MACS were analysed together with NFAT (left panels) and separately (right panels).

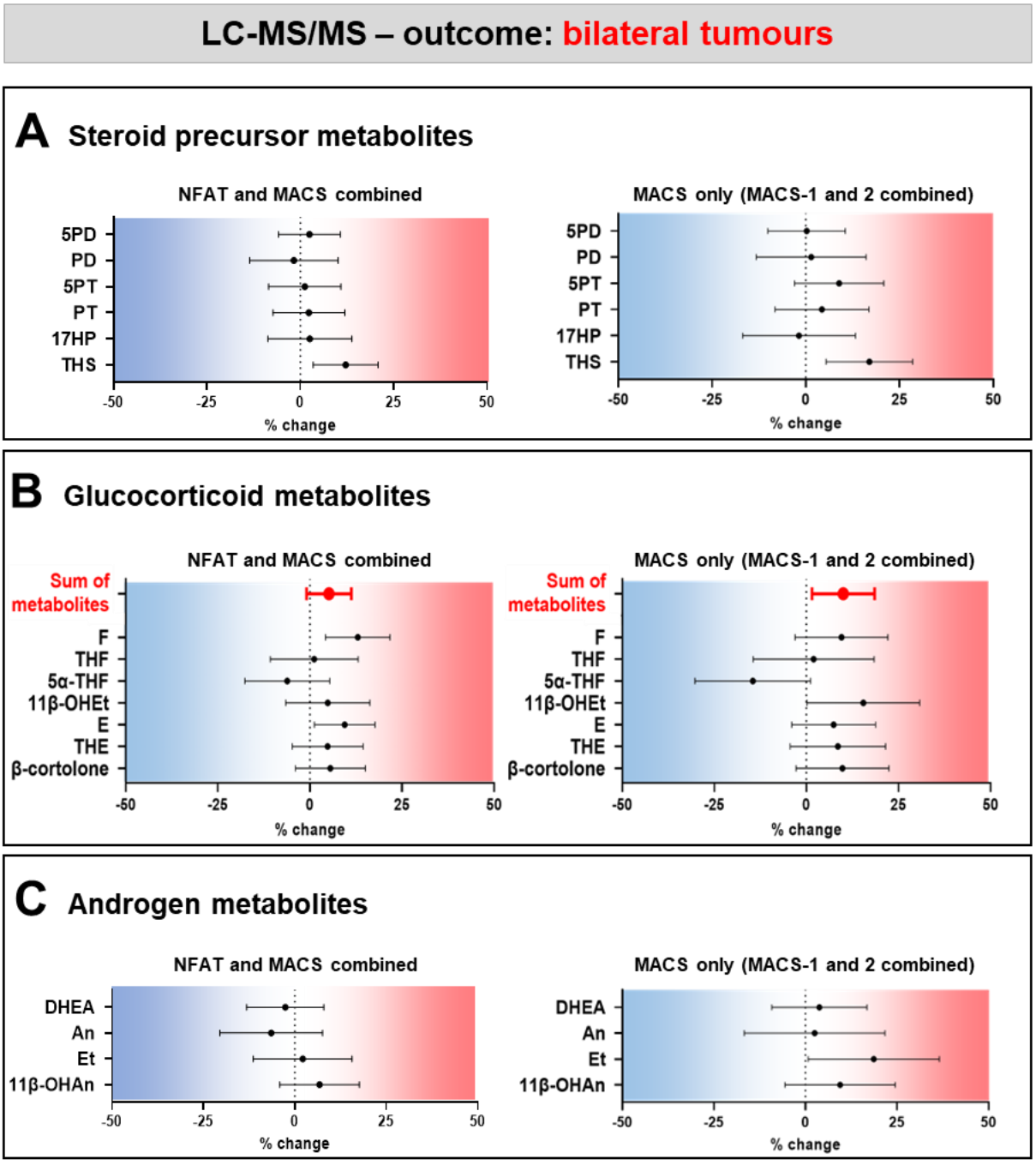

Figure 4.13: Generalised matrix learning vector quantisation to classify persons with adrenal incidentalomas, with and without bilateral adrenal tumours, based on 24-hour urinary steroid excretion. Urine steroid metabolites were measured by LC-MS/MS. The results are averaged over 30 selected independent runs. Data of persons with non-functioning adrenal tumours (NFAT) and mild autonomous cortisol secretion (MACS) were combined. Panel A: two-dimensional embedding of the samples; each dot is the projection of the entire steroid metabolome of a person with adrenal tumours; the big circles represent the class prototypes. Panel B: training receiver operating characteristic (ROC) curve showing the performance of a classification model. Panel C: prototype vectors for the 17 steroid metabolites of the two classes (1, 5PD; 2, PD; 3, 5PT; 4, PT; 5, 17HP; 6, THS; 7, F; 8, THF; 9, 5α-THF; 10, 11β-OHEt; 11, E; 12, THE; 13, β-cortolone; 14, DHEA; 15, An; 16, Et; 17, 11β-OHAn); columns above and below the 0 represent increased or decreased steroid excretion relative to the other class, respectively, and the height of the column indicates the degree of the change. Panel D: relevance (mean ± standard deviation) of each steroid metabolite for the multi-class classification; metabolites on the left-hand side of the graph are more relevant for the classification.

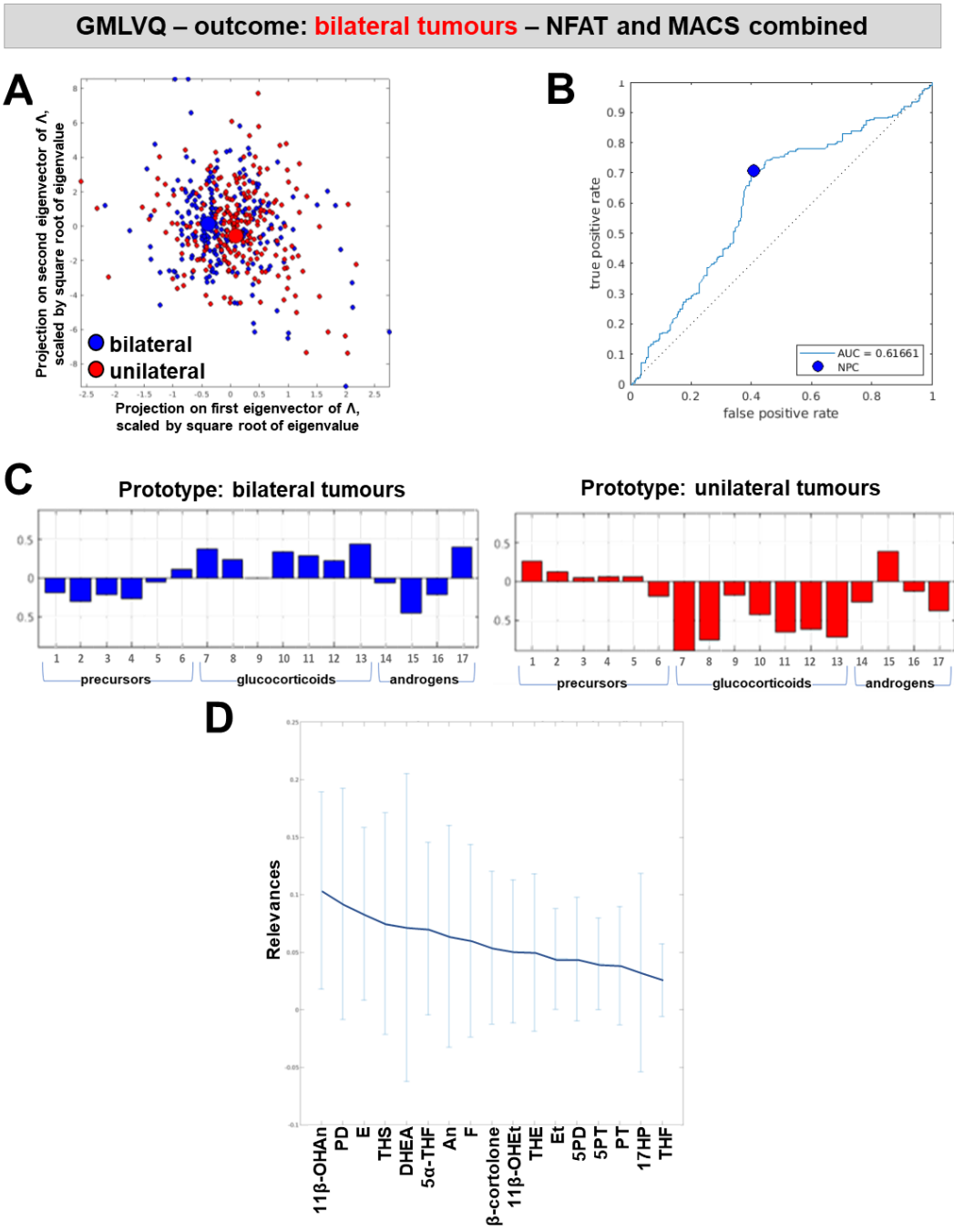

Figure 4.14: Generalised matrix learning vector quantisation to classify persons with mild autonomous cortisol secretion (MACS), with and without bilateral adrenal tumours, based on 24-hour urinary steroid excretion. Urine steroid metabolites were measured by LC-MS/MS. The results are averaged over 30 selected independent runs. Data of persons with possible and definitive MACS were combined. Panel A: two-dimensional embedding of the samples; each dot is the projection of the entire steroid metabolome of a person with adrenal tumours; the big circles represent the class prototypes. Panel B: training receiver operating characteristic (ROC) curve showing the performance of a classification model. Panel C: prototype vectors for the 17 steroid metabolites of the two classes (1, 5PD; 2, PD; 3, 5PT; 4, PT; 5, 17HP; 6, THS; 7, F; 8, THF; 9, 5α-THF; 10, 11β-OHEt; 11, E; 12, THE; 13, β-cortolone; 14, DHEA; 15, An; 16, Et; 17, 11β-OHAn); columns above and below the 0 represent increased or decreased steroid excretion relative to the other class, respectively, and the height of the column indicates the degree of the change. Panel D: relevance (mean ± standard deviation) of each steroid metabolite for the multi-class classification; metabolites on the left-hand side of the graph are more relevant for the classification.

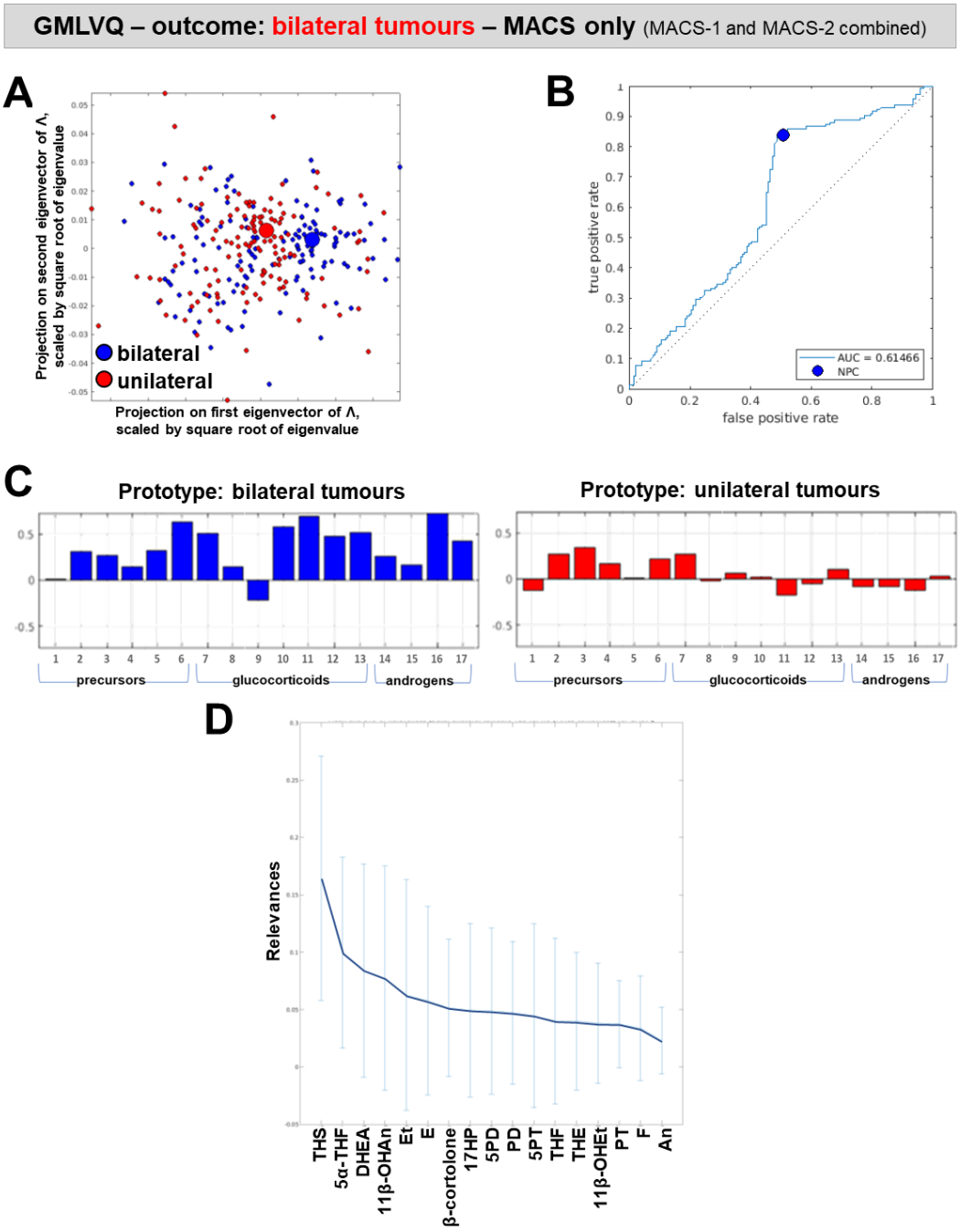

4.4. Discussion

In this cross-sectional study, changes in the 24-hour urine steroid metabolome were characterised by a progressive decrease in androgen excretion and a progressive increase in glucocorticoid excretion across MACS-1, MACS-2, and CS compared with NFAT. These changes correlated with the increased cardiometabolic burden observed in this cohort (**Chapter 3**).

Our results provide insights into the pathophysiology of steroid metabolism in the context of autonomous cortisol secretion. The reduced adrenal androgen output in MACS and CS is in line with the lack of pituitary ACTH stimulation due to negative feedback from the adrenal-derived autonomous cortisol secretion (i.e., ACTH-independent autonomous cortisol secretion) (79). Only a few retrospective studies have so far evaluated the use of mass spectrometry-based multi-steroid profiling for the detection of autonomous cortisol secretion in persons with benign adrenal tumours. Small-scale studies on the 24-hour urine steroid metabolome measured by GC-MS showed similar findings to the much larger prospective cohort presented here, with increased TSH and glucocorticoid metabolite excretion and reduced androgen metabolite excretion in persons with MACS and ACTH-independent CS (39, 75, 140-144). Two studies have previously analysed the 24-hour urine steroid metabolome by LC-MS in a total of 104 persons with benign adrenal tumours and various degrees of autonomous cortisol secretion, consistently showing increased urinary glucocorticoid metabolite excretion in MACS and CS (41, 145, 146). Several studies have also assessed the use of serum and plasma steroid metabolome profiling in NFAT, MACS and CS, showing varying degrees of glucocorticoid excess and androgen suppression in the presence of autonomous cortisol secretion (107, 146-154).

Urinary steroid metabolite ratios can provide information about the activity of enzymes involved in steroid metabolism (2). The analysis of the steroid metabolome of persons with MACS and CS revealed that increasing degrees of autonomous cortisol secretion correlated with a progressive decrease in 5α-reductase activity, a key step in cortisol inactivation (**Figure 4.15**).

Figure 4.15: 5α-Reductase activity in persons with non-functioning adrenal tumours (NFAT) possible mild autonomous cortisol secretion (MACS-1), definitive mild autonomous cortisol secretion (MACS-2), and Cushing's syndrome. Steroid A-ring reduction is an essential step for the inactivation of glucocorticoids and mineralocorticoids, as well as the peripheral activation and inactivation of androgens. A-ring reduction involves two reduction steps: 5α/β-reduction followed by 3α-reduction. 5α-Reduction is catalysed by 5α-reductase type 1 (SRD5A1, mainly expressed in the liver) and 5α-reductase type 2 (SRD5A2, mainly expressed in the reproductive system), whilst the aldo-keto reductase family 1 member D1 (AKR1D1) is responsible for 5β-reduction. 3α-Reduction is catalysed by several aldo-keto reductase family 1 members, particularly the liver-specific AKR1C4 (3α-hydroxysteroid dehydrogenase). The A-ring reduction of cortisol, primarily happening in the liver, is shown in the top left panel. The ratio of urinary 5α-tetrahydrocortisol over tetrahydrocortisol is an indicator of 5α-reductase vs. 5β-reductase activity (top right panel). This is also reflected by the ratios of other 5α-tetrahydro and tetrahydro metabolites (bottom panels).

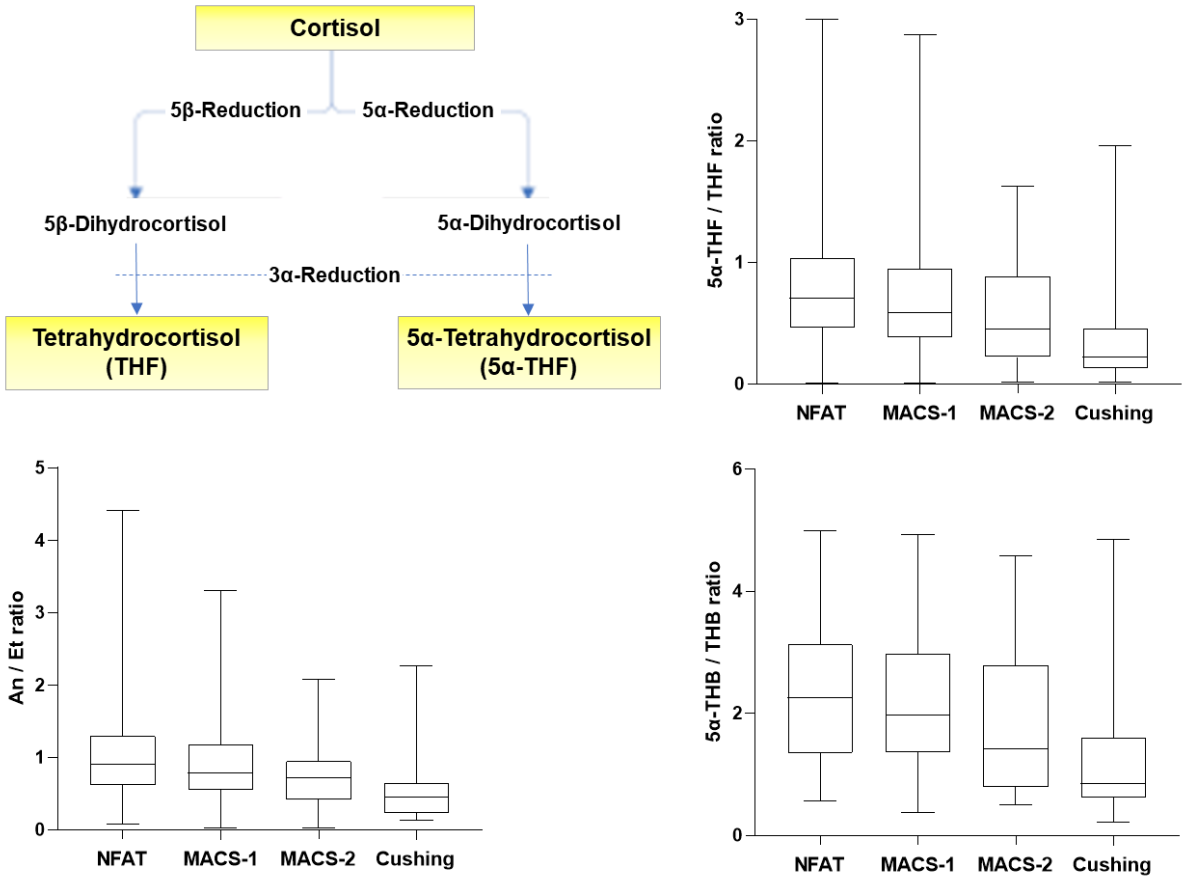

Decreased 5α-reductase activity was previously described in persons with CS (155, 156), but the reason for this is unclear. Possible explanations include substrate saturation, inhibition by other adrenal steroids, or product inhibition. Circulating androgens (often low-suppressed in autonomous cortisol secretion) and free fatty acids (often deranged in autonomous cortisol secretion; see **Chapter 5**) can also affect 5α-reductase expression and function (157, 158). Regardless of the mechanism responsible, it is intriguing to speculate that decreased 5α-reductase activity and cortisol inactivation may result in higher exposure of target organs to cortisol, contributing to the detrimental metabolic effects of autonomous cortisol secretion.

Another observation in this study was that persons with ACTH-independent CS had increased mineralocorticoid metabolite excretion, as already shown in another independent cohort (39). Whilst an increase in mineralocorticoid precursor metabolites can be expected in the context of intense adrenal stimulation of persons with CS secondary to ectopic ACTH production (159), the reason for this in the context of ACTH-independent autonomous cortisol secretion is less clear. Considering that only 11-deoxycorticosterone and corticosterone metabolites were significantly increased in persons with CS (tetrahydro-11-deoxycorticosterone and tetrahydrocorticosterone, respectively), it is possible to speculate that a reduced aldosterone synthase (CYP11B2) activity may be responsible for mineralocorticoid precursor accumulation; this could be related to paracrine/autocrine negative feedback loop on CYP11B2 mediated by the mineralocorticoid receptor activation by cortisol (160). A further possible explanation for these changes is reduced 5α-reductase activity, which is involved in the downstream metabolism of mineralocorticoids (**Figure 4.15**).

We found that persons with adrenal incidentalomas and hypertension – particularly those with MACS – had increased glucocorticoid metabolite excretion. This points towards the potential contribution of cortisol excess to the development of hypertension in persons with MACS. In line with this hypothesis, two studies measuring the serum steroid metabolome of persons with MACS found that cortisol correlated with waist circumference, several cardiovascular risk factors, and the risk of requiring three or more anti-hypertensive medications (150, 152).

We did not observe an obvious correlation between glucocorticoid metabolite excretion and type 2 diabetes. However, the excretion of 11β-hydroxyandrosterone, the metabolite of the major adrenal androgen precursor 11β-hydroxyandrostenedione, was significantly increased in persons with type 2 diabetes, as well as those with hypertension. Whilst increased androgen generation in the context of ACTH-independent autonomous cortisol secretion is apparently counterintuitive, two mechanisms can potentially explain these findings. In healthy individuals, most 11β-hydroxyandrosterone originates from the adrenal androgen 11β-hydroxyandrostenedione; however, it can also be generated in the downstream metabolism of cortisol (**Figure 1.3**) (161) and this pathway is expected to be upregulated in the context of autonomous cortisol secretion. Furthermore, the generation of cortisol from 11-deoxycortisol and of 11β-hydroxyandrostenedione from androstenedione is catalysed by the same enzyme – CYP11B1. Increased expression of CYP11B1 has been found in tumour tissue of persons undergoing adrenalectomy for MACS and CS (162, 163), and therefore increased generation of 11β-hydroxyandrostenedione is expected (164). Steroids downstream of 11β-hydroxyandrostenedione are active 11-oxygenated androgens (11-keto-testosterone

and 11-keto-5α-dihydrotestosterone), whose excess has been linked to increased cardiometabolic disease in women (165). Considering that most persons with MACS are women, it is therefore intriguing to speculate that 11-oxygenated androgens may contribute to and be a hallmark of their increased risk of developing hypertension and type 2 diabetes.

We observed increased glucocorticoid and glucocorticoid precursor metabolite excretion in persons with bilateral adrenal tumours, who carried an increased cardiometabolic burden (**Chapter 3**). Whilst subjects with autonomous cortisol secretion due to established primary bilateral macronodular adrenal hyperplasia were excluded from this study, undiagnosed cases cannot be ruled out (43). Persons with primary bilateral macronodular adrenal hyperplasia have been found to have increased plasma 11-deoxycortisol levels (166), which mirrors the increased urinary excretion of THS observed in the present study. A study comparing the serum steroid profiling of adrenal incidentalomas also found that persons with bilateral tumours had higher baseline, ACTH-stimulated, and post-dexamethasone cortisol levels, as well as higher ACTH-stimulated 11-deoxycortisol levels than those with unilateral tumours (154). These data suggest that at least a subset of persons with bilateral adrenal tumours have dysregulated steroidogenesis characterised by increased glucocorticoid output; this hypothesis would have to be validated in the context of systematic screening for somatic and germline mutations associated with primary bilateral macronodular adrenal hyperplasia in a large cohort of persons with bilateral adrenal tumours.

Strengths of this study include the prospective recruitment, the large sample size, and the centralised urine multi-steroid metabolite profiling by mass spectrometry, which could be correlated to the degree of autonomous cortisol secretion and clinical

outcomes of interest. Weaknesses of the present study include its cross-sectional design, precluding establishing a causal relationship between the observed changes in the steroid metabolome and the increased cardiometabolic burden of persons with MACS. Nonetheless, the similarities in the steroid metabolome of MACS and ACTH-independent CS suggest that autonomous cortisol secretion is at least a contributor to the increased risk of hypertension and type 2 diabetes in this population. Longitudinal data linking cardiometabolic outcomes and changes in the steroid metabolome, as well as interventional studies assessing changes in the steroid metabolome post-intervention, are needed to conclusively prove a causal relationship.

In conclusion, the steroid data suggest that NFAT, MACS-1 and MACS-2 represent a progressive continuum of increasing autonomous cortisol secretion, rather than clearly distinct classes. Urine steroid metabolomics has the potential for metabolic risk stratification of affected individuals and may identify persons who can benefit from targeted interventions to mitigate the adverse consequences of cortisol excess.

CHAPTER 5

Untargeted serum metabolomics to dissect the impact of autonomous cortisol secretion on global metabolism

5.1. Research strategy

We selected a subgroup of 291 EURINE-ACT study participants with benign adrenocortical adenomas and available 1mg-overnight dexamethasone suppression test (1mg-DST): 104 with non-functioning adrenal tumours (NFAT); 70 with possible mild autonomous cortisol secretion (MACS-1); 70 with definitive mild autonomous cortisol secretion (MACS-2); 47 with Cushing's syndrome (CS) (**Figure 5.1**).

Figure 5.1: Overview of the research strategy and methods used for the untargeted serum metabolomics of persons with adrenal tumours. HILIC, hydrophilic interaction chromatography; UHPLC-MS, ultra-high performance liquid chromatography-mass spectrometry.

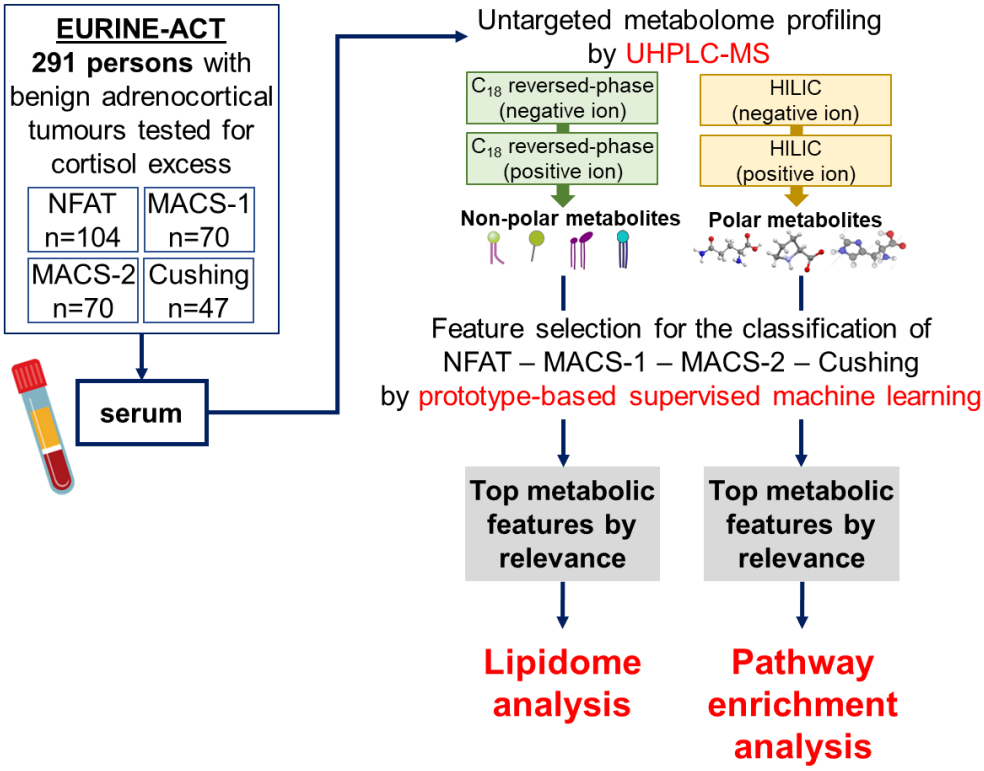

Untargeted serum metabolome profiling was carried out using four different assays by ultra-high performance liquid chromatography-mass spectrometry (UHPLC-MS) to maximise the number of polar and non-polar metabolic features detected. Thousands of metabolic features were detected in each sample.

Prototype-based supervised machine learning was used to analyse this wealth of information. Specifically, two classifiers (generalised matrix learning vector quantisation [GMLVQ] and ordinal regression [OR]) were employed to rank metabolic features according to how relevant they were for the classification of benign adrenal tumours across the spectrum of autonomous cortisol secretion. The rationale for employing machine learning and two independent classifiers was two-fold. First, untargeted metabolome profiling data are traditionally reported as relative concentration changes between different groups. Whilst this approach provides a bird's-eye view of the most obvious metabolic perturbations in the group(s) of interest, it does not take into consideration the relationships between different metabolic features and information that is key for biological interpretation can be lost (for example, a metabolic feature may not be substantially increased or decreased, but it may be important in relationship with other features and metabolic pathways to answer a specific research question). Because of this, machine learning is a powerful approach to handling multi-dimensional data and investigating the relationship between different datapoints based on the outcome of interest. The decision to employ two independent classifiers was based on the exploratory nature of the research question combined with the novelty of using machine learning for untargeted metabolome data modelling. Showing agreement between the two approaches provides reassurance that the observed perturbations are indeed biologically relevant.

After ranking polar and non-polar metabolic features separately according to relevance, the top 500 features were selected for biological interpretation. This cut-off was chosen to cast the net wide enough to retain sufficient information and capture the most relevant metabolic perturbations whilst limiting confounding noise linked to the untargeted nature of the method and the high number of metabolic features detected.

5.2. Methods

5.2.1. *Subjects*

772 of the 1305 EURINE-ACT study participants with benign adrenocortical adenomas and available 1mg-DST provided a serum sample at the time of the baseline assessment for their newly diagnosed adrenal tumours. Of these, 291 were selected for untargeted serum metabolome profiling (**Table 5.1**). The samples were aliquoted on the day of collection and stored locally at -80 °C. The samples were transported on dry ice to the University of Birmingham, United Kingdom, for centralised untargeted serum metabolome profiling in the Phenome Centre Birmingham.

Table 5.1: Clinical characteristics of the persons who underwent untargeted serum metabolome profiling. Values are reported as median (interquartile range), unless otherwise stated. Differences across the groups were assessed using one-way ANOVA (for numerical variables) and chi-square test (for categorical variables). Abbreviations: BMI, body mass index.

	NFAT (n=104)	MACS-1 (n=70)	MACS-2 (n=70)	Adrenal CS (n=47)	p-value
Women, n (%)	83 (79.8)	70 (100)	70 (100)	42 (89.4)	<0.001
Age at diagnosis (years)	58 (48-66)	64 (56-68)	64 (55-69)	48 (41-60)	<0.001
BMI (kg/m^2)	28.8 (26.0-32.8)	29.1 (25.2-33.7)	29.3 (24.5-34.9)	28.9 (25.2-32.9)	0.941
Hypertension, n (%)	72 (69.2)	51 (72.9)	56 (80%)	33 (70.2)	0.447
Type 2 diabetes, n (%)	30 (28.8)	25 (35.7)	25 (35.7)	14 (29.8)	0.694
Dyslipidaemia, n (%)	30 (28.8)	26 (37.1)	29 (41.4)	10 (21.3)	0.088

Subjects were matched for BMI and prevalence of hypertension, type 2 diabetes, and dyslipidaemia to minimise the confounding effect of body weight and comorbidities on the metabolome. The age distribution of the cohort reflects that of the EURINE-ACT cohort, with CS cases being significantly younger than those with NFAT and MACS (**Chapter 3**). For the MACS-1 and MACS-2 groups, only women were selected since women make up for ~70% of MACS cases and sex affects the serum metabolome (167). Some men were included in the NFAT group (i.e., the control group) to match the number of men with CS and of men with adrenocortical cancer (the latter feeding into a sub-study on the global metabolome in adrenocortical cancer not shown here).

5.2.2. *Raw data acquisition and processing*

Biological samples were prepared and analysed using the following steps:

1. Serum aliquots stored at -80°C were selected for analysis.
2. Samples were randomised to determine the sample preparation order. This order was assessed to ensure that all the metadata (age, sex, BMI, and disease classification) was randomised and there were no patterns/correlation with sample preparation order (e.g., all female samples were at the start of the order and all male samples were at the end of the order).
3. On the day of sample preparation, serum aliquots were removed from the -80°C freezer and were allowed to thaw on wet ice.
4. Once thawed, a 120 µL serum aliquot from all biological samples was transferred to a single tube and vortex mixed. This single tube sample is called the pooled quality control (QC) sample (e.g., if there are 20 biological samples then the single tube will contain 20 aliquots).

5. 50 µL of each biological sample and the pooled QC sample were prepared for analysis applying a hydrophilic interaction chromatography (HILIC) UHPLC-MS assay by deproteinisation with 150 µL of acetonitrile/methanol (1/1 (v/v)). For the pooled QC sample, this step was repeated and multiple aliquots prepared based on how many QC samples were required for the analytical run (e.g., if 20 QC samples are required, 20 aliquots were separately prepared – see step 7).
6. 50 µL of each biological sample and the pooled QC sample were prepared for analysis applying a C18 reversed-phase lipidomics UHPLC-MS assay by deproteinisation with 150 µL of isopropanol. For the pooled QC sample, this step was repeated and multiple aliquots prepared based on how many QC samples were required for the analytical run (e.g., if 20 QC samples are required, 20 aliquots were separately prepared).
7. Samples were analysed according to a randomised analysis order (re-randomised to ensure sample preparation order did not correlate with sample analysis order). First, 10 pooled QC samples were analysed for system equilibration and MS/MS data acquisition, then cycles of 7 samples were analysed (where the first 6 were biological samples and the last a pooled QC sample), and finally two pooled QC samples were analysed at the end of the analytical batch. A system blank sample was analysed after the first five QC samples and as the last sample of each batch.
8. Samples were analysed using UHPLC-MS (Thermo Fisher Scientific Ultimate3000 UHPLC system coupled to a Thermo Fisher Scientific Q Exactive Focus mass spectrometer) as described previously (110, 168-170). Two assays were applied to increase the coverage of metabolites detected; polar (water-soluble) metabolites were analysed by HILIC UHPLC-MS and non-polar (lipid) metabolites by C_{18}

reversed-phase lipidomics UHPLC-MS (171). All samples were analysed separately in positive and negative ion modes to increase the number of metabolites detected (171). The methods applied are reported in (171).

9. Each injected sample (blank, QC sample, biological sample) generated a single raw data file. The open-source software XCMS deconvoluted each data file (i.e., it picked and reported all peaks present) and then data from different raw data files were integrated to generate a raw data processed data matrix (172). In total, four distinct data matrices were generated: HILIC positive ion mode; HILIC negative ion mode; C_{18} positive ion mode; C_{18} negative ion mode. Each data matrix comprised samples (columns) x metabolite features (rows) with chromatographic single ion chromatogram peak areas reported when a metabolite feature was detected for a sample; a non-numerical value meant the metabolite was not detected for that sample.
10. Signal correction was performed to minimise run-order associated drift in response by applying quality control-based robust locally estimated scatterplot smoothing signal correction (110).
11. The data for the pooled QC samples were used to filter the data based on metabolic features and the mean and relative standard deviation were calculated. Any metabolic feature with a relative standard deviation >30% was removed from the data matrix to retain high-quality data.
12. Metabolic features that were detected in <90% of the pooled QC samples were removed from the data matrix to remove low-quality data/noise.
13. Data were normalised applying probabilistic quotient normalisation.

14. Metabolic features were annotated applying the in-house software BEAMS (see: https://more.bham.ac.uk/bamcg/resources/beams/) and where feasible by comparison of retention time and higher-energy collisional dissociation MS/MS mass spectra acquired for QC samples to an in-house retention time and MS/MS library or the mass spectral library mzCloud (https://www.mzcloud.org/). All metabolic features were annotated according to level 2 or 3 as defined by the Metabolomics Standards Initiative (173). All non-lipid metabolites were grouped into classes based on KEGG metabolic pathway involvement by applying pathway enrichment analysis in MetaboAnalyst (174).

5.2.3. *Data modelling by machine learning*

The flow of data modelling and interpretation involved the following steps:

1. Between 2500 and 3000 metabolic features were identified and quantified (varying numbers based on the UHPLC-MS method and ion mode used). The relative concentrations were expressed as normalised peak areas (mean ± 95%CI).
2. The relative concentrations of the metabolic features were normalised and log-transformed to reduce the skewness of the dataset.
3. Missing data were handled by k-nearest neighbour imputation (175). This method imputes each missing value using the mean value from the k nearest neighbours found using the Euclidean distance (176).
4. Metabolomic data were analysed using prototype-based supervised machine learning. Specifically, two distinct classifiers were used: GMLVQ and OR. These classifiers were also used for the urine steroid metabolite profiling data and further details can be found in **Chapter 4**. GMLVQ and OR were used to determine the

relevance of each metabolic feature for the classification of benign adrenal tumours across the spectrum of autonomous cortisol secretion, i.e., the four-class classification NFAT – MACS-1 – MACS-2 – CS. The relevance of each metabolic feature was expressed as median rank and interquartile range (the smaller the rank, the more relevant that metabolic feature). Since two UHPLC-MS methods were used (HILIC and C_{18}; each using two ion modes) and two classifiers applied, eight lists of ordered metabolic features were generated (four for GMLVQ and four for OR) (**Figure 5.2**).

5. After visual inspection of the plots of the metabolic features ordered by their relevance, an arbitrary cut-off of the top 500 metabolites was chosen for biological interpretation (**Figure 5.2**). This cut-off was deemed to offer an acceptable compromise between including too much noise (i.e., the risk of including metabolic features that are not very relevant for the classification of autonomous cortisol secretion and may mask underlying metabolic processes) or too little information (i.e., the risk of excluding metabolic features that point towards key metabolic perturbations linked to autonomous cortisol secretion).
6. The four ranking lists generated by GMLVQ were merged and the same was done for OR, yielding one list of metabolic features for GMLVQ and one list of metabolic features for OR. Duplicate metabolic features across the various ranking lists were removed.

Figure 5.2: Relevance plots of the metabolic features measured by ultra-high performance liquid chromatography-mass spectrometry and analysed by machine learning. Four datasets were generated (HILIC UHPLC-MS, negative ion mode; HILIC UHPLC-MS, positive ion mode; C18 reversed-phase UHPLC-MS, negative ion mode; C18 reversed-phase UHPLC-MS, positive ion mode) and the metabolic features ranked by generalised matrix learning vector quantisation (GMLVQ) and ordinal regression (OR). The lower the rank, the more relevant a metabolic feature for the classifications of persons with mild autonomous cortisol secretion and Cushing's syndrome. The red dotted lines show the chosen cut-off of 500 metabolic features.

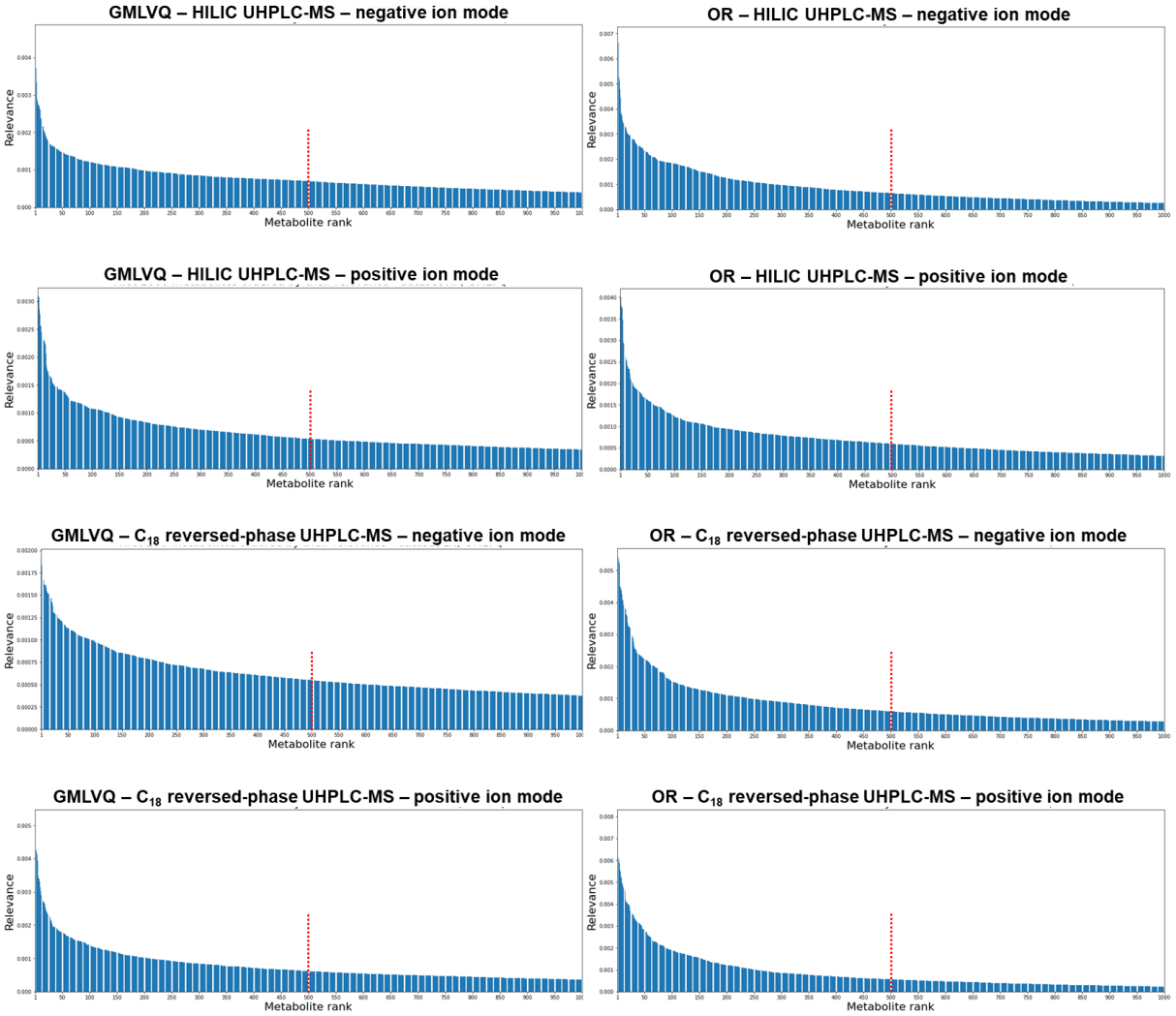

5.2.4. *Data interpretation*

The metabolite feature concentrations in persons with MACS-1, MACS-2, and CS were expressed as fold-changes using persons with NFAT as the reference group. This analysis was carried out separately for the metabolite lists generated by GMLVQ and OR. Moreover, non-polar and polar metabolic features were analysed separately:

Non-polar metabolic features (measured by C_{18} reversed-phase UHPLC-MS): the lipidome was analysed by grouping non-polar metabolic features into classes related to chemical structure or metabolic function. Only classes where 20 or more metabolite features were selected by GMLVQ or OR were brought forward for biological interpretation. This arbitrary cut-off was deemed sufficient to identify biologically meaningful changes in persons with MACS and CS whilst reducing the risk of reporting spurious results linked to the inherent variability of the metabolome.

Polar metabolites (measured by HILIC UHPLC-MS): pathway enrichment analysis was used to identify which metabolic pathways had metabolic features that were over-represented and had significant perturbations to their concentrations. One-way ANOVA with *post hoc* analysis to correct for multiple comparisons using false discovery rate was used to identify the most affected metabolic pathways in persons with MACS and CS; p-values <0.05 were considered statistically significant. Pathway enrichment analysis was performed using MetaboAnalyst end box and whisker plots were constructed using data normalised by sum (174).

5.3. Results

5.3.1. *Lipidome analysis*

GMLVQ and OR identified the same top 6 lipid classes as the most perturbed across the spectrum of autonomous cortisol secretion (**Table 5.2** and **Figure 5.3**). There was only a partial overlap between the metabolic features identified by the two classifiers; nonetheless, the metabolic perturbations observed in the 6 lipid classes, expressed as fold-changes, were very similar when assessed by GMLVQ or OR (**Figures 5.4-5.16**). Glycerophospholipids were the class with the most metabolic features identified by machine learning, followed by several bioactive lipid classes, triacylglycerides, and acylcarnitines. Glycerophospholipids were increasingly perturbed with the increasing degree of autonomous cortisol secretion (**Figure 5.4**); this trend was mostly driven by the glycerophospholipid subclasses phosphatidylcholines and – to a lesser extent – phosphatidylethanolamines (**Figures 5.5-5.11**). Conversely, phosphatidylinositols and phosphatidylserines were downregulated in CS but not MACS.

Lysoglycerophospholipids were progressively abnormal in MACS-1, MACS-2 and CS compared to NFAT (**Figure 5.12**), whilst triacylglycerides and ceramides were more perturbed in CS than MACS (**Figures 5.13-5.14**).

Obvious trends for sphingolipids were not observed (**Figure 5.15**), whilst acylcarnitines were upregulated in MACS and downregulated in CS (**Figure 5.16**).

Table 5.2: Most relevant non-polar metabolic features for the classification of benign adrenal tumours based on machine learning analysis. The number of metabolic features identified by generalised matrix learning vector quantisation (GMLVQ), ordinal regression (OR), as well as the number of overlapping features between the two classifiers, are listed separately. Only metabolite classes were classifiers identified ≥20 features were selected for further analysis (shown in bold).

Metabolite class	**Number of metabolic features identified by machine learning**		
	GMLVQ	**OR**	**overlapping**
Glycerophospholipids (GPLs)	297	207	82
GPLs (phosphatidylcholine, PC)	82	49	19
GPLs (phosphatidylinositol, PI)	22	23	10
GPLs (phosphatidylethanolamine, PE)	26	16	4
GPLs (phosphatidylserine, PS)	15	12	1
GPLs (phosphatidic acid, PA)	11	8	3
GPLs (phosphatidylglycerol, PG)	9	5	1
GPLs (mixed)*	132	94	44
Lysoglycerophospholipids	76	80	35
Triacylglycerides	70	72	33
Ceramides	65	73	24
Sphingolipids	53	42	23
Acylcarnitines	22	21	12
Oxidised fatty acids	11	7	4
Fatty acids	9	13	4
Bile acids	7	4	3
Cardiolipins	7	8	2
Diacylglycerides	6	9	6
Acyl amino acids	4	6	1
Cholesterol metabolism	8	6	4
Steroid metabolism	3	1	1
GPL synthesis	3	3	1
Vitamin A metabolism	2	3	/
Vitamin D metabolism	1	/	/
Mixed class†	39	37	17
Peptides†	22	16	6

* This includes metabolic features that belong to the glycerophospholipid class, but it is unknown which subclass they belong to. Therefore, they have been included in the overall analysis of the glycerophospholipid class but have been excluded from subclass analyses.

† These classes include metabolic features that have not been attributed to specific metabolite classes. Therefore, they have not been used for biological interpretation.

Figure 5.3: Most perturbed lipid classes in persons with benign adrenal tumours and autonomous cortisol secretion. Panel A: The number of metabolic features identified by generalised matrix learning vector quantisation (GMLVQ) and ordinal regression (OR) are reported for each class as Venn diagrams. The circle areas and the overlapping areas (showing the number of features identified by both classifiers) are directly proportional to the number of features. Panel B: Schematic overview of the six most perturbed lipid classes and their main physiological functions.

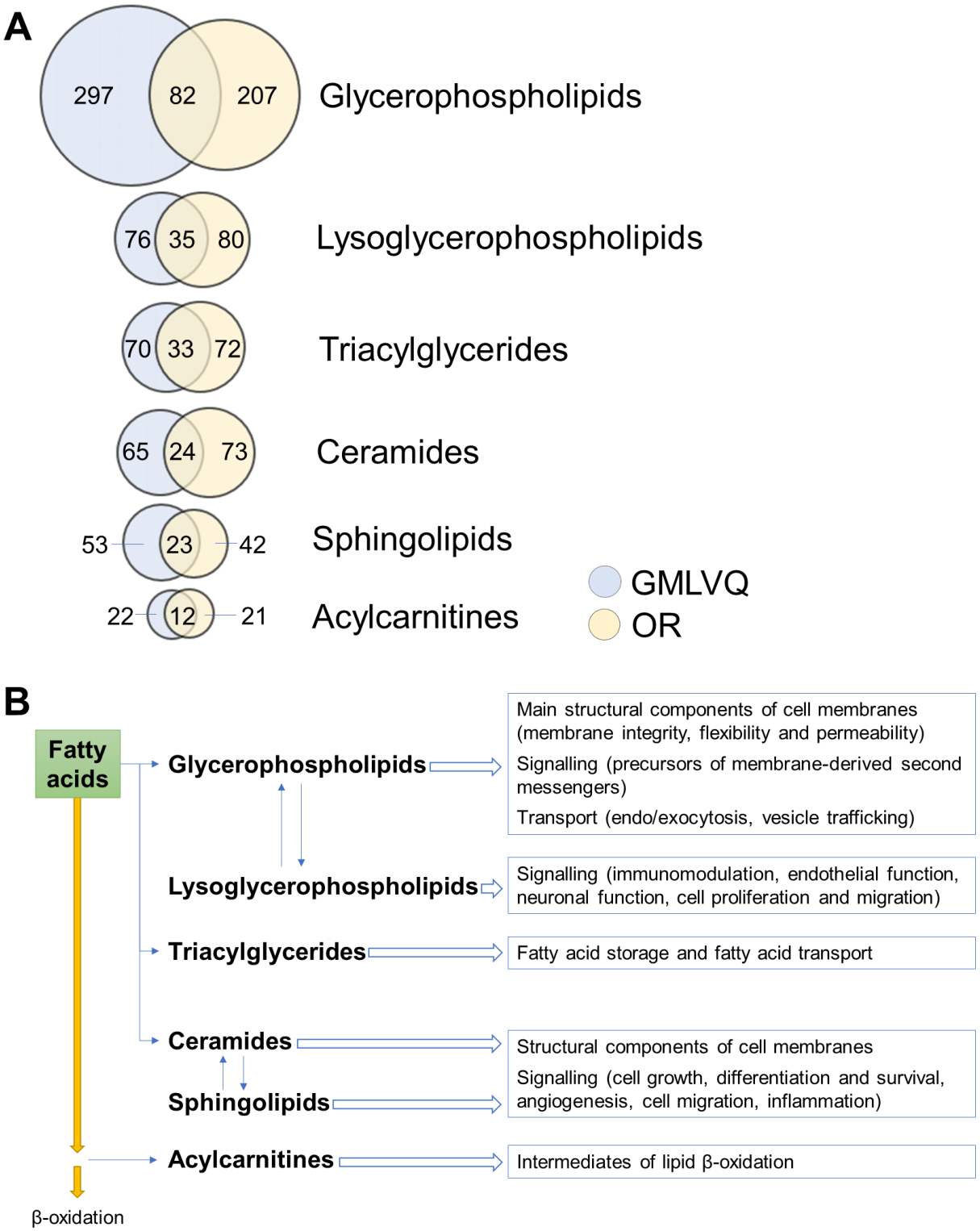

Figure 5.4: Changes of serum glycerophospholipids across the spectrum of autonomous cortisol secretion. Metabolic features identified by ordinal regression (OR, panel A) and generalised matrix learning vector quantisation (GMLVQ, panel B) are presented separately. Relative concentrations in possible mild autonomous cortisol secretion (MACS-1), definitive mild autonomous cortisol secretion (MACS-2), and Cushing's syndrome (CS) are shown as fold-changes compared to non-functioning adrenal tumours (NFAT); fold-changes are log2 transformed so that 0 equals to no change and values above and below 0 represent symmetrical degrees of change. The graph on the left shows the overall trend of the metabolic class in MACS-1, MACS-2 and CS, and fold-changes are shown as boxplots, with boxes representing the median and interquartile range, and whiskers representing the 5th to 95th centile; results are presented separately for all features combined, increased features only, and decreased features only. The graphs on the right show the fold-changes of single features (dots) and their relevance rank on the y-axis; the lower the rank, the more relevant a metabolic feature for the classifications of persons with benign adrenal tumours and autonomous cortisol secretion. Results are shown for the top 500 and top 150 metabolic features.

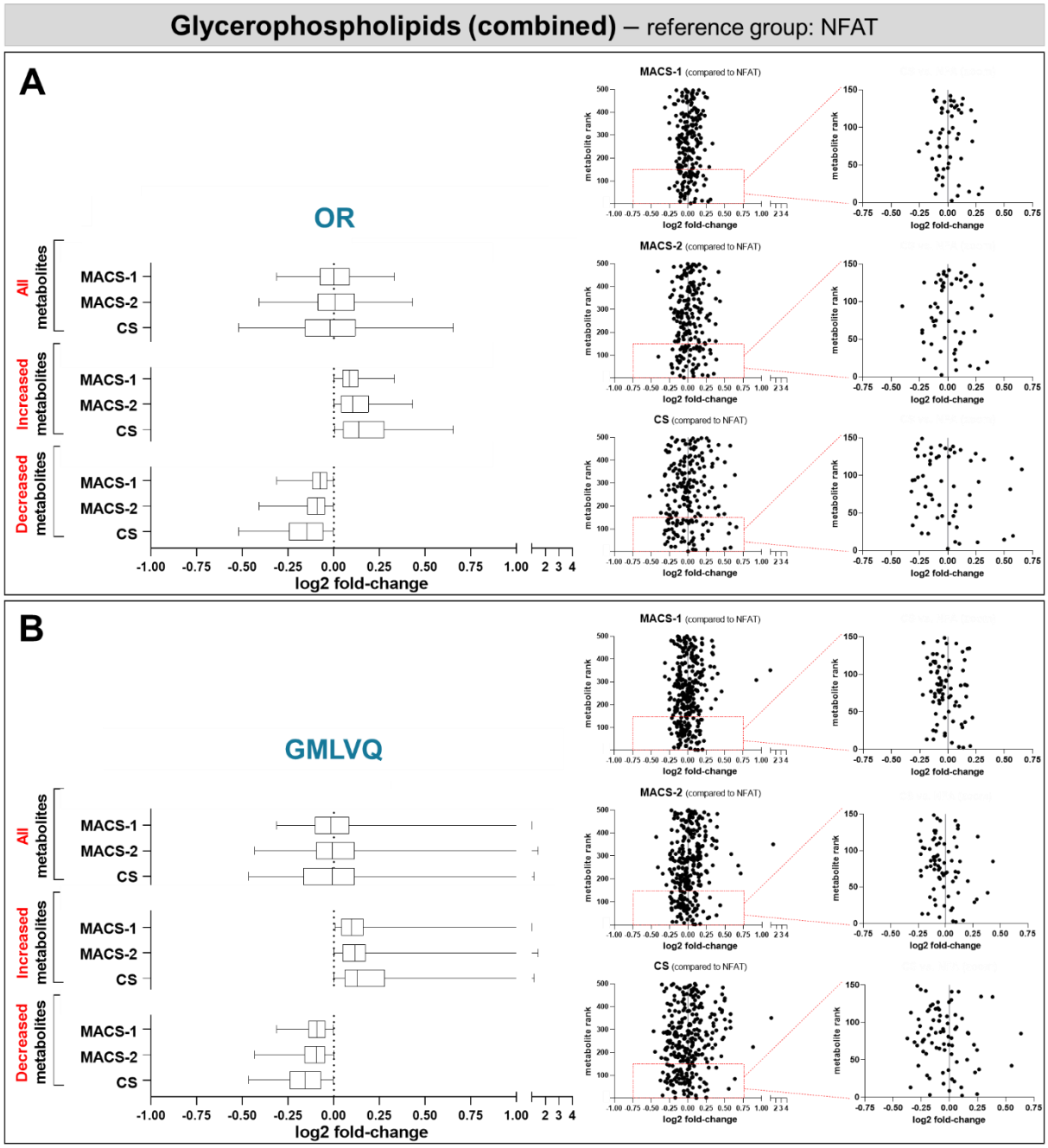

Figure 5.5: Glycerophospholipid synthetic pathways. Phosphatidylcholine is synthesised via two pathways. The major pathway is the Kennedy pathway and involves the addition of cytidine diphosphate-choline (CDP-choline) to the phosphatidic acid derivative diacylglycerol. Phosphatidyl-choline can also be synthesised through the action of phosphatidylethanolamine N-methyltransferase (PEMT), which converts phosphatidyl-ethanolamine to phosphatidylcholine. Phosphatidylethanolamine is also synthesised via the Kennedy pathway, where the multifunctional enzymes catalyse the addition of CDP-ethanolamine to diacylglycerol. Phosphatidylethanolamine can also be synthesised by phosphatidylserine decarboxylase. Phosphatidylserine is synthesised from CDP-diacylglycerol, phosphatidylcholine, and phosphatidylethanolamine via phosphatidylserine synthase. Phosphatidyl-inositol is derived from the CDP-diacylglycerol by phosphatidylinositol synthase. Phosphatidylglycerol is synthesised from CDP-diacylglycerol via a multi-step process involving phosphatidylglycerol phosphate synthase, and phosphatidylglycerol phosphate phosphatase. Cardiolipin can then be synthesised from phosphatidylglycerol via cardiolipin synthase. Figure reproduced and adapted from (177).

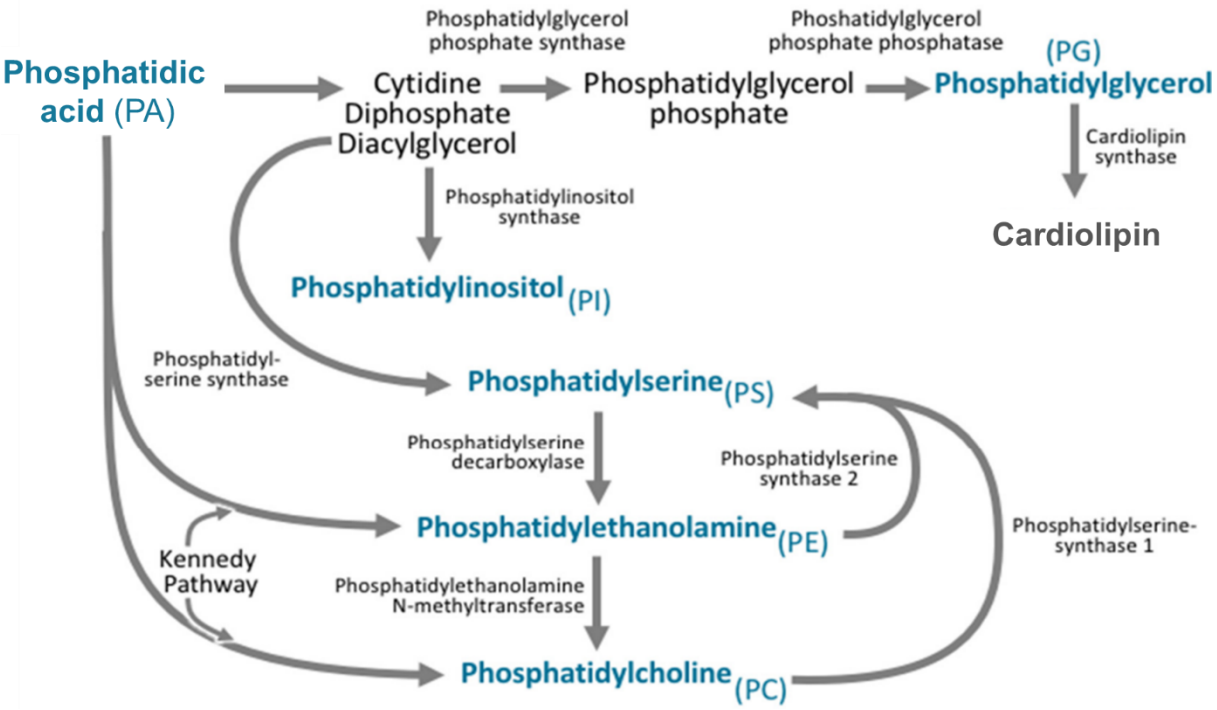

Figure 5.6: Changes of the phosphatidic acid glycerophospholipid subclass across the spectrum of autonomous cortisol secretion. Metabolic features identified by ordinal regression (OR, panel A) and generalised matrix learning vector quantisation (GMLVQ, panel B) are presented separately. Relative concentrations in possible mild autonomous cortisol secretion (MACS-1), definitive mild autonomous cortisol secretion (MACS-2), and Cushing's syndrome (CS) are shown as fold-changes compared to non-functioning adrenal tumours (NFAT); fold-changes are log2 transformed so that 0 equals to no change and values above and below 0 represent symmetrical degrees of change. The graph on the left shows the overall trend of the metabolic class in MACS-1, MACS-2 and CS, and fold-changes are shown as boxplots, with boxes representing median and interquartile range, and whiskers representing 5th to 95th centile; results are presented separately for all features combined, increased features only, and decreased features only. The graphs on the right show the fold-changes of single features (dots) and their relevance rank on the y-axis; the lower the rank, the more relevant a metabolic feature for the classifications of persons with benign adrenal tumours and autonomous cortisol secretion. Results are shown for the top 500 and top 150 metabolic features.

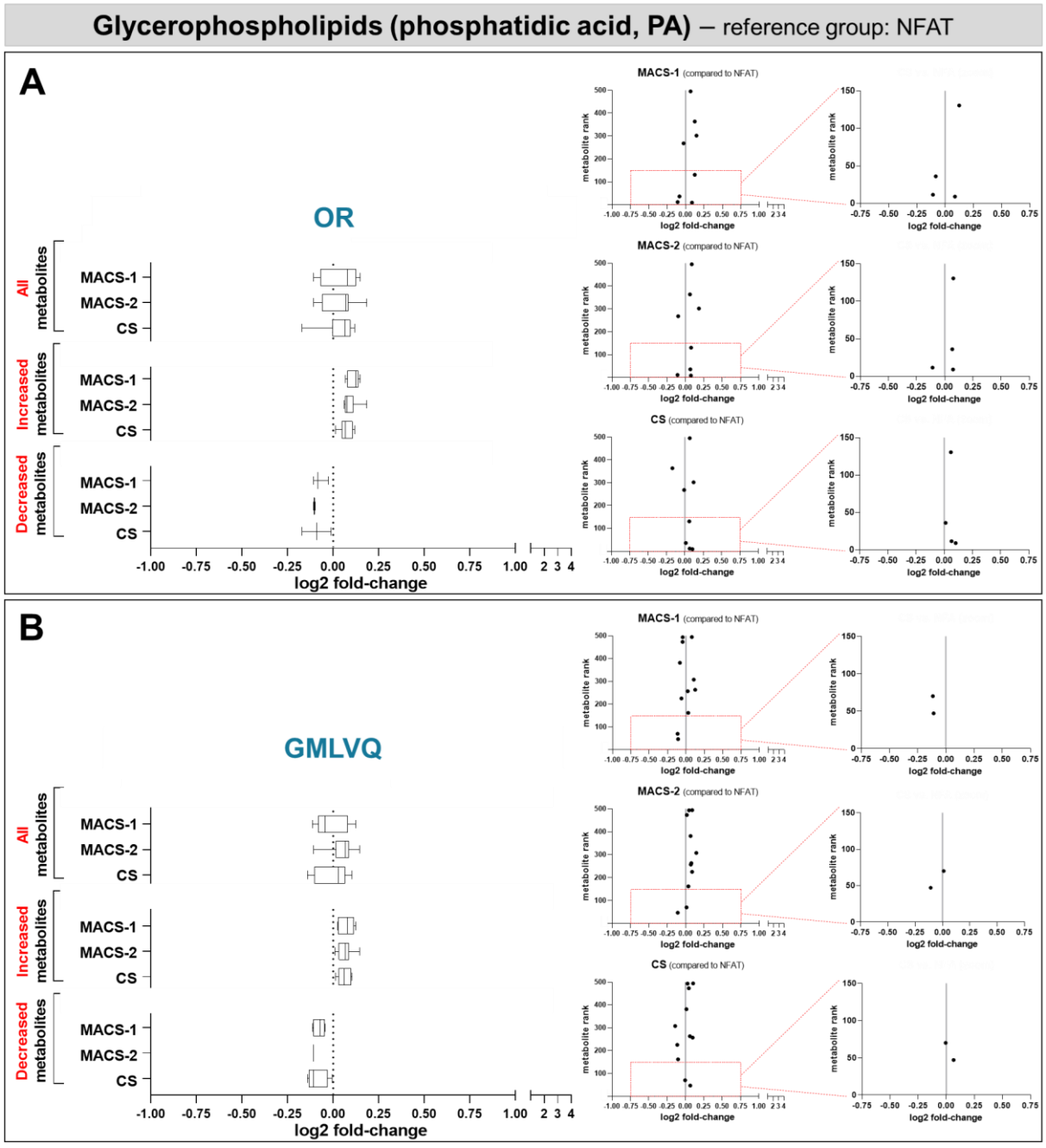

Figure 5.7: Changes of the phosphatidylinositol glycerophospholipid subclass across the spectrum of autonomous cortisol secretion. Metabolic features identified by ordinal regression (OR, panel A) and generalised matrix learning vector quantisation (GMLVQ, panel B) are presented separately. Relative concentrations in possible mild autonomous cortisol secretion (MACS-1), definitive mild autonomous cortisol secretion (MACS-2), and Cushing's syndrome (CS) are shown as fold-changes compared to non-functioning adrenal tumours (NFAT); fold-changes are log2 transformed so that 0 equals to no change and values above and below 0 represent symmetrical degrees of change. The graph on the left shows the overall trend of the metabolic class in MACS-1, MACS-2 and CS, and fold-changes are shown as boxplots, with boxes representing median and interquartile range, and whiskers representing 5th to 95th centile; results are presented separately for all features combined, increased features only, and decreased features only. The graphs on the right show the fold-changes of single features (dots) and their relevance rank on the y-axis; the lower the rank, the more relevant a metabolic feature for the classifications of persons with benign adrenal tumours and autonomous cortisol secretion. Results are shown for the top 500 and top 150 metabolic features.

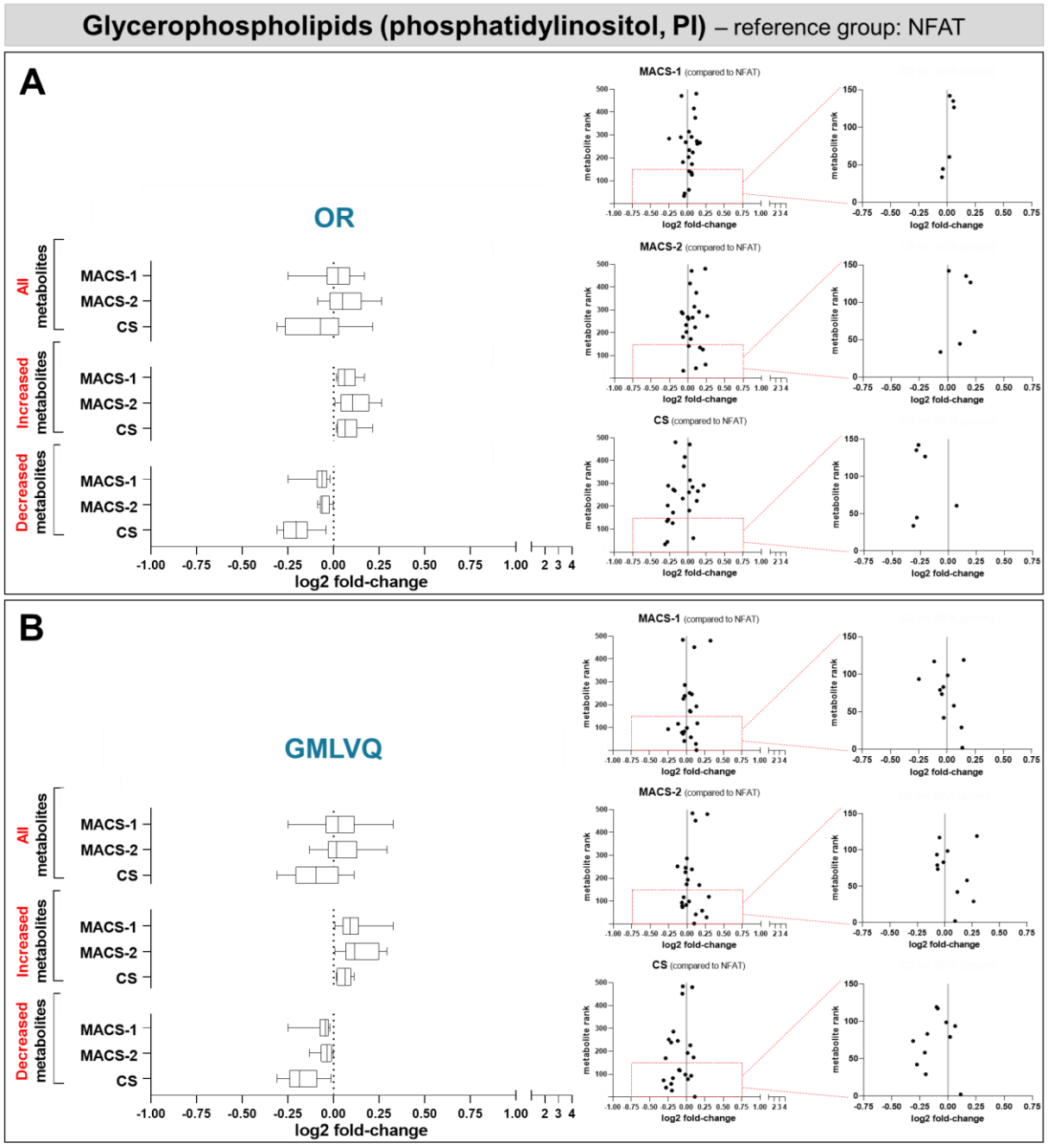

Figure 5.8: Changes of the phosphatidylglycerol glycerophospholipid subclass across the spectrum of autonomous cortisol secretion. Metabolic features identified by ordinal regression (OR, panel A) and generalised matrix learning vector quantisation (GMLVQ, panel B) are presented separately. Relative concentrations in possible mild autonomous cortisol secretion (MACS-1), definitive mild autonomous cortisol secretion (MACS-2), and Cushing's syndrome (CS) are shown as fold-changes compared to non-functioning adrenal tumours (NFAT); fold-changes are log2 transformed so that 0 equals to no change and values above and below 0 represent symmetrical degrees of change. The graph on the left shows the overall trend of the metabolic class in MACS-1, MACS-2 and CS, and fold-changes are shown as boxplots, with boxes representing median and interquartile range, and whiskers representing 5th to 95th centile; results are presented separately for all features combined, increased features only, and decreased features only. The graphs on the right show the fold-changes of single features (dots) and their relevance rank on the y-axis; the lower the rank, the more relevant a metabolic feature for the classifications of persons with benign adrenal tumours and autonomous cortisol secretion. Results are shown for the top 500 and top 150 metabolic features.

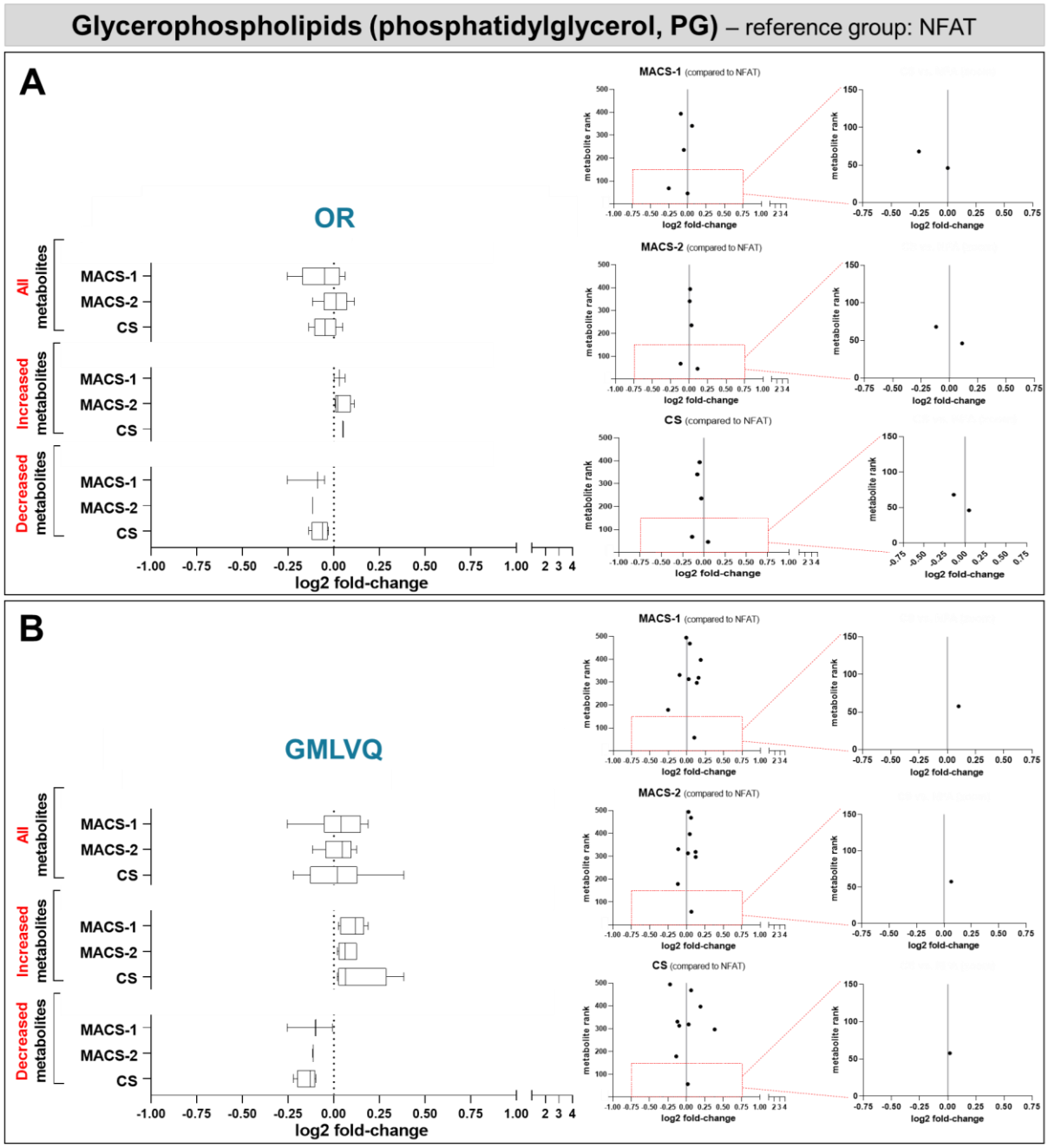

Figure 5.9: Changes of the phosphatidylserine glycerophospholipid subclass across the spectrum of autonomous cortisol secretion. Metabolic features identified by ordinal regression (OR, panel A) and generalised matrix learning vector quantisation (GMLVQ, panel B) are presented separately. Relative concentrations in possible mild autonomous cortisol secretion (MACS-1), definitive mild autonomous cortisol secretion (MACS-2), and Cushing's syndrome (CS) are shown as fold-changes compared to non-functioning adrenal tumours (NFAT); fold-changes are log2 transformed so that 0 equals to no change and values above and below 0 represent symmetrical degrees of change. The graph on the left shows the overall trend of the metabolic class in MACS-1, MACS-2 and CS, and fold-changes are shown as boxplots, with boxes representing median and interquartile range, and whiskers representing 5th to 95th centile; results are presented separately for all features combined, increased features only, and decreased features only. The graphs on the right show the fold-changes of single features (dots) and their relevance rank on the y-axis; the lower the rank, the more relevant a metabolic feature for the classifications of persons with benign adrenal tumours and autonomous cortisol secretion. Results are shown for the top 500 and top 150 metabolic features.

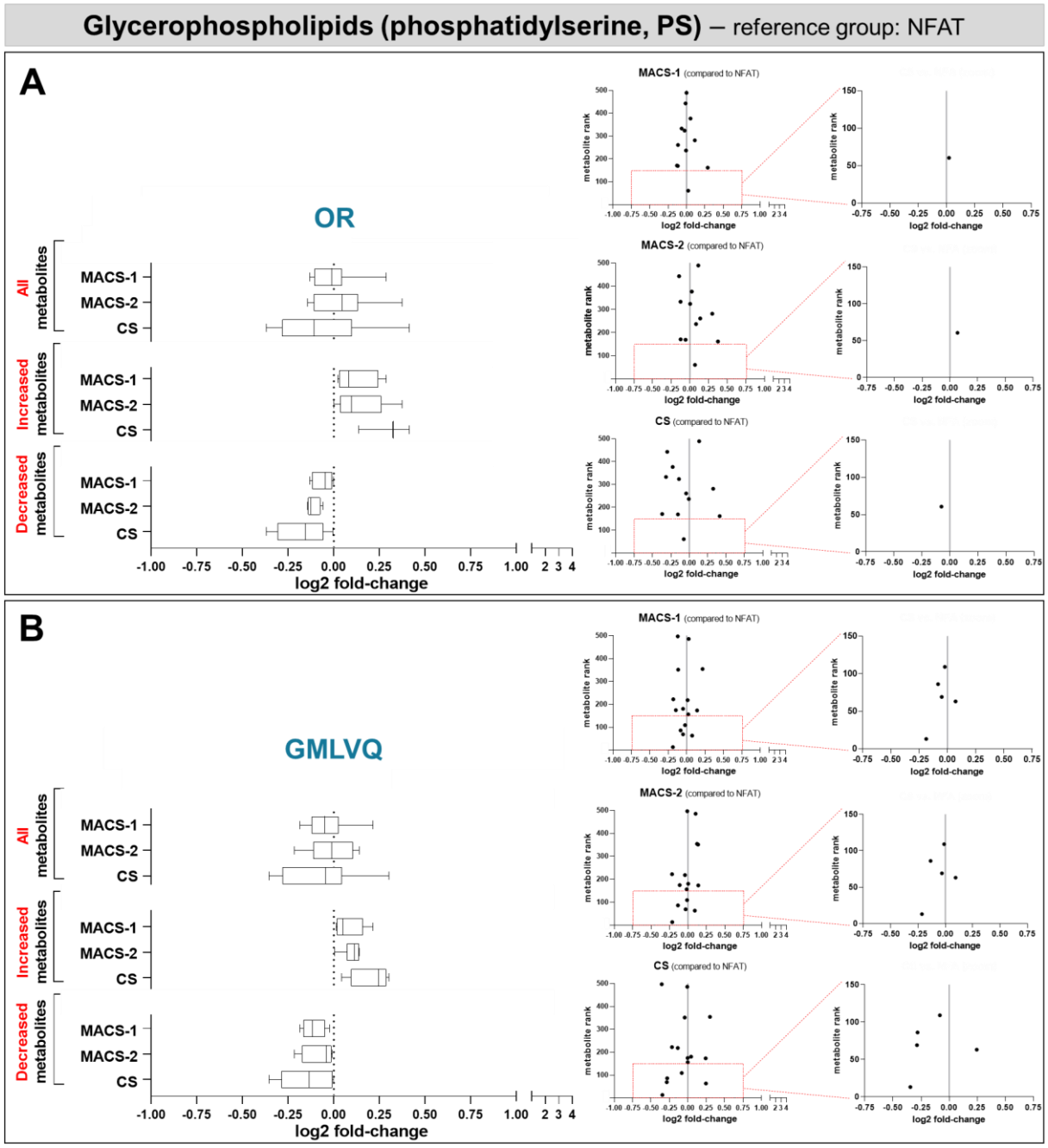

Figure 5.10: Changes of the phosphatidylethanolamine glycerophospholipid subclass across the spectrum of autonomous cortisol secretion. Metabolic features identified by ordinal regression (OR, panel A) and generalised matrix learning vector quantisation (GMLVQ, panel B) are presented separately. Relative concentrations in possible mild autonomous cortisol secretion (MACS-1), definitive mild autonomous cortisol secretion (MACS-2), and Cushing's syndrome (CS) are shown as fold-changes compared to non-functioning adrenal tumours (NFAT); fold-changes are log2 transformed so that 0 equals to no change and values above and below 0 represent symmetrical degrees of change. The graph on the left shows the overall trend of the metabolic class in MACS-1, MACS-2 and CS, and fold-changes are shown as boxplots, with boxes representing median and interquartile range, and whiskers representing 5th to 95th centile; results are presented separately for all features combined, increased features only, and decreased features only. The graphs on the right show the fold-changes of single features (dots) and their relevance rank on the y-axis; the lower the rank, the more relevant a metabolic feature for the classifications of persons with benign adrenal tumours and autonomous cortisol secretion. Results are shown for the top 500 and top 150 metabolic features.

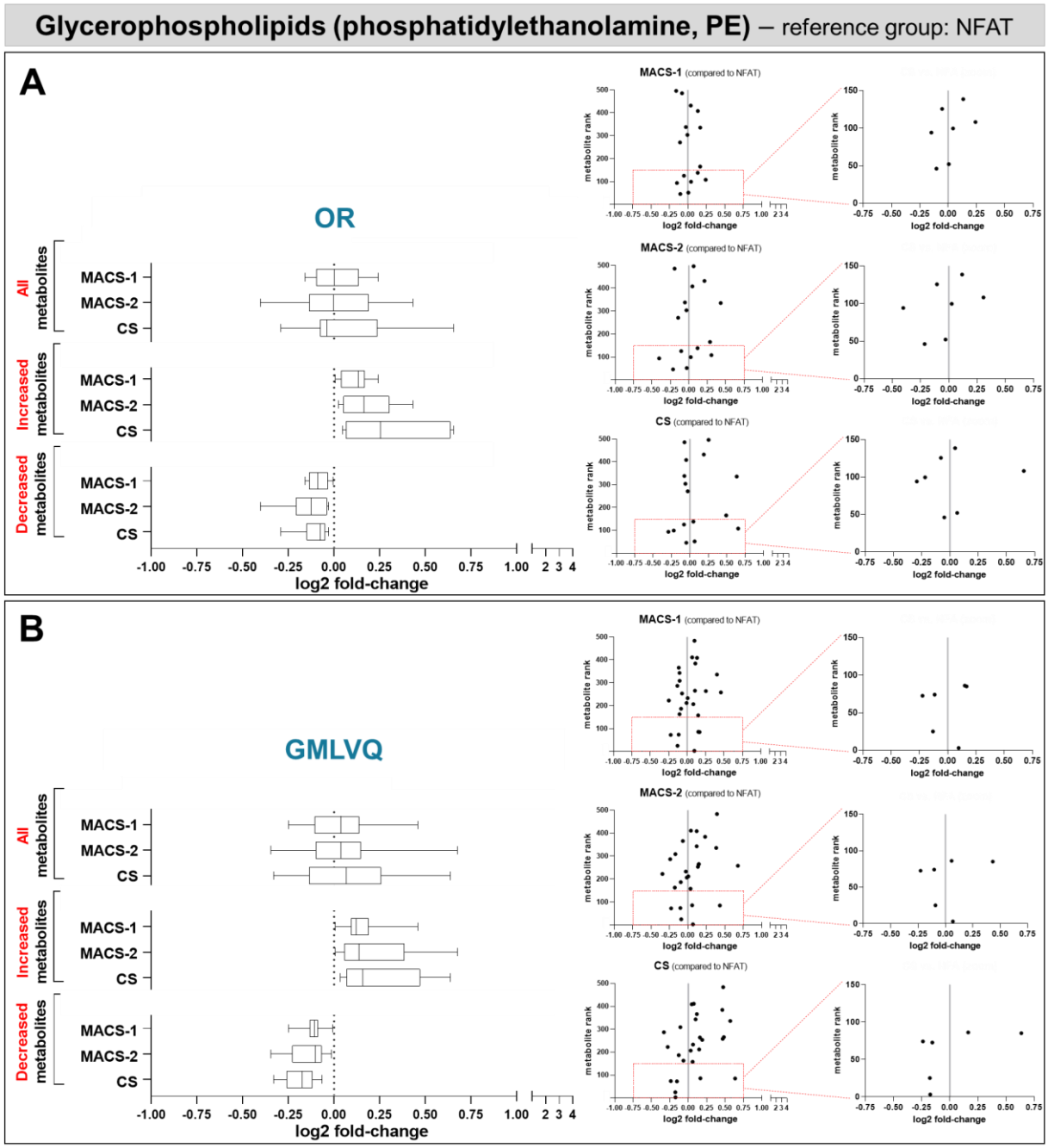

Figure 5.11: Changes of the phosphatidylcholine glycerophospholipid subclass across the spectrum of autonomous cortisol secretion. Metabolic features identified by ordinal regression (OR, panel A) and generalised matrix learning vector quantisation (GMLVQ, panel B) are presented separately. Relative concentrations in possible mild autonomous cortisol secretion (MACS-1), definitive mild autonomous cortisol secretion (MACS-2), and Cushing's syndrome (CS) are shown as fold-changes compared to non-functioning adrenal tumours (NFAT); fold-changes are log2 transformed so that 0 equals to no change and values above and below 0 represent symmetrical degrees of change. The graph on the left shows the overall trend of the metabolic class in MACS-1, MACS-2 and CS, and fold-changes are shown as boxplots, with boxes representing median and interquartile range, and whiskers representing 5th to 95th centile; results are presented separately for all features combined, increased features only, and decreased features only. The graphs on the right show the fold-changes of single features (dots) and their relevance rank on the y-axis; the lower the rank, the more relevant a metabolic feature for the classifications of persons with benign adrenal tumours and autonomous cortisol secretion. Results are shown for the top 500 and top 150 metabolic features.

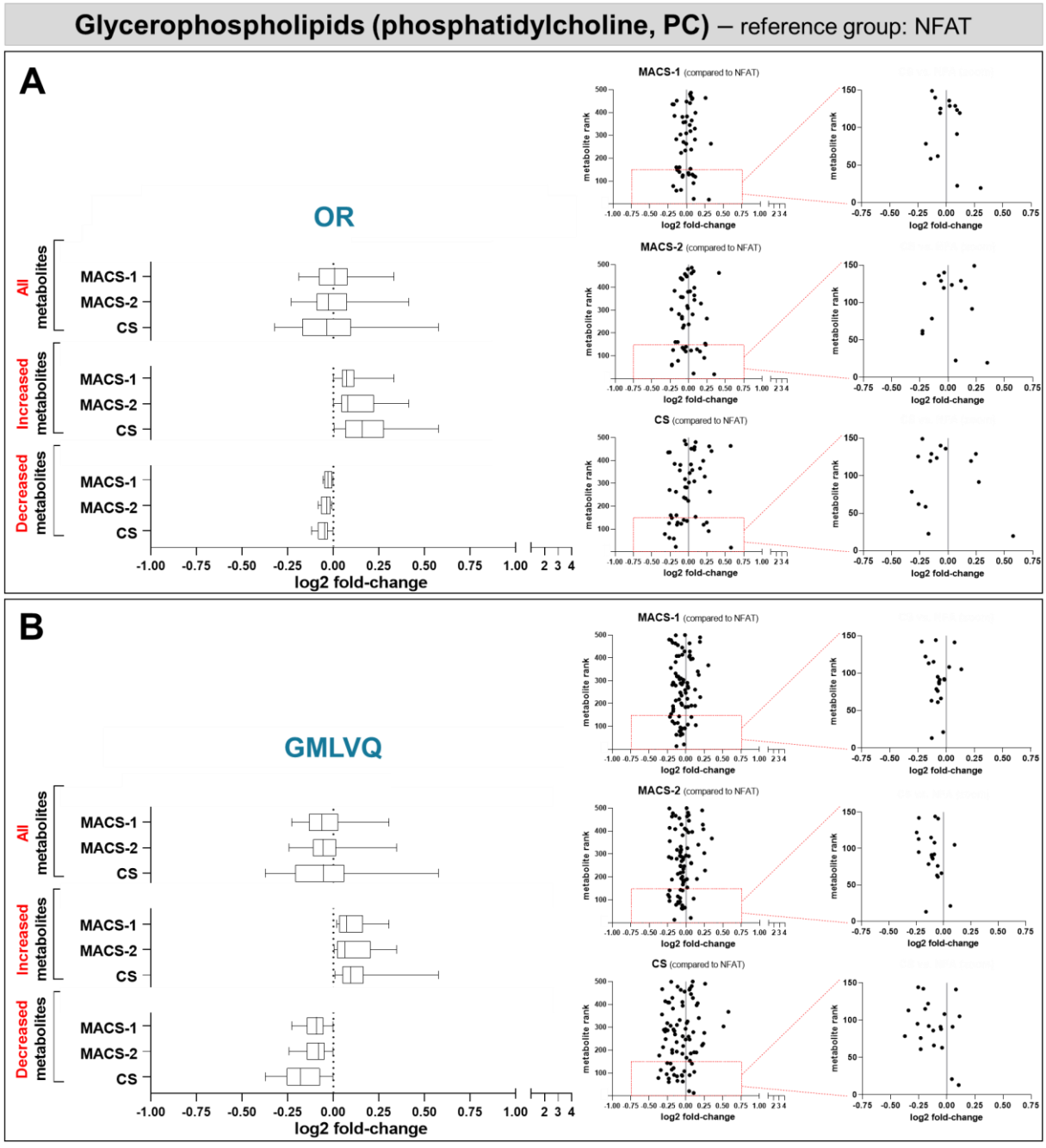

Figure 5.12: Changes of serum lysoglycerophospholipids across the spectrum of autonomous cortisol secretion. Metabolic features identified by ordinal regression (OR, panel A) and generalised matrix learning vector quantisation (GMLVQ, panel B) are presented separately. Relative concentrations in possible mild autonomous cortisol secretion (MACS-1), definitive mild autonomous cortisol secretion (MACS-2), and Cushing's syndrome (CS) are shown as fold-changes compared to non-functioning adrenal tumours (NFAT); fold-changes are log2 transformed so that 0 equals to no change and values above and below 0 represent symmetrical degrees of change. The graph on the left shows the overall trend of the metabolic class in MACS-1, MACS-2 and CS, and fold-changes are shown as boxplots, with boxes representing median and interquartile range, and whiskers representing 5th to 95th centile; results are presented separately for all features combined, increased features only, and decreased features only. The graphs on the right show the fold-changes of single features (dots) and their relevance rank on the y-axis; the lower the rank, the more relevant a metabolic feature for the classifications of persons with benign adrenal tumours and autonomous cortisol secretion. Results are shown for the top 500 and top 150 metabolic features.

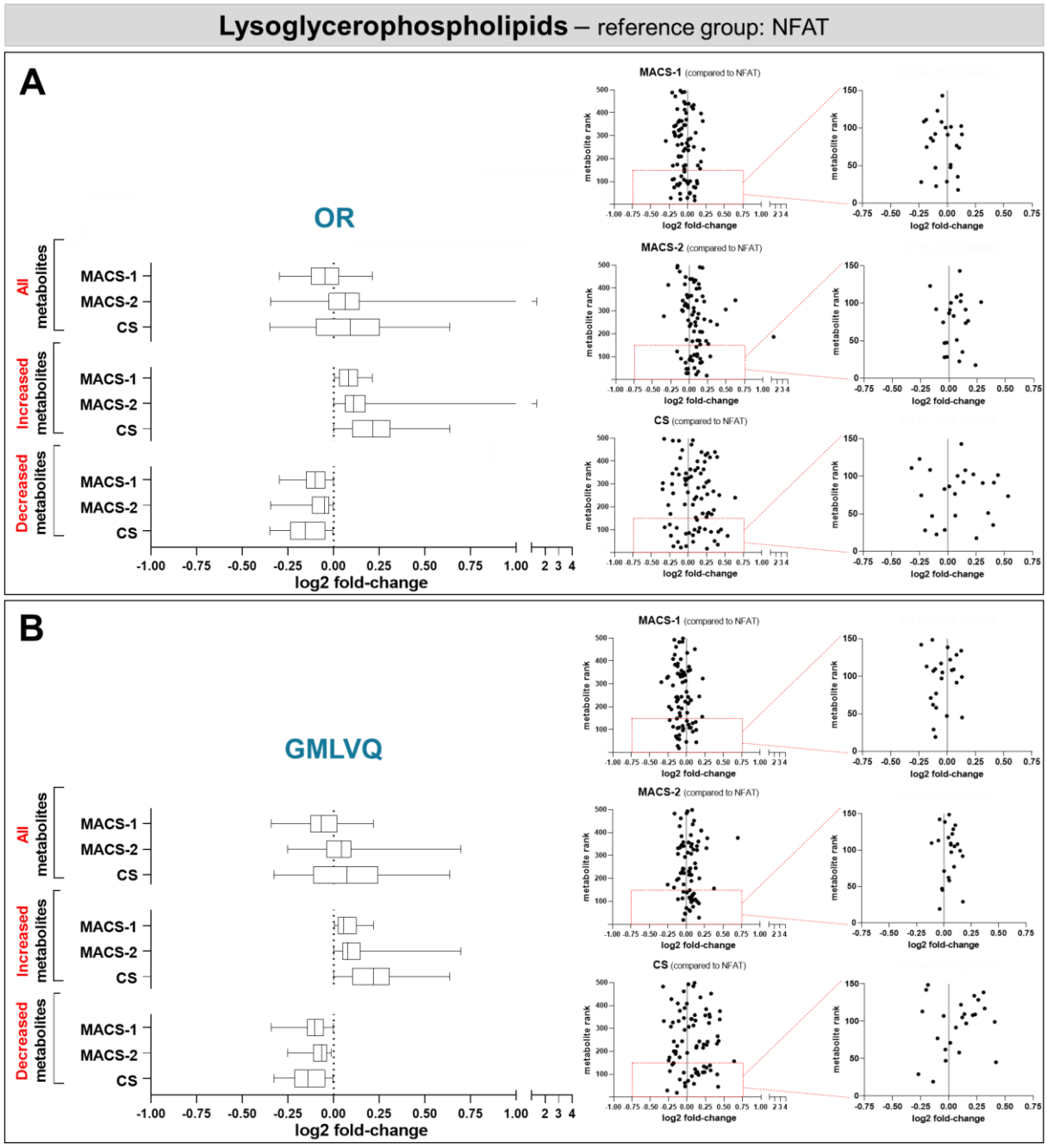

Figure 5.13: Changes of serum triglycerides across the spectrum of autonomous cortisol secretion. Metabolic features identified by ordinal regression (OR, panel A) and generalised matrix learning vector quantisation (GMLVQ, panel B) are presented separately. Relative concentrations in possible mild autonomous cortisol secretion (MACS-1), definitive mild autonomous cortisol secretion (MACS-2), and Cushing's syndrome (CS) are shown as fold-changes compared to non-functioning adrenal tumours (NFAT); fold-changes are log2 transformed so that 0 equals to no change and values above and below 0 represent symmetrical degrees of change. The graph on the left shows the overall trend of the metabolic class in MACS-1, MACS-2 and CS, and fold-changes are shown as boxplots, with boxes representing median and interquartile range, and whiskers representing 5th to 95th centile; results are presented separately for all features combined, increased features only, and decreased features only. The graphs on the right show the fold-changes of single features (dots) and their relevance rank on the y-axis; the lower the rank, the more relevant a metabolic feature for the classifications of persons with benign adrenal tumours and autonomous cortisol secretion. Results are shown for the top 500 and top 150 metabolic features.

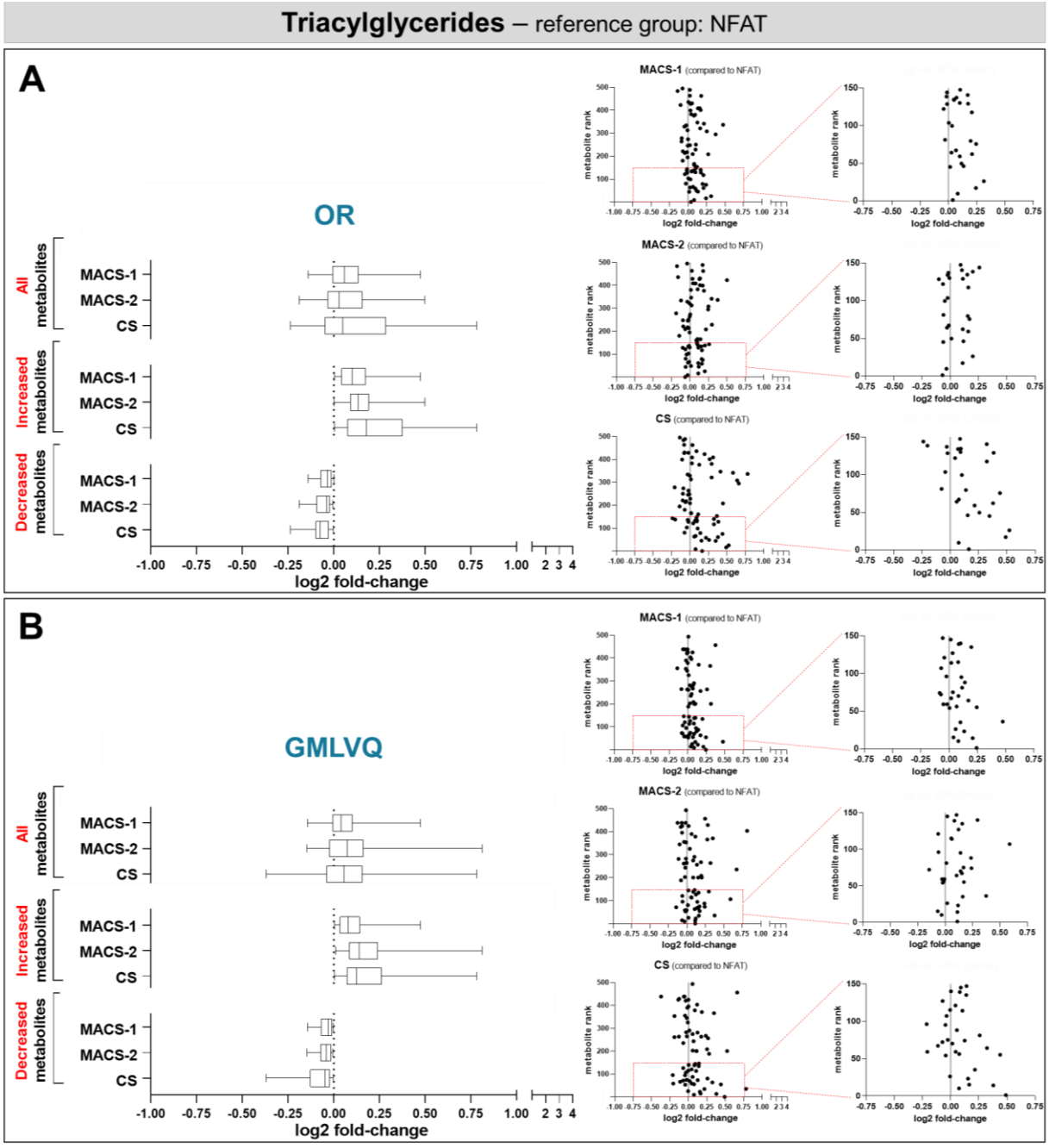

Figure 5.14: Changes of serum ceramides across the spectrum of autonomous cortisol secretion. Metabolic features identified by ordinal regression (OR, panel A) and generalised matrix learning vector quantisation (GMLVQ, panel B) are presented separately. Relative concentrations in possible mild autonomous cortisol secretion (MACS-1), definitive mild autonomous cortisol secretion (MACS-2), and Cushing's syndrome (CS) are shown as fold-changes compared to non-functioning adrenal tumours (NFAT); fold-changes are log2 transformed so that 0 equals to no change and values above and below 0 represent symmetrical degrees of change. The graph on the left shows the overall trend of the metabolic class in MACS-1, MACS-2 and CS, and fold-changes are shown as boxplots, with boxes representing median and interquartile range, and whiskers representing 5th to 95th centile; results are presented separately for all features combined, increased features only, and decreased features only. The graphs on the right show the fold-changes of single features (dots) and their relevance rank on the y-axis; the lower the rank, the more relevant a metabolic feature for the classifications of persons with benign adrenal tumours and autonomous cortisol secretion. Results are shown for the top 500 and top 150 metabolic features.

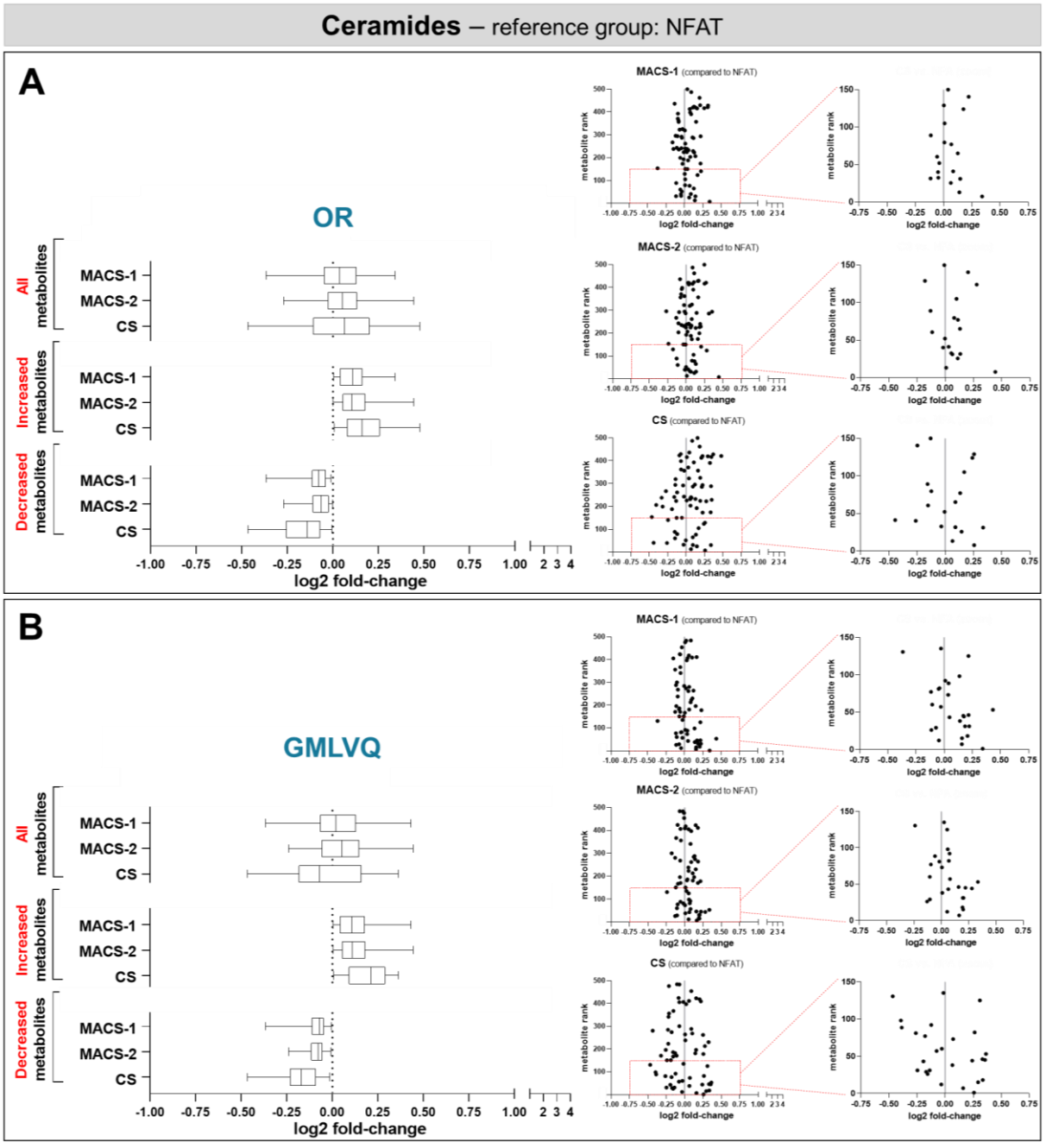

Figure 5.15: Changes of serum sphingolipids across the spectrum of autonomous cortisol secretion. Metabolic features identified by ordinal regression (OR, panel A) and generalised matrix learning vector quantisation (GMLVQ, panel B) are presented separately. Relative concentrations in possible mild autonomous cortisol secretion (MACS-1), definitive mild autonomous cortisol secretion (MACS-2), and Cushing's syndrome (CS) are shown as fold-changes compared to non-functioning adrenal tumours (NFAT); fold-changes are log2 transformed so that 0 equals to no change and values above and below 0 represent symmetrical degrees of change. The graph on the left shows the overall trend of the metabolic class in MACS-1, MACS-2 and CS, and fold-changes are shown as boxplots, with boxes representing median and interquartile range, and whiskers representing 5th to 95th centile; results are presented separately for all features combined, increased features only, and decreased features only. The graphs on the right show the fold-changes of single features (dots) and their relevance rank on the y-axis; the lower the rank, the more relevant a metabolic feature for the classifications of persons with benign adrenal tumours and autonomous cortisol secretion. Results are shown for the top 500 and top 150 metabolic features.

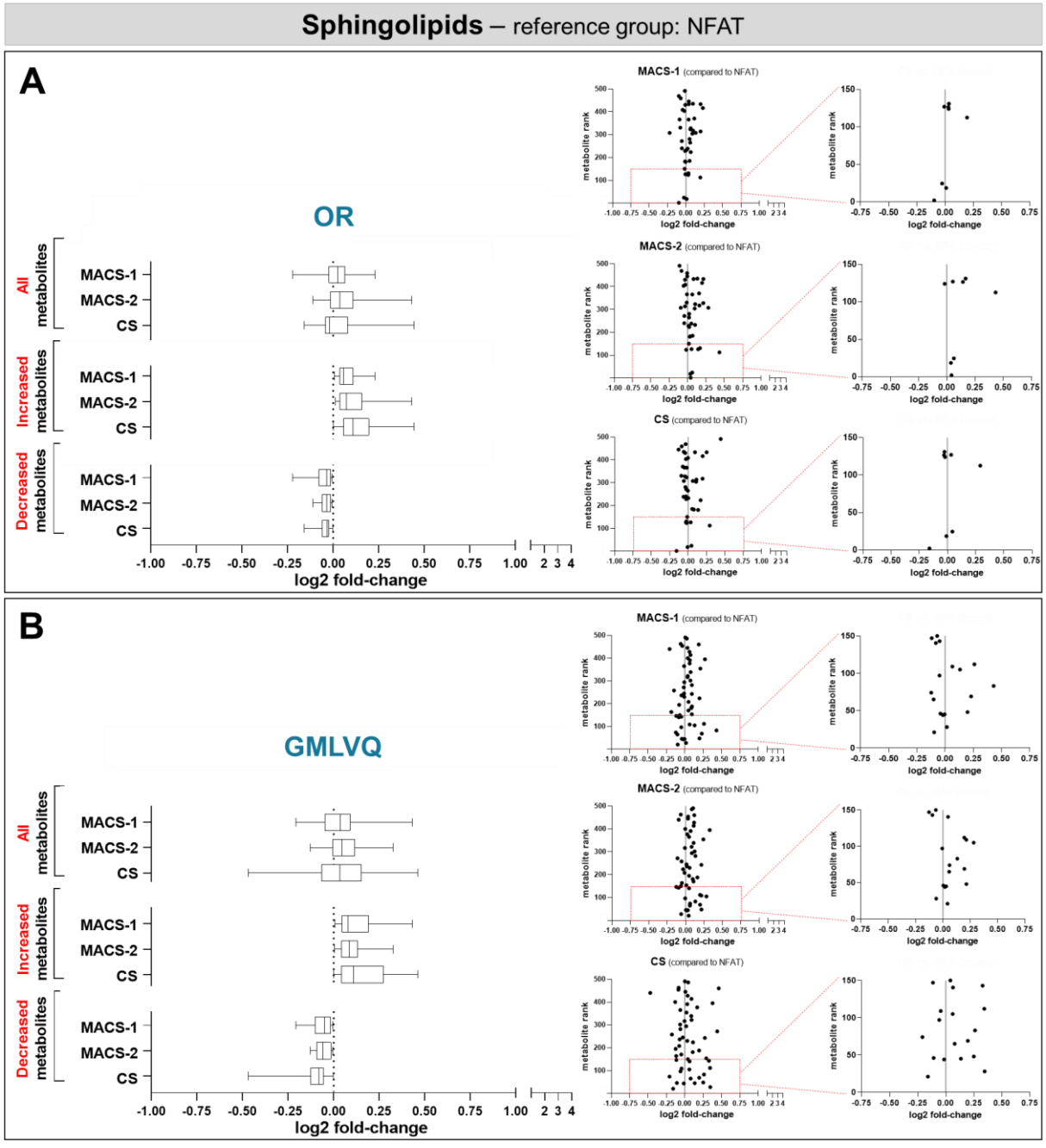

Figure 5.16: Changes of serum acylcarnitines across the spectrum of autonomous cortisol secretion. Metabolic features identified by ordinal regression (OR, panel A) and generalised matrix learning vector quantisation (GMLVQ, panel B) are presented separately. Relative concentrations in possible mild autonomous cortisol secretion (MACS-1), definitive mild autonomous cortisol secretion (MACS-2), and Cushing's syndrome (CS) are shown as fold-changes compared to non-functioning adrenal tumours (NFAT); fold-changes are log2 transformed so that 0 equals to no change and values above and below 0 represent symmetrical degrees of change. The graph on the left shows the overall trend of the metabolic class in MACS-1, MACS-2 and CS, and fold-changes are shown as boxplots, with boxes representing median and interquartile range, and whiskers representing 5th to 95th centile; results are presented separately for all features combined, increased features only, and decreased features only. The graphs on the right show the fold-changes of single features (dots) and their relevance rank on the y-axis; the lower the rank, the more relevant a metabolic feature for the classifications of persons with benign adrenal tumours and autonomous cortisol secretion. Results are shown for the top 500 and top 150 metabolic features.

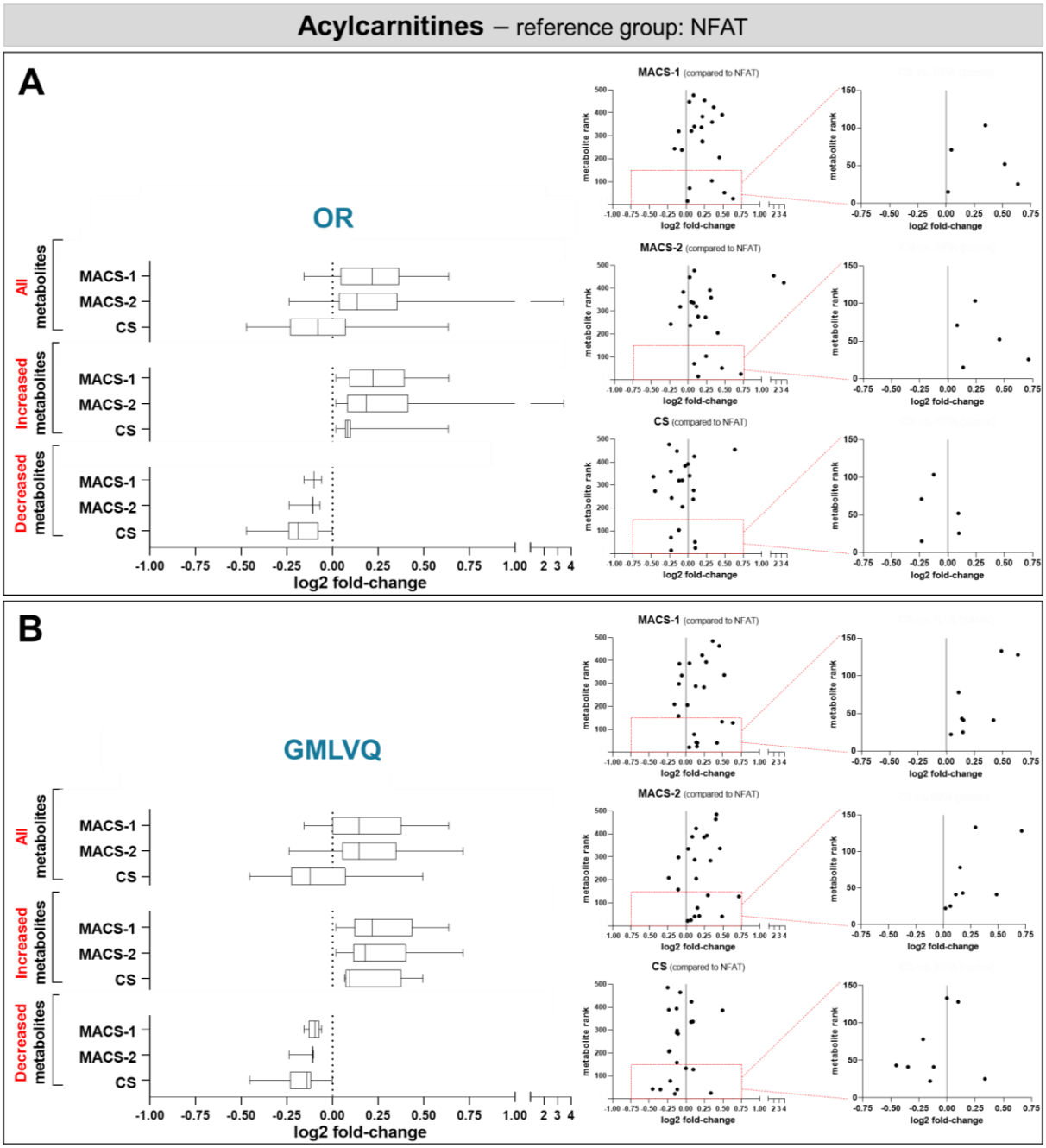

5.3.2. *Pathway enrichment analysis*

The pathway enrichment analysis results are reported in **Tables 5.3-5.4**. GMLVQ and OR agreed on identifying the arginine & proline and histidine metabolic pathways as the key pathways affected by autonomous cortisol secretion (**Figures 5.17-5.19**). The relative concentrations of selected metabolites belonging to these classes are reported for NFAT, MACS-1, MACS-2, and CS in **Figure 5.20**.

Both classifiers also identified tryptophan metabolism as potentially relevant in persons with MACS and CS, but this pathway did not remain significant after false discovery rate correction. Valine, leucine and isoleucine biosynthesis and alanine, aspartate and glutamate metabolism were identified as potentially relevant by OR but not GMLVQ (**Figure 5.17**).

Table 5.3: Pathway enrichment analysis based on metabolic feature ranking by ordinal regression. Pathway enrichment analysis was carried out on the top 500 polar metabolic features identified by hydrophilic interaction chromatography (HILIC) ultra-high performance liquid chromatography-mass spectrometry (UHPLC-MS) in the positive and negative ion modes and ranked in order of relevance by ordinal regression (OR). One-way ANOVA was used to compare persons with benign adrenal tumours and different degrees of autonomous cortisol secretion; non-corrected and false discovery rate (FDR)-corrected p-values for the various pathways identified are reported. The "match status" column shows the number of metabolites belonging to a specific pathway that OR assigned to the top 500 over the total number of metabolites in that pathway (e.g., 17 out of 38 metabolites of the arginine and proline metabolism pathway are found in the top 500 list generated by OR). The "annotated compound names" reports the list of metabolites belonging to a specific pathway; the metabolites found in the top 500 list generated by OR are shown in bold.

Pathway Name	**Non-corrected p-value**	**FDR-corrected p-value**	**Match Status**	**Annotated compound names**
Arginine and proline metabolism	<0.0001	<0.0001	17/38	**L-Arginine**; N(omega)-Hydroxyarginine; **Guanidinoacetate**; **Creatine**; 4-Aminobutanoate; Agmatine; Putrescine; 4-Aminobutyraldehyde; S-Adenosylmethioninamine; S-Adenosyl-L-methionine; Spermidine; N-Acetylputrescine; N4-Acetylaminobutanal; Spermine; **trans-3-Hydroxy-L-proline**; D-Proline; (4R)-4-Hydroxy-2-oxoglutarate; L-erythro-4-Hydroxyglutamate; **L-4-Hydroxyglutamate semialdehyde**; **L-1-Pyrroline-3-hydroxy-5-carboxylate**; **Hydroxyproline**; L-Proline; **cis-4-Hydroxy-D-proline**; **(S)-1-Pyrroline-5-carboxylate**; L-Glutamyl 5-phosphate; **L-Glutamate**; **L-Glutamate 5-semialdehyde**; **L-Ornithine**; Peptide; Nitric oxide; Phosphocreatine; 4-Guanidinobutanoate; **4-Acetamidobutanoate**; Homocarnosine; **1-Pyrroline-2-carboxylate**; **Glyoxylate**; **Pyruvate**; **1-Pyrroline-4-hydroxy-2-carboxylate**
Histidine metabolism	<0.0001	<0.0001	10/16	**L-Glutamate**; **4-Imidazolone-5-propanoate**; Urocanate; **L-Histidine**; Carnosine; **Imidazole-4-acetaldehyde**; **N-**

				Methylhistamine; Methylimidazole acetaldehyde; **Histamine**; **N(pi)-Methyl-L-histidine**; N-Formyl-L-aspartate; **N-Formimino-L-glutamate**; beta-Alanyl-N(pi)-methyl-L-histidine; **Imidazole-4-acetate**; **Methylimidazoleacetic acid**; L-Aspartate
Valine, leucine, and isoleucine biosynthesis	<0.0001	0.0029	6/8	**L-Threonine**; **(S)-3-Methyl-2-oxopentanoic acid**; **L-Leucine**; 3-Methyl-2-oxobutanoic acid; **2-Oxobutanoate**; **L-Isoleucine**; 4-Methyl-2-oxopentanoate; **L-Valine**
Alanine, aspartate, and glutamate metabolism	0.0018	0.0309	10/28	**N-Acetyl-L-aspartate**; 2-Oxosuccinamate; L-Aspartate; **L-Asparagine**; D-Aspartate; N-(L-Arginino)succinate; N6-(1,2-Dicarboxyethyl)-AMP; L-Alanine; **Succinate semialdehyde**; **L-Glutamate**; 4-Aminobutanoate; **L-Glutamine**; Ammonia; **2-Oxoglutaramate**; **(S)-1-Pyrroline-5-carboxylate**; N-Acetylaspartylglutamate; N-Acetylaspartylglutamylglutamate; Citrate; Oxaloacetate; Fumarate; **Pyruvate**; **N-Carbamoyl-L-aspartate**; **Succinate**; 2-Oxoglutarate; Carbamoyl phosphate; D-Glucosamine 6-phosphate; 5-Phosphoribosylamine; beta-Citryl-L-glutamate
Aminoacyl-tRNA biosynthesis*	<0.0001	0.0042	16/48	**L-Asparagine**; **L-Histidine**; **L-Phenylalanine**; **L-Arginine**; **L-Glutamine**; L-Cysteine; **Glycine**; L-Aspartate; L-Serine; **L-Methionine**; **L-Valine**; L-Alanine; **L-Lysine**; **L-Isoleucine**; **L-Leucine**; **L-Threonine**; **L-Tryptophan**; L-Methionyl-tRNA; **10-Formyltetrahydrofolate**; **L-Tyrosine**; L-Proline; **L-Glutamate**; Glutaminyl-tRNA; L-Asparaginyl-tRNA(Asn); L-Seryl-tRNA(Sec); O-Phosphoseryl-tRNA(Sec); L-Histidyl-tRNA(His); L-Phenylalanyl-tRNA(Phe); L-Arginyl-tRNA(Arg); L-Cysteinyl-tRNA(Cys); Glycyl-tRNA(Gly); L-Aspartyl-tRNA(Asp); L-Seryl-tRNA(Ser); L-Valyl-tRNA(Val); L-Alanyl-tRNA; L-Lysyl-tRNA; L-Isoleucyl-tRNA(Ile); L-Leucyl-tRNA; L-Threonyl-tRNA(Thr); L-Tryptophanyl-tRNA(Trp); Tetrahydrofolate; N-Formylmethionyl-tRNA; L-Tyrosyl-tRNA(Tyr); L-Prolyl-tRNA(Pro); L-Glutamyl-tRNA(Glu); L-Glutamyl-tRNA(Gln); L-Aspartyl-tRNA(Asn); L-Selenocysteinyl-tRNA(Sec)
Tryptophan metabolism	0.0336	0.3060	10/41	**L-Tryptophan**; Melatonin; N-Acetylserotonin; **Serotonin**; **5-Hydroxyindoleacetate**; 5-Hydroxykynurenamine; 5-Hydroxykynurenine; 5-Hydroxy-L-tryptophan; L-Formylkynurenine; Acetoacetyl-CoA; (S)-3-Hydroxybutanoyl-CoA; Crotonoyl-CoA; Glutaryl-CoA; **2-Oxoadipate**; 2-Aminomuconate semialdehyde; 2-Amino-3-carboxymuconate semialdehyde; **3-Hydroxyanthranilate**; **L-Kynurenine**; Formylanthranilate; 3-Hydroxy-L-kynurenine; 3-Hydroxykynurenamine; **Indole-3-acetaldehyde**; 5-Hydroxy-N-formylkynurenine; 5-Hydroxyindoleacetaldehyde; Tryptamine; Indolepyruvate; Formyl-N-acetyl-5-methoxykynurenamine; 6-Hydroxymelatonin; **Formyl-5-hydroxykynurenamine**; **5-Methoxyindoleacetate**; 4,6-Dihydroxyquinoline; Acetyl-CoA; 2-Aminomuconate; **Anthranilate**; Cinnavalininate; 4-(2-Amino-3-hydroxyphenyl)-2,4-dioxobutanoate; 4-(2-Aminophenyl)-2,4-dioxobutanoate; 4,8-Dihydroxyquinoline; Indole-3-acetate; N-Methylserotonin; N-Methyltryptamine
Arginine biosynthesis	0.0057	0.0793	6/14	**L-Glutamate**; **L-Arginine**; **N-Acetylornithine**; N-(L-Arginino)succinate; **L-Citrulline**; L-Aspartate; Carbamoyl phosphate; **L-Ornithine**; Ammonia; **L-Glutamine**; 2-Oxoglutarate; N-Acetyl-L-glutamate; Urea; Fumarate
Pyrimidine metabolism	0.0088	0.1051	11/39	UDP; **L-Glutamine**; Carbamoyl phosphate; (S)-Dihydroorotate; **Orotidine 5'-phosphate**; UMP; UTP; **Uridine**; 5,6-Dihydrouracil; **3-Ureidopropionate**; CTP; CDP; CMP; **Cytidine**; dCDP; dCMP; dCTP; **Deoxycytidine**; dUTP; dUDP; dUMP; **Deoxyuridine**; dTDP; dTTP; dTMP; **Thymidine**; **Thymine**; (R)-5,6-Dihydrothymine; (R)-3-Ureidoisobutyrate; P1,P4-Bis(5'-uridyl) tetraphosphate; 2'-Deoxy-5-hydroxymethylcytidine-5'-diphosphate; **N-Carbamoyl-L-aspartate**; Orotate; 5-Phospho-alpha-D-ribose 1-diphosphate;

				Uracil; beta-Alanine; **2-Deoxy-D-ribose 1-phosphate**; (R)-3-Amino-2-methylpropanoate; 2'-Deoxy-5-hydroxymethylcytidine-5'-triphosphate
Caffeine metabolism	0.0316	0.3060	4/10	1,7-Dimethylxanthine; **1-Methylxanthine**; Theobromine; **7-Methylxanthine**; Caffeine; 1-Methyluric acid; **3,7-Dimethyluric acid**; **1,7-Dimethyluric acid**; 5-Acetylamino-6-formylamino-3-methyluracil; 7-Methyluric acid
Butanoate metabolism	0.0364	0.3060	5/15	(R)-3-Hydroxybutanoate; **Acetoacetate**; (S)-3-Hydroxy-3-methylglutaryl-CoA; Acetyl-CoA; Acetoacetyl-CoA; (S)-3-Hydroxybutanoyl-CoA; Crotonoyl-CoA; 4-Aminobutanoate; **L-Glutamate**; Butanoyl-CoA; **Succinate semialdehyde**; Butanoic acid; 2-Oxoglutarate; **Succinate**; **2-Hydroxyglutarate**
Glycine, serine, and threonine metabolism	0.0568	0.4336	8/33	L-Serine; Choline; Betaine aldehyde; Betaine; **Guanidinoacetate**; 3-Phospho-D-glycerate; N,N-Dimethylglycine; L-Cystathionine; **Glycine**; O-Phospho-L-serine; Sarcosine; 5,10-Methylenetetrahydrofolate; **L-Threonine**; Lipoylprotein; Aminoacetone; D-Glycerate; [Protein]-S8-aminomethyldihydrolipoyllysine; Tetrahydrofolate; Dihydrolipoylprotein; 2-Phospho-D-glycerate; D-Serine; Hydroxypyruvate; **Creatine**; 3-Phosphonooxypyruvate; L-Cysteine; **2-Oxobutanoate**; **Glyoxylate**; L-2-Amino-3-oxobutanoic acid; **Pyruvate**; CO2; **5-Aminolevulinate**; Methylglyoxal; Ammonia
Purine metabolism	0.0725	0.5077	13/65	GDP; **Xanthine**; D-Ribose 5-phosphate; **L-Glutamine**; 5-Phospho-alpha-D-ribose 1-diphosphate; 5-Phosphoribosylamine; 5'-Phosphoribosylglycinamide; 2-(Formamido)-N1-(5'-phosphoribosyl)acetamidine; 1-(5'-Phosphoribosyl)-5-amino-4-imidazolecarboxamide; 1-(5'-Phosphoribosyl)-5-amino-4-(N-succinocarboxamide)-imidazole; 1-(5-Phospho-D-ribosyl)-5-amino-4-imidazolecarboxylate; 1-(5'-Phosphoribosyl)-5-formamido-4-imidazolecarboxamide; 3',5'-Cyclic AMP; ATP; ADP; dADP; AMP; N6-(1,2-Dicarboxyethyl)-AMP; IMP; **Adenosine**; **dAMP**; **Deoxyadenosine**; Deoxyinosine; Xanthosine; IDP; GMP; Xanthosine 5'-phosphate; **Hypoxanthine**; **Inosine**; **Guanine**; **Deoxyguanosine**; Allantoate; Guanosine 3',5'-bis(diphosphate); Guanosine 3'-diphosphate 5'-triphosphate; GTP; dGMP; dGDP; Guanosine; 3',5'-Cyclic GMP; Sulfate; Adenylyl sulfate; 5'-Phosphoribosyl-N-formylglycinamide; ITP; XTP; P1,P4-Bis(5'-adenosyl)tetraphosphate; dGTP; P1,P4-Bis(5'-xanthosyl) tetraphosphate; alpha-D-Ribose 1-phosphate; ADP-ribose; **Adenine**; dIDP; dITP; P1,P3-Bis(5'-adenosyl) triphosphate; dATP; 5-Hydroxy-2-oxo-4-ureido-2,5-dihydro-1H-imidazole-5-carboxylate; **Urate**; **Aminoimidazole ribotide**; Ammonia; (S)-Ureidoglycolate; Urea; 3'-Phosphoadenylyl sulfate; P1,P4-Bis(5'-guanosyl) tetraphosphate; 2'-Deoxyinosine 5'-phosphate; **5-Amino-4-imidazolecarboxyamide**; (S)-Allantoin
Phenylalanine, tyrosine, and tryptophan biosynthesis	0.0856	0.5531	2/4	Phenylpyruvate; **L-Phenylalanine**; **L-Tyrosine**; 3-(4-Hydroxyphenyl)pyruvate
* The aminoacyl-tRNA biosynthesis group includes all amino acids and for this reason is often perturbed in untargeted metabolomics studies. However, this group is not specific to a metabolic pathway.				

Table 5.4: Pathway enrichment analysis based on metabolic feature ranking by generalised matrix learning vector quantisation. Pathway enrichment analysis was carried out on the top 500 polar metabolic features identified by hydrophilic interaction chromatography (HILIC) ultra-high performance liquid chromatography-mass spectrometry (UHPLC-MS) in the positive and negative ion modes and ranked in order of relevance by generalised matrix learning vector quantisation (GMLVQ). One-way ANOVA was used to compare persons with benign adrenal tumours and different degrees of autonomous cortisol secretion; non-corrected and false discovery rate (FDR)-corrected p-values for the various pathways identified are reported. The "match status" column shows the number of metabolites belonging to a specific pathway that GMLVQ assigned to the top 500 over the total number of metabolites in that pathway (e.g., 12 out of 38 metabolites of the arginine and proline metabolism pathway are found in the top 500 list generated by GMLVQ). The "annotated compound names" reports the list of metabolites belonging to a specific pathway; the metabolites found in the top 500 list generated by GMLVQ are shown in bold.

Pathway Name	Non-corrected p-value	FDR-corrected p-value	Match status	Annotated compound names
Arginine and proline metabolism	<0.0001	0.0015	12/38	**L-Arginine**; N(omega)-Hydroxyarginine; Guanidinoacetate; **Creatine**; 4-Aminobutanoate; Agmatine; Putrescine; 4-Amino-butyraldehyde; S-Adenosylmethioninamine; S-Adenosyl-L-methionine; Spermidine; N-Acetylputrescine; N4-Acetylamino-butanal; Spermine; **trans-3-Hydroxy-L-proline**; D-Proline; (4R)-4-Hydroxy-2-oxoglutarate; L-erythro-4-Hydroxyglutamate; **L-4-Hydroxyglutamate semialdehyde**; **L-1-Pyrroline-3-hydroxy-5-carboxylate**; **Hydroxyproline**; L-Proline; **cis-4-Hydroxy-D-proline**; (S)-1-Pyrroline-5-carboxylate; L-Glutamyl 5-phosphate; L-Glutamate; **L-Glutamate 5-semialdehyde**; **L-Ornithine**; Peptide; Nitric oxide; Phosphocreatine; **4-Guanidinobutanoate**; 4-Acetamidobutanoate; Homocarnosine; 1-Pyrroline-2-carboxylate; Glyoxylate; **Pyruvate**; **1-Pyrroline-4-hydroxy-2-carboxylate**
Histidine metabolism	<0.0001	0.0401	6/16	L-Glutamate; **4-Imidazolone-5-propanoate**; **Urocanate**; L-Histidine; Carnosine; Imidazole-4-acetaldehyde; **N-Methylhistamine**; Methylimidazole acetaldehyde; Histamine; **N(pi)-Methyl-L-histidine**; N-Formyl-L-aspartate; **N-Formimino-L-glutamate**; beta-Alanyl-N(pi)-methyl-L-histidine; Imidazole-4-acetate; **Methylimidazoleacetic acid**; L-Aspartate
Tryptophan metabolism	0.0402	0.6748	7/41	L-Tryptophan; Melatonin; N-Acetylserotonin; Serotonin; 5-Hydroxyindoleacetate; **5-Hydroxykynurenamine**; 5-Hydroxykynurenine; **5-Hydroxy-L-tryptophan**; L-Formylkynure-nine; Acetoacetyl-CoA; (S)-3-Hydroxybutanoyl-CoA; Crotonoyl-CoA; Glutaryl-CoA; 2-Oxoadipate; 2-Aminomuconate semi-aldehyde; 2-Amino-3-carboxymuconate semialdehyde; 3-Hydroxy-anthranilate; **L-Kynurenine**; Formylanthranilate; 3-Hydroxy-L-kynurenine; 3-Hydroxykynurenamine; **Indole-3-acetaldehyde**; 5-Hydroxy-N-formylkynurenine; 5-Hydroxyindoleacetaldehyde; Tryptamine; Indolepyruvate; Formyl-N-acetyl-5-methoxykynuren-amine; 6-Hydroxymelatonin; Formyl-5-hydroxykynurenamine; **5-Methoxyindoleacetate**; **4,6-Dihydroxyquinoline**; Acetyl-CoA; 2-Aminomuconate; Anthranilate; Cinnavalininate; 4-(2-Amino-3-hydroxyphenyl)-2,4-dioxobutanoate; 4-(2-Aminophenyl)-2,4-dioxobutanoate; **4,8-Dihydroxyquinoline**; Indole-3-acetate; N-Methylserotonin; N-Methyltryptamine
Phenylalanine, tyrosine, and tryptophan biosynthesis	0.0342	0.6748	2/4	Phenylpyruvate; **L-Phenylalanine**; **L-Tyrosine**; 3-(4-Hydroxyphenyl)pyruvate
Phenylalanine metabolism	0.0395	0.6748	3/10	Phenylacetaldehyde; **L-Phenylalanine**; Phenethylamine; Pheny-lpyruvate; Benzoyl-CoA; Phenylacetic acid; 2-Hydroxyphenyl-acetate; 2-Hydroxy-3-phenylpropenoate; **Hippurate**; **L-Tyrosine**
Arginine biosynthesis	0.0950	1	3/14	L-Glutamate; **L-Arginine**; N-Acetylornithine; N-(L-Arginino)succinate; **L-Citrulline**; L-Aspartate; Carbamoyl phosphate; **L-Ornithine**; Ammonia; L-Glutamine; 2-Oxoglutarate; N-Acetyl-L-glutamate; Urea; Fumarate

Figure 5.17: Pathway enrichment analysis in persons with benign adrenal tumours and autonomous cortisol secretion. The number of metabolic features identified by generalised matrix learning vector quantisation (GMLVQ) and ordinal regression (OR) are reported as a Venn diagram. The circle areas and of the overlapping area (showing the number of features identified by both classifiers) are directly proportional to the number of features. The metabolic pathways identified as significant by one or both machine learning classifiers are shown. Abbreviations: FDR, false discovery rate.

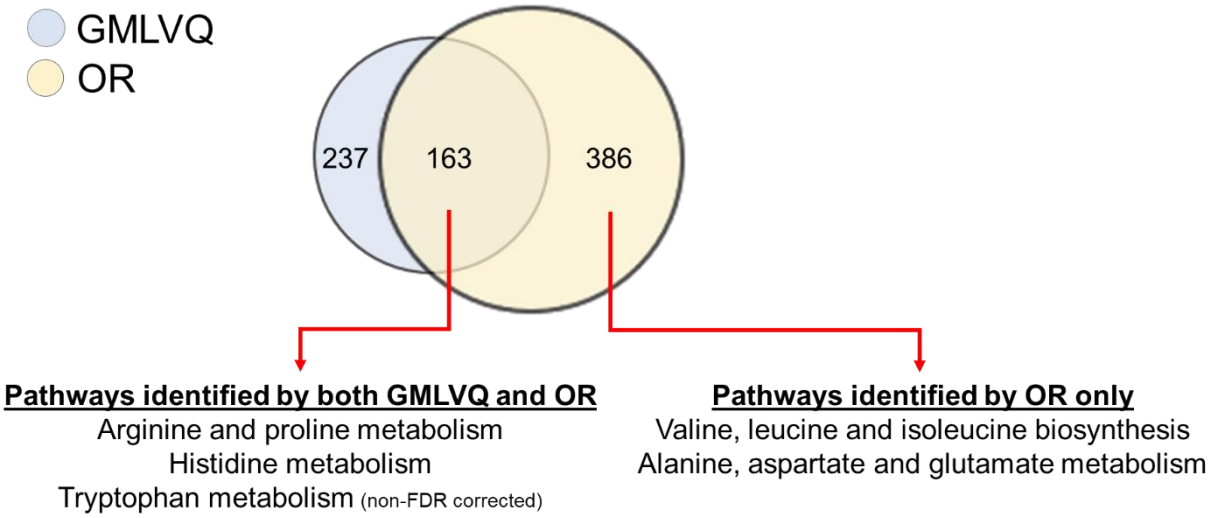

Figure 5.18: Arginine and proline metabolism. The metabolites identified by machine learning are circled in red. Generated with KEGG (178).

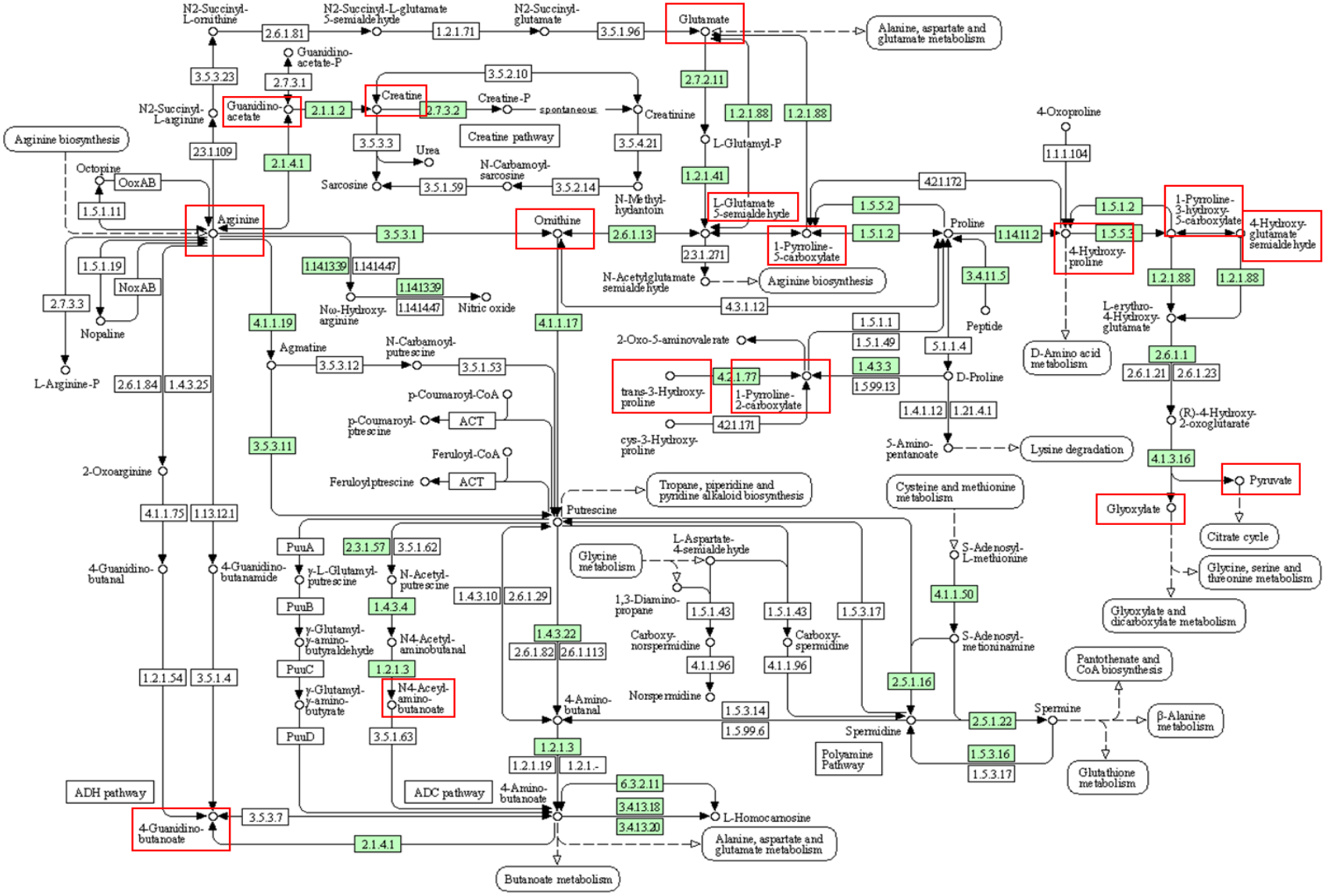

Figure 5.19: Histidine metabolism. The metabolites identified by machine learning are circled in red. Generated with KEGG (178).

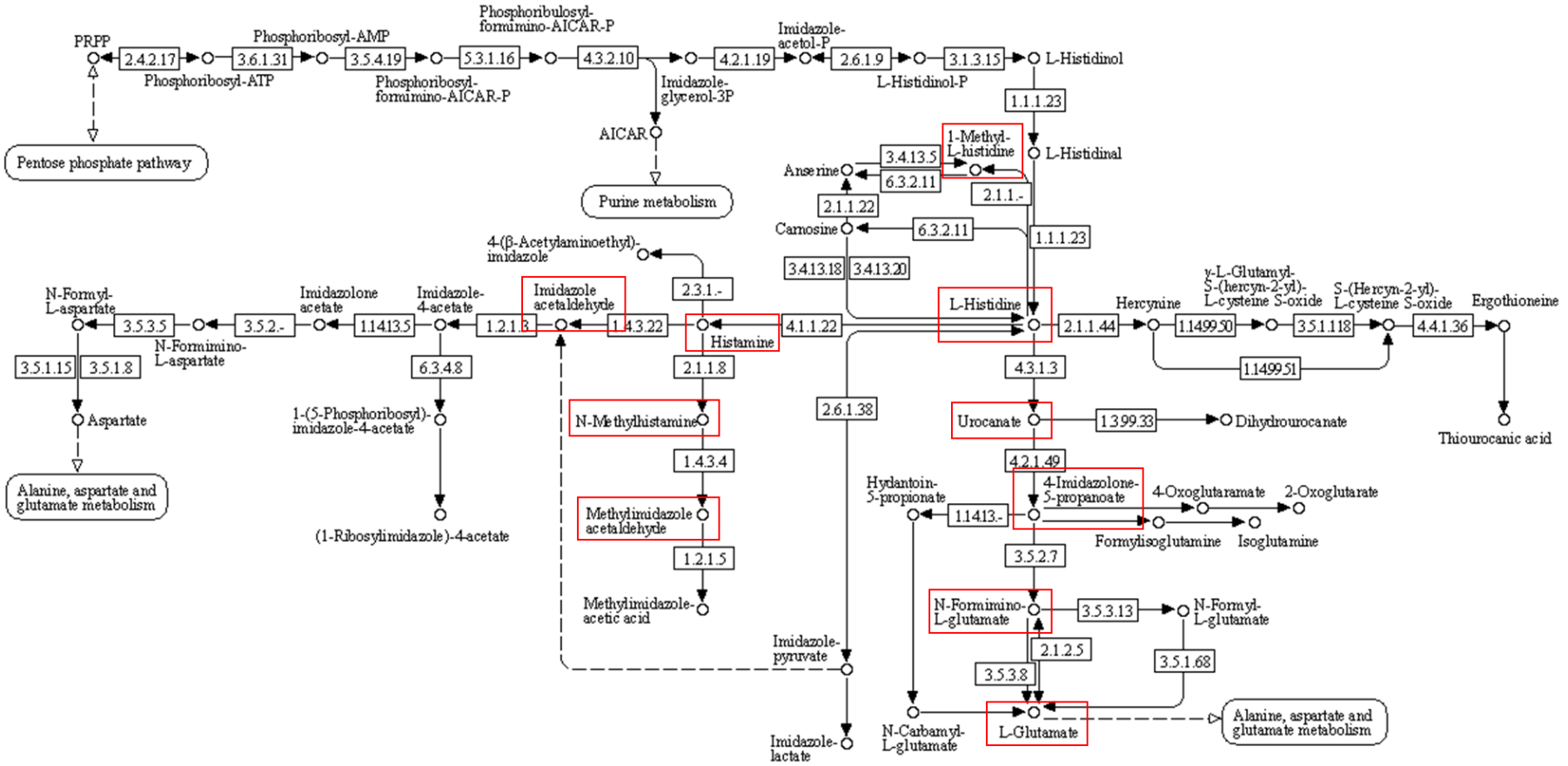

Figure 5.20: Concentrations of selected metabolites of the arginine & proline and histidine metabolic pathways. Box and whisker plot describing normalised relative intensity values in the concentration of selected metabolites in persons with non-functioning adrenal tumours (NFAT), possible mild autonomous cortisol secretion (MACS-1), definitive mild autonomous cortisol secretion (MACS-2), and Cushing's syndrome (CS).

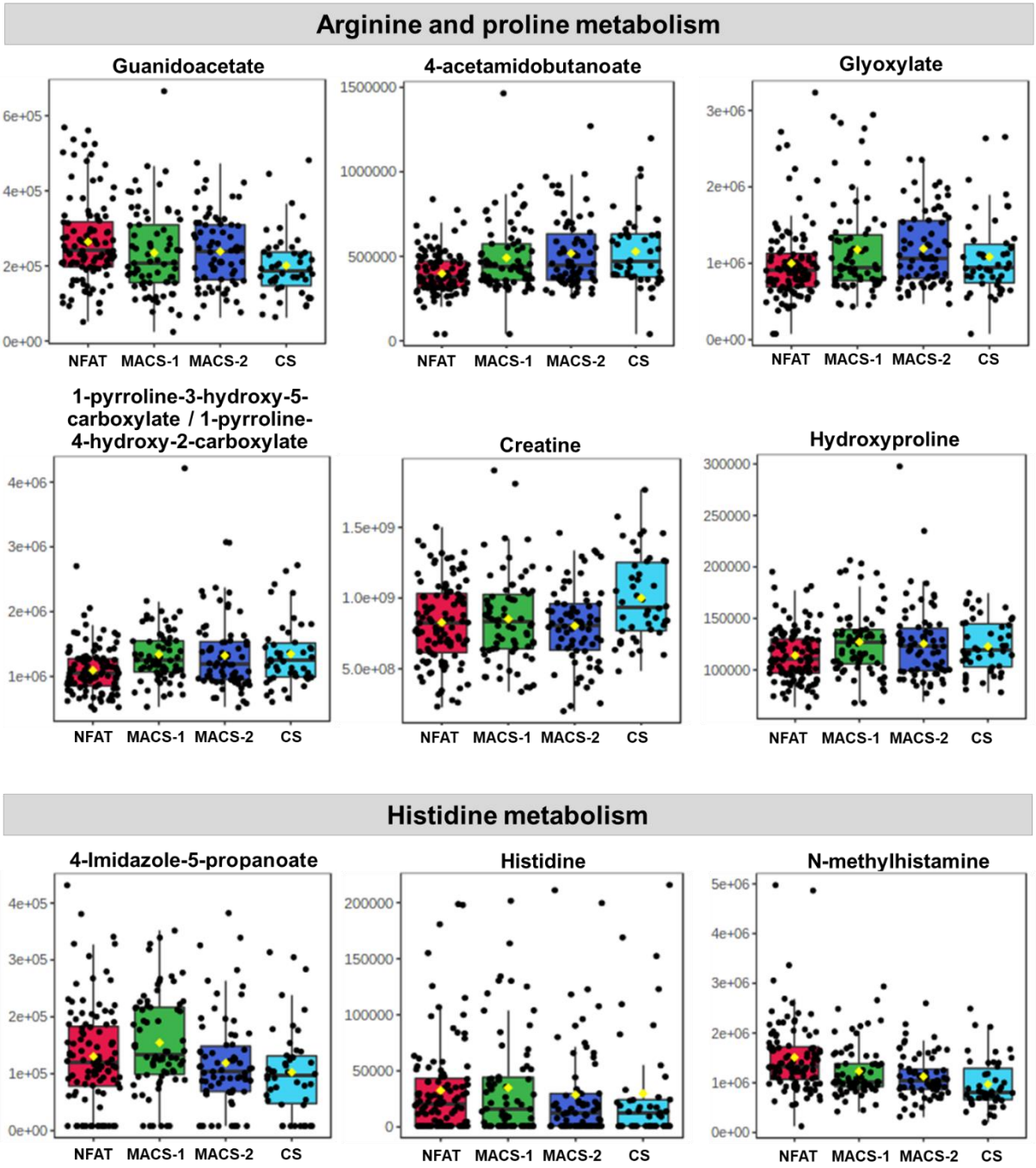

5.4. Discussion

The present study focused on the analysis of the untargeted serum metabolome in a large cohort of persons with benign adrenal tumours. Data modelling by machine learning revealed extensive perturbations in the lipidome and amino acid metabolism which correlated with the degree of autonomous cortisol secretion, providing insights into the crosstalk between cortisol excess and human metabolism.

Glycerophospholipids were the lipid class most affected by the cortisol excess, with progressively increased derangement in MACS-1, MACS-2, and CS. These changes were primarily driven by phosphatidylcholines and phosphatidylethanolamines that, in addition to being the most abundant structural components of cell membranes, are involved in the regulation of lipid metabolism, lipoprotein secretion, and whole-body energy metabolism by supporting mitochondrial function (179). Abnormal levels of these glycerophospholipids in mitochondrial membranes have been linked to the development of mitochondrial dysfunction leading to cardiovascular disease and metabolic syndrome (180, 181). Moreover, phosphatidylcholines and phosphatidylethanolamines can influence insulin signalling in the skeletal muscle, possibly by disrupting calcium signalling (182, 183), hence impacting glucose disposal and energy metabolism (184, 185). An imbalance of phosphatidylcholines and phosphatidylethanolamines can also lead to dysfunctional membranes of cytosolic lipid droplets, leading to reduced capacity for storing excess lipids into droplets and chronic elevation of circulating fatty acids, which can accumulate in non-adipose tissues resulting in lipotoxicity (186, 187). Phosphatidylethanolamines and phosphatidylcholines have also been proposed as biomarkers for major depressive disorders (188), type 2 diabetes (189-191), and cardiovascular events (189).

The association between autonomous cortisol secretion and glycerophospholipids has been investigated before. Zoran et al. recently published the results of the targeted plasma metabolome profiling of 40 persons with CS and hypertension and – in agreement with the present study – found that several phosphatidylcholines could discriminate cases from controls (192). A further study by Di Dalmazi et al. utilising a targeted plasma metabolome profiling in a smaller cohort of persons with NFAT, MACS and CS, found that autonomous cortisol secretion correlated with abnormal concentrations of several phosphatidylcholines (193). The concentrations of these metabolites also showed a negative association with post-DST cortisol levels, corroborating the hypothesis that the more severe the cortisol excess, the more perturbed the glycerophospholipids. Similarly, a recently published study by Vega-Beyhart et al. assessing the serum metabolome of 25 persons with CS, found altered levels of phosphatidylcholines and phosphatidylethanolamines that correlated with 24-hour urinary free cortisol and post-DST cortisol levels (194). The authors also identified dysregulation of the Kennedy pathway in CS, which leads to the *de novo* synthesis of phosphatidylcholines and phosphatidylethanolamines (**Figure 5.5**).

Untargeted serum metabolomics identified the downregulation of phosphatidylinositols and phosphatidylserines in persons with CS. These glycerophospholipids act as precursors of membrane-derived second messengers involved in many trafficking and signalling pathways. Dysregulation of their metabolism can lead to pro-inflammatory and pro-atherosclerotic changes (195), hypercoagulable states (195), as well as insulin resistance and type 2 diabetes (191, 196). It is therefore intriguing to speculate that perturbations of these glycerophospholipid subclasses contribute to the cardiometabolic burden of CS.

A key finding of this study was the dysregulation of several bioactive lipid classes in the lipidome of persons with MACS and CS. Ceramides and other sphingolipids regulate several pathophysiological mechanisms including cell cycle, inflammation, angiogenesis, and intracellular trafficking (197). An imbalance between glycerophospholipids and these pro-inflammatory bioactive lipids has been proposed as a hallmark of lipotoxicity and is associated with multiple chronic inflammatory diseases including obesity, type 2 diabetes, non-alcoholic fatty liver disease, cardiovascular events, and cancer (191, 197, 198). Similarly, lysoglycerophospholipids play a role in cell signalling including immunomodulation, insulin resistance, and endothelial function (199), and have been proposed as biomarkers for obesity, cardiovascular events, and type 2 diabetes (191, 200-204). The studies by Zoran et al. (192) and Vega-Beyhart et al. (194) found similar changes in these bioactive lipid classes in persons with CS, supporting the hypothesis that part of the increase cardiometabolic burden of autonomous cortisol secretion is driven by abnormal lipid-dependent cell signalling.

The lipidome analysis further identified acylcarnitines, intermediate products of lipid β-oxidation, as perturbed in persons with autonomous cortisol secretion. Interestingly, these were upregulated in MACS and downregulated in CS. Our findings differ from the study by Di Dalmazi et al., where persons with MACS and CS presented a similar trend of lower levels of short-/medium-chain acylcarnitines and a relative increase of long-chain acylcarnitines (193). Higher levels of long-chain acylcarnitines in persons with CS were also observed by Zoran et al. (192), but not Vega-Beyhart et al. (194). Alterations in acylcarnitines point toward dysfunctional lipid β-oxidation and mitochondrial stress, which are associated with the risk of developing insulin resistance

and type 2 diabetes (191, 205, 206). This raises the interesting possibility that acylcarnitines may be used as biomarkers for the identification of persons with MACS at higher cardiometabolic risk. The reasons for the different acylcarnitines concentrations in MACS and CS are unclear but could be related to the duration and severity of the cortisol excess, as well as the acute inhibitory effect of cortisol excess on enzymes involved in lipid β-oxidation (207).

Pathway enrichment analysis identified abnormal concentrations of several amino acids in persons with MACS and CS (**Tables 5.3-5.4**). The arginine & proline and histidine metabolic pathways were primarily affected by autonomous cortisol secretion, but changes in aromatic amino acids (tryptophan metabolism), branched-chain amino acids (valine, leucine, and isoleucine biosynthesis), and derivatives of citric acid cycle intermediates (alanine, aspartate, and glutamate metabolism) were also observed.

Alterations of arginine and proline metabolism have been linked to cardiovascular disease and the development of type 2 diabetes (208-210), possibly because of reduced generation of arginine-derived nitric oxide leading to pro-inflammatory changes, mitochondrial dysfunction and oxidative stress (211, 212). The disruption of the arginine-nitric oxide pathway has also been observed in experimental models of glucocorticoid-induced hypertension (213), suggesting a contributing role to the pathogenesis of hypertension in autonomous cortisol secretion in addition to mineralocorticoid receptor activation by cortisol and increased vascular tone (214). Furthermore, arginine is a precursor of polyamines, involved in oxidative stress and cortisol-related immunomodulation (215); increase levels of the polyamine spermidine have been observed in persons with CS (192, 193) and linked to the presence of

catabolic signs of cortisol excess such as proximal myopathy, skin thinning, and easy bruising (193).

Histidine and related metabolites were downregulated in MACS and CS (**Figure 5.20**). Histidine was found to dampen inflammation and ameliorate insulin sensitivity (216). Moreover, histidine derivatives such as carnosine play a major role in protecting the skeletal muscle from oxidative stress and low levels of histidine have been associated with sarcopaenia (217, 218). In line with these observations, Di Dalmazi et al. found that lower histidine concentrations correlated with the severity of autonomous cortisol secretion and with catabolic signs including proximal myopathy (193).

Strengths of the present study include the large sample size and the prospective recruitment, which differentiate it from three previous studies focusing on similar research questions (192-194). The metabolome profiling by four distinct assays yielded a comprehensive overview of the metabolic perturbations associated with autonomous cortisol secretion, and the reliability of the results obtained is supported by the agreement between two independent machine learning classifiers. Limitations of the present study include its cross-sectional design and the non-standardised sample collection in relation to the time of the day and food intake, which can have impacted the variability of the serum metabolome. A further limitation is that study participants were not matched for age and sex. When serum samples were selected for analysis, matching for BMI and cardiometabolic disease prevalence was prioritised over other parameters; moreover, in the MACS group (a condition that primarily affects postmenopausal women) only women were included to minimise the sex differences in the untargeted metabolome across the spectrum of autonomous cortisol secretion.

In conclusion, MACS and CS were associated with a lipidome signature suggestive of pro-inflammatory changes, incomplete lipid β-oxidation, and lipotoxicity, as well as perturbed amino acid metabolism reflecting oxidative stress and protein catabolism. These results offer possible mechanistic insights on how MACS and CS lead to metabolic dysfunction and cardiometabolic disease and hold the promise of risk stratification of affected individuals.

CHAPTER 6

Conclusions and future directions

I presented in this thesis the characteristics of the largest prospective study to date on persons with benign adrenocortical tumours and different degrees of autonomous cortisol secretion, from non-functioning adrenal tumours (NFAT) to possible mild autonomous cortisol secretion (MACS-1), definitive mild autonomous cortisol secretion (MACS-2), and clinically overt Cushing's syndrome (CS).

Firstly, I presented the clinical characteristics of the 1305 persons included in the study, with a particular focus on MACS which accounted for almost half of the cases. I showed that MACS primarily affects post-menopausal women, who often present with larger and bilateral adrenal tumours. I also demonstrated a progressively higher cardiometabolic burden with increasing cortisol excess, particularly a higher prevalence and severity of hypertension and type 2 diabetes in persons with MACS compared to NFAT.

Secondly, I presented the results of the centralised multi-steroid metabolite profiling by liquid chromatography-tandem mass spectrometry of the 24-hour urine samples collected by the 1305 study participants at the time of adrenal tumour diagnosis. After applying linear regression and prototype-based supervised machine learning, I demonstrated progressive changes in the steroid metabolome across the spectrum NFAT – MACS-1 – MACS-2 – CS, characterised by increasing urinary excretion of glucocorticoid and glucocorticoid precursor metabolites and decreasing excretion of androgen metabolites. I also observed increased glucocorticoid excretion in persons

with bilateral adrenal tumours. I further stratified persons with MACS according to the presence of hypertension and type 2 diabetes and found that an increased cardiometabolic burden was associated with higher urinary excretion of 11-oxygenated androgen metabolites, suggesting a causative contribution of these hormones to the cardiometabolic risk profile of MACS.

In the last part of the thesis, I presented the metabolic perturbations associated with autonomous cortisol secretion after analysing the untargeted serum metabolome of 291 persons with benign adrenocortical tumours. Two independent prototype-based supervised machine learning methods and pathway enrichment analysis were employed for selection of the most relevant metabolic perturbations. I showed that persons with MACS and CS have a lipidome signature characterised by compromised cell membrane integrity, abnormal levels of pro-inflammatory bioactive lipids hallmark of lipotoxicity, and dysfunctional mitochondrial lipid β-oxidation. Moreover, I observed abnormal arginine & proline and histidine metabolism in MACS and CS, which points towards an association between autonomous cortisol secretion, oxidative stress, abnormal insulin signalling, and protein catabolism.

In conclusion, I showed that MACS is a very frequent cause of cardiometabolic disease that primarily affects women. The urine steroid metabolome revealed progressive changes across the spectrum of autonomous cortisol secretion, indicative of ACTH-independent glucocorticoid excess. This was reflected in progressive perturbations of the lipid, protein, and energy metabolism, indicative of a causative contribution of cortisol excess to the high cardiometabolic burden observed in MACS. These findings provide mechanistic insights into the metabolic consequences of cortisol excess and

observed changes hold promise for risk stratification in MACS, a highly relevant and previously largely overlooked metabolic risk condition.

The results presented in this thesis lay the foundation for my future research activity. I intend to continue dissecting the cardiometabolic impact of MACS to improve the diagnosis, risk stratification, and management of this common condition. The key next steps that I envisage are described below.

Integrating the steroid and untargeted metabolome data: First, I plan to combine the urine multi-steroid metabolome and serum untargeted metabolome profiling results that are already available to me. This would provide not only further insights into the crosstalk between steroid and global metabolism but also the groundwork for biomarker identification. The results I presented in this thesis are mostly hypothesis-generating and inform the pathophysiology of autonomous cortisol secretion. The next natural step is to use this wealth of information to select possible biomarkers of increased cardiometabolic risk, which could be translated to the clinic for patient risk stratification and targeted treatment.

Examining the tissue-specific consequences of MACS: I devised an experimental medicine study called *Adrenal Incidentalomas causing Metabolic dysfunction due to Mild Autonomous Cortisol Secretion (AIM-MACS)*. Persons with MACS and matched controls would undergo systemic and tissue-specific blood sampling of the adipose tissue and skeletal muscle using the arterio-venous difference technique (219). Assessments would be carried out in the post-absorptive state and after a mixed meal test coupled with the use of isotope-labelled triacylglycerides. Outcomes of the study include parameters of glucose metabolism and tissue-specific rates of glucose uptake, lipid kinetics between the adipose tissue and the skeletal muscle, the steroid

metabolome in the adipose tissue and skeletal muscle, and the untargeted metabolome in the adipose tissue and skeletal muscle.

Testing novel interventions for MACS: I devised a proof-of-concept, dose-escalation study called *Effects of OSIlodrostat on the CORTicosteroid metabolome in patients with mild autonomous cortisol excess (OSI-CORT)*. Currently, adrenalectomy is the only treatment option for MACS, but persons with MACS are often elderly and have multiple co-morbidities that increase their surgical risk. I hypothesise that the CYP11B1 inhibitor osilodrostat, given at doses lower than those recommended for CS, is a potential therapy to reduce the cardiometabolic burden of MACS and avoid surgery. In this study, I would assess how osilodrostat affects the urinary steroid metabolome and test the hypothesis that low-dose osilodrostat can significantly reduce urinary glucocorticoid excretion. Persons with MACS would receive incremental doses of osilodrostat for 4 weeks in a stepwise approach (lowest dose 0.5mg/day, highest dose 2mg/day). During the study, participants would provide urine collections for urine multi-steroid profiling. I expect to identify the minimum effective dose of osilodrostat required to significantly reduce urine glucocorticoid excretion. The results of the study would inform the design of a larger phase 2b clinical trial focusing on the impact of osilodrostat treatment on the cardiometabolic burden of persons with MACS.

In-depth phenotyping of persons with and without adrenal tumours: I plan to access the UK biobank platform, a large prospective study that has collected phenotypic and genotypic data of >500,000 adults (220). By focusing on persons who underwent cross-sectional imaging of the abdomen, I would be able to select persons with incidentally discovered adrenal tumours and carefully matched controls. This approach would not only provide robust data about the prevalence of adrenal tumours in the

general population but would allow for correlating imaging with phenotypic and genotypic information.

Investigating the functional status changes of adrenal incidentalomas: I am setting up a retrospective, multi-centre study called *DEXamethasone suppression test follow-up study in Adrenal Incidentalomas (DEX-AI)* to determine how many persons initially diagnosed with NFAT and MACS change their functional status over time. Whilst the risk of developing CS in persons initially diagnosed with NFAT or MACS during long-term follow-up is negligible (<0.1%), 4-22% of persons initially classified as NFAT can develop an abnormal 1mg-overnight dexamethasone suppression test (1mg-DST) during follow-up; however, the evidence behind this comes from small-scale studies that did not focus on clinical outcomes (15, 21, 78). Through the DEX-AI multi-centre study, I aim to determine the proportion of persons with benign adrenal incidentalomas who develop incident changes in 1mg-DST results and to correlate this with clinical, radiological, and hormonal outcomes.

Patient-reported outcome measures in adrenal incidentalomas: Persons with MACS have an increased cardiometabolic burden which correlates with frailty and reduced quality of life (21, 85), but validated questionnaires for persons diagnosed with benign adrenal incidentalomas are lacking. Through patient-reported outcome measures, I aim to develop patient-derived questionnaires that can be used in the clinic to monitor clinical outcomes and quality of life. This would become an additional asset for decision-making in the management of persons with MACS.

REFERENCES

1. Schiffer L, Barnard L, Baranowski ES, Gilligan LC, Taylor AE, Arlt W, et al. Human steroid biosynthesis, metabolism and excretion are differentially reflected by serum and urine steroid metabolomes: A comprehensive review. J Steroid Biochem Mol Biol. 2019;194:105439.
2. Storbeck KH, Schiffer L, Baranowski ES, Chortis V, Prete A, Barnard L, et al. Steroid Metabolome Analysis in Disorders of Adrenal Steroid Biosynthesis and Metabolism. Endocr Rev. 2019;40(6):1605-25.
3. Prete A, Yan Q, Al-Tarrah K, Akturk HK, Prokop LJ, Alahdab F, et al. The cortisol stress response induced by surgery: A systematic review and meta-analysis. Clin Endocrinol (Oxf). 2018;89(5):554-67.
4. Gathercole LL, Lavery GG, Morgan SA, Cooper MS, Sinclair AJ, Tomlinson JW, et al. 11beta-Hydroxysteroid dehydrogenase 1: translational and therapeutic aspects. Endocr Rev. 2013;34(4):525-55.
5. Tomlinson JW, Walker EA, Bujalska IJ, Draper N, Lavery GG, Cooper MS, et al. 11beta-hydroxysteroid dehydrogenase type 1: a tissue-specific regulator of glucocorticoid response. Endocr Rev. 2004;25(5):831-66.
6. Bradlow HL, Zumoff B, Gallagher TF, Hellman L**.** Tetrahydrocortisol metabolism in man. Steroids. 1968;12(3):303-8.
7. Zumoff B, Bradlow HL, Gallagher TF, Hellman L**.** Metabolism of tetrahydrocortisone in health and disease. J Clin Endocrinol Metab. 1968;28(9):1330-4.
8. Ged C, Rouillon JM, Pichard L, Combalbert J, Bressot N, Bories P, et al. The increase in urinary excretion of 6 beta-hydroxycortisol as a marker of human

hepatic cytochrome P450IIIA induction. Br J Clin Pharmacol. 1989;28(4):373-87.

9. Reimondo G, Castellano E, Grosso M, Priotto R, Puglisi S, Pia A, et al. Adrenal Incidentalomas are Tied to Increased Risk of Diabetes: Findings from a Prospective Study. J Clin Endocrinol Metab. 2020;105(4).

10. Ebbehoj A, Li D, Kaur RJ, Zhang C, Singh S, Li T, et al. Epidemiology of adrenal tumours in Olmsted County, Minnesota, USA: a population-based cohort study. Lancet Diabetes Endocrinol. 2020;8(11):894-902.

11. Ichijo T, Ueshiba H, Nawata H, Yanase T**.** A nationwide survey of adrenal incidentalomas in Japan: the first report of clinical and epidemiological features. Endocr J. 2020;67(2):141-52.

12. Mantero F, Terzolo M, Arnaldi G, Osella G, Masini AM, Ali A, et al. A survey on adrenal incidentaloma in Italy. Study Group on Adrenal Tumors of the Italian Society of Endocrinology. J Clin Endocrinol Metab. 2000;85(2):637-44.

13. Mao JJ, Dages KN, Suresh M, Bancos I**.** Presentation, disease progression and outcomes of adrenal gland metastases. Clin Endocrinol (Oxf). 2020;93(5):546-54.

14. Delivanis DA, Erickson D, Atwell TD, Natt N, Maraka S, Schmit GD, et al. Procedural and clinical outcomes of percutaneous adrenal biopsy in a high-risk population for adrenal malignancy. Clin Endocrinol (Oxf). 2016;85(5):710-6.

15. Elhassan YS, Alahdab F, Prete A, Delivanis DA, Khanna A, Prokop L, et al. Natural History of Adrenal Incidentalomas With and Without Mild Autonomous Cortisol Excess: A Systematic Review and Meta-analysis. Ann Intern Med. 2019;171(2):107-16.

16. Li D, El Kawkgi OM, Henriquez AF, Bancos I**.** Cardiovascular risk and mortality in patients with active and treated hypercortisolism. Gland Surg. 2020;9(1):43-58.

17. Deutschbein T, Reimondo G, Di Dalmazi G, Bancos I, Patrova J, Vassiliadi DA, et al. Age-dependent and sex-dependent disparity in mortality in patients with adrenal incidentalomas and autonomous cortisol secretion: an international, retrospective, cohort study. Lancet Diabetes Endocrinol. 2022.

18. Bancos I, Taylor AE, Chortis V, Sitch AJ, Jenkinson C, Davidge-Pitts CJ, et al. Urine steroid metabolomics for the differential diagnosis of adrenal incidentalomas in the EURINE-ACT study: a prospective test validation study. Lancet Diabetes Endocrinol. 2020;8(9):773-81.

19. Cyranska-Chyrek E, Szczepanek-Parulska E, Olejarz M, Ruchala M**.** Malignancy Risk and Hormonal Activity of Adrenal Incidentalomas in a Large Cohort of Patients from a Single Tertiary Reference Center. Int J Environ Res Public Health. 2019;16(10).

20. Iniguez-Ariza NM, Kohlenberg JD, Delivanis DA, Hartman RP, Dean DS, Thomas MA, et al. Clinical, Biochemical, and Radiological Characteristics of a Single-Center Retrospective Cohort of 705 Large Adrenal Tumors. Mayo Clin Proc Innov Qual Outcomes. 2018;2(1):30-9.

21. Bancos I, Prete A**.** Approach to the Patient With Adrenal Incidentaloma. J Clin Endocrinol Metab. 2021;106(11):3331-53.

22. Hamidi O, Raman R, Lazik N, Iniguez-Ariza N, McKenzie TJ, Lyden ML, et al. Clinical course of adrenal myelolipoma: A long-term longitudinal follow-up study. Clin Endocrinol (Oxf). 2020;93(1):11-8.

23. Dages KN, Kohlenberg JD, Young WF, Jr., Murad MH, Prokop L, Rivera M, et al. Presentation and outcomes of adrenal ganglioneuromas: A cohort study and a systematic review of literature. Clin Endocrinol (Oxf). 2021.

24. Ahn SH, Kim JH, Baek SH, Kim H, Cho YY, Suh S, et al. Characteristics of Adrenal Incidentalomas in a Large, Prospective Computed Tomography-Based Multicenter Study: The COAR Study in Korea. Yonsei Med J. 2018;59(4):501-10.

25. Gruber LM, Hartman RP, Thompson GB, McKenzie TJ, Lyden ML, Dy BM, et al. Pheochromocytoma Characteristics and Behavior Differ Depending on Method of Discovery. J Clin Endocrinol Metab. 2019;104(5):1386-93.

26. Canu L, Van Hemert JAW, Kerstens MN, Hartman RP, Khanna A, Kraljevic I, et al. CT Characteristics of Pheochromocytoma: Relevance for the Evaluation of Adrenal Incidentaloma. J Clin Endocrinol Metab. 2019;104(2):312-8.

27. Gruber LM, Strajina V, Bancos I, Murad MH, Dy BM, Young WF, et al. Not all adrenal incidentalomas require biochemical testing to exclude pheochromocytoma: Mayo clinic experience and a meta-analysis. Gland Surg. 2020;9(2):362-71.

28. Fassnacht M, Arlt W, Bancos I, Dralle H, Newell-Price J, Sahdev A, et al. Management of adrenal incidentalomas: European Society of Endocrinology Clinical Practice Guideline in collaboration with the European Network for the Study of Adrenal Tumors. Eur J Endocrinol. 2016;175(2):G1-G34.

29. Vaidya A, Hamrahian A, Bancos I, Fleseriu M, Ghayee HK**.** The Evaluation of Incidentally Discovered Adrenal Masses. Endocr Pract. 2019;25(2):178-92.

30. Dinnes J, Bancos I, Ferrante di Ruffano L, Chortis V, Davenport C, Bayliss S, et al. MANAGEMENT OF ENDOCRINE DISEASE: Imaging for the diagnosis of malignancy in incidentally discovered adrenal masses: a systematic review and meta-analysis. Eur J Endocrinol. 2016;175(2):R51-64.

31. Corwin MT, Navarro SM, Malik DG, Loehfelm TW, Fananapazir G, Wilson M, et al. Differences in Growth Rate on CT of Adrenal Adenomas and Malignant Adrenal Nodules. AJR Am J Roentgenol. 2019;213(3):632-6.

32. Michalowska I, Cwikla JB, Michalski W, Wyrwicz LS, Prejbisz A, Szperl M, et al. Growth Rate of Paragangliomas Related to Germline Mutations of the Sdhx Genes. Endocr Pract. 2017;23(3):342-52.

33. Sanford T, Gomella PT, Siddiqui R, Su D, An JY, Bratslavsky G, et al. Long term outcomes for patients with von Hippel-Lindau and Pheochromocytoma: defining the role of active surveillance. Urol Oncol. 2021;39(2):134 e1- e8.

34. Delivanis DA, Bancos I, Atwell TD, Schmit GD, Eiken PW, Natt N, et al. Diagnostic performance of unenhanced computed tomography and (18) F-fluorodeoxyglucose positron emission tomography in indeterminate adrenal tumours. Clin Endocrinol (Oxf). 2018;88(1):30-6.

35. Schloetelburg W, Ebert I, Petritsch B, Weng AM, Dischinger U, Kircher S, et al. Adrenal wash-out CT: moderate diagnostic value in distinguishing benign from malignant adrenal masses. Eur J Endocrinol. 2021;186(2):183-93.

36. Woo S, Suh CH, Kim SY, Cho JY, Kim SH**.** Pheochromocytoma as a frequent false-positive in adrenal washout CT: A systematic review and meta-analysis. Eur Radiol. 2018;28(3):1027-36.

37. He X, Caoili EM, Avram AM, Miller BS, Else T**.** 18F-FDG-PET/CT Evaluation of Indeterminate Adrenal Masses in Noncancer Patients. J Clin Endocrinol Metab. 2021;106(5):1448-59.

38. Athimulam S, Grebe S, Bancos I**.** Steroid profiling in the diagnosis of mild and overt Cushing's syndrome. Best Pract Res Clin Endocrinol Metab. 2021:101488.

39. Arlt W, Lang K, Sitch AJ, Dietz AS, Rhayem Y, Bancos I, et al. Steroid metabolome analysis reveals prevalent glucocorticoid excess in primary aldosteronism. JCI Insight. 2017;2(8).

40. Bancos I, Arlt W**.** Diagnosis of a malignant adrenal mass: the role of urinary steroid metabolite profiling. Curr Opin Endocrinol Diabetes Obes. 2017;24(3):200-7.

41. Hines JM, Bancos I, Bancos C, Singh RD, Avula AV, Young WF, et al. High-Resolution, Accurate-Mass (HRAM) Mass Spectrometry Urine Steroid Profiling in the Diagnosis of Adrenal Disorders. Clin Chem. 2017;63(12):1824-35.

42. Herndon J, Nadeau AM, Davidge-Pitts CJ, Young WF, Bancos I**.** Primary adrenal insufficiency due to bilateral infiltrative disease. Endocrine. 2018;62(3):721-8.

43. Bouys L, Chiodini I, Arlt W, Reincke M, Bertherat J**.** Update on primary bilateral macronodular adrenal hyperplasia (PBMAH). Endocrine. 2021;71(3):595-603.

44. Dahia PL**.** Pheochromocytoma and paraganglioma pathogenesis: learning from genetic heterogeneity. Nat Rev Cancer. 2014;14(2):108-19.

45. Petr EJ, Else T**.** Adrenocortical carcinoma (ACC): When and why should we consider germline testing? Presse Med. 2018;47(7-8 Pt 2):e119-e25.

46. Bausch B, Schiavi F, Ni Y, Welander J, Patocs A, Ngeow J, et al. Clinical Characterization of the Pheochromocytoma and Paraganglioma Susceptibility Genes SDHA, TMEM127, MAX, and SDHAF2 for Gene-Informed Prevention. JAMA Oncol. 2017;3(9):1204-12.

47. Benn DE, Robinson BG, Clifton-Bligh RJ**.** 15 YEARS OF PARAGANGLIOMA: Clinical manifestations of paraganglioma syndromes types 1-5. Endocr Relat Cancer. 2015;22(4):T91-103.

48. Boikos SA, Xekouki P, Fumagalli E, Faucz FR, Raygada M, Szarek E, et al. Carney triad can be (rarely) associated with germline succinate dehydrogenase defects. Eur J Hum Genet. 2016;24(4):569-73.

49. Carney JA**.** Carney triad: a syndrome featuring paraganglionic, adrenocortical, and possibly other endocrine tumors. J Clin Endocrinol Metab. 2009;94(10):3656-62.

50. Crona J, Taieb D, Pacak K**.** New Perspectives on Pheochromocytoma and Paraganglioma: Toward a Molecular Classification. Endocr Rev. 2017;38(6):489-515.

51. Else T, Greenberg S, Fishbein L**.** Hereditary Paraganglioma-Pheochromocytoma Syndromes. In: Adam MP, Ardinger HH, Pagon RA, et al., eds. GeneReviews((R)). Seattle (WA); 1993.

52. Gatta-Cherifi B, Chabre O, Murat A, Niccoli P, Cardot-Bauters C, Rohmer V, et al. Adrenal involvement in MEN1. Analysis of 715 cases from the Groupe d'etude des Tumeurs Endocrines database. Eur J Endocrinol. 2012;166(2):269-79.

53. Lenders JW, Eisenhofer G, Mannelli M, Pacak K**.** Phaeochromocytoma. Lancet. 2005;366(9486):665-75.

54. MacFarland SP, Mostoufi-Moab S, Zelley K, Mattei PA, States LJ, Bhatti TR, et al. Management of adrenal masses in patients with Beckwith-Wiedemann syndrome. Pediatr Blood Cancer. 2017;64(8).

55. Shuch B, Ricketts CJ, Vocke CD, Valera VA, Chen CC, Gautam R, et al. Adrenal nodular hyperplasia in hereditary leiomyomatosis and renal cell cancer. J Urol. 2013;189(2):430-5.

56. Vaidya A, Carey RM**.** Evolution of the Primary Aldosteronism Syndrome: Updating the Approach. J Clin Endocrinol Metab. 2020;105(12).

57. Funder JW, Carey RM, Mantero F, Murad MH, Reincke M, Shibata H, et al. The Management of Primary Aldosteronism: Case Detection, Diagnosis, and Treatment: An Endocrine Society Clinical Practice Guideline. J Clin Endocrinol Metab. 2016;101(5):1889-916.

58. Buitenwerf E, Berends AMA, van Asselt ADI, Korteweg T, Greuter MJW, Veeger NJM, et al. Diagnostic Accuracy of Computed Tomography to Exclude Pheochromocytoma: A Systematic Review, Meta-analysis, and Cost Analysis. Mayo Clin Proc. 2019;94(10):2040-52.

59. Ceccato F, Artusi C, Barbot M, Lizzul L, Pinelli S, Costantini G, et al. Dexamethasone measurement during low-dose suppression test for suspected hypercortisolism: threshold development with and validation. J Endocrinol Invest. 2020;43(8):1105-13.

60. Ueland GA, Methlie P, Kellmann R, Bjorgaas M, Asvold BO, Thorstensen K, et al. Simultaneous assay of cortisol and dexamethasone improved diagnostic

accuracy of the dexamethasone suppression test. Eur J Endocrinol. 2017;176(6):705-13.

61. Nieman LK, Biller BM, Findling JW, Newell-Price J, Savage MO, Stewart PM, et al. The diagnosis of Cushing's syndrome: an Endocrine Society Clinical Practice Guideline. J Clin Endocrinol Metab. 2008;93(5):1526-40.

62. Giordano R, Marinazzo E, Berardelli R, Picu A, Maccario M, Ghigo E, et al. Long-term morphological, hormonal, and clinical follow-up in a single unit on 118 patients with adrenal incidentalomas. Eur J Endocrinol. 2010;162(4):779-85.

63. Prete A, Paragliola RM, Bottiglieri F, Rota CA, Pontecorvi A, Salvatori R, et al. Factors predicting the duration of adrenal insufficiency in patients successfully treated for Cushing disease and nonmalignant primary adrenal Cushing syndrome. Endocrine. 2017;55(3):969-80.

64. Raff H, Auchus RJ, Findling JW, Nieman LK**.** Urine free cortisol in the diagnosis of Cushing's syndrome: is it worth doing and, if so, how? J Clin Endocrinol Metab. 2015;100(2):395-7.

65. Sereg M, Toke J, Patocs A, Varga I, Igaz P, Szucs N, et al. Diagnostic performance of salivary cortisol and serum osteocalcin measurements in patients with overt and subclinical Cushing's syndrome. Steroids. 2011;76(1-2):38-42.

66. Ueland GA, Grinde T, Methlie P, Kelp O, Lovas K, Husebye ES**.** Diagnostic testing of autonomous cortisol secretion in adrenal incidentalomas. Endocr Connect. 2020;9(10):963-70.

67. Ceccato F, Barbot M, Albiger N, Antonelli G, Zilio M, Todeschini M, et al. Daily salivary cortisol and cortisone rhythm in patients with adrenal incidentaloma. Endocrine. 2018;59(3):510-9.

68. O'Shea PM, Griffin TP, Denieffe S, Fitzgibbon MC**.** The aldosterone to renin ratio in the diagnosis of primary aldosteronism: Promises and challenges. Int J Clin Pract. 2019;73(7):e13353.

69. Lenders JW, Duh QY, Eisenhofer G, Gimenez-Roqueplo AP, Grebe SK, Murad MH, et al. Pheochromocytoma and paraganglioma: an endocrine society clinical practice guideline. J Clin Endocrinol Metab. 2014;99(6):1915-42.

70. Darr R, Kuhn M, Bode C, Bornstein SR, Pacak K, Lenders JWM, et al. Accuracy of recommended sampling and assay methods for the determination of plasma-free and urinary fractionated metanephrines in the diagnosis of pheochromocytoma and paraganglioma: a systematic review. Endocrine. 2017;56(3):495-503.

71. Eisenhofer G, Prejbisz A, Peitzsch M, Pamporaki C, Masjkur J, Rogowski-Lehmann N, et al. Biochemical Diagnosis of Chromaffin Cell Tumors in Patients at High and Low Risk of Disease: Plasma versus Urinary Free or Deconjugated O-Methylated Catecholamine Metabolites. Clin Chem. 2018;64(11):1646-56.

72. Kahramangil B, Kose E, Remer EM, Reynolds JP, Stein R, Rini B, et al. A Modern Assessment of Cancer Risk in Adrenal Incidentalomas: Analysis of 2219 Patients. Ann Surg. 2020.

73. Hong AR, Kim JH, Park KS, Kim KY, Lee JH, Kong SH, et al. Optimal follow-up strategies for adrenal incidentalomas: reappraisal of the 2016 ESE-ENSAT guidelines in real clinical practice. Eur J Endocrinol. 2017;177(6):475-83.

74. Lopez D, Luque-Fernandez MA, Steele A, Adler GK, Turchin A, Vaidya A**.** "Nonfunctional" Adrenal Tumors and the Risk for Incident Diabetes and Cardiovascular Outcomes: A Cohort Study. Ann Intern Med. 2016;165(8):533-42.

75. Arlt W, Biehl M, Taylor AE, Hahner S, Libe R, Hughes BA, et al. Urine steroid metabolomics as a biomarker tool for detecting malignancy in adrenal tumors. J Clin Endocrinol Metab. 2011;96(12):3775-84.

76. Morelli V, Reimondo G, Giordano R, Della Casa S, Policola C, Palmieri S, et al. Long-term follow-up in adrenal incidentalomas: an Italian multicenter study. J Clin Endocrinol Metab. 2014;99(3):827-34.

77. Di Dalmazi G, Vicennati V, Garelli S, Casadio E, Rinaldi E, Giampalma E, et al. Cardiovascular events and mortality in patients with adrenal incidentalomas that are either non-secreting or associated with intermediate phenotype or subclinical Cushing's syndrome: a 15-year retrospective study. Lancet Diabetes Endocrinol. 2014;2(5):396-405.

78. Rengarajan L., Knowles G., Asia M., Elhassan Y.S., Arlt W., Ronchi C.L., Prete A. Should the 1mg-overnight dexamethasone suppression test be repeated in patients with benign adrenal incidentalomas and no overt hormone excess? Presented at Society for Endocrinology BES 2021, Edinburgh, UK. Endocrine Abstracts 77. ISSN 1479-6848.

79. Lacroix A, Feelders RA, Stratakis CA, Nieman LK**.** Cushing's syndrome. Lancet. 2015;386(9996):913-27.

80. Beuschlein F, Fassnacht M, Assie G, Calebiro D, Stratakis CA, Osswald A, et al. Constitutive activation of PKA catalytic subunit in adrenal Cushing's syndrome. N Engl J Med. 2014;370(11):1019-28.

81. Albiger NM, Occhi G, Sanguin F, Iacobone M, Casarrubea G, Ferasin S, et al. Adrenal nodules in patients with Cushing's disease: prevalence, clinical significance and follow-up. J Endocrinol Invest. 2011;34(8):e204-9.

82. Borretta G, Terzolo M, Cesario F, Meineri I, Pia A, Angeli A**.** Coexistence of unilateral adrenal macronodule and Cushing's disease. Report of two cases. J Endocrinol Invest. 1996;19(2):131-5.

83. Di Dalmazi G, Vicennati V, Pizzi C, Mosconi C, Tucci L, Balacchi C, et al. Prevalence and Incidence of Atrial Fibrillation in a Large Cohort of Adrenal Incidentalomas: A Long-Term Study. J Clin Endocrinol Metab. 2020;105(8).

84. Morelli V, Palmieri S, Lania A, Tresoldi A, Corbetta S, Cairoli E, et al. Cardiovascular events in patients with mild autonomous cortisol secretion: analysis with artificial neural networks. Eur J Endocrinol. 2017;177(1):73-83.

85. Singh S, Atkinson EJ, Achenbach SJ, LeBrasseur N, Bancos I**.** Frailty in Patients With Mild Autonomous Cortisol Secretion is Higher Than in Patients with Nonfunctioning Adrenal Tumors. J Clin Endocrinol Metab. 2020;105(9).

86. Kjellbom A, Lindgren O, Puvaneswaralingam S, Londahl M, Olsen H**.** Association Between Mortality and Levels of Autonomous Cortisol Secretion by Adrenal Incidentalomas : A Cohort Study. Ann Intern Med. 2021;174(8):1041-9.

87. Zhang CD, Li D, Kaur RJ, Ebbehoj A, Singh S, Atkinson EJ, et al. Cardiometabolic Outcomes and Mortality in Patients with Adrenal Adenomas in a Population-based Setting. J Clin Endocrinol Metab. 2021;106(11):3320-30.

88. Chiodini I, Morelli V, Masserini B, Salcuni AS, Eller-Vainicher C, Viti R, et al. Bone mineral density, prevalence of vertebral fractures, and bone quality in patients with adrenal incidentalomas with and without subclinical hypercortisolism: an Italian multicenter study. J Clin Endocrinol Metab. 2009;94(9):3207-14.

89. Chiodini I, Guglielmi G, Battista C, Carnevale V, Torlontano M, Cammisa M, et al. Spinal volumetric bone mineral density and vertebral fractures in female patients with adrenal incidentalomas: the effects of subclinical hypercortisolism and gonadal status. J Clin Endocrinol Metab. 2004;89(5):2237-41.

90. Chiodini I, Viti R, Coletti F, Guglielmi G, Battista C, Ermetici F, et al. Eugonadal male patients with adrenal incidentalomas and subclinical hypercortisolism have increased rate of vertebral fractures. Clin Endocrinol (Oxf). 2009;70(2):208-13.

91. Li D, Kaur RJ, Zhang CD, Ebbehoj A, Singh S, Atkinson EJ, et al. Risk of bone fractures after the diagnosis of adrenal adenomas: a population-based cohort study. Eur J Endocrinol. 2021;184(4):597-606.

92. Bancos I, Alahdab F, Crowley RK, Chortis V, Delivanis DA, Erickson D, et al. THERAPY OF ENDOCRINE DISEASE: Improvement of cardiovascular risk factors after adrenalectomy in patients with adrenal tumors and subclinical Cushing's syndrome: a systematic review and meta-analysis. Eur J Endocrinol. 2016;175(6):R283-R95.

93. Salcuni AS, Morelli V, Eller Vainicher C, Palmieri S, Cairoli E, Spada A, et al. Adrenalectomy reduces the risk of vertebral fractures in patients with monolateral adrenal incidentalomas and subclinical hypercortisolism. Eur J Endocrinol. 2016;174(3):261-9.

94. Belokovskaya R, Ravikumar A, Arumugam D, Izadmehr S, Goddard GM, Geer EB, et al. Mifepristone Treatment for Mild Autonomous Cortisol Secretion Due to Adrenal Adenomas: A Pilot Study. Endocr Pract. 2019;25(8):846-53.

95. Debono M, Harrison RF, Chadarevian R, Gueroult C, Abitbol JL, Newell-Price J**.** Resetting the Abnormal Circadian Cortisol Rhythm in Adrenal Incidentaloma Patients With Mild Autonomous Cortisol Secretion. J Clin Endocrinol Metab. 2017;102(9):3461-9.

96. Debono M, Chadarevian R, Eastell R, Ross RJ, Newell-Price J**.** Mifepristone reduces insulin resistance in patient volunteers with adrenal incidentalomas that secrete low levels of cortisol: a pilot study. PLoS One. 2013;8(4):e60984.

97. Dennedy MC, Annamalai AK, Prankerd-Smith O, Freeman N, Vengopal K, Graggaber J, et al. Low DHEAS: A Sensitive and Specific Test for the Detection of Subclinical Hypercortisolism in Adrenal Incidentalomas. J Clin Endocrinol Metab. 2017;102(3):786-92.

98. Yener S, Yilmaz H, Demir T, Secil M, Comlekci A**.** DHEAS for the prediction of subclinical Cushing's syndrome: perplexing or advantageous? Endocrine. 2015;48(2):669-76.

99. Carafone LE, Zhang CD, Li D, Lazik N, Hamidi O, Hurtado MD, et al. Diagnostic Accuracy of Dehydroepiandrosterone Sulfate and Corticotropin in Autonomous Cortisol Secretion. Biomedicines. 2021;9(7).

100. Bourdeau I, El Ghorayeb N, Gagnon N, Lacroix A**.** MANAGEMENT OF ENDOCRINE DISEASE: Differential diagnosis, investigation and therapy of bilateral adrenal incidentalomas. Eur J Endocrinol. 2018;179(2):R57-R67.

101. Osswald A, Reincke M**.** Response to the Letter to the Editor: "Long-Term Outcome of Primary Bilateral Macronodular Adrenocortical Hyperplasia After Unilateral Adrenalectomy". J Clin Endocrinol Metab. 2020;105(2).

102. Young WF, Jr., du Plessis H, Thompson GB, Grant CS, Farley DR, Richards ML, et al. The clinical conundrum of corticotropin-independent autonomous cortisol secretion in patients with bilateral adrenal masses. World J Surg. 2008;32(5):856-62.

103. Ueland GA, Methlie P, Jossang DE, Sagen JV, Viste K, Thordarson HB, et al. Adrenal Venous Sampling for Assessment of Autonomous Cortisol Secretion. J Clin Endocrinol Metab. 2018;103(12):4553-60.

104. Shackleton C, Pozo OJ, Marcos J**.** GC/MS in Recent Years Has Defined the Normal and Clinically Disordered Steroidome: Will It Soon Be Surpassed by LC/Tandem MS in This Role? J Endocr Soc. 2018;2(8):974-96.

105. Wudy SA, Schuler G, Sanchez-Guijo A, Hartmann MF**.** The art of measuring steroids: Principles and practice of current hormonal steroid analysis. J Steroid Biochem Mol Biol. 2018;179:88-103.

106. Schiffer L, Adaway JE, Arlt W, Keevil BG**.** A liquid chromatography-tandem mass spectrometry assay for the profiling of classical and 11-oxygenated androgens in saliva. Ann Clin Biochem. 2019;56(5):564-73.

107. Berke K, Constantinescu G, Masjkur J, Kimpel O, Dischinger U, Peitzsch M, et al. Plasma Steroid Profiling in Patients With Adrenal Incidentaloma. J Clin Endocrinol Metab. 2022;107(3):e1181-e92.

108. Snaterse G, van Dessel LF, Taylor AE, Visser JA, Arlt W, Lolkema MP, et al. Validation of circulating steroid hormone measurements across different matrices by liquid chromatography-tandem mass spectrometry. Steroids. 2021;167:108800.

109. Krone N, Hughes BA, Lavery GG, Stewart PM, Arlt W, Shackleton CH**.** Gas chromatography/mass spectrometry (GC/MS) remains a pre-eminent discovery tool in clinical steroid investigations even in the era of fast liquid chromatography tandem mass spectrometry (LC/MS/MS). J Steroid Biochem Mol Biol. 2010;121(3-5):496-504.

110. Dunn WB, Broadhurst D, Begley P, Zelena E, Francis-McIntyre S, Anderson N, et al. Procedures for large-scale metabolic profiling of serum and plasma using gas chromatography and liquid chromatography coupled to mass spectrometry. Nat Protoc. 2011;6(7):1060-83.

111. Dunn WB, Broadhurst DI, Atherton HJ, Goodacre R, Griffin JL**.** Systems level studies of mammalian metabolomes: the roles of mass spectrometry and nuclear magnetic resonance spectroscopy. Chem Soc Rev. 2011;40(1):387-426.

112. Biehl M. (2022) The Shallow and the Deep: A biased introduction to neural networks and old school machine learning. University of Groningen. https://research.rug.nl/en/publications/the-shallow-and-the-deep-a-biased-introduction-to-neural-networks.

113. Kubat M. An introduction to machine learning. Springer, 2017.

114. Funder JW, Carey RM, Fardella C, Gomez-Sanchez CE, Mantero F, Stowasser M, et al. Case detection, diagnosis, and treatment of patients with primary aldosteronism: an endocrine society clinical practice guideline. J Clin Endocrinol Metab. 2008;93(9):3266-81.

115. Calhoun DA, Jones D, Textor S, Goff DC, Murphy TP, Toto RD, et al. Resistant hypertension: diagnosis, evaluation, and treatment. A scientific statement from the American Heart Association Professional Education Committee of the Council for High Blood Pressure Research. Hypertension. 2008;51(6):1403-19.

116. American Diabetes A**.** 2. Classification and Diagnosis of Diabetes: Standards of Medical Care in Diabetes-2021. Diabetes Care. 2021;44(Suppl 1):S15-S33.

117. Arnett DK, Blumenthal RS, Albert MA, Buroker AB, Goldberger ZD, Hahn EJ, et al. 2019 ACC/AHA Guideline on the Primary Prevention of Cardiovascular Disease: A Report of the American College of Cardiology/American Heart Association Task Force on Clinical Practice Guidelines. Circulation. 2019;140(11):e596-e646.

118. Barros AJ, Hirakata VN**.** Alternatives for logistic regression in cross-sectional studies: an empirical comparison of models that directly estimate the prevalence ratio. BMC Med Res Methodol. 2003;3:21.

119. Cole TJ**.** Sympercents: symmetric percentage differences on the 100 log(e) scale simplify the presentation of log transformed data. Stat Med. 2000;19(22):3109-25.

120. Chiodini I, Torlontano M, Scillitani A, Arosio M, Bacci S, Di Lembo S, et al. Association of subclinical hypercortisolism with type 2 diabetes mellitus: a case-control study in hospitalized patients. Eur J Endocrinol. 2005;153(6):837-44.

121. Petramala L, Olmati F, Concistre A, Russo R, Mezzadri M, Soldini M, et al. Cardiovascular and metabolic risk factors in patients with subclinical Cushing. Endocrine. 2020;70(1):150-63.

122. Oki K, Yamane K, Nakanishi S, Shiwa T, Kohno N**.** Influence of adrenal subclinical hypercortisolism on hypertension in patients with adrenal incidentaloma. Exp Clin Endocrinol Diabetes. 2012;120(4):244-7.

123. Kasperlik-Zaluska AA, Otto M, Cichocki A, Roslonowska E, Slowinska-Srzednicka J, Jeske W, et al. Incidentally discovered adrenal tumors: a lesson from observation of 1,444 patients. Horm Metab Res. 2008;40(5):338-41.

124. Invitti C, Pecori Giraldi F, de Martin M, Cavagnini F**.** Diagnosis and management of Cushing's syndrome: results of an Italian multicentre study. Study Group of the Italian Society of Endocrinology on the Pathophysiology of the Hypothalamic-Pituitary-Adrenal Axis. J Clin Endocrinol Metab. 1999;84(2):440-8.

125. Vassiliadi DA, Ntali G, Vicha E, Tsagarakis S**.** High prevalence of subclinical hypercortisolism in patients with bilateral adrenal incidentalomas: a challenge to management. Clin Endocrinol (Oxf). 2011;74(4):438-44.

126. Olsen H, Nordenstrom E, Bergenfelz A, Nyman U, Valdemarsson S, Palmqvist E**.** Subclinical hypercortisolism and CT appearance in adrenal incidentalomas: a multicenter study from Southern Sweden. Endocrine. 2012;42(1):164-73.

127. Raverot V, Richet C, Morel Y, Raverot G, Borson-Chazot F**.** Establishment of revised diagnostic cut-offs for adrenal laboratory investigation using the new Roche Diagnostics Elecsys((R)) Cortisol II assay. Ann Endocrinol (Paris). 2016;77(5):620-2.

128. Chortis V, Bancos I, Nijman T, Gilligan LC, Taylor AE, Ronchi CL, et al. Urine Steroid Metabolomics as a Novel Tool for Detection of Recurrent Adrenocortical Carcinoma. J Clin Endocrinol Metab. 2020;105(3).

129. Kamrath C, Hartmann MF, Pons-Kuhnemann J, Wudy SA**.** Urinary GC-MS steroid metabotyping in treated children with congenital adrenal hyperplasia. Metabolism. 2020;112:154354.

130. Wilkes EH, Rumsby G, Woodward GM**.** Using Machine Learning to Aid the Interpretation of Urine Steroid Profiles. Clin Chem. 2018;64(11):1586-95.

131. Schneider P., Biehl M., Hammer B. Adaptive relevance matrices in learning vector quantization. Neural Comput. 2009;21(12):3532-61.

132. Biehl M, Schneider P, Smith D, Stiekema H, Taylor AE, Hughes B, et al. Matrix relevance LVQ in steroid metabolomics based classification of adrenal tumors. In: ESANN. 2012.

133. Biehl M, Hammer B, Villmann T. Prototype-based models in machine learning. In: Wiley Interdisciplinary Reviews: Cognitive Science 7.2 (2016), pp. 92–111.

134. Biehl M. A collection of no-nonsense GMLVQ demo code. 2020. url: https://www.cs.rug.nl/~biehl/gmlvq.

135. Tang F., Tiño P. Ordinal regression based on learning vector quantization, Neural Networks 93 (2017) 76–88, doi: 10.1016/j.neunet.2017.05.006.

136. Fouad S., Tiño P. Adaptive Metric Learning Vector Quantization for Ordinal Classification, Neural computation 24 11 (2012) 2825–2851.

137. Chu W., Keerthi SS. Support Vector Ordinal Regression, Neural Comput. 19 (3) (2007-03) 792–815, doi: 10.1162/neco.2007.19.3.792.

138. Shashua A., Levin A. Ranking with Large Margin Principle: Two Approaches, in: Proceedings of the 15th International Conference on Neural Information Processing Systems, in: NIPS'02, MIT Press, 2002, pp. 961–968. http://dl.acm. org/citation.cfm?id=296 8618.296 8738.

139. Frank E., Hall M. A Simple Approach to Ordinal Classification, in: L. De Raedt, P. Flach (Eds.), Machine Learning: ECML 2001, 2001, pp. 145–156.

140. Kikuchi E, Yanaihara H, Nakashima J, Homma K, Ohigashi T, Asakura H, et al. Urinary steroid profile in adrenocortical tumors. Biomed Pharmacother. 2000;54 Suppl 1:194s-7s.

141. Homoki J, Holl R, Teller WM**.** [Urinary steroid profile in Cushing syndrome and in tumors of the adrenal cortex]. Klin Wochenschr. 1987;65(15):719-26.

142. Kotlowska A, Puzyn T, Sworczak K, Stepnowski P, Szefer P**.** Metabolomic Biomarkers in Urine of Cushing's Syndrome Patients. Int J Mol Sci. 2017;18(2).

143. Tiu SC, Chan AO, Taylor NF, Lee CY, Loung PY, Choi CH, et al. Use of urinary steroid profiling for diagnosing and monitoring adrenocortical tumours. Hong Kong Med J. 2009;15(6):463-70.

144. Velikanova LI, Shafigullina ZR, Lisitsin AA, Vorokhobina NV, Grigoryan K, Kukhianidze EA, et al. Different Types of Urinary Steroid Profiling Obtained by High-Performance Liquid Chromatography and Gas Chromatography-Mass

Spectrometry in Patients with Adrenocortical Carcinoma. Horm Cancer. 2016;7(5-6):327-35.

145. Brossaud J, Ducint D, Corcuff JB**.** Urinary glucocorticoid metabolites: biomarkers to classify adrenal incidentalomas? Clin Endocrinol (Oxf). 2016;84(2):236-43.

146. Maser-Gluth C, Reincke M, Allolio B, Schulze E**.** Metabolism of glucocorticoids and mineralocorticoids in patients with adrenal incidentalomas. Eur J Clin Invest. 2000;30 Suppl 3:83-6.

147. Hana V, Jr., Jezkova J, Kosak M, Krsek M, Hana V, Hill M**.** Serum steroid profiling in Cushing's syndrome patients. J Steroid Biochem Mol Biol. 2019;192:105410.

148. Masjkur J, Gruber M, Peitzsch M, Kaden D, Di Dalmazi G, Bidlingmaier M, et al. Plasma Steroid Profiles in Subclinical Compared With Overt Adrenal Cushing Syndrome. J Clin Endocrinol Metab. 2019;104(10):4331-40.

149. Eisenhofer G, Masjkur J, Peitzsch M, Di Dalmazi G, Bidlingmaier M, Gruber M, et al. Plasma Steroid Metabolome Profiling for Diagnosis and Subtyping Patients with Cushing Syndrome. Clin Chem. 2018;64(3):586-96.

150. Di Dalmazi G, Fanelli F, Mezzullo M, Casadio E, Rinaldi E, Garelli S, et al. Steroid Profiling by LC-MS/MS in Nonsecreting and Subclinical Cortisol-Secreting Adrenocortical Adenomas. J Clin Endocrinol Metab. 2015;100(9):3529-38.

151. Ueshiba H, Segawa M, Hayashi T, Miyachi Y, Irie M**.** Serum profiles of steroid hormones in patients with Cushing's syndrome determined by a new HPLC/RIA method. Clin Chem. 1991;37(8):1329-33.

152. Di Dalmazi G, Fanelli F, Zavatta G, Ricci Bitti S, Mezzullo M, Repaci A, et al. The Steroid Profile of Adrenal Incidentalomas: Subtyping Subjects With High Cardiovascular Risk. J Clin Endocrinol Metab. 2019;104(11):5519-28.

153. Ku EJ, Lee C, Shim J, Lee S, Kim KA, Kim SW, et al. Metabolic Subtyping of Adrenal Tumors: Prospective Multi-Center Cohort Study in Korea. Endocrinol Metab (Seoul). 2021;36(5):1131-41.

154. Huayllas MKP, Smith LM, Gallagher JC, Netzel BC, Singh RJ, Kater CE**.** Steroidogenesis in patients with adrenal incidentalomas: Extended steroid profile measured by liquid chromatography-mass spectrometry after ACTH stimulation and dexamethasone suppression. Clin Endocrinol (Oxf). 2021;95(1):29-40.

155. Stewart PM, Walker BR, Holder G, O'Halloran D, Shackleton CH**.** 11 beta-Hydroxysteroid dehydrogenase activity in Cushing's syndrome: explaining the mineralocorticoid excess state of the ectopic adrenocorticotropin syndrome. J Clin Endocrinol Metab. 1995;80(12):3617-20.

156. Phillipou G**.** Investigation of urinary steroid profiles as a diagnostic method in Cushing's syndrome. Clin Endocrinol (Oxf). 1982;16(5):433-9.

157. Liang T, Liao S**.** Inhibition of steroid 5 alpha-reductase by specific aliphatic unsaturated fatty acids. Biochem J. 1992;285 (Pt 2):557-62.

158. Li J, Ding Z, Wang Z, Lu JF, Maity SN, Navone NM, et al. Androgen regulation of 5alpha-reductase isoenzymes in prostate cancer: implications for prostate cancer prevention. PLoS One. 2011;6(12):e28840.

159. Ulick S, Wang JZ, Blumenfeld JD, Pickering TG**.** Cortisol inactivation overload: a mechanism of mineralocorticoid hypertension in the ectopic adrenocorticotropin syndrome. J Clin Endocrinol Metab. 1992;74(5):963-7.

160. Chong C, Hamid A, Yao T, Garza AE, Pojoga LH, Adler GK, et al. Regulation of aldosterone secretion by mineralocorticoid receptor-mediated signaling. J Endocrinol. 2017;232(3):525-34.

161. Shackleton CH, Neres MS, Hughes BA, Stewart PM, Kater CE**.** 17-Hydroxylase/C17,20-lyase (CYP17) is not the enzyme responsible for side-chain cleavage of cortisol and its metabolites. Steroids. 2008;73(6):652-6.

162. Bassett MH, Mayhew B, Rehman K, White PC, Mantero F, Arnaldi G, et al. Expression profiles for steroidogenic enzymes in adrenocortical disease. J Clin Endocrinol Metab. 2005;90(9):5446-55.

163. Cao C, Yang X, Li L, Sun R, Xian Y, Lv W, et al. Increased expression of CYP17 and CYP11B1 in subclinical Cushing's syndrome due to adrenal adenomas. Int J Urol. 2011;18(10):691-6.

164. Teuber JP, Nanba K, Turcu AF, Chen X, Zhao L, Else T, et al. Intratumoral steroid profiling of adrenal cortisol-producing adenomas by liquid chromatography- mass spectrometry. J Steroid Biochem Mol Biol. 2021;212:105924.

165. Schiffer L, Kempegowda P, Arlt W, O'Reilly MW**.** MECHANISMS IN ENDOCRINOLOGY: The sexually dimorphic role of androgens in human metabolic disease. Eur J Endocrinol. 2017;177(3):R125-R43.

166. Hannah-Shmouni F, Berthon A, Faucz FR, Briceno JM, Maria AG, Demidowich A, et al. Mass spectrometry-based steroid profiling in primary bilateral

macronodular adrenocortical hyperplasia. Endocr Relat Cancer. 2020;27(7):403-13.

167. Krumsiek J, Mittelstrass K, Do KT, Stuckler F, Ried J, Adamski J, et al. Gender-specific pathway differences in the human serum metabolome. Metabolomics. 2015;11(6):1815-33.

168. Hazlehurst JM, Oprescu AI, Nikolaou N, Di Guida R, Grinbergs AE, Davies NP, et al. Dual-5alpha-Reductase Inhibition Promotes Hepatic Lipid Accumulation in Man. J Clin Endocrinol Metab. 2016;101(1):103-13.

169. O'Reilly MW, Kempegowda P, Walsh M, Taylor AE, Manolopoulos KN, Allwood JW, et al. AKR1C3-Mediated Adipose Androgen Generation Drives Lipotoxicity in Women With Polycystic Ovary Syndrome. J Clin Endocrinol Metab. 2017;102(9):3327-39.

170. Chacko S, Mamas MA, El-Omar M, Simon D, Haseeb S, Fath-Ordoubadi F, et al. Perturbations in cardiac metabolism in a human model of acute myocardial ischaemia. Metabolomics. 2021;17(9):76.

171. Southam AD, Pursell H, Frigerio G, Jankevics A, Weber RJM, Dunn WB**.** Characterization of Monophasic Solvent-Based Tissue Extractions for the Detection of Polar Metabolites and Lipids Applying Ultrahigh-Performance Liquid Chromatography-Mass Spectrometry Clinical Metabolic Phenotyping Assays. J Proteome Res. 2021;20(1):831-40.

172. Smith CA, Want EJ, O'Maille G, Abagyan R, Siuzdak G**.** XCMS: processing mass spectrometry data for metabolite profiling using nonlinear peak alignment, matching, and identification. Anal Chem. 2006;78(3):779-87.

173. Sumner LW, Amberg A, Barrett D, Beale MH, Beger R, Daykin CA, et al. Proposed minimum reporting standards for chemical analysis Chemical Analysis Working Group (CAWG) Metabolomics Standards Initiative (MSI). Metabolomics. 2007;3(3):211-21.

174. Chong J, Wishart DS, Xia J**.** Using MetaboAnalyst 4.0 for Comprehensive and Integrative Metabolomics Data Analysis. Curr Protoc Bioinformatics. 2019;68(1):e86.

175. Pan R., Yang T., Cao J., Lu K., Zhang Z.. Missing data imputation by K nearest neighbours based on grey relational structure and mutual information. Applied Intelligence, 43:614{632, 2015.

176. Pedregosa F., Varoquaux G., Gramfort A., Michel V., Thirion B., Grisel O., et al. Scikit-learn: Machine learning in Python. Journal of Machine Learning Research, 12:2825{2830, 2011.

177. Tracey TJ, Steyn FJ, Wolvetang EJ, Ngo ST**.** Neuronal Lipid Metabolism: Multiple Pathways Driving Functional Outcomes in Health and Disease. Front Mol Neurosci. 2018;11:10.

178. Kanehisa M**.** Toward understanding the origin and evolution of cellular organisms. Protein Sci. 2019;28(11):1947-51.

179. van der Veen JN, Kennelly JP, Wan S, Vance JE, Vance DE, Jacobs RL**.** The critical role of phosphatidylcholine and phosphatidylethanolamine metabolism in health and disease. Biochim Biophys Acta Biomembr. 2017;1859(9 Pt B):1558-72.

180. Supale S, Li N, Brun T, Maechler P**.** Mitochondrial dysfunction in pancreatic beta cells. Trends Endocrinol Metab. 2012;23(9):477-87.

181. Ren J, Pulakat L, Whaley-Connell A, Sowers JR**.** Mitochondrial biogenesis in the metabolic syndrome and cardiovascular disease. J Mol Med (Berl). 2010;88(10):993-1001.

182. Funai K, Lodhi IJ, Spears LD, Yin L, Song H, Klein S, et al. Skeletal Muscle Phospholipid Metabolism Regulates Insulin Sensitivity and Contractile Function. Diabetes. 2016;65(2):358-70.

183. Funai K, Song H, Yin L, Lodhi IJ, Wei X, Yoshino J, et al. Muscle lipogenesis balances insulin sensitivity and strength through calcium signaling. J Clin Invest. 2013;123(3):1229-40.

184. Storlien LH, Jenkins AB, Chisholm DJ, Pascoe WS, Khouri S, Kraegen EW**.** Influence of dietary fat composition on development of insulin resistance in rats. Relationship to muscle triglyceride and omega-3 fatty acids in muscle phospholipid. Diabetes. 1991;40(2):280-9.

185. Chang W, Hatch GM, Wang Y, Yu F, Wang M**.** The relationship between phospholipids and insulin resistance: From clinical to experimental studies. J Cell Mol Med. 2019;23(2):702-10.

186. Listenberger LL, Han X, Lewis SE, Cases S, Farese RV, Jr., Ory DS, et al. Triglyceride accumulation protects against fatty acid-induced lipotoxicity. Proc Natl Acad Sci U S A. 2003;100(6):3077-82.

187. Guo Y, Walther TC, Rao M, Stuurman N, Goshima G, Terayama K, et al. Functional genomic screen reveals genes involved in lipid-droplet formation and utilization. Nature. 2008;453(7195):657-61.

188. Liu X, Zheng P, Zhao X, Zhang Y, Hu C, Li J, et al. Discovery and validation of plasma biomarkers for major depressive disorder classification based on liquid chromatography-mass spectrometry. J Proteome Res. 2015;14(5):2322-30.

189. Meikle PJ, Wong G, Barlow CK, Weir JM, Greeve MA, MacIntosh GL, et al. Plasma lipid profiling shows similar associations with prediabetes and type 2 diabetes. PLoS One. 2013;8(9):e74341.

190. Semba RD, Gonzalez-Freire M, Moaddel R, Sun K, Fabbri E, Zhang P, et al. Altered Plasma Amino Acids and Lipids Associated With Abnormal Glucose Metabolism and Insulin Resistance in Older Adults. J Clin Endocrinol Metab. 2018;103(9):3331-9.

191. Morze J, Wittenbecher C, Schwingshackl L, Danielewicz A, Rynkiewicz A, Hu FB, et al. Metabolomics and Type 2 Diabetes Risk: An Updated Systematic Review and Meta-analysis of Prospective Cohort Studies. Diabetes Care. 2022;45(4):1013-24.

192. Erlic Z, Reel P, Reel S, Amar L, Pecori A, Larsen CK, et al. Targeted Metabolomics as a Tool in Discriminating Endocrine From Primary Hypertension. J Clin Endocrinol Metab. 2021;106(4):1111-28.

193. Di Dalmazi G, Quinkler M, Deutschbein T, Prehn C, Rayes N, Kroiss M, et al. Cortisol-related metabolic alterations assessed by mass spectrometry assay in patients with Cushing's syndrome. Eur J Endocrinol. 2017;177(2):227-37.

194. Vega-Beyhart A, Iruarrizaga M, Pane A, Garcia-Eguren G, Giro O, Boswell L, et al. Endogenous cortisol excess confers a unique lipid signature and metabolic network. J Mol Med (Berl). 2021;99(8):1085-99.

195. Darabi M, Kontush A**.** Phosphatidylserine in atherosclerosis. Curr Opin Lipidol. 2016;27(4):414-20.

196. Bridges D, Saltiel AR**.** Phosphoinositides: Key modulators of energy metabolism. Biochim Biophys Acta. 2015;1851(6):857-66.

197. Rodriguez-Cuenca S, Pellegrinelli V, Campbell M, Oresic M, Vidal-Puig A**.** Sphingolipids and glycerophospholipids - The "ying and yang" of lipotoxicity in metabolic diseases. Prog Lipid Res. 2017;66:14-29.

198. Green CD, Maceyka M, Cowart LA, Spiegel S**.** Sphingolipids in metabolic disease: The good, the bad, and the unknown. Cell Metab. 2021;33(7):1293-306.

199. Tan ST, Ramesh T, Toh XR, Nguyen LN**.** Emerging roles of lysophospholipids in health and disease. Prog Lipid Res. 2020;80:101068.

200. Yin X, Willinger CM, Keefe J, Liu J, Fernandez-Ortiz A, Ibanez B, et al. Lipidomic profiling identifies signatures of metabolic risk. EBioMedicine. 2020;51:102520.

201. Markgraf DF, Al-Hasani H, Lehr S**.** Lipidomics-Reshaping the Analysis and Perception of Type 2 Diabetes. Int J Mol Sci. 2016;17(11).

202. Razquin C, Toledo E, Clish CB, Ruiz-Canela M, Dennis C, Corella D, et al. Plasma Lipidomic Profiling and Risk of Type 2 Diabetes in the PREDIMED Trial. Diabetes Care. 2018;41(12):2617-24.

203. Liu P, Zhu W, Chen C, Yan B, Zhu L, Chen X, et al. The mechanisms of lysophosphatidylcholine in the development of diseases. Life Sci. 2020;247:117443.

204. Matsumoto T, Kobayashi T, Kamata K**.** Role of lysophosphatidylcholine (LPC) in atherosclerosis. Curr Med Chem. 2007;14(30):3209-20.

205. Mihalik SJ, Goodpaster BH, Kelley DE, Chace DH, Vockley J, Toledo FG, et al. Increased levels of plasma acylcarnitines in obesity and type 2 diabetes and identification of a marker of glucolipotoxicity. Obesity (Silver Spring). 2010;18(9):1695-700.

206. Guasch-Ferre M, Hruby A, Toledo E, Clish CB, Martinez-Gonzalez MA, Salas-Salvado J, et al. Metabolomics in Prediabetes and Diabetes: A Systematic Review and Meta-analysis. Diabetes Care. 2016;39(5):833-46.

207. Letteron P, Brahimi-Bourouina N, Robin MA, Moreau A, Feldmann G, Pessayre D**.** Glucocorticoids inhibit mitochondrial matrix acyl-CoA dehydrogenases and fatty acid beta-oxidation. Am J Physiol. 1997;272(5 Pt 1):G1141-50.

208. Yu E, Ruiz-Canela M, Razquin C, Guasch-Ferre M, Toledo E, Wang DD, et al. Changes in arginine are inversely associated with type 2 diabetes: A case-cohort study in the PREDIMED trial. Diabetes Obes Metab. 2019;21(2):397-401.

209. Chen S, Akter S, Kuwahara K, Matsushita Y, Nakagawa T, Konishi M, et al. Serum amino acid profiles and risk of type 2 diabetes among Japanese adults in the Hitachi Health Study. Sci Rep. 2019;9(1):7010.

210. Gunther SH, Khoo CM, Tai ES, Sim X, Kovalik JP, Ching J, et al. Serum acylcarnitines and amino acids and risk of type 2 diabetes in a multiethnic Asian population. BMJ Open Diabetes Res Care. 2020;8(1).

211. Pitocco D, Zaccardi F, Di Stasio E, Romitelli F, Santini SA, Zuppi C, et al. Oxidative stress, nitric oxide, and diabetes. Rev Diabet Stud. 2010;7(1):15-25.

212. Montagnani M, Quon MJ**.** Insulin action in vascular endothelium: potential mechanisms linking insulin resistance with hypertension. Diabetes Obes Metab. 2000;2(5):285-92.

213. Ong SL, Whitworth JA**.** Glucocorticoid-induced hypertension and the nitric oxide system. Expert Rev Endocrinol Metab. 2012;7(3):273-80.

214. Cicala MV, Mantero F**.** Hypertension in Cushing's syndrome: from pathogenesis to treatment. Neuroendocrinology. 2010;92 Suppl 1:44-9.

215. Bjelakovic G, Stojanovic I, Jevtovic Stoimenov T, Pavlovic D, Kocic G, Rossi S, et al. Metabolic correlations of glucocorticoids and polyamines in inflammation and apoptosis. Amino Acids. 2010;39(1):29-43.

216. DiNicolantonio JJ, McCarty MF, JH OK**.** Role of dietary histidine in the prevention of obesity and metabolic syndrome. Open Heart. 2018;5(2):e000676.

217. Toyoshima K, Nakamura M, Adachi Y, Imaizumi A, Hakamada T, Abe Y, et al. Increased plasma proline concentrations are associated with sarcopenia in the elderly. PLoS One. 2017;12(9):e0185206.

218. Lu Y, Karagounis LG, Ng TP, Carre C, Narang V, Wong G, et al. Systemic and Metabolic Signature of Sarcopenia in Community-Dwelling Older Adults. J Gerontol A Biol Sci Med Sci. 2020;75(2):309-17.

219. Manolopoulos KN, O'Reilly MW, Bujalska IJ, Tomlinson JW, Arlt W**.** Acute Hypercortisolemia Exerts Depot-Specific Effects on Abdominal and Femoral Adipose Tissue Function. J Clin Endocrinol Metab. 2017;102(4):1091-101.

220. Sudlow C, Gallacher J, Allen N, Beral V, Burton P, Danesh J, et al. UK biobank: an open access resource for identifying the causes of a wide range of complex diseases of middle and old age. PLoS Med. 2015;12(3):e1001779.